ORGANIC CONTAMINANTS DESTRUCTION USING THE UV/FREE CHLORINE PROCESS: MECHANISMS AND MODELING

A Dissertation
Presented to
The Academic Faculty

by

Weiqiu Zhang

In Partial Fulfillment
of the Requirements for the Degree
Doctor of Philosophy in the
School of Civil and Environmental Engineering

Georgia Institute of Technology
May 2020

ORGANIC CONTAMINANTS DESTRUCTION USING THE UV/FREE CHLORINE PROCESS: MECHANISMS AND MODELING

Approved by:

Dr. John C. Crittenden, Advisor
School of Civil and Environmental Engineering
Georgia Institute of Technology

Dr. Sotira Yiacoumi
School of Civil and Environmental Engineering
Georgia Institute of Technology

Dr. Yongsheng Chen
School of Civil and Environmental Engineering
Georgia Institute of Technology

Dr. Donggang Yao
School of Materials Science and Engineering
Georgia Institute of Technology

Dr. Ching-Hua Huang
School of Civil and Environmental Engineering
Georgia Institute of Technology

Date Approved: December 6th, 2019

This doctoral thesis is humbly dedicated to:

My parents, Douzhi Zhang & Jun Hou

and

The love of my life, Dr. Haosheng Wu

ACKNOWLEDGEMENTS

Foremost, I would like to express my sincere gratitude to my advisor Dr. John C. Crittenden for the continuous support throughout my Ph.D. study and research. Dr. Crittenden guides me to finish my doctoral thesis with his patience, enthusiasm and expertise. Over the past four and half years, Dr. Crittenden educates me to grow into an independent researcher as my mentor. His attitudes of hard-working, passion and curiosity for science always inspire me to overcome all difficulties encountered in my research. I shall be benefited for my entire life from Dr. Crittenden's spirit of constant exploration of knowledge in science. I would also like to appreciate my doctoral thesis committee members at Georgia Institute of Technology (Georgia Tech): Dr. Yongsheng Chen, Dr. Ching-Hua Huang, Dr. Sotira Yiacoumi, and Dr. Donggang Yao for their continuous encouragement and professional suggestions for my research.

Besides my advisor and thesis committee members at Georgia Tech, I would like to appreciate my master's degree advisor Dr. Mitchell Small from Department of Civil and Environmental Engineering, Carnegie Mellon University. Dr. Small introduced me to the area of environmental modeling and educated me build solid mathematical and programing background for my Ph.D. research. I would also thank Dr. Amelia Wang, Dr. Sharon Blei, Dr. Pawan Bareja, Dr. Yufen Han from Wells Fargo Inc. for their help of my computer skill development and support of my early career.

My acknowledgements extends to faculty, students and staff at Brook Byers Institute for Sustainable Systems and School of Civil and Environmental Engineering: Dr. Michael Chang, Susan Ryan, Gray Burchfield, Kathryn Jonell, Dr. Xiaoyang Meng, Su Liu, Osvaldo Broesicke, Junchen Yan, Zefang Chen, Kaihang Zhang, Dr. Dong Wang, Dr.

Jinming Luo. I also thank my collaborators and visiting scholars Dr. Shiqing Zhou, Dr. Shumin Zhu, Yangtao Wu, Julong Sun and Dr. Can Wang.

I would like to acknowledge the following foundations, institutes and assistantships for their funding supports: Brook Byers Institute of Sustainable Systems and High Tower Chair and Georgia Research Alliance at Georgia Tech, Chinese Council Scholarship.

Outside of my research and study, I would express my great appreciation to my friends back in China and here in USA: Wenjing Gao, Yujing Xue, Yu Liao, Zhiling Sun, Yi Zhou, Yuan Fang, Xicheng Xiong, Yaye Wang, Qinyu Li, Ting Li, etc. for their friendships.

My deepest acknowledge belongs to my family. My beloved parents, Douzhi Zhang and Jun Hou provide me unconditional love, the best education and always encourage me to chase my dreams. My husband, Dr. Haosheng Wu fully supports me with tremendous love during my pursuit of Ph.D. degree. I greatly value Dr. Wu's academic contributions and deeply appreciate his belief in me. Thanks for the many years of happiness and continual inspiration that Dr. Wu has brought for me. I would like to give endless gratitude to my deceased grandparents, they passed away before the completion of my Ph.D. degree. I will be forever grateful for the values they instilled in me since my childhood. Finally, my parents in law, my sister in law, uncles, aunties and cousins deserve my wholehearted thanks as well. I would never have been able to complete my doctoral thesis without the love from you all.

TABLE OF CONTENTS

LIST OF TABLES

LIST OF FIGURES

LIST OF SYMBOLS AND ABBREVIATIONS

AOPs	Advanced Oxidation Processes
GCM	Group Contribution Method
DBPs	Disinfection Byproducts
DBPFPs	Disinfection Byproducts Formation Potentials
POCs	Persistent Organic Contaminants
TCE	Trichloroethylene
PPCPs	Pharmaceuticals and Personal Care Products
EDCs	Endocrine Disrupting Compounds
RCS	Reactive Chlorine Species
SPSS	Simplified Pseudo-Steady State
PMS	Peroxymonosulfate
LFERs	Linear Free Energy Relationships
ODEs	Ordinary Differential Equations
NOM	Nature Organic Matters
PS	Persulfate
UV	Ultraviolet
DRG	Directed Relation Graph
NIST	National Institute of Standards and Technology
LP	Low Pressure
SBACs	Substituted Benzoic Acid Compounds
QASR	Quantitative Structure Activity Relationships
DPD	Diethyl-P-Phenylene Diamine

HPLC	High-Performance Liquid Chromatography
VWD	Variable Wavelength Detector
SD	Sample Deviation
OF	Objective Function
BDF	Backward Differentiation Formula
EE/O	Electrical Energy Requirement for One Order Magnitude Degradation
TMP	Trimethoprim
CBZ	Carbamazepine
PT-GC-MS	Purge-and-Trap Gas Chromatography-Mass Spectrometry
TCM	Trichloromethane
DCAN	Dichloroacetonitrile
SMILES	Simplified Molecular Input Line Entry System
DA	Double Bond Addition
XE	HCl Elimination
OA	Oxygen Addition
PB	Bimolecular Decay of Peroxyl Radicals
S	Special Reactions
BS	β Scission
XR	Recombination of Cl·/Cl_2^-· with carbon centered radicals
HX	Hydrolysis of Carbonyl Chloride Group
HC	Hydrolysis of Carbonyl Group
HA	Hydrogen Abstraction

OT	1,2-Shift of Oxyl radicals
PH	$HO_2^{\cdot}$ Elimination of Peroxyl Radicals
ClE	Homolytic Cleavage of C-Cl Bond
HS	Hydrolysis Reactions
ClR	Chlorination

SUMMARY

Advanced oxidation processes (AOPs) are effective technologies to oxidize recalcitrant organic contaminants in the aqueous phase. The UV/free chlorine process has gained attention as a promising AOP technology, and it generates various reactive radicals (i.e. HO•, Cl•, Cl_2^-• and ClO•) at room temperature and pressure**.** These electrophilic radicals eventually mineralize refractory organic contaminants into CO_2 and H_2O. Compared with other common AOPs (e.g. UV/H_2O_2 and UV/Persulfate processes), the UV/free chlorine process has many advantages, for example (1) it has much lower chemical reagent costs; (2) it has higher energy efficiency; (3) it is only slightly impacted by chloride ions (Cl^-) (We found Cl^- significantly inhibits the effectiveness of the UV/Persulfate process). For large scale applications, understanding the degradation mechanisms is critical to the design of the UV/free chlorine process that has the lowest energy consumption and greatest toxicity reduction. A number of related studies have shed light on the degradation of some selected organic compounds (e.g., atrazine, naproxen, etc.). However, these previous studies of the UV/free chlorine process have not comprehensively examined the mechanistically complex radicals-initiated chain reactions. Many researches have conducted experiments to determine the degradation mechanisms. However, these experimental studies are very time consuming and expensive. With respect to developing kinetic models that can simulate the reaction pathways in the UV/free chlorine process, most studies have used simplified lumped reactions or invoked the simplified pseudo steady state assumption because the rate constants between reactive radicals and organic compounds are unknown. Accordingly, conducting experiments and developing simplified kinetic models would be impossible to fully elucidate the oxidation mechanisms of all

organic contaminants that may be found in the aqueous phase (Chemical Abstracts Service lists about more than 147 million compounds).

To overcome the above-mentioned challenges, we developed a first principles-based kinetic model to predict the oxidation of organic compounds in the UV/free chlorine process. First, we collected photolysis and chemical reactions that describe the oxidation of target organic compounds from literature. Second, we developed a rate constants estimator to predict the rarely reported second-order rate constants between reactive radicals and organic compounds (i.e. $k_{HO\cdot/R}$, $k_{Cl\cdot/R}$, $k_{Cl_2^-\cdot/R}$ and $k_{ClO\cdot/R}$). $k_{HO\cdot/R}$ was estimated by the group contribution method (GCM). $k_{Cl\cdot/R}$, $k_{Cl_2^-\cdot/R}$ and $k_{ClO\cdot/R}$ were estimated by using the genetic algorithm that was fit to our experimental data (i.e. experimental observed time-dependent concentration profiles of target organic compounds). Third, we developed a stiff ordinary differential equations solver using Gear's method to predict the time-dependent concentration profiles of target organic compounds, and our prediction results agreed with our experimental data for various operational conditions. Accordingly, our first principles-based kinetic model was successfully verified using our experimental data. Based on our UV/free chlorine kinetic model, we developed four quantitative structure activity relationships using Hammett constants of organic compounds and our predicted rate constants. We then determined relative contribution of these reactive radicals and photolysis, and, we found ClO· was the dominant radicals for organic contaminants oxidation. We also optimized the operational conditions (i.e. UV intensity and free chlorine dosage) that has the lowest energy consumption. Furthermore, we successfully implemented graph theory to develop a computerized pathway generator, which was built based on the predefined reaction mechanisms from experimental

observations. The pathway generator can automatically predict all possible reactions and byproducts/intermediates that are involved in the degradation of target organic contaminants during the UV/free chlorine process (e.g. the degradation of TCE involves more than 200 byproducts /intermediates and more than 1,000 reactions). Therefore, the pathway generator significantly advances our understanding about the degradation pathways. However, we have noticed that it is difficult to estimate the rate constants of all possible involved reactions at current stage, because we only have very limited amount of experimental data (e.g., we do not have data on peroxyl radicals reactions) to develop a GCM. Consequently, future work will mainly focus on developing new methods (e.g. quantum chemistry) to estimate the rate constants of all possible involved reactions, and then predicting the time-dependent concentration profiles of byproducts. Finally, we investigated the disinfection byproducts (DBPs) and disinfection byproducts formation potentials (DBPFPs) in the UV/free chlorine process. In practical applications, natural organic matter can react with residual free chlorine to produce toxic DBPs. As a result, both the micropollutants and the DBPFPs must be decreased. Therefore, we need determine the controlling factor (i.e., organic contaminant destruction or DBPFPs reduction) in the design of the UV/free chlorine system. Overall, our study can be used to design the most cost-effective UV/free chlorine process.

CHAPTER 1. INTRODUCTION

1.1 Significance and Objectives

With the rapidly development of global economy in the past century, numerous persistent organic contaminants (POCs) (e.g. pesticides, solvents, pharmaceuticals, etc.) have been extensively used in industrial and agriculture areas.[1] In recent years, POCs are widely distributed in aqueous environment after intentionally/unintentionally released.[2] POCs are potentially for long-range transport because bioaccumulation and persistence in environment with acute toxicity.[3] Therefore, the occurrences of persistent organic contaminants in water matrix become a global pollution issue and cause very serious adverse impacts on human health and ecological systems. For example, trichloroethylene (TCE) polluted the groundwater at Minneapolis in 2013, which resulted in the increasing of cancer rate and birth defects;[4] pharmaceuticals and personal care products (PPCPs) and endocrine disrupting compounds (EDCs) can be toxicity at low concentration and pose risks to public health in China, India, Brazil;[5] petroleum oil were spilled into the Gulf of Mexico over 87 days in 2010, which caused serious distress to the marine ecosystems, such as the rate of baby dolphin deaths raised in the area[6]. These negative impacts indicate a need of tertiary wastewater treatment processes for the removal of refractory organic contaminants before they are discharged into natural environment.[7] In Switzerland, removal of refractory organic contaminants is mandatory for wastewater treatment plants and Germany will follow suit.[7]

Research studies about the removal of persistent organic contaminants from aqueous phase exponentially increased after year 2000 . Among various tertiary wastewater treatment technologies that have been applied to remove persistent organic contaminants,

advanced oxidation processes (AOPs) are most effective technologies because of generating various highly reactive radicals at room temperature and pressure. These electrophilic radicals initially target the electron-rich sites of POCs, and further degrade POCs into carbon dioxide and water by the subsequent radical-initiated chain reactions. However, other tertiary wastewater treatment technologies do not always mineralize POCs. For example, biological process-based conventional wastewater treatment technologies are unable to eliminate non-biodegradable organic contaminants, and may still result in a high portion of these contaminants can enter into aquatic environment;[8,9] advanced physical chemical wastewater treatment technologies including adsorption, reverse osmosis membranes and air striping only transfer persistent organic compounds from aqueous phase to another phase (e.g. solid phase).[10]

AOPs were first proposed in 1980s for drinking water treatment in United States.[11] Conventional hydroxyl radicals (HO•)-based AOPs (e.g., ultraviolet light combined with hydrogen peroxide (UV/H_2O_2) and ozone combined with hydrogen peroxide (H_2O_2/O_3)) have been successfully applied for the destruction of a variety of organic contaminants. HO• acts as strong oxidant (standard reduction potential, $E^o(HO\bullet/H_2O) = 2.73V$),[12,13] and non-selectively targets organic compounds at close to the diffusion-limited rate (i.e.,1-8×10^{10} $M^{-1}s^{-1}$).[12] However, there are some obstacles to the widely application of conventional HO•-based AOPs. For the H_2O_2/O_3 process, the primary concern is the formation of bromate (BrO_3^-) from the reaction of O_3 with bromide ions (Br^-) in water matrix.[10] Bromate is a carcinogenic pollutant and poses high risks for human health.[14] For the UV/H_2O_2 process, major limitations include: ***(1)*** the need for an expensive chemical reagent (H_2O_2) to maintain the operation; ***(2)*** low energy efficiency due to the poor UV

light-absorption characteristics of H_2O_2;[15] and, ***(3)*** concerns about residual H_2O_2 after treatment (e.g., residual H_2O_2 reacts rapidly with chlorine, which would result in increasing chlorine dosage to maintain a chlorine residual in the distribution system, and thereby increases operational costs).[16] Recently, the UV/persulfate (PS) process has been considered as an alternative AOP technology, which generates persulfate radicals $SO_4^{-}\bullet$ (standard reduction potential E° ($SO_4^{-}\bullet$/ SO_4^{2-}) = 3.1 V) to selectively destroy refractory organic contaminants.[17,18,19] Nevertheless, one major concern regarding the UV/PS process is the impact of the chloride ions (Cl^-), as Qian et al. reported that the UV/PS process is completely ineffective to destruct perfluorinated compounds when Cl^- is present.[20]

In aqueous environment, the oxidation states of chlorine element range from -1 to +7, namely, Cl^-, HOCl/OCl^-, HOClO/$OClO^-$, ClO_2, ClO_2^-, $HOClO_2$/$OClO_2^-$, ClO_3^-, ClO_4^-.[21] Cl^- is the one of the most stable oxidation state of chlorine element in water matrix. Meanwhile, Cl^- is one of the most commonly found anions in water matrices, for example, Cl^- is present at approximately 0.001 M in freshwater and 0.1 M in industrial wastewater.[22,23,24] As a result, the wastewater treated by AOPs inevitably contains Cl^-. Many experimental studies have been conducted and reported the Cl^--related impacts on certain organic compounds destruction in the UV/PS process.[20,25,26,27,28,29,30,31,32,33,34,35,36] However, a quantitative insight and the fundamental understanding of the impact of Cl^- on the UV/PS remains challenging because ***(1)*** experimentally screening the impact of Cl^- on all organic contaminants that may be present in water matrix is time consuming and cost prohibitive, ***(2)*** the sophisticated radical chain reactions typically involved in AOPs limit most current studies to only qualifying the effects of Cl^- on a particular compound (rather than

determining the intrinsic mechanism and quantifying the Cl^- impact). Consequently, an in-depth mathematical modeling study of the effect of Cl^- on the UV/PS process is critical for the cost-effective application of the UV/PS in wastewater treatment. In this study, we will first develop a mathematical model to investigate the impact of Cl^- on the UV/PS process by comparing the destruction rate of organic contaminants when Cl^- is not present/present.

The UV/free chlorine ($HOCl/OCl^-$) process has become another promising AOP technology. The photolysis of free chlorine initially produces HO• and Cl•, and Cl• is a very strong oxidant with a standard reduction potential comparable to that of HO• ($E^o(Cl\bullet/Cl^-)$ = 2.4 V).[37] The secondary radicals generated in the UV/free chlorine process are $Cl_2^-\bullet$ ($E^o(Cl_2^-\bullet/Cl_2(aq))$ = 0.67 V) and ClO• ($E^o(ClO\bullet/ClO^-)$ = 1.39 V).[13] Compared with conventional AOPs and the UV/PS process, the UV/free chlorine process has the following advantages: ***(1)*** the chemical reagent costs is much cheaper (the market price is $250/metric ton for NaOCl, $800/metric ton for $Na_2S_2O_8$, and $500/metric ton for H_2O_2); ***(2)*** the treatment efficiency is higher with less chemical consumption and shorter treatment time (e.g., trichloroethylene, MIB);[38] ***(3)*** the energy efficiency is higher because free chlorine has greater UV light-absorption characteristics. The quantum yields of free chlorine (0.9-1.45 for HOCl, 0.8-0.97 for OCl^-) are higher than those of both H_2O_2 (0.5) and $S_2O_8^{2-}$ (0.7) at a wavelength of 254 nm.[15,39,40] In addition, the molar extinction coefficients of HOCl and OCl^- are 59 and 66 $M^{-1}cm^{-1}$ respectively,[37] which are much higher than the values for H_2O_2 (17.9 $M^{-1}cm^{-}$1-19.6 $M^{-1}cm^{-1}$) and $S_2O_8^{2-}$ (20.07 $M^{-1}cm^{-1}$).[15,20] Sichel et al. reported that the UV/free chlorine process achieved energy reductions of approximately 75% compared with the UV/H_2O_2 process;[41] ***(4)*** free chlorine is the most commonly used disinfectant, thus existing infrastructure can be utilized with only addition of a UV light

source;[42] ***(5)*** residual free chlorine after treatment can be used for residual disinfection in distribution systems, therefore, no further quenching is needed;[43] and, ***(6)*** many experimental studies have reported that a moderate concentration of Cl^- has a negligible impact on the oxidation of various organic contaminants (e.g., benzoic acid, clofibric acid, ibuprofen, carbamazepine, caffeine) by the UV/free chlorine process.[37,44,45,46,47] Overall, the UV/free chlorine process is more cost-effective than conventional AOPs and the UV/persulfate process. MIOX Inc. reported that the UV/free chlorine process could save $10,800 annually for groundwater remediation compared with the UV/H_2O_2 process at a flow rate of 416 gal/min.[48]

The above-mentioned benefits have positioned the UV/free chlorine process as one of the most promising AOPs to oxidize POCs. However, current studies on the UV/free chlorine process are still largely at the theoretical level or laboratory-scale,[49] because ***(1)*** the involved chain reactions are mechanistically complex; ***(2)*** the second-order rate constants of reactive chlorine species (RCS: Cl·, Cl_2^-· and ClO·) reacting with most organic contaminants are lacking. Consequently, for the application of UV/free at industrial scale with lowest energy consumption and least toxicity, it is necessary to understand the degradation mechanisms of organic contaminants in this process. Many related experimental studies have investigated the degradation mechanisms of some selected organic compounds in the UV/free chlorine process, for example (i) reporting the treatment efficiency of atrazine, [50] desethylatrazine,[41] sulfamethoxazole[41] under various water matrix conditions; (ii) determining the rate constants for RCS reacting with PPCPs,[51] DEET[47] and Caffeine[47] by the competition kinetic method; (iii) detecting the major byproducts generated from the oxidation of benzalkonium chlorides,[52] naproxen,[53]

paracetamol[54]. Although the experimental studies are time consuming and present a challenge for screening all organic contaminants, they still laid foundation for further kinetic modeling studies. Some kinetic models have been developed for the oxidization of various organic contaminants in the UV/free chlorine process, such as benzoic acid, [37] carbamazepine,[46] acrylamide,[55] phenacetin,[56] ibuprofen, [45] clofibric acid, [44] polyvinyl alcohol,[57] chloramphenicol, [58] iodoform,[59] trimethoprim,[60] bezafibrate. [61] However, most of these kinetic models invoked lumped reactions for simplification, or, utilized the simplified pseudo-steady state (SPSS) assumption for the kinetic description of free radicals species in the system. The SPSS assumption indicates that the net formation rates of free radicals are zero. Therefore, these simplified kinetic models only estimated the pseudo-first-order rate constants to quantify the overall oxidization rates under certain experimental conditions, rather than elucidated the oxidization rate contributions for all the reactive radicals that are involved (e.g., HO• and RCS). Recently, a few studies used some commercial software/tools (e.g., Simbiology, Kintecus) to simulate the kinetic performance of the UV/free chlorine process.[62] Even though the SPSS assumption was not used, these commercial software/tools can only be applied to very limited organic contaminants that have reported rate constants with HO• and RCS.

In general, conducting experiments and developing simplified kinetic models would be impossible to fully elucidate the oxidation mechanisms of all organic contaminants that may be found in the aqueous phase (Chemical Abstracts Service lists about more than 147 million compounds). Consequently, quantitative insights into the degradation mechanisms of organic contaminants are still insufficient for the UV/free chlorine process. An attractive alternative for overcoming these challenges is to develop a first-principles based kinetic

model without SPSS assumption. Various kinetic models based on first-principles have been successfully implemented to describe the degradation mechanisms of HO· based and SO_4^{-}· based AOPs, which included UV/H_2O_2 process,[63,64,65] UV/TiO_2 process,[65] H_2O_2/O_3 process, UV/PS process,[20] CoFeNi/Peroxymonosulfate (PMS) process,[66] ascorbic acid/PMS process.[67] Accordingly, several useful computer tools have been developed and used for these first principles-based kinetic models: ***(1)*** Li et al. developed a pathway generator based on the graph theory to automatically predict the elementary reactions included in the degradation pathways of HO· targeting organic compounds. For example, full degradation pathway of acetone in the UV/ H_2O_2 process contains 285 species and 3639 reactions,[68] and the generated pathway have been validated with experimental observations.[63,68]. However, this pathway generator is insufficient to predict organic contaminants destruction in the UV/free chlorine process because not only HO· but also Cl·, Cl_2^{-}· and ClO· are involved; ***(2)*** Daisuke et al. developed a friendly used rate constants estimator for HO· reacting with organic contaminants by group contribution method (GCM).[69] GCM hypothesizes that the reaction mechanisms of HO· (H abstraction, addition into unsaturated bond) and the effect of neighboring functional groups determine $k_{HO\cdot/R}$. GCM has been successfully applied for estimating $k_{HO\cdot/R}$ for many organic contaminants in the aqueous phase, and the predicted value of $k_{HO\cdot/R}$ typically has an error factor of 0.5–2;[69,70] ***(3)*** Daisuke et al. also developed a linear free energy relationships (LFERs) to estimate rate constants for HO· reactions,[71]Cl· adducts,[72] oxygen addition reactions,[73] unimolecular and bimolecular peroxyl radical decay reactions.[73] LFERs was based on the transition state theory, and the kinetic reaction rate constant of a given elementary reaction is linearly dependent on the free energy change from reactants to

transition state; ***(4)*** Qian et al. implemented genetic algorithm to estimate rate constant for $SO_4^{-}\cdot$ reacting with organic contaminants by fitting experimental data with the minimum objective function;[20] ***(5)*** Guo et al. have implemented gear's algorithm and kinetic Monte Carlo algorithm to solve the stiff ordinary differential equations (ODEs) for conventional HO• -based AOPs systems (e.g. UV/H_2O_2 and UV/TiO_2 processes.[64,65] With the consideration of these computer tools developed for HO• based and $SO_4^{-}\cdot$ based AOPs, it is feasible to develop a first principles-based kinetic model for the UV/free chlorine process.

Accordingly, we will develop a first principles-based kinetic model that can be utilized to fully explore the oxidation mechanisms of organic compounds in the UV/free chlorine process in this study. Specifically, we will first collect all possible elementary reactions regarding the oxidation of target organic compounds. Then, we will develop a second-rate constants estimator to predict the rarely reported second-order rate constants between organic contaminants and reactive radicals in the UV/free chlorine process (i.e. RCS and HO•). Then, we will develop a stiff ordinary differential equations solver to predict the time-dependent concentration profiles of target organic compounds. Our prediction results will be compared with our experimental data for various water matrix conditions, such as various free chlorine dosage, various pH, various Cl^- concentrations, various nature organic matters (NOM) concentrations, various bicarbonate/carbonate concentrations, etc. After verifying our first- principles based kinetic model by comparing with our experimental data: ***(1)*** we can develop four quantitative structure activity relationships using Hammett constants of organic compounds and our predicted rate constants; ***(2)*** we can determine relative contribution of these reactive radicals and photolysis and explore the dominant contributor for the oxidation; ***(3)*** we also optimized the operational conditions (i.e. UV

intensity and free chlorine dosage) that has the lowest energy consumption. Furthermore, we will implement graph theory to develop a computerized pathway generator for the UV/free chlorine process, which was built based on the predefined reaction mechanisms from experimental observations. The pathway generator can automatically predict all possible reactions and byproducts/intermediates that are yielded from the degradation of target organic contaminants in the UV/free chlorine process. Consequently, pathway generator can significantly advance our understanding about the detailed pathways of mineralization various organic contaminants into inorganic compounds. Additionally, we will investigate the disinfection byproducts formation potentials (DBPFPs) in the UV/free chlorine process, because NOM typically exists in real water and can react with residual free chlorine to produce toxic DBPs. As a result, we need consider the decreasing of both the micropollutants and the DBPFPs for the design of the UV/free chlorine process in practical application.

This study will provide researchers and engineers with a comprehensive tool to quantitatively evaluate the performance of the UV/free chlorine process in treating numerous contaminants and gain detailed insight into the fate of their byproducts. Our study can be used to design experiments and the most cost-effective AOPs for industrial applications, such as optimal chemical dosages, water matrix conditions, and light intensity. Our study can also help discover new theoretical knowledge by validating experimental results, such as novel degradation mechanisms and isotope effects. Furthermore, this study can be used for other elementary reaction-based systems, such as disinfection byproduct formation, combustion and polymerization processes. The success of this study will be a powerful tool used to address important societal concerns. For

example, water scarcity is one of the most challenging global issues, the availability of high-quality freshwater sources continues to decrease due to population growth, urbanization and climate change. Water reuse is an important option to the water scarcity problem. This study can help guide the most cost-effective AOP technology and recycle water rapidly.

1.2 Structure of This Dissertation

This dissertation consists of the introductory part, three main chapters, and appendices. After this introductory chapter, Chapter 2 discusses development of a mathematical to investigate the impact of Cl^- on the UV/PS process and UV/H_2O_2 process. The work from this chapter has been published in Zhang et al. (Zhang et al., 2018). [39] In Chapter 3, a first-principles based kinetic model has been developed for the oxidation of target organic contaminants in the UV/free chlorine process. The work from this chapter has been published in Zhou and Zhang et al.(Zhou and Zhang et al.,(co-first authors) 2019).[74] Chapter 4 presents the feasible study of the UV/free chlorine process oxidizing pharmaceuticals in practical application, the study mainly includes ***(1)*** the impact of water matrix scenarios (pH, Cl^-, alkalinity, NOM) on the oxidation rate of pharmaceuticals; ***(2)*** DBPs formation during the pretreatment of the UV/free chlorine process. The work fin this chapter will be submitted in ***(1)*** Wu and Zhang et al. (Wu and Zhang et al., 2019), ***(2)*** Wang, Wang and Zhang et al. (Wang, Wang and Zhang et al., 2019). Chapter 5 addresses the development for the pathway generator for the UV/free chlorine process. This work will be submitted in Zhang et al. Conclusions and future work will be the last chapter (Chapter 6). Appendices cover the detailed equations, data, procedures of calculations and development process and computational code examples.

CHAPTER 2. IMPACT OF CHLORIDE IONS ON UV/H2O2 AND UV/PERSULFATE ADVANCED OXIDATION PROCESSES

†*work from this chapter has been published and presented in the following citation:*

Zhang, Weiqiu., Zhou, Shiqing., Sun, Julong., Meng, Xiaoyang., Luo, Jinming., Zhou, Dandan., & Crittenden, John. (2018). Impact of chloride ions on UV/H_2O_2 and UV/persulfate advanced oxidation processes. *Environmental science & technology*, *52*(13), 7380-7389.

Zhang, Weiqiu., Crittenden, John. Impact of chloride ions on UV/H_2O_2 and UV/persulfate advanced oxidation processes. The 256th American Chemistry Society National Meeting & Exposition. August 19, 2018 - August 23, 2018. Boston, Massachusetts, USA.

2.1 Abstract

Chloride ion (Cl^-) is one of the most common anions in the aqueous environment. A mathematical model was developed to determine and quantify the impact of Cl^- on the oxidization rate of organic compounds at the beginning stage of UV/persulfate (PS) and UV/H_2O_2 processes. We examined two cases for the UV/PS process: ***(1)*** when the target organic compounds react only with sulfate radicals, the ratio of the destruction rate of the target organic compound when Cl^- is present to the rate when Cl^- is not present (designated as $r_R^{Cl^-}/r_R$) is no larger than 1.942%, and ***(2)*** when the target organic compounds can react with sulfate radicals, hydroxyl radicals and chlorine radicals, $r_R^{Cl^-}/r_R$ can be no larger than 60%. Hence, Cl^- significantly reduces the organic destruction rate in the UV/PS process. In the UV/H_2O_2 process, we found that Cl^- has a negligible effect on the organic contaminants oxidation rate. Our simulation results agree with the experimental results very well. Accordingly, our mathematical model is a reliable method for determining whether Cl^- will adversely impact organic compounds destruction by the UV/PS and UV/H_2O_2 processes.

2.2 Introduction

Ultraviolet (UV)-driven advanced oxidation processes (AOPs) are popular drinking water and wastewater treatment techniques for the destruction of refectory organic contaminants owing to their great oxidative capability and efficiency.[11,75,76,77] In addition, AOPs are useful for controlling toxic disinfection by-products (the secondary organic contaminants) in aqueous phase.[78,79] AOPs produce various highly reactive radicals at ambient temperature and atmospheric pressure.[10] These electrophilic radicals can directly

decompose electron-rich organic compounds into water, mineral acids and CO_2.[80] For example, hydroxyl radicals (HO·) can be produced via UV/H_2O_2 or UV/persulfate (PS) processes, and sulfate radicals (SO_4^{-}·) can be generated by the UV/PS process. Both HO· ($E^o(HO\cdot/OH^-) = 2.74$ V) [12] and SO_4^{-}· ($E^o(SO_4^{-}\cdot/SO_4^{2-}) = 3.1$ V) [19,25] are very strong oxidants. The industrial-scale implementation of AOPs is ramping up rapidly, especially for UV/H_2O_2 and UV/PS processes. The momentum mainly comes from the increasing need for water reuse and more demanding regulations on organic contaminants.[11,26,27,75,81,82] Nevertheless, one major concern regarding UV/H_2O_2 and UV/PS processes is the impact of the commonly found chloride ion (Cl^-), as Qian et al. reported that UV/PS is completely ineffective to destruct perfluorinated compounds when Cl^- is present.[20] This is an important finding because perfluorinated compounds cannot be destroyed by hydroxyl radical. Consequently, an in-depth study of the effect of Cl^- on UV/H_2O_2 and UV/PS processes is critical for the cost-effective application of these AOPs in wastewater treatment.

Cl^- is one of the most common anions in water matrices; for example, Cl^- is present at approximately 0.001 M in freshwater and 0.1 M in industrial wastewater.[22,23,24] Some experimental studies have been conducted that shed light on the impact of Cl^- on only certain organic oxidization rates in the UV/H_2O_2 and UV/PS processes (e.g. atenolol,[76] atrazine,[34] propranolol,[31] chloramphenicol,[32] etc.). However, a quantitative insight with the fundamental and comprehensive understanding of the impact of Cl^- on the UV/H_2O_2 and UV/PS processes remains challenging because: ***(1)*** experimentally screening the impact of Cl^- on all organic contaminants that may be present in the water matrix is time consuming and cost prohibitive,[30,83,84] ***(2)*** the sophisticated radical chain reactions

typically involved in AOPs limit most current experimental studies to only qualifying the effects of Cl^- on a particular compound (rather than determining the intrinsic mechanism and quantifying Cl^- impacts for any compound), and (3) Cl^- can react with $SO_4^{\cdot-}$ in the UV/PS process or HO· in both the UV/H_2O_2 and UV/PS process to form chlorine radicals (Cl·), which are also strong oxidants ($E^o(Cl\cdot/Cl^-) = 2.4$ V) and can oxidize organic contaminants.[37] The reactivity of Cl· can be higher than that of HO· or $SO_4^{\cdot-}$ depending on the structure of the organic compounds (e.g., benzene, pyridine, etc. have second order rate constants).[37] However, possible reactions between the generated Cl· and organic contaminants and related effects have not been considered in most of the UV/PS and UV/H_2O_2 studies so far.[30,83,84] We proposed a promising method to overcome the above mentioned difficulties by developing a mathematical model based on elementary reactions and kinetic data reported for the UV/PS and UV/H_2O_2 processes.[20,84,85] Modeling studies have been reported to investigate the mechanism of organic degradation in UV/H_2O_2 and UV/PS processes, for example, many studies developed kinetic models with pseudo steady state assumption or utilize commercial software (e.g. Kinetucs) to predict the parent organic compounds degradation rate in UV/PS and UV/H_2O_2 process, such as ionophore antibiotics,[84] chlorobenzene,[86] acetaminophen,[87] haloacetonitriles,[88] etc. However, to the best of our knowledge, no attempt has been made to establish a mathematical model to investigate the impact of Cl^- by comparing the destruction rate in AOPs when Cl^- is not present/present. Herein, we developed a novel algorithm based on a mathematical model to determine and quantify the impact of Cl^- on the oxidation of all organic contaminants in both the UV/PS and UV/H_2O_2 process. Furthermore, our model can elucidate the detailed mechanisms through which Cl^- impacts the oxidation rate. Beside Cl^-, natural organic

matter (NOM), bicarbonate (HCO_3^-) and carbonate (CO_3^{2-}) (HCO_3^-/CO_3^{2-}) are also commonly found in water matrices, and these species may also scavenge $SO_4^-\cdot$, HO· and Cl·.[89,90] Consequently, the model we developed can also be used to investigate the combined impacts of organic compound oxidation by (i) Cl^- and NOM and (ii) Cl^- and HCO_3^-/CO_3^{2-} on the UV/PS and UV/H_2O_2 processes.

To validate our model, we conducted experimental studies on the degradation of benzoic acid by the UV/PS and UV/H_2O_2 processes. The simulation results are consistent with the experimental results. Furthermore, our model results also agree well with the reported experimental results for more than 20 compounds. Hence, our modeling approach is rational. This model can help make policy decisions, for example, by quickly determining whether the application of UV/PS and UV/H_2O_2 processes in the presence of Cl^- is cost effective (e.g., in a water reuse facility to determine whether reverse osmosis would help by removing chloride ion).

2.3 Materials and Methods

In the UV/PS process, $SO_4^-\cdot$, HO· and Cl· can be produced in the presence of Cl^-. These three radicals are strong oxidants and can oxidize most electron-rich organic compounds. However, for organic compounds with strong polarized bonds (e.g., perfluorinated compounds), only $SO_4^-\cdot$ can destroy these compounds.[20,91] As a result, we can examine two situations for the UV/PS process to determine the impact of Cl^-: ***(1)*** organic compounds that react only with $SO_4^-\cdot$ and ***(2)*** organic compounds that can react with $SO_4^-\cdot$, HO· and Cl· (the latter two are produced from the reaction between: (i) $SO_4^-\cdot$ with H_2O and (ii) $SO_4^-\cdot$ with Cl^-). In the UV/H_2O_2 process, HO· and Cl· are produced in the presence of Cl^-, and these two radicals can oxidize target organic compounds.

2.3.1 Modeling approach

The effects of Cl^- on the UV/PS and UV/H_2O_2 processes were investigated by comparing the organic destruction rate when Cl^- is present to the rate when Cl^- is not present. The quenching ratio (Q_R) can be used to quantify the fraction of radical oxidizing the target organic compound. Q_R is defined as the rate of radical oxidizing the target organic compound as compared to the rate of all reactions of this radical.[10] If the quenching ratio significantly decreases when Cl^- is present (less radical will oxidize the target organic compound), then Cl^- lowers the rate of target organic compound destruction.

UV/PS and UV/H_2O_2 processes involve complex elementary reactions. Therefore, we used the directed relation graph (DRG) method to remove all unimportant elementary reactions to reduce computational time. Based on the DRG method, some elementary reactions can be ignored if the ratio between the reaction rate and the interested reactant overall consumption rate is less than 0.05%.[64] The DRG method has been successfully applied to remove unimportant elementary reactions for various AOPs in on-the-fly kinetic models.[63,64] All elementary reactions and rate constants used in this study are included in **Table A.1** and **Table A.2 in Appendix A**. These elementary reactions have been used in validated kinetic models for UV/PS and UV/H_2O_2 process.[20,63,64,65,92] Reactions between $Cl_2^-\cdot$ and the organic compounds were not considered in this study because ***(1)*** $Cl_2^-\cdot$ is generally much less reactive than HO· and Cl·,[37] and, ***(2)*** based on the DRG method, the ratio between the rate of $Cl_2^-\cdot$ reacting with organic compounds and the overall consumption rate of $Cl_2^-\cdot$ is very low (0.018%) (**Text A.4.7 in Appendix A**). Based on these elementary reactions, reaction networks were developed to determine the reaction pathway. **Figure 2.1** illustrates the network in the UV/PS process in which organic

compounds can react with $SO_4^{-}\cdot$, HO· and Cl·. The network in the UV/PS process in which organic compounds react only with $SO_4^{-}\cdot$ and the network in the UV/H_2O_2 process are provided in **Figure A.1** and **Figure A.2 in Appendix A**.

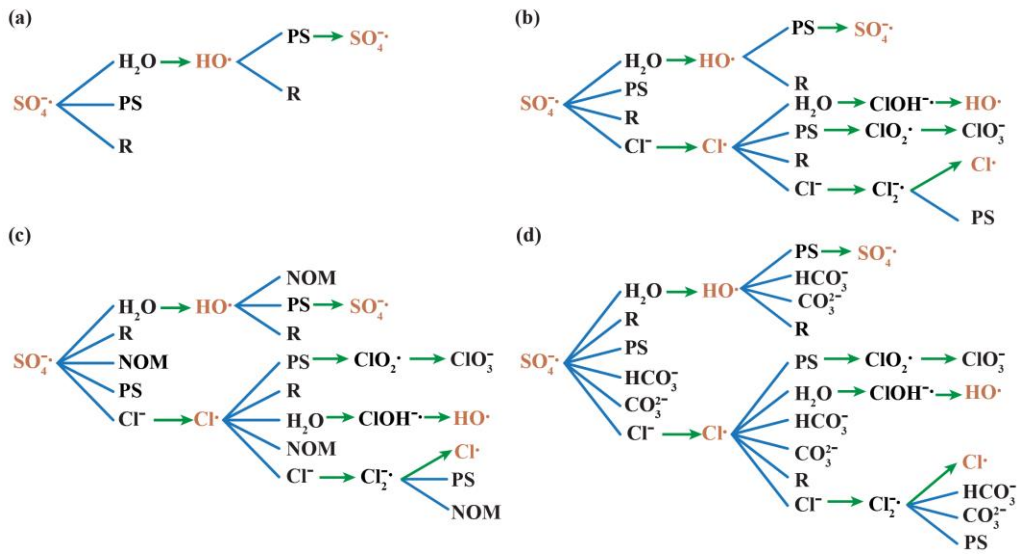

Figure 2.1. UV/PS elementary reaction network (when organic compounds can react with HO·, $SO_4^{-}\cdot$ and Cl·). (a) Cl^- is not present, (b) only Cl^- is present, (c) Cl^- and NOM are present, and (d) Cl^-, HCO_3^-/ CO_3^{2-} are present. The blue lines represent reactions between two compounds, and the green arrows represent the generation of the reaction products.

This mathematical model was developed based on the simplified pseudo-steady-state (SPSS) assumption (assuming all photons are absorbed by the system).[15,20] The SPSS assumes that all species (e.g., R, Cl^-, PS, H_2O_2, NOM, HCO_3^- and CO_3^{2-}) maintain their initial concentrations, which notably, would yield the greatest impact on Cl^-.[84] This simplification allows us to develop an algebraic algorithm (rather that a set of ordinary differential equations (ODEs) that must be solved) to describe the impact of Cl^- at the beginning of the oxidation process (see the Excel sheet in the SI). All equations (eq A.63 – eq A.158) in the algebraic algorithm were derived from the validated UV/H_2O_2 and UV/PS kinetic models.[20,63,64,65,92]

In this study, we varied the Cl^- concentration while the concentrations of the other components were fixed at feasible values. The Cl^- concentration varied from 0.001 M to 0.1 M.[22,23,24] The concentration of organics was assumed to be 10^{-4} M, and [PS]/[R] or $[H_2O_2]$/[R] was assumed to be 100, as reported in the literature.[20,27,76] The surface water or ground water matrix contains typically 2 $mg \cdot L^{-1}$ NOM (ranges from 1 $mg \cdot L^{-1}$ to 3 $mg \cdot L^{-1}$),[10] 3 mM HCO_3^- and 0.14 μM CO_3^{2-} and has a pH of 6 (ranges from 6 to 8.5).[93] We used these conditions for further analysis. The National Institute of Standards and Technology (NIST) database reported the rate constants of 22 organics reacting with $SO_4^- \cdot$, HO· and Cl·.[85] Qian et al. reported rate constants of 6 perfluorinated compounds reacting with $SO_4^- \cdot$.[20] These values, tabulated in **Table A.3 in Appendix A**, cover the wide range of rate constants used in this study.

Because some of the rate constants used here were estimated without considering the ionic strength, the ionic strength was not considered in this manuscript to simplify the calculation. Nevertheless, we also developed an algorithm including ionic strength by replacing all species concentrations with species activities in eq A.63 – eq A.158 (see Excel sheet in the SI). The species activity is equal to the ionic strength coefficient (γ_i) times the species concentration. For molecular species (uncharged) such as weak acids and organic species, γ_i is very close to 1.0 based on the Setschenow equation.[94] For charged species, γ_i was calculated from the Davies equation (eq 2.1).[95]

$$\log \gamma_i = -AZ^2 \left(\frac{\sqrt{I}}{1+\sqrt{I}} - 0.3I \right) \tag{2.1}$$

where A is 0.51, Z is the ionic charge, I is the ionic strength ($I = \frac{1}{2} \sum C_i Z_i^2$), and C_i is the concentration of ionic species i.

2.3.2 Experimental procedures

UV/PS and UV/H_2O_2 experiments were conducted in a UV reactor with a low-pressure (LP) UV lamp (6 W LPUV lamp, 4P-SE, Philips) in a quartz sleeve placed in the center of the system. The reactor is illustrated in **Figure 3.1 in Chapter 3**. The UV intensity (P_{UV}) and the effective path length (L) were determined to be 1.97×10^{-6} Einstein s^{-1} L^{-1} and 6.3 cm, respectively, using atrazine and hydrogen peroxide as actinometers.[59] The detailed procedures of determining I_0 and L are provided in **Chapter 3.3.2** At each designed sampling time, 5 mL of sample was quenched by excess $Na_2S_2O_3$ and analyzed immediately. The detailed procedures of detecting oxidants (PS and H_2O_2) concentration are provided in **Text A.7 in Appendix A**.[96] The sources of the chemicals and reagents are provided in **Text A.8 in Appendix A**. The analytical details are provided in **Text A.9 in Appendix A**.

2.4 Results and Discussion

Here we discuss the impact of Cl^- on the UV/PS process for two cases: ***(1)*** target organic compounds react only with $SO_4^{\cdot-}$ and ***(2)*** target organic compounds can react with $SO_4^{\cdot-}$, HO· and Cl·. Then we discuss the effects of Cl^- on the UV/H_2O_2 process.

2.4.1 UV/PS process case 1: organic compounds react only with $SO_4^{\cdot-}$.

When Cl^- is present, the quenching ratio Q_1 can be used to quantify the scavenging effect of Cl^- on $SO_4^{\cdot-}$. Q_1 is defined in eq 2.2 as the rate of $SO_4^{\cdot-}$ oxidizing organic compound divided by the rate of $SO_4^{\cdot-}$ reacting with all components in the water matrix (**Figure A.1(b)** and **Text A.3.2 in Appendix A**). In other words, Q_1 equals the fraction of $SO_4^{\cdot-}$ reacting with organic compounds when Cl^- is present, and therefore, the value of Q_1 is between 0%

and 100%. When Q_1 is larger, more $SO_4^{-}\cdot$ can react with organic compounds, and therefore, Cl^- has less of a scavenging effect on $SO_4^{-}\cdot$, and vice versa.

$$Q_1 = \frac{k_{SO_4^{-}\cdot/R}[R]_0}{k_{SO_4^{-}\cdot/R}[R]_0 + k_2[Cl^-]_0 + k_3[PS]_0} \tag{2.2}$$

where k_2, k_3 and $k_{SO_4^{-}\cdot/R}$ are the second-order rate constants for the reactions of (i) Cl^- and $SO_4^{-}\cdot$, (ii) PS and $SO_4^{-}\cdot$, and (iii) R and $SO_4^{-}\cdot$, respectively. k_2 and k_3 have known values (**Table A.1 in Appendix A**), and the value of $k_{SO_4^{-}\cdot/R}$ depends on the target organic compound. Three lines are drawn in **Figure 2.2** representing a quenching ratio Q_1 of 0.1, 0.5, and 0.9 to illustrate the impact of Cl^-. These three lines are ***(1)*** for a quenching ratio of Q_1 = 0.1, (a line for 10% quenching was obtained by substituting $k_2 = 4.7\times10^8\ M^{-1}\cdot s^{-1}$, $k_3 = 0.095\ M^{-1}\cdot s^{-1}$ and $[PS]_0$ = 0.01 M into eq 2.2 to obtain the yellow dashed line, $k_{SO_4^{-}\cdot/R} = 5.2\times10^7 \frac{[Cl^-]}{[R]} + 1.05$); ***(2)*** for a quenching ratio of Q_1 = 0.5, (a line for 50% quenching was obtained with of k_2, k_3 and $[PS]_0$ and is shown as the blue dashed line, $k_{SO_4^{-}\cdot/R} = 4.7\times10^8 \frac{[Cl^-]}{[R]} + 9.5$); and ***(3)*** similarly, for a quenching ratio of Q_1 = 0.9, a line for 90% quenching was obtained (the green dashed line, $k_{SO_4^{-}\cdot/R} = 4.23\times10^9 \frac{[Cl^-]}{[R]} + 85.5$). The $k_{SO_4^{-}\cdot/R}$ of 6 organic compounds that only react with $SO_4^{-}\cdot$ were plotted by different symbols in **Figure 2.2**. $k_{SO_4^{-}\cdot/R}$ typically ranges from $10^5\ M^{-1}\cdot s^{-1}$ to $10^8\ M^{-1}\cdot s^{-1}$ (**Table A.3 in Appendix A**) [20] and $[Cl^-]/[R]$ ranges from 10 to 1000. Therefore, these organic compounds are all located well below the 10% quenching ratio line, which indicates that far less than 10% of $SO_4^{-}\cdot$ can react with these organic compounds. The values of Q_1 for these 6 organic compounds under different Cl^- concentrations are summarized in **Table 2.1**. The maximum value of Q_1 is 0.0194 when $k_{SO_4^{-}\cdot/R} = 9.31\times10^7\ M^{-1}\cdot s^{-1}$ and $[Cl^-]/[R]$ =

10. Accordingly, $SO_4^-\cdot$ reacts much faster with Cl^- than with the organic compound (a maximum of only 1.94% $SO_4^-\cdot$ reacts with the organic compound when Cl^- is present.) In contrast, 99.999% $SO_4^-\cdot$ reacts with the organic compound when Cl^- is not present (**Text A.3.1 in Appendix A**). Therefore, in the presence of Cl^-, the UV/PS process will not be able to destroy organic compounds that react only with $SO_4^-\cdot$. As $[Cl^-]/[R]$ increases, the fraction of $SO_4^-\cdot$ reacting with a certain organic compound (Q_1) significantly decreases, as shown in **Table 2.1**. Consequently, a higher Cl^- concentration causes a greater inhibitory effect. In addition, an experimental study indicated that PFOA will not be destroyed by $SO_4^-\cdot$ until all Cl^- are converted into ClO_3^-.[20] This can be attributed to the fact that $SO_4^-\cdot$ reacts with Cl^- much faster than with PFOA. Hence, $SO_4^-\cdot$ will react with Cl^- to produce $Cl\cdot$ rather than reacting with PFOA. $Cl\cdot$ will then mostly react with PS to form $ClO_2\cdot$, and $ClO_2\cdot$ will react with $SO_4^-\cdot$ to generate ClO_3^-. Only after the above-mentioned reactions have occurred will $SO_4^-\cdot$ react with PFOA.

Table 2.1. Fraction of $SO_4^-\cdot$ reacting with organics in the presence of different Cl^- concentration

Organic Compound	$k_{SO_4^-\cdot/R}$ ($M^{-1}s^{-1}$)	Fraction of $SO_4^-\cdot$ reacting with the organic compound			
		Cl^- is not present	Cl^- is present		
			$[Cl^-]/[R]$ = 10	$[Cl^-]/[R]$ = 100	$[Cl^-]/[R]$ = 1000
PFOA	2.59×10^5	99.999%	0.00551%	0.000551%	0.0000551%
PFHpA	2.68×10^5	99.999%	0.00570%	0.000570%	0.0000570%
PFHeA	7.02×10^5	99.999%	0.0149%	0.00149%	0.000149%
PFPeA	1.26×10^6	99.999%	0.0268%	0.00268%	0.000268%
PFPBA	1.05×10^7	99.999%	0.223%	0.0223%	0.000223%
PFPrA	9.31×10^7	99.999%	1.942%	0.197%	0.0198%

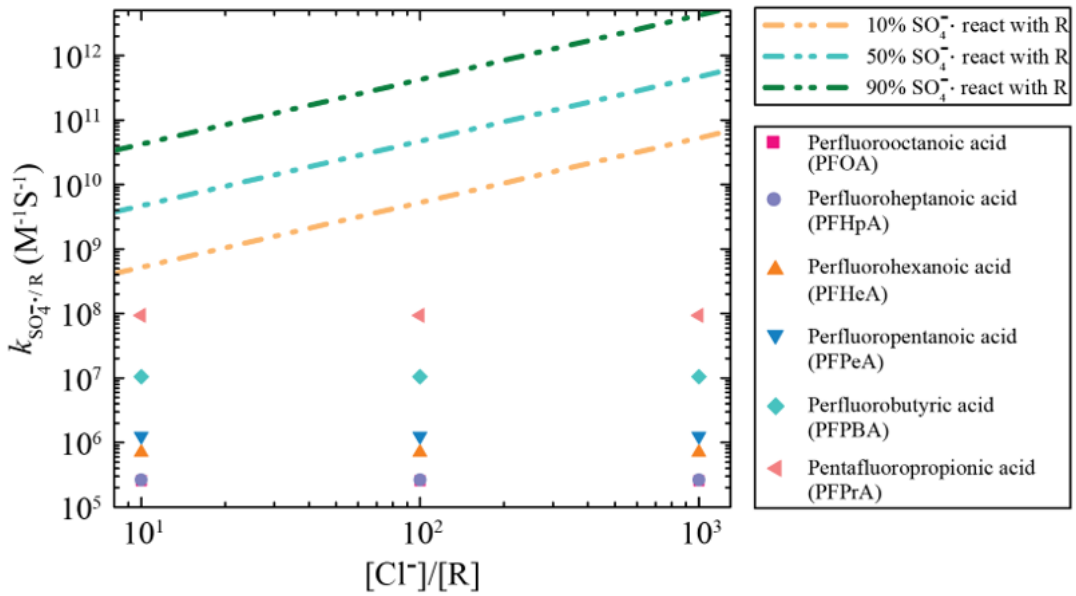

Figure 2.2. The fraction of $SO_4^{\cdot-}$ reacting with organic compounds (Q_1). This figure plots $k_{SO_4^{\cdot-}/R}$ vs. [Cl^-]/[R], where $k_{SO_4^{\cdot-}/R}$ is the second-order rate constant needed to achieve the desired quenching. The yellow dashed line represents criteria 1 (Q_1 = 0.1), the blue dashed line represents criteria 2 (Q_1 = 0.5), and the green dashed line represents criteria 3 (Q_1 = 0.9). The $k_{SO_4^{\cdot-}/R}$ values of six organics that only react with $SO_4^{\cdot-}$ are plotted by different symbols.

When NOM is present (**Table A.1(c) in Appendix A**), the quenching ratio Q_{S3} quantifies the scavenging effect of NOM on $SO_4^{\cdot-}$ (**Text A.3.3 in Appendix A**). As **Table A.4 in Appendix A** shows, the fraction of $SO_4^{\cdot-}$ reacting with a certain organic compound significantly decreases when NOM is present. At most 8.68% $SO_4^{\cdot-}$ reacts with the organic compounds (**Text A.3.3**) when $k_{SO_4^{\cdot-}/R}$ = 9.31×10^7 $M^{-1}\cdot s^{-1}$ and [Cl^-]/[R] = 10. Thus, NOM inhibits the organic oxidation rate, which can be attributed to the following phenomena: ***(1)*** NOM will absorb UV light and reduce the $SO_4^{\cdot-}$ production rate via PS photolysis [10,37] and ***(2)*** NOM scavenges $SO_4^{\cdot-}$.[89] The complete mechanism of NOM activating PS to produce $SO_4^{\cdot-}$ is not fully understood at this time.[20] However, the amount of $SO_4^{\cdot-}$ activated by NOM in the UV/PS process will be small compared to that in photolysis. Hence, this effect was not considered in this study. When Cl^- and NOM are present (**Figure**

A.1(c)), the quenching ratio Q_{S4} quantifies the scavenging effect of NOM and Cl^- on $SO_4^-\cdot$ (**Text A.3.4**). As **Table A.4** shows, the fraction of $SO_4^-\cdot$ reacting with a certain organic compound (Q_{S4}) significantly decreases when NOM and Cl^- are both present. **Table A.4** also indicates that as $[Cl^-]/[R]$ increases, the fraction of $SO_4^-\cdot$ reacting with the target organic compound significantly decreases. At most 0.936% $SO_4^-\cdot$ reacts with the organic compounds when $k_{SO_4^-\cdot/R} = 9.31\times10^7\ M^{-1}\cdot s^{-1}$ and $[Cl^-]/[R] = 10$. Consequently, Cl^- and NOM will significantly inhibit the destruction of organic compounds that react only with $SO_4^-\cdot$ in the UV/PS process. In addition, **Table 2.1** and **Table A.4** show that, for a certain target compound and with the same Cl^- and NOM concentration, greater inhibition occurs in the presence of both Cl^- and NOM than either Cl^- or NOM alone. Hence, Cl^- and NOM have a synergistic inhibitory effect.

When HCO_3^-/CO_3^{2-} are present (**Figure A.1(d) in Appendix A**), the quenching ratio Q_{S5} quantifies the scavenging effect of HCO_3^-/CO_3^{2-} on $SO_4^-\cdot$ (**Text A.3.5 in Appendix A**). As **Table A.5 in Appendix A** shows, the fraction of $SO_4^-\cdot$ reacting with organic compounds (Q_{S5}) significantly decreases when HCO_3^-/CO_3^{2-} is present. Thus, HCO_3^-/CO_3^{2-} significantly inhibits other organics. When Cl^- and HCO_3^- / CO_3^{2-} are present (**Figure A.1(d) in Appendix A**), the quenching ratio Q_{S6} quantifies the scavenging effect of HCO_3^-/CO_3^{2-} on $SO_4^-\cdot$ (**Text A.3.6 in Appendix A**). As **Table A.5 in Appendix A** shows, the fraction of $SO_4^-\cdot$ reacting with a certain organic compound significantly decreases when Cl^- and HCO_3^-/CO_3^{2-} are both present. **Table A.5 in Appendix A** also indicates that as $[Cl^-]/[R]$ increases, the fraction of $SO_4^-\cdot$ reacting with organic compounds decreases (**Text A.3.6 in Appendix A**). Consequently, Cl^- and HCO_3^-/CO_3^{2-} will significantly inhibit the destruction of organic compounds that react only with $SO_4^-\cdot$ in the UV/PS process. Furthermore, **Table**

2.1 and **Table A.5 in Appendix A** show that, for a certain target compound and with the same Cl^- and HCO_3^-/CO_3^{2-} concentration, greater inhibition occurs in the presence of both Cl^- and HCO_3^-/CO_3^{2-} than either Cl^- or HCO_3^-/CO_3^{2-} alone. Hence, Cl^- and HCO_3^-/CO_3^{2-} have a synergistic inhibitory effect. In addition, carbonate system depends on pH. As the total carbonate concentration remain constants, $[HCO_3^-]$ decreases and $[CO_3^{2-}]$ increases if pH increases. Since CO_3^{2-} has higher rate constant with $SO_4^-\cdot$ than HCO_3^-, greater inhibition will occur with higher pH.

2.4.2 UV/PS process case 2: organic compounds that can react with $SO_4^-\cdot$, $HO\cdot$ and $Cl\cdot$

This section discusses situations including (i) when Cl^- is present and the organic compounds can be destroyed by $SO_4^-\cdot$, $HO\cdot$ and $Cl\cdot$ and (ii) when Cl^- is not present and organic compounds can be destroyed by $SO_4^-\cdot$ and $HO\cdot$. We report the rate constants for 22 organic compounds reacting with $SO_4^-\cdot$, $HO\cdot$ and $Cl\cdot$ in **Table A.3 in Appendix A**. First, we compared the rate of organic compound destruction by $SO_4^-\cdot$ when Cl^- is present to the rate when Cl^- is not present. As indicated in **Table A.6 in Appendix A**, the fraction of $SO_4^-\cdot$ reacting with a certain organic compound decreases significantly in the presence of Cl^-. The reason is that $SO_4^-\cdot$ reacts with Cl^- much faster than the organic compound to produce $Cl\cdot$. The fraction of $SO_4^-\cdot$ reacting with a certain organic compound also decreases significantly as $[Cl^-]/[R]$ increases (**Table A.6 in Appendix A**).

Second, we compared the rate of organic compound destruction by $HO\cdot$ when Cl^- is present to the rate when Cl^- is not present. The fraction of $HO\cdot$ reacting with a certain organic compound significantly decreases in the presence of Cl^- (**Table A.7 in Appendix A**). This can be attributed to the following facts: ***(1)*** $SO_4^-\cdot$ reacts with Cl^- much faster than H_2O and this decreases $HO\cdot$ generation and ***(2)*** $Cl\cdot$ reacts with H_2O to increase $HO\cdot$

generation. With the consideration of these two factors together, we found that HO· generation is suppressed in the presence of Cl^- (**Text A.4.2 in Appendix A**). Decreased HO· generation was also reported in another experimental study.[20] Furthermore, the fraction of HO· reacting with a certain organic compound also decreases more significantly as $[Cl^-]/[R]$ increases **(Table A.7 in Appendix A)**.

Third, we compared the rate of organic compound destruction by Cl· when Cl^- is present to the rate when Cl^- is not present. The quenching ratio Q_2 in eq 2.3 can be used to quantify the Cl^- scavenging effect on Cl·. Q_2 is defined as the rate of Cl· oxidizing organic compound divided by the rate of Cl· reacting with all components in the water matrix (**Text A.4.2 in Appendix A**). In other words, Q_2 is the fraction of Cl· reacting with the organic compound.

$$Q_2 = \frac{k_{Cl\cdot/R}[R]_0}{k_{Cl\cdot/R}[R]_0 + k_6[PS]_0 + k_7[H_2O] + \left(k_5 - \frac{k_5 k_9}{k_9 + k_{10}[PS]_0}\right)[Cl^-]_0} \tag{2.3}$$

where k_5, k_6,k_7,k_{10} and $k_{Cl\cdot/R}$ are the second-order rate constants for reactions of (i) Cl^- and Cl·, (ii) PS and Cl·, (iii) H_2O and Cl·, (iv) PS and Cl_2^-·, and (v) R and Cl·, respectively. k_9 is the first-order rate constant for Cl_2^-· generating Cl·. k_5, k_6, k_7, k_9, and k_{10} have known values (**Table A.1 in Appendix A**), and $k_{Cl\cdot/R}$ depends on the structure of the organic compound and typically ranges from 10^5 $M^{-1}\cdot s^{-1}$ to 1.5×10^{10} $M^{-1}\cdot s^{-1}$ (**Table A.3 in Appendix A**). Similar to **Figure 2.2**, three lines are drawn in **Figure 2.3** for quenching ratios of 0.1 (yellow dashed line), 0.5 (blue dashed line) and 0.9 (green dashed line) to illustrate the gradual decline in the Cl^- scavenging effect on Cl· (**Text A.4.2 in Appendix A**). In **Figure 2.3**, 22 organic compounds were clustered in three distinct groups, marked by pink, purple, and black, depending on the value of $k_{Cl\cdot/R}$. The values of Q_2 for the 22

organic compounds are summarized in **Table A.8 in Appendix A**. According to **Figure 2.3** and **Table A.8 in Appendix A**, organic compounds with a $k_{Cl\cdot/R}$ value less than 3×10^{9} $M^{-1}\cdot s^{-1}$ (marked in pink and purple) all lie below the 0.1 quenching ratio line. Therefore, far less than 10% Cl· reacts with these organic compounds, as indicated in **Table A.8 in Appendix A**. Consequently, the reaction between Cl· and the organic compound is negligible when $k_{Cl\cdot/R}$ is less than 3×10^{9} $M^{-1}\cdot s^{-1}$. Meanwhile, the discussion is more complicated for organic compounds with a $k_{Cl\cdot/R}$ value larger than 3×10^{9} $M^{-1}\cdot s^{-1}$ (marked in black): ***(1)*** when $[Cl^-]/[R]$ is as high as 1000, the compounds all lie below the 10% quenching line, which indicates that the reaction between Cl· and the organic compound is negligible, and ***(2)*** when $[Cl^-]/[R]$ is 100 or 10, the compounds all lie above the 10% quenching ratio line, which indicates that more than 10% Cl· reacts with these organic compounds, and **Table A.8 in Appendix A** shows that at most 33.42% Cl· reacts with these organic compounds when $k_{Cl\cdot/R} = 1.2\times10^{10}$ $M^{-1}\cdot s^{-1}$ and $[Cl^-]/[R] = 10$. Consequently, the reaction of Cl· with the organic compound ($k_{Cl\cdot/R}$ larger than 3×10^{9} $M^{-1}\cdot s^{-1}$) becomes important when $[Cl^-]/[R]$ is below 100.

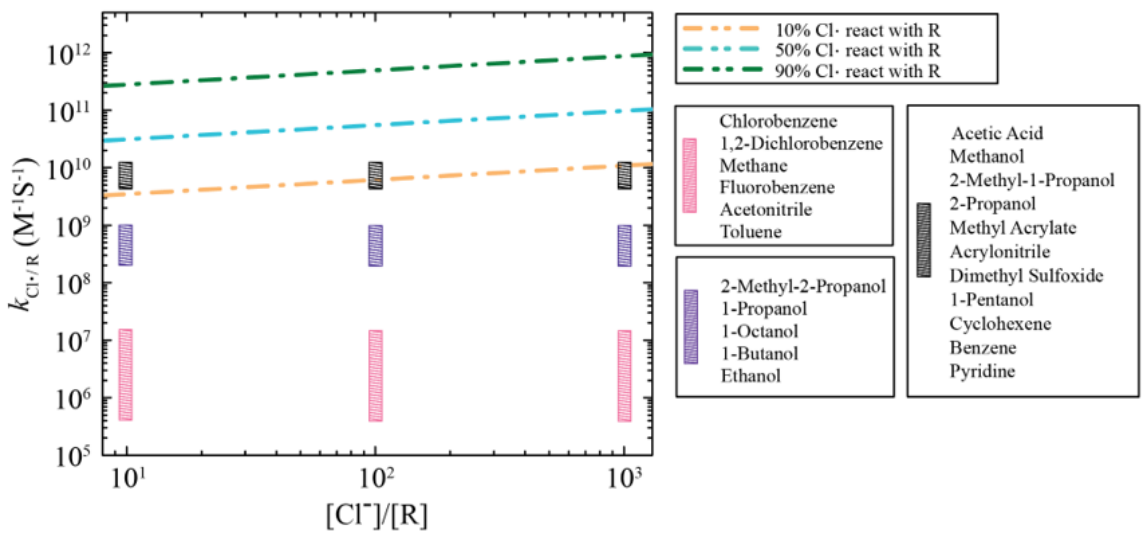

Figure 2.3. The fraction of Cl· reacting with organic compounds (Q_2). This figure plots $k_{Cl\cdot/R}$ vs. [Cl⁻]/[R]. The yellow dashed line represents criteria 1 (Q_2 = 0.1), the blue dashed line represents criteria 2 (Q_2 = 0.5), and the green dashed line represents criteria 3 (Q_2 = 0.9). The $k_{Cl\cdot/R}$ values of 22 organic compounds that react with $SO_4^{-}\cdot$, HO·, and Cl· are clustered in three groups (pink, purple, and black).

Finally, the impact of Cl^- on the UV/PS process for organic compounds that can react with $SO_4^{-}\cdot$, HO· and Cl· is difficult to determine because of the following contradictory facts: (i) the organic destruction rate by $SO_4^{-}\cdot$ and HO· significantly decreases for all organic compounds when Cl^- is present, but (ii) $SO_4^{-}\cdot$ mainly reacts with Cl^- to produce Cl·, and the reaction of Cl· with organic compounds ($k_{Cl\cdot/R}$ larger than 3×10^9 $M^{-1}\cdot s^{-1}$) is important. This increases the organic destruction rate when chloride is present. Hence, these two competing factors must be combined to investigate the overall result. We compared the organic compound destruction rate induced by $SO_4^{-}\cdot$, HO· and Cl· when Cl^- is present ($r_R^{Cl^-}$) to the rate induced by $SO_4^{-}\cdot$ and HO· when Cl^- is not present (r_R). If the maximum value of the ratio between $r_R^{Cl^-}$ and r_R ($r_R^{Cl^-}/r_R$) is less than 1, then Cl^- must inhibit the UV/PS process. $r_R^{Cl^-}/r_R$ in eq A.102 is a function of 4 variables: (i) $k_{Cl\cdot/R}$, (ii) $k_{HO\cdot/R}$, (iii) $k_{SO_4^{-}\cdot/R}$, and (iv) [Cl^-]. $r_R^{Cl^-}/r_R$ is a monotonically increasing function of $k_{Cl\cdot/R}$ and a monotonically decreasing function of [Cl^-]. $k_{Cl\cdot/R}$ typically ranges from 1×10^5 $M^{-1}\cdot s^{-1}$

to 1.5×10^{10} $M^{-1}\cdot s^{-1}$ and $[Cl^-]$ ranges from 0.001 M to 0.1 M, the maximum value of $r_R^{Cl^-}/r_R$ can be reached when $k_{Cl\cdot/R} = 1.5\times10^{10}$ $M^{-1}\cdot s^{-1}$ and $[Cl^-] = 0.001$ M. **Figure 2.4** is the heat map showing the values of $r_R^{Cl^-}/r_R$ with all possible combinations of $k_{HO\cdot/R}$ and $k_{SO_4^-\cdot/R}$ when $k_{Cl\cdot/R} = 1.5\times10^{10}$ $M^{-1}\cdot s^{-1}$ and $[Cl^-] = 0.001$ M. **Figure 2.4** clearly indicates that the maximum value of $r_R^{Cl^-}/r_R$ is 0.6. Therefore, Cl^- inhibits the organic compound destruction rate induced by $SO_4^-\cdot$, HO· and Cl· in the UV/PS process. The values of $r_R^{Cl^-}/r_R$ for these 22 organic compounds are summarized in **Table A.9 in Appendix A**. As $[Cl^-]/[R]$ increases, for a certain organic compound, the destruction rate induced by $SO_4^-\cdot$ and HO· will decrease because a smaller fraction of $SO_4^-\cdot$, HO· and Cl· can react with the organic compound (**Table A.6 - Table A.8 in Appendix A**). Consequently, the organic destruction rate further decreases as $[Cl^-]/[R]$ increases.

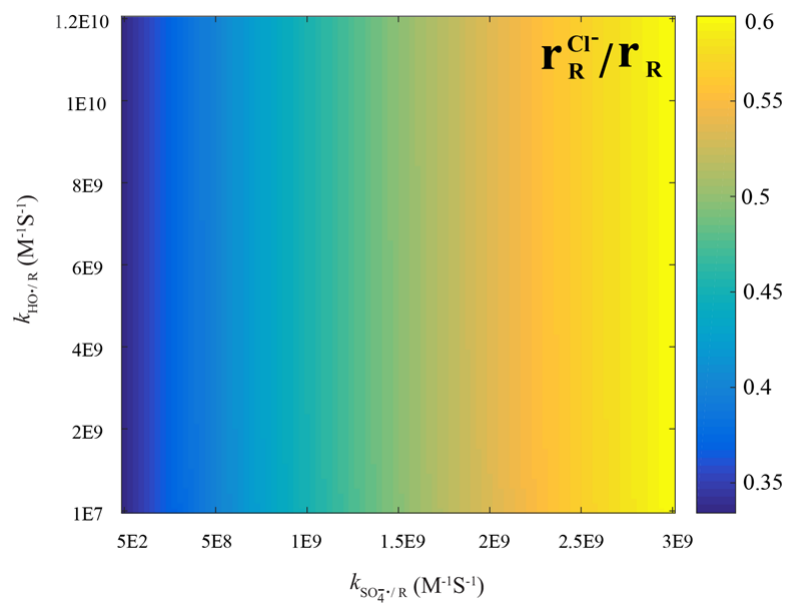

Figure 2.4. The ratio between the organic destruction rate by $SO_4^-\cdot$, HO· and Cl· when Cl^- is present ($r_R^{Cl^-}$) to the organic destruction rate by $SO_4^-\cdot$, HO· when Cl^- is not present (r_R) when $k_{Cl\cdot/R} = 1.5\times10^{10}$ $M^{-1}\cdot s^{-1}$ and $[Cl^-] = 0.001$ M. If the ratio is less than 1, Cl^- inhibits the UV/PS process where the target organic compound can react with $SO_4^-\cdot$, HO· and Cl·.

When NOM is present (**Figure 2.1(c)**), the fraction of $SO_4^{\cdot-}$ and HO· reacting with an organic compound significantly decreases, as summarized in **Table A.10** and **Table A.11 in Appendix A**, respectively. The organic destruction rate by $SO_4^{\cdot-}$ and HO· reaches a maximum, 46.04%, when NOM is present compared to the rate when NOM is not present (**Text A4.3 in Appendix A**). Hence, NOM has an inhibitory effect. When Cl^- and NOM are present (**Figure 2.1(c)**), the fraction of $SO_4^{\cdot-}$ and HO· reacting with the organic compound significantly decreases, as summarized in **Table A.10** and **Table A.11 in Appendix A**, respectively. In addition, the quenching ratio Q_{S16} quantifies the Cl^- scavenging effect on Cl·. At most only 17.52% Cl· can react with the organic compound (**Table A.12** and **Text A.4.4 in Appendix A**). Overall, the organic destruction rate is at most 29.60% of the rate when Cl^- and NOM are not present when $k_{SO_4^{\cdot-}/R} = 3\times10^9\ M^{-1}\cdot s^{-1}$, $k_{HO\cdot/R} = 1.2\times10^{10}\ M^{-1}\cdot s^{-1}$, $k_{Cl\cdot/R} = 1.5\times10^{10}\ M^{-1}\cdot s^{-1}$, and $[Cl^-]/[R] = 10$. Therefore, Cl^- and NOM significantly inhibit the UV/PS process from destroying organics that react with $SO_4^{\cdot-}$, HO·, and Cl·. As $[Cl^-]/[R]$ increases, the Cl^- inhibition effect is enhanced (**Table A.13 in Appendix A**). Moreover, by comparing the same organic compound and the same Cl^- and NOM concentration in **Table A.9** and **Table A.13 in Appendix A**, we can conclude that greater inhibition occurs in the presence of both Cl^- and NOM than either Cl^- or NOM alone. Hence, Cl^- and NOM have a synergistic inhibitory effect.

When HCO_3^-/CO_3^{2-} is present (**Figure 2.1(d)**), the fraction of $SO_4^{\cdot-}$ and HO· reacting with an organic compound decreases slightly for a few reactive organic compounds and decreases significantly for other organic compounds, as summarized in **Table A.14** and **Table A.15 in Appendix A**, respectively. The organic destruction rate by $SO_4^{\cdot-}$ and HO· is at most 96.64% of the rate when HCO_3^-/CO_3^{2-} is not present (**Text A.4.5 in Appendix A**).

Thus, HCO_3^-/CO_3^{2-} slightly inhibits the destruction of a few of the most reactive organic compounds (e.g., benzene, toluene) but significantly inhibits the destruction rate of other organic compounds [97,98]. When Cl^- and HCO_3^-/CO_3^{2-} are present (**Figure 2.1(d)**), the fraction of $SO_4^-\cdot$ and HO· reacting with organic compound significantly decreases, as summarized in **Table A.14** and **Table A.15 in Appendix A**, respectively. In addition, the quenching ratio Q_{A21} quantifies the Cl^- scavenging effect on Cl ·. The values of Q_{A21} for 22 organic compounds are summarized in **Table A.16 in Appendix A**. At most only 12.88% Cl · will react with organic compounds (**Table A.16** and **Text A.4.6 in Appendix A**). Overall, the organic destruction rate is at most 42.13% of the rate when Cl^- or HCO_3^-/CO_3^{2-} is not present when $k_{SO_4^-\cdot/R} = 3\times10^9\ M^{-1}\cdot s^{-1}$, $k_{HO\cdot/R} = 1.2\times10^{10}\ M^{-1}\cdot s^{-1}$ and $k_{Cl\cdot/R} = 1.5\times10^{10}\ M^{-1}\cdot s^{-1}$. Consequently, Cl^- and HCO_3^-/CO_3^{2-} will significantly inhibit the destruction of organics that react with $SO_4^-\cdot$, HO·, and Cl· in the UV/PS process. As $[Cl^-]/[R]$increases, the Cl^- inhibition effect is enhanced (**Table A.17 in Appendix A**). Furthermore, comparing **Table A.9** and **Table A.17 in Appendix A**, for the same organic compound and the same Cl^- concentration, greater inhibition occurs in the presence of both Cl^- and HCO_3^-/CO_3^{2-} than either Cl^- or HCO_3^-/CO_3^{2-} alone. Thus, Cl^- and HCO_3^-/CO_3^{2-} have a synergistic inhibitory effect. In addition, as we discussed above, $[HCO_3^-]$ decreases and $[CO_3^{2-}]$ increases if pH increases. Since CO_3^{2-} has higher rate constant with $SO_4^-\cdot$, HO· and Cl· than HCO_3^-, greater inhibition will occur with higher pH.

2.4.3 UV/H_2O_2 process: organic compounds that can react with HO· and Cl·

HO· is not scavenged by Cl^- to generate $ClOH^-\cdot$ because $ClOH^-\cdot$ rapidly dissociates to form HO·.[19] To prove this, we compared the reaction rate of $ClOH^-\cdot$ producing HO· to the rates of all $ClOH^-\cdot$ reactions (shown as Ratio in eq 2.4):

$$\text{Ratio} = \frac{k_8[\text{ClOH}^-\cdot]_{ss,0}^{Cl^-}}{k_8[\text{ClOH}^-\cdot]_{ss,0}^{Cl^-} + k_{21}[Cl^-]_0[\text{ClOH}^-\cdot]_{ss,0}^{Cl^-} + k_{22}[H^+][\text{ClOH}^-\cdot]_{ss,0}^{Cl^-}} \tag{2.4}$$

where k_8 is the first-order rate constant for $ClOH^-\cdot$ generating HO· and k_{21} and k_{22} are the second-order rate constants for reactions of (i) Cl^- and $ClOH^-\cdot$ (produces $Cl_2^-\cdot$) and (ii) H^+ and $ClOH^-\cdot$ (produces Cl·), respectively. k_8, k_{21} and k_{22} have known values (**Table A.2 in Appendix A**). The value of Ratio is approximately 0.999. Thus, the dominant reaction path for $ClOH^-\cdot$ is to produce HO·, while the production of Cl· from $ClOH^-\cdot$ is negligible. As a result, the organic destruction rate by Cl· is negligible compared to the destruction rate by HO·.

When Cl^- is present, the quenching ratio Q_3 can be used to quantify the Cl^- scavenging effect on HO· (**Text A.5.2 in Appendix A**). Q_3 is defined in eq 2.5 as the organic destruction rate of HO· divided by the rate of HO· reacting with all components in the water matrix. In other words, Q_3 is the fraction of HO· reacting with organic compounds.

$$Q_3 = \frac{k_{HO\cdot/R}[R]_0}{k_{HO\cdot/R}[R]_0 + k_{19}[H_2O_2]_0 + \frac{k_{21}[Cl^-]_0 + k_{22}[H^+]}{k_8 + k_{21}[Cl^-]_0 + k_{22}[H^+]} k_{20}[Cl^-]_0} \tag{2.5}$$

where k_{19}, k_{20} and $k_{HO\cdot/R}$ are the second-order rate constants for reactions of (i) H_2O_2 and HO·, (ii) Cl^- and HO·, and (iii) R and HO·, respectively. k_8, k_{19}, k_{20}, k_{21}, and k_{22} have known values (**Table A.2 in Appendix A**). The value of $k_{HO\cdot/R}$ depends on the structure of the organic compound and typically ranges from 10^7 $M^{-1}\cdot s^{-1}$ to 1.2×10^{10} $M^{-1}\cdot s^{-1}$.[85] The pH is 6, $[H_2O_2]$ is 0.01 M, [R] is 0.001 M, and $[Cl^-]$ ranges from 0.001 M to 0.1 M for the denominator of in eq 2.6:

$$\frac{k_{21}[Cl^-] + k_{22}[H^+]}{k_8 + k_{21}[Cl^-] + k_{22}[H^+]} k_{20}[Cl^-]_0 \ll k_{HO\cdot/R}[R]_0 + k_{19}[H_2O_2]_0 \tag{2.6}$$

As a result, Q_3 becomes eq 2.7:

$$Q_3 \approx \frac{k_{HO\cdot/R}[R]}{k_{HO\cdot/R}[R]+k_{19}[H_2O_2]} \tag{2.7}$$

Eq 2.7 is the same as eq A.53. Eq 2.7 is the fraction of HO· reacting with the organic compound (Q_3) when Cl^- is present, and eq A.53 is the fraction of HO· reacting with the organic compound (Q_{A23}) when Cl^- is not present. Therefore, Cl^- has a negligible impact on the oxidation of organic compounds in the UV/H_2O_2 process. We report the rate constants for 22 organics reacting with HO· and Cl· in **Table A.3 in Appendix A**. The values of Q_3 for the 22 organic compounds exposed to different Cl^- concentrations are summarized in **Table A.18 in Appendix A**. **Table A.18 in Appendix A** also indicates that regardless of whether Cl^- is present (from 0.001 M to 0.1 M), the fraction of HO· reacting with a certain organic compound (Q_3) is almost the same. Even when Cl^- is as high as 0.7 M (seawater),[99] it still only has a slight effect on the UV/H_2O_2 process.[100]

When NOM is present (**Figure A.2(c) in Appendix A**), the quenching ratio Q_{S25} is used to quantify the Cl^- scavenging effect on HO· (**Text A.5.3 in Appendix A**). As **Table A.19 in Appendix A** indicates, the fraction of HO· reacting with a certain organic compound significantly decreases in the presence of NOM. At most, 40.16% HO· reacts with an organic compound when $k_{HO\cdot/R} = 1.2\times10^{10}\ M^{-1}\cdot s^{-1}$ (very large). When NOM is not present, at most 81.63% HO· reacts with an organic compound when $k_{HO\cdot/R} = 1.2\times10^{10}\ M^{-1}\cdot s^{-1}$. Consequently, NOM limits the effectiveness of the UV/H_2O_2 process. When HCO_3^-/CO_3^{2-} is present (**Figure A.2(d) in Appendix A**), the quenching ratio Q_{S26} is used to quantify the HCO_3^-/CO_3^{2-} scavenging effect on HO· (**Text A.5.4 in Appendix A**). As **Table A.19 in Appendix A** indicates, the fraction of HO· reacting with a certain organic compound (Q_{S26})

slightly decreases in the presence of HCO_3^-/CO_3^{2-}. Consequently, HCO_3^-/CO_3^{2-} slightly limits the effectiveness of the UV/H_2O_2 process because of the low concentration of HCO_3^-/CO_3^{2-} in the water matrix.[97,98] In addition, [HCO_3^-] decreases and [CO_3^{2-}] increases if pH increases. Since CO_3^{2-} has higher rate constant with HO· and Cl· than HCO_3^-, greater inhibition will occur with higher pH.

2.5 Model Validation

It is necessary to emphasize that all elementary reactions and kinetic equations, which used to develop our mathematical model, have been validated in HO· based AOPs and SO_4^-· based AOPs kinetic models under different water matrices (ultra-water, surface water and wastewater with Cl^-, NOM and HCO_3^-/CO_3^{2-}) , for example, (i) 1,2-dibromo-3-chloropropane,[15] acetone,[64] TCE [64,92] and polyethylene glycol,[63] triethylene glycol,[63] diethylene glycol [63] degradation in UV/H_2O_2; (ii) PFOA degradation in UV/PS,[20] Congo red and Rhodamine B degradation in CoFeNi/Peroxymonosulfate,[66] microcystin-LR in ascorbic acid/PMS.[67] These validated elementary reactions and kinetic equations are prerequisites to guarantee the reliability of our Cl^- impact mathematical model. To validate our mathematical model again, we conducted the experiment for benzoic acid (BA) oxidization by the UV/PS process in the presence of different Cl^- concentrations. BA was chosen for model validation because it has reported rate constants with SO_4^-·, HO· and Cl· ($k_{SO_4^-\cdot/BA} = 1.2\times10^9\ M^{-1}\cdot s^{-1}$ [18]; $k_{HO\cdot/R} = 4.3\times10^9\ M^{-1}\cdot s^{-1}$ [101]; $k_{Cl\cdot/R} = 1.2\times10^{10}\ M^{-1}\cdot s^{-1}$ [102]). The pseudo-first-order equation (eq 2.8) was employed to evaluate the BA degradation reaction kinetics.

$$C/C_0 = \exp(-k_{obs}\times t) \quad (2.8)$$

where C is the BA concentration at time t, C_0 is the initial BA concentration, and k_{obs} is the pseudo-first-order reaction constant. According to the semi-log plots in **Figure 2.5**, the pseudo-first-order rate constant is 0.0092 s^{-1} when Cl^- is not present, 0.0043 s^{-1} when Cl^- is 0.01 M, 0.0023 s^{-1} when Cl^- is 0.1 M. As a result, the experimental results indicated that the BA degradation rate decreased by 53.3% in the presence of 0.01 M Cl^- and by 75.0% in the presence of 0.1 M Cl^-. Under the same conditions, our mathematical model predicted that the BA degradation rate would decrease by 58.8% in the presence of 0.01 M Cl^- and by 71.2% in the presence of 0.1 M Cl^-. In addition, we conducted BA degradation in UV/H_2O_2 process. As our mathematical model prediction, the experimental results also indicated that Cl^- (ranges from 0 M to 0.1 M) has negligible impact on BA oxidation rate in UV/H_2O_2 (**Figure 2.6**). Consequently, the results of our mathematical model agree with the experimental results very well.

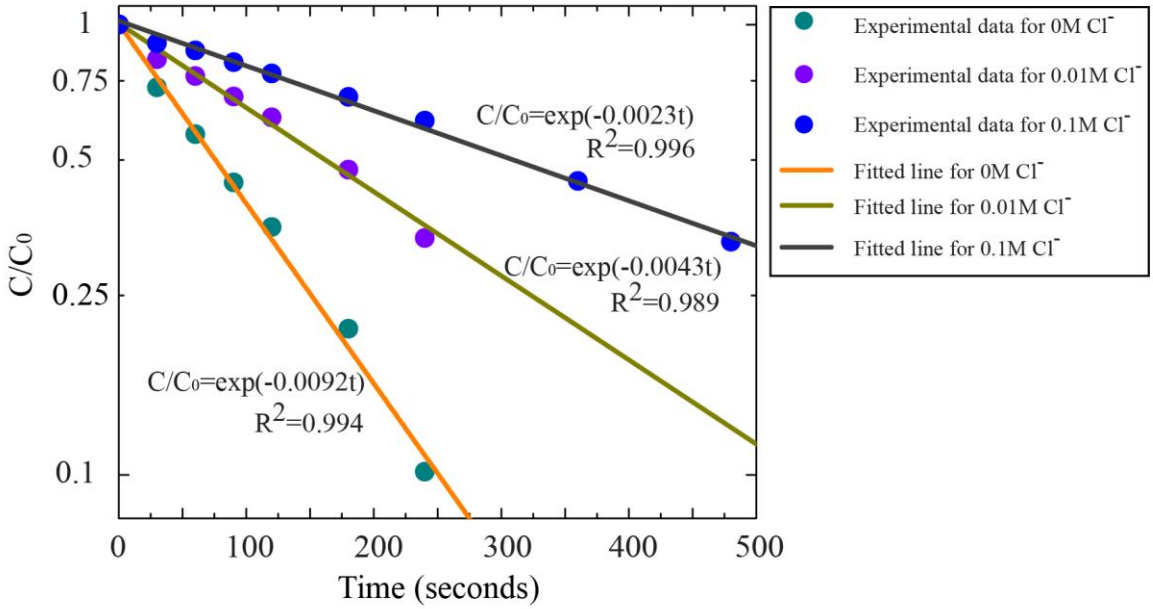

Figure 2.5. Pseudo-first-order semi-log plots for BA degradation by the UV/PS process. The dots show the experimental results, and the solid lines represent the fitted lines. Experimental Conditions: UV intensity = 1.97×10^{-6} Einstein/L·s, [BA] = 0.1 mM, PS dosage = 10 mM, [Cl^-] = 0 M to 0.1 M, and pH = 7.

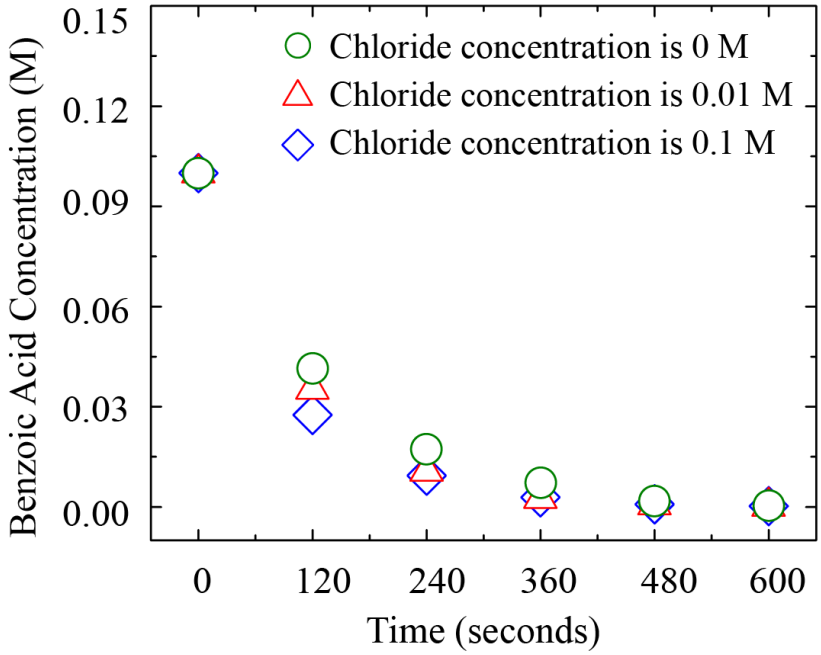

Figure 2.6. Model validation for benzoic acid degradation in UV/H_2O_2 process. Experimental Conditions: UV intensity = 1.97×10^{-6} Einstein/L·s, [H_2O_2] = 0.01 M, initial [BA]=0.1 M, [Cl^-]=0 M~0.1 M, pH=7.

Furthermore, many research groups have already independently and carefully evaluated Cl^- problem for certain organic compounds in UV/PS and UV/H_2O_2 processes with experimental methods. These experimental results were reviewed to validate our modeling approach. For a UV/PS process that destroys organic compounds that only react with $SO_4^{\cdot-}$, Cl^- inhibits PFOA degradation.[20] In the UV/PS reaction of organic compounds that react with $SO_4^{\cdot-}$, HO·, and Cl·, Cl^- has been reported to inhibit the degradation of biphenyl,[26] polychlorinated biphenyls,[26] azathioprine,[27] humic acid,[28] sulfamethoxazole,[31] propranolol,[31] carbamazepine,[31] acyclovir,[31] lamivudine,[31] chloramphenicol,[32] acetaminophen,[33] atrazine[103] and atenolol,[34] 1,4-dioxane,[104] diclofenac,[105] diethyl phthalate.[106] On the other hand, Cl^- has less of an inhibitory effect on 2,4,6-trichloroanisole,[25] mono-chlorophenols,[35] and trichloroethylene.[36] This is because they have very high second-order rate constants with Cl· (e.g., TCE is 4.88×10^{10} $M^{-1}\cdot s^{-1}$).[107]

In the UV/H_2O_2 process, Cl^- has a slight inhibitory effect for iodinated trihalomethanes,[83] monensin,[84] salinomycin,[84] narasin,[84] humic acid,[28] acetyl-sulfamethoxazole,[30] trimethoprim,[30] sulfamethoxazole,[31] propranolol,[31] carbamazepine,[31] atrazine,[31] lamivudine,[31] 4-nitrophenol,[108] phenol (seawater condition) [100] and atenolol.[34] These experimental observations are in general agreement with the conclusions reached in this study.

2.6 Model Implication

A mathematical model was developed based on validated elementary reactions and kinetic data with SPSS assumption to investigate Cl^- impact at the beginning stages of UV/PS and UV/H_2O_2 processes. The simulation conditions in this study are: [PS] or [H_2O_2] is 0.01 M, [R] is 0.0001 M, [Cl^-] ranges from 0.001 M to 0.1 M, [NOM] is 2 mg/L, [HCO_3^-] is 3 mM and [CO_3^{2-}] is 0.14 μM. The model indicates the inhibition effect of Cl^- on UV/PS. NOM or HCO_3^-/CO_3^{2-} inhibits the organic oxidization rate in UV/PS process. Greater inhibition occurs when NOM and Cl^- or HCO_3^-/CO_3^{2-} and Cl^- are present. Thus, NOM and Cl^- or HCO_3^-/CO_3^{2-} and Cl^- have synergistic inhibition effect. The model describes the slight impact of Cl^- on UV/H_2O_2 process. NOM or high concentrations of HCO_3^-/CO_3^{2-} inhibits organic compound oxidation rate in UV/H_2O_2. The presence of Cl^- does not inhibit the UV/H_2O_2 process more than NOM or HCO_3^-/CO_3^{2-}. Our model prediction results agree with experimental results very well.

We further developed a user-friendly algorithm based on the mathematical model to quantify the effects of Cl^- at the beginning stage of UV/PS and UV/H_2O_2 processes, as engineers are likely to encounter situations in real applications that were not discussed in this manuscript, for example, different pH, different NOM in different water matrix, etc.

Users can input their specific feasible conditions and kinetic parameters to obtain the ratio of the organic destruction rate when Cl^- is present to the rate when Cl^- is not present. In addition, the impact of the ionic strength on the reaction activity is considered in the mathematical model. It is worth noting that the results calculated from this algorithm is a boundary to quantify Cl^- impact at the beginning stage of UV/PS and UV/H_2O_2 processes. If the later generated intermediates have higher rate constants with radicals, then greater Cl^- inhibition will occur because less fraction of radicals reacting with the target organic compounds. This mathematical model is provided as an Excel sheet in https://pubs.acs.org/doi/abs/10.1021/acs.est.8b01662.

2.7 Acknowledgement

This work was supported by the Brook Byers Institute for Sustainable Systems, Hightower Chair and the Georgia Research Alliance at the Georgia Institute of Technology, NSF Award #0854416, and the China Scholarship Council. The views and ideas expressed herein are solely the authors and do not represent the ideas of the funding agencies in any form.

CHAPTER 3. OXIDATION MECHANISMS OF THE UV/FREE CHLORINE PROCESS: KINETIC MODELING AND QUANTITATIVE STRUCTURE ACTIVITY RELATIONSHIPS

†*work from this chapter has been published and presented in the following citation:*

Zhou, Shiqing., **Zhang, Weiqiu.**, Sun, Julong., Zhu, Shumin., Li, Ke., Meng, Xiaoyang., Luo, Jinming., Shi, Zhou., Zhou, Dandan. and Crittenden, John., 2019. Oxidation Mechanisms of the UV/Free Chlorine Process: Kinetic Modeling and Quantitative Structure Activity Relationships. *Environmental science & technology*, 53(8), pp.4335-4345. (**Zhang, Weiqiu and Shiqing Zhou are co-first authors**)

3.1 Abstract

Recently, the UV/free chlorine process has gained attention as a promising technology for destroying refractory organic contaminants in the aqueous phase. We have developed a kinetic model based on first principles to describe the kinetics and mechanisms of the oxidation of organic contaminants in the UV/free chlorine process. Substituted benzoic acid compounds (SBACs) were chosen as the target parent contaminants. We determined the second-order rate constants between SBACs and reactive chlorine species (RCS; including Cl•, Cl_2^-• and ClO•) by fitting our model to the experimental results. We then predicted the concentration profiles of SBACs under various operational conditions. We analyzed the kinetic data and predicted concentration profiles of reactive radicals (HO• and RCS), we found that ClO • was the dominant radicals for SBACs destruction. In addition, we established quantitative structure activity relationships (QSARs) that can help predict the second-order rate constants for SBACs destruction by each type of reactive radicals using SBACs Hammett constants. Our first-principles-based kinetic model has been verified using experimental data. Our model can facilitate a design for the most cost-effective application of the UV/free chlorine process. For example, our model can determine the optimum chlorine dosage and UV light intensity that result in the lowest energy consumption.

3.2 Introduction

Advanced oxidation processes (AOPs) are effective technologies to destroy recalcitrant organic contaminants in the aqueous phase.[107,109,110] AOPs create highly reactive radicals at room temperature and pressure. These electrophilic radicals eventually mineralize refractory organic contaminants into CO_2 and H_2O. Recently, the UV/free chlorine

($HOCl/OCl^-$) process has been considered a promising AOP technology and was originally introduced by Watts and Linden,[111] and this process generates HO• and reactive chlorine species (RCS, including Cl•, Cl_2^-• and ClO•).[37,40] Compared with other common AOPs (e.g. UV/H_2O_2 and UV/Persulfate processes), the UV/free chlorine process has the following advantages: ***(1)*** it has much lower chemical reagent costs (the market price per ton: $250 for NaOCl, $500 for H_2O_2 and $800 for $Na_2S_2O_8$); ***(2)*** it has higher treatment efficiency with less oxidant consumption and shorter treatment time (e.g., trichloroethylene);[38] ***(3)*** it has higher energy efficiency because $HOCl/OCl^-$ has a greater UV light-absorption characteristics (quantum yield and molar absorption coefficient); [15,39,40] ***(4)*** it can be implemented in existing disinfection infrastructure with only addition of a UV light source;[42] ***(5)*** there is no need for quenching residual free chlorine;[43] and, ***(6)*** Cl^- does not inhibit destruction of organic contaminants in the UV/free chlorine process.[37,44,45,46], which has been observed in the UV/Persulfate process.[20,39] Overall, the UV/free chlorine process appears to be more cost-effective to destroy refractory organic contaminants.

For the wide scale industrial application, it is critical to design the UV/free chlorine process with lowest energy consumption. Therefore, we need to understand the degradation mechanisms of organic contaminants in this process. However, current studies of the UV/free chlorine process have not examined the mechanistically complex radicals-initiated chain reactions,[49] because there is a lack of RCS kinetic data. Many related experimental studies have shed light on the degradation of some selected organic compounds (e.g. atrazine, [50] naproxen,[53] desethylatrazine,[41] etc.)[52]. These experimental studies have laid foundation for further kinetic modeling studies, which could advance our

understanding about the degradation mechanisms of organic contaminants in a cost and time efficient way.

Some kinetic models have been developed for the destruction of various organic contaminants (e.g. benzoic acid, [37] carbamazepine,[46] acrylamide,[55] etc.)[44,45,51,56,57,58,59,60,61] in the UV/free chlorine process. However, most of these studies used the simplified pseudo-steady-state (SPSS) assumption (i.e., the net formation rates of free radicals are zero) for simplification. Although invoking the SPSS assumption has achieved various levels of success; for example, pseudo-first-order rate constants estimated from these models can quantify the overall oxidization rates under certain experimental conditions. However, the SPSS models are unable to elucidate the oxidization rate contributions for all the reactive radicals that are involved (e.g., HO· and RCS). Some studies determined the second-order rate constants for RCS reacting with selected organic contaminants by the competition kinetic method, [47,51] which adopts the SPSS assumption and presents a challenge for screening all organic contaminants. Commercial software (e.g., Simbiology) has been used to simulate the performance of the UV/free chlorine process.[62] It did not invoke the SPSS assumption but it is unable to determine unknown RCS kinetic data. In conclusion, quantitative insight in the degradation mechanisms of organic contaminants is still insufficient for the UV/free chlorine process.

An attractive alternative for overcoming these challenges is to develop a first-principles-based kinetic model without SPSS assumption. Kinetic models based on first-principles have been successfully implemented to describe the degradation mechanisms of HO· based and SO_4^-· based AOPs.[20,63,64,65,66,67,112] In this study, we developed a novel first-principles-based kinetic model for the UV/free chlorine process, which includes all

reasonably proposed photochemical and chemical reactions regarding the degradation of parent organic contaminants.[37,43,47] Substituted benzoic compounds (SBACs) were chosen as the target organic contaminants.

The objectives in developing this first-principle-based kinetic model for the UV/free chlorine process include: ***(1)*** determining the unknown second-order rate constants between organic contaminants and RCS by fitting our experimental results; ***(2)*** predicting the performance of organic contaminants destruction in this process under different operational conditions; ***(3)*** interpreting the oxidization mechanisms of organic contaminants by determining relative contribution of each type reactive radicals and photolysis; ***(4)*** establishing quantitative structure activity relationships (QSARs) that can help determine the second-order rate constants for each type of reactive radicals; [113] and, finally, ***(5)*** developing the model that can be used to design the most cost-effective UV/free chlorine process (i.e., lowest energy usage) .

3.3 Materials and Methods

3.3.1 Chemicals

These are the six target organic compounds (SBACs): 3-methylbenzoic acid, 4-fluorobenzoic acid, 2-chlorobenzoic acid, 2-iodobenzoic acid, 3-cyanobenzoic acid and 3-nitrobenzoic acid. All chemicals were at least of analytical grade. A NaOCl stock solution was prepared by dissolving chlorine gas into the sodium hydroxide solution, and the concentration of active chlorine was standardized by the diethyl-p-phenylene diamine (DPD) colorimetric method (Hach, Anachemia Canada Inc). HPLC grade methanol was purchased from Sigma-Aldrich (USA). Dipotassium hydrogen phosphate and potassium dihydrogen phosphate were purchased from Sinopharm Chemical Reagent Co. (China).

Benzoic acid (BA), 3-Methylbenzoic acid, 4-Fluorobenzoic acid, 2-Chlorobenzoic acid, 2-Iodobenzoic acid, 3-Cyanobenzoic acid and 3-Nitrobenzoic acid were purchased from Sigma-Aldrich (USA). All solutions were prepared using ultrapure water from a Milli-Q water purification system. The chemical properties and structures of these substituted benzoic acid compounds (SBACs) are listed in **Table 3.1**. The extinction coefficient for each SBAC was obtained from our experimental detection by UV spectrophotometer (UV-1770, Hitachi, Japan). The Hammett constants for the SBACs were collected from the literature,[114] and, the Hammett constant for the ortho position (σ_o) substituted was assumed to be the same as the Hammett constant for the para position substituted (σ_p) if the value of σ_o is not available in the literature.[70,114]

Table 3.1. Chemical properties and structures of SBACs

No.	**Name**	**Molecular Formula**	**Structure**	**Extinction Coefficient ($M^{-1}cm^{-1}$)**	**Hammett Constant**
1	3-Methylbenzoic acid	$C_8H_8O_2$ 136.15	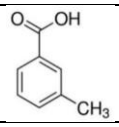	3100	-0.069
2	4-Fluorobenzoic acid	$C_7H_5FO_2$ 140.11	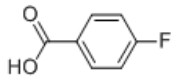	3200	0.062
3	2-Chlorobenzoic acid	$C_7H_5ClO_2$ 156.57	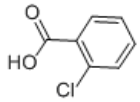	7300	0.227
4	2-Iodobenzoic acid	$C_7H_5IO_2$ 248.02	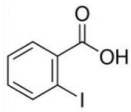	6600	0.276
5	3-Cyanobenzoic acid	$C_8H_5NO_2$ 147.13	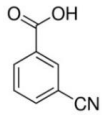	3000	0.56
6	3-Nitrobenzoic acid	$C_7H_5NO_4$ 167.12	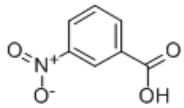	5200	0.71

3.3.2 Experimental procedures

UV irradiation experiments were conducted in a 1-L stainless steel UV reactor with a 6-W low-pressure Hg lamp placed in the center of the batch reactor as shown in **Figure 3.1**. The reaction temperature was maintained at 25 ± 1 °C with a continuous recirculation system. Chlorine dosages of 0.5, 1, 2 and 4 mg L^{-1} were added to the reactor and the initial concentration of SBACs was 5 μM. The solution pH was buffered to be 7.2 by the addition of 2.0 mM phosphate buffer solution. At each sampling time, 1.0 mL of solution was sampled and quenched immediately by excess $Na_2S_2O_3$.

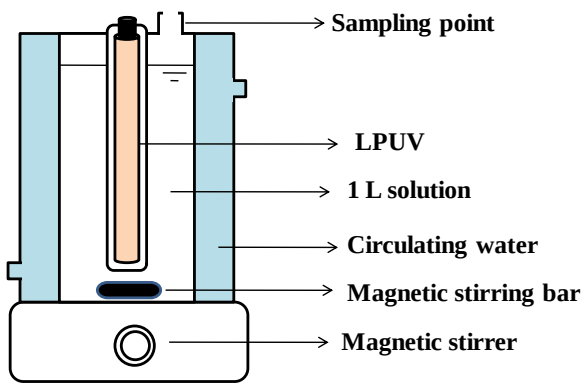

Figure 3.1. Schematic schemes of UV reactor

The UV intensity (P_{UV}) and the effective path length (L) can be determined by detecting concentration profile of a target organic compound during the UV irradiation alone. According to the Beer-Lambert Law, the photolysis kinetics of the target organic compound in batch reactor (r_R^{UV}) is expressed in eq 3.1:

$$r_R^{UV} = \frac{dC_t}{dt} = -\phi P_{UV}(1-\exp(-2.303\varepsilon C_t L)) \quad (3.1)$$

where, C_t is the target organic compound concentration at time t (M); ϕ is the quantum yield of target organic compound; P_{UV} is the UV intensity (Einstein s^{-1} L^{-1}), ε is the target organic compound molar absorption coefficient ($M^{-1}cm^{-1}$) at wavelength 254 nm; L is the effective

path length (cm). In this study, the values of P_{UV} and L were determined at wavelength 254 nm.

We first used dilute atrazine as the target organic compound to determine the UV intensity. Eq 3.1 can be simplified into eq 3.2 as the $2.303\varepsilon_{atrazine}C_tL$ is large:[59]

$$C_0 - C_t = \phi_{atrazine}P_{UV}t \tag{3.2}$$

where, C_0 is the initial concentration of atrazine (10^{-4}M); $\phi_{atrazine}$ is 0.046;[115] $\varepsilon_{atrazine}$ is 3498 $M^{-1}cm^{-1}$.[116] We detected atrazine concentrations at different time (C_t), and then plotted the figure C_t-C_0 vs. time (t). As a result, the slope of this plot is $\phi_{atrazine}P_{UV}$. Therefore, P_{UV} equals to the slope divided by $\phi_{atrazine}$. **Figure 3.2** indicates the result of photolysis of dilute atrazine under UV irradiation at 254 nm. The slope of **Figure 3.2** is 0.0908 and therefore the UV intensity is determined as 1.97×10^{-6} Einstein s^{-1} L^{-1}.The UV photo flux (Einstein s^{-1}) equals to the P_{UV} times the batch reactor volume (L).

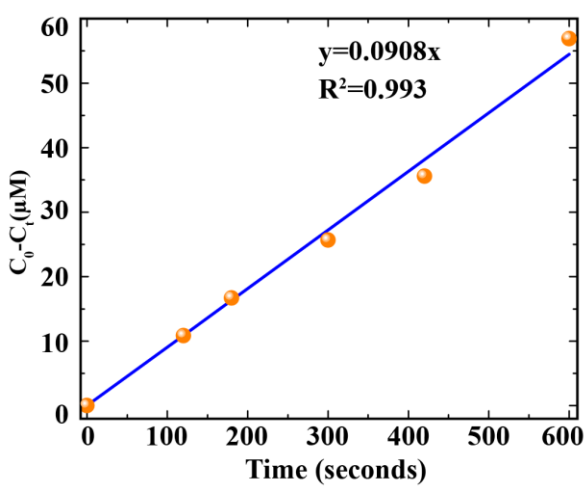

Figure 3.2. Photolysis of dilute atrazine under UV irradiation at 254 nm ([atrazine]$_0$=100μM).

After determining the UV intensity, we used dilute H_2O_2 solution as the target organic compound to determine the effective path length. Eq 3.1 can be simplified into eq 3.3 if $2.303\varepsilon_{H_2O_2}C_tL$ is small:[37,59]

$$\ln(C_t / C_0) = -2.303\phi_{H_2O_2} P_{UV} \varepsilon_{H_2O_2} Lt = -k_{obs} t \quad (3.3)$$

where, C_0 is the initial concentration of H_2O_2 (10^{-4} M), $\phi_{H_2O_2}$ is 0.5; $\varepsilon_{H_2O_2}$ is 17.9 $M^{-1}cm^{-1}$ -19.6 $M^{-1}cm^{-1}$. We detected H_2O_2 concentrations at different time (C_t), and then plotted the figure $\ln(C_0/C_t)$ vs. time (t). As a result, the slope of this plot is k_{obs} (k_{obs} is the pseudo first order rate constant, s^{-1}). It is obvious that k_{obs} equals to $2.303\phi_{H_2O_2} P_{UV} \varepsilon_{H_2O_2} L$. Therefore, L equals to k_{obs} divided by $2.303\phi_{H_2O_2} P_{UV} \varepsilon_{H_2O_2}$ (P_{UV} has been determined and $\phi_{H_2O_2}$, $\varepsilon_{H_2O_2}$ are already known). **Figure 3.3** indicates the results of photolysis of dilute H_2O_2 under UV irradiation at 254 nm. The slope of **Figure 3.3** is 0.00028 and therefore the effective path length is determined as 6.3 cm.

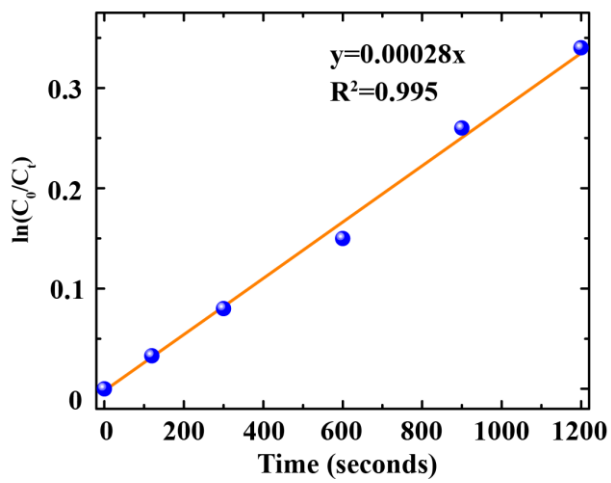

Figure 3.3. Photolysis of dilute H_2O_2 under UV irradiation at 254 nm ($[H_2O_2]_0$=100μM).

3.3.3 Analytical Methods

A high-performance liquid chromatography (HPLC) system (Agilent 1260, USA) equipped with a C18 column (150 mm × 4.6 mm × 5 μm, Agilent, USA), and, a variable wavelength detector (VWD) set at 227 nm was used to detect the concentrations of BA and SBACs. A mobile phase consisting of 50% methanol and 50% phosphoric acid (10 mM) at a flow rate of 1 mL min^{-1} was used for separation.

3.3.4 Modeling Approach

Our first-principles based kinetic model was developed by the following steps, and the general information flow of our kinetic model is shown in **Figure 3.4**.

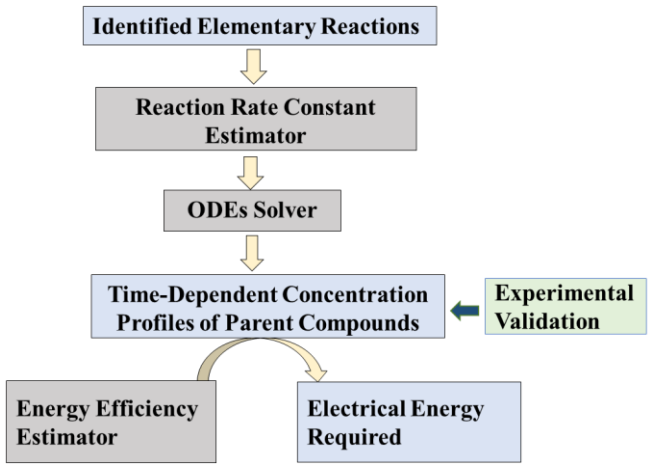

Figure 3.4. Information flow diagram of the first-principles based kinetic model.

The first step was to identify photolysis and all possible elementary reactions regarding the destruction of target organic compounds from the literature,[37,43,47] which were collected in **Table B.1 in Appendix B.** The photolysis rates of free chlorine generating the primary radicals HO· and Cl· are given in eq 3.4 and eq 3.5:

$$r_{uv,HOCl} = \phi_{HOCl} P_{UV} f_{HOCl} (1 - 10^{-A}) \tag{3.4}$$

$$r_{uv,OCl^-} = \phi_{OCl^-} P_{UV} f_{OCl^-} (1 - 10^{-A}) \tag{3.5}$$

where,

$$A = \left(\varepsilon_{HOCl} C_{HOCl} + \varepsilon_{OCl^-} C_{OCl^-} + \sum_i \varepsilon_i C_i \right) L$$

$$f_{HOCl} = \frac{\varepsilon_{HOCl} C_{HOCl}}{\varepsilon_{HOCl} C_{HOCl} + \varepsilon_{OCl^-} C_{OCl^-} + \sum_i \varepsilon_i C_i}; f_{OCl^-} = \frac{\varepsilon_{OCl^-} C_{OCl^-}}{\varepsilon_{HOCl} C_{HOCl} + \varepsilon_{OCl^-} C_{OCl^-} + \sum_i \varepsilon_i C_i}$$

ϕ_{HOCl} is the quantum yield of HOCl (0.9-1.45);[40] ϕ_{OCl^-} is the quantum yield of OCl^- (0.8-0.97);[40] ϕ_R is the quantum yield of the target organic compound, the value of ϕ_R is 0 if the

target organic compound is not degraded by UV alone. $\phi_R P_{UV} f_R (1-10^{-A})$ is the photolysis rate of SBACs, in M·s^{-1} (if the SBAC cannot be destructed by UV alone, then this term becomes 0 M·s^{-1}). ε_{HOCl} is the extinction coefficient of HOCl (59 M^{-1}cm^{-1});[37] ε_{OCl^-} is the extinction coefficient of OCl$^-$ (66 M^{-1}cm^{-1});[37] ε_R is the extinction coefficient of SBAC (**Table 3.1**); $\sum_i \varepsilon_i C_i$ is the absorptivity of all light absorbing species (e.g. target organic compounds, NOM, byproducts, etc.) in cm^{-1}. L is the effective pathlength (6.3 cm).

The second-order rate constant for each elementary reaction is also reported in **Table B.1 in Appendix B**.[20,37,39,43,85] However, the kinetic data for HO·, Cl·, Cl_2^-· and ClO· reacting with target organic compounds ($k_{HO\cdot/R}$, $k_{Cl\cdot/R}$, $k_{Cl_2^-\cdot/R}$ and $k_{ClO\cdot/R}$) are rarely reported previously. Therefore, the second step was to estimate the rarely reported second-order rate constants for reactive radicals oxidizing organic contaminants ($k_{HO\cdot/R}$, $k_{Cl\cdot/R}$, $k_{Cl_2^-\cdot/R}$ and $k_{ClO\cdot/R}$). $k_{HO\cdot/R}$ were estimated by the group contribution method (GCM). GCM hypothesizes that the reaction mechanisms of HO· and the effect of neighboring functional groups determine $k_{HO\cdot/R}$. GCM has been successfully applied for estimating $k_{HO\cdot/R}$ of many organic contaminants in the aqueous phase, and the predicted value of $k_{HO\cdot/R}$ typically has an error factor of 0.5–2.[69,70] However, the current version of GCM is unable to predict the second-order rate constants of RCS reacting with target organic compounds. Therefore, we estimated $k_{Cl\cdot/R}$, $k_{Cl_2^-\cdot/R}$ and $k_{ClO\cdot/R}$ by fitting the experimental data of concentration profiles of target organic compounds. The sample deviation (SD, which is also objective function (OF)) in eq 3.6 reflects whether the simulation results fit the experimental data well:[20]1

$$SD=\sqrt{\frac{1}{n-1}\sum\left[\left(C_{exp}-C_{cal}\right)/C_{exp}\right]^2} \tag{3.6}$$

where n is the number of experimental data points, and, C_{exp} and C_{cal} are the experimental and calculated concentrations of the target organic compound at each time point, respectively. **Appendix D** includes a source code of objective function developed in MATLAB R2018b. In this work, we combined the pattern search algorithm and the genetic algorithm to achieve the global minimum OF for the best fit. [117,118,119] The PS and GA algorithms are effective for solving global minimum problems. These two types algorithms are not developed based on the Jacobian method, which uses derivatives of the objective function to determine the best fit, therefore could avoid trapping at local minima. PS operates by searching a set of points (pattern) and expanding or shrinking until no more points within the pattern have a lower objective function value than the current point.[117] GA mimics the biological evolution process to solve the optimization problem with global minimal OF.[118] Compared to the PS algorithm, the GA algorithm typically achieves better solutions but incurs much greater computational cost if the search range of each parameter is very large (e.g., the range of $k_{Cl\cdot/R}$ value is typically within the magnitude 10^5 to 10^9).[119] As a result, to balance the computational efficiency and the accuracy of results, we implemented the PS algorithm first to narrow the subsequent search range for the GA algorithm. **Appendix E** includes a source code of pattern search algorithm developed in MATLAB R2018b, and **Appendix F** include a source code of genetic algorithm in MATLAB R2018b.

The third step was to predict the concentration profiles of organic contaminants. To describe the destruction of parent organic contaminants, the mass balance for all species in the batch reactor create a set of ODEs, which are listed in eq B.1 - eq B.40 **in Appendix B**. The ODEs **in Appendix B** are stiff because the rate constants have a very large range

(e.g., the range of $k_{Cl\cdot/R}$ value is typically within the magnitude 10^5 to 10^9). As a result, some reactions occurs slowly, and others occur rapidly.[119] Consequently, the major challenges for solving stiff ODEs are the very expensive computational cost and the extremely unstable results. To overcome these difficulties, Gear's algorithm was selected to solve the stiff ODEs system. Gear's algorithm is based on the backward differentiation formula (BDF). The general formula for BDF is given in eq 3.7:[120]

$$\sum_{k=0}^{s} a_k y_{n+k} = h\beta f(t_{n+s,} y_{n+s}) \tag{3.7}$$

where h is the step size; $t_n = t_0 + nh$; f is the first derivative of y_{n+s}; and a_k and β are coefficients whose values depend on the step order s (e.g., if s is 1, a_0 is −1, a_1 is 1, and β is 1; if s is 2, a_0 is 1/3, a_1 is −4/3, a_2 is 1 and β is 2/3).[120] Gear's algorithm has been reported to be one of the most efficient and stable stiff ODE solvers. **Appendix F** includes a source code about the implementation of gear's algorithm in MATLAB R2018b. The fourth step was to evaluate the energy efficiency per order of destruction of parent compound. Finally, our model was validated by comparing the modeling results to the experimental data.

3.3.5 Quantitative structure activity relationship (QSAR) model development

We developed four QSAR models to help us further explore the reactivity of HO•, Cl•, Cl_2^-• and ClO• with SBACs. QSAR models are regression models that linearly relate chemical descriptor to the rate constants of structurally closed organic compounds.[121] QSARs have been successfully developed to determine the rate constants of a wide variety of oxidants (e.g., HO•, SO_4^-•, O_3) reacting with organic contaminants.[70,113,122] Previous studies have not attempted to simultaneously establish QSAR models for each type of RCS.[43,51] In this study, Hammett constants (σ) were chosen as the chemical descriptor and this is one of the most commonly employed substituent descriptor.[43,70,123] The values of σ

for SBACs have been reported by Hansch et al.[114] The values of $k_{Cl\cdot/R}$, $k_{Cl_2^-\cdot/R}$ and $k_{ClO\cdot/R}$ were determined by fitting our model to the data, the values of $k_{HO\cdot/R}$ were determined by GCM. The general Hammett equation is given in eq 3.8.[124]

$$\log k = \log k_0 + \rho\sigma \tag{3.8}$$

where k is the rate constant between a certain SBAC and RCS in $M^{-1}s^{-1}$; k_0 is the rate constant between BA and RCS in $M^{-1}s^{-1}$; and ρ is the slope of the regression line, which reflects the sensitivity of the reaction rate constant to the electronic effect of the additional functional group.[121]

3.4 Results and Discussion

3.4.1 Estimation of second-order rate constants for RCS with SBACs

Benzoic acid (BA) is the best candidate as a reference organic contaminant and can be used to firstly validate our model because some rate constants for BA destruction has been reported.[37,85] The prediction results of the concentration profiles of BA under different initial concentration of free chlorine are shown in **Figure 3.5**. Accordingly, the value of objective function is 0.028 for 1 ppm free chlorine; the objective function is 0.155 for 2 ppm free chlorine; the objective function is 0.182 for 4 ppm free chlorine. In general, our first-principles-based kinetic model successfully predicted the degradation of BA in the UV/free chlorine process under various experimental conditions.

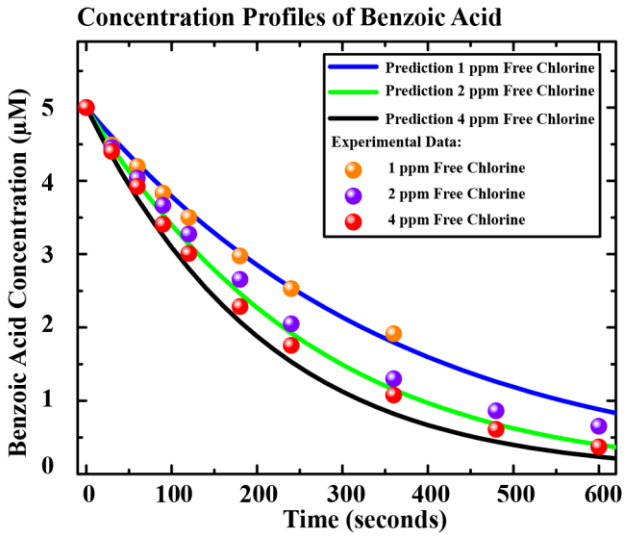

Figure 3.5. Prediction results for BA degradation in UV/free chlorine process. Experimental conditions: UV intensity $=1.97\times10^{-6}$ Einstein/L·s; free chlorine dosage range, 1 ppm to 4 ppm; initial concentration of BA = 5×10^{-6} M; pH was buffered at 7.2. The symbols represent experimental data and the lines represent model results.

Our experiments showed that none of these SBACs were oxidized by free chlorine alone, four were oxidized by UV alone (4-fluorobenzoic acid, 2-chlorobenzoic acid, 2-iodobenzoic acid and 3-nitrobenzoic acid). By fitting the experimental data for degradation by UV alone (**Text C.1 in Appendix C**), the quantum yields for these four SBACs were determined to be (i) 0.00144 for 4-fluorobenzoic acid; (ii) 0.0028 for 2-chlorobenzoic acid; (iii) 0.0132 for 2-iodobenzoic acid; and, (iv) 0.0005 for 3-nitrobenzoic acid. Then we fitted the experimental data for the UV/free chlorine process and included the photolysis rate. Dashed lines in **Figure 3.6** show the experimental data fitting results for these SBACs to determine the second-order rate constants toward RCS. As shown in **Figure 3.6(a)**, the time-dependent concentration profile for 3-methylbenzoic acid was fitted for 1 ppm initial free chlorine. The rate constants for $k_{HO\cdot/R}$, $k_{Cl\cdot/R}$, $k_{Cl_2^-\cdot/R}$ and $k_{ClO\cdot/R}$ are 4.28×10^9 $M^{-1}s^{-1}$, 1.64×10^9 $M^{-1}s^{-1}$, 6.81×10^4 $M^{-1}s^{-1}$ and 1.21×10^6 $M^{-1}s^{-1}$, respectively. The minimum

value of the objective function (OF_{min}) is 0.0737. Eq.1 is the sample deviation and it becomes the standard deviation if we have a large set of model data comparisons. In case where it is the standard deviation and the error between model calculations follows a Gaussian curve, 68% of data are within ± 7.37% of the model calculations (this is a good fit). We often do not have a large number of model data comparisons, and thus OF_{min} is not the standard deviation but it is still a good metric to report regarding the model fits. As shown in **Figure 3.6(b)**, the time-dependent concentration profile for 4-fluorobenzoic acid was fit for 2 ppm initial free chlorine. The rate constants for $k_{HO\cdot/R}$, $k_{Cl\cdot/R}$, $k_{Cl_2^-\cdot/R}$ and $k_{ClO\cdot/R}$ were determined to be 3.48×10^9 $M^{-1}s^{-1}$, 7.92×10^8 $M^{-1}s^{-1}$, 5.20×10^4 $M^{-1}s^{-1}$ and 1.27×10^6 $M^{-1}s^{-1}$, respectively, and, the OF_{min} is 0.121. As shown in **Figure 3.6(c)**, the time-dependent concentration profile for 2-chlorobenzoic acid was fit for 1 ppm initial free chlorine. The rate constants for $k_{HO\cdot/R}$, $k_{Cl\cdot/R}$, $k_{Cl_2^-\cdot/R}$ and $k_{ClO\cdot/R}$ were determined to be 3.31×10^9 $M^{-1}s^{-1}$, 6.00×10^8 $M^{-1}s^{-1}$, 3.00×10^4 $M^{-1}s^{-1}$ and 8.00×10^5 $M^{-1}s^{-1}$, respectively, and, the OF_{min} is 0.0400. As shown in **Figure 3.6(d)**, the time-dependent concentration profile for 2-iodobenzoic acid was fit for 1 ppm initial free chlorine. The rate constant for $k_{HO\cdot/R}$, $k_{Cl\cdot/R}$, $k_{Cl_2^-\cdot/R}$ and $k_{ClO\cdot/R}$ were determined to be 2.78×10^9 $M^{-1}s^{-1}$, 3.85×10^8 $M^{-1}s^{-1}$, 2.00×10^4 $M^{-1}s^{-1}$ and 8.82×10^5 $M^{-1}s^{-1}$, respectively, and, the OF_{min} is 0.0520. As shown in **Figure 3.6(e)**, the time-dependent concentration profile for 3-cyanobenzoic acid was fit for 1 ppm initial free chlorine. The rate constants for $k_{HO\cdot/R}$, $k_{Cl\cdot/R}$, $k_{Cl_2^-\cdot/R}$ and $k_{ClO\cdot/R}$ were determined to be 1.76×10^9 $M^{-1}s^{-1}$, 6.35×10^7 $M^{-1}s^{-1}$, 1.89×10^4 $M^{-1}s^{-1}$ and 8.11×10^5 $M^{-1}s^{-1}$, respectively, and, the OF_{min} is 0.0294. As shown in **Figure 3.6(f)**, the time-dependent concentration profile for 3-nitrobenzoic acid was fit for 1 ppm initial free chlorine. The rate constants for $k_{HO\cdot/R}$, $k_{Cl\cdot/R}$, $k_{Cl_2^-\cdot/R}$ and $k_{ClO\cdot/R}$ were determined to be 1.72×10^9 $M^{-1}s^{-1}$,

4.18×10^{7} $M^{-1}s^{-1}$, 1.08×10^{4} $M^{-1}s^{-1}$ and 5.05×10^{5} $M^{-1}s^{-1}$, respectively, and, the OF_{min} is 0.0189. Accordingly, our dynamic kinetic model successfully fit all these experimental data. Overall, for the oxidation of these SBACs, $k_{HO\cdot/R}$ ranges from 1×10^{9} $M^{-1}s^{-1}$ to 5×10^{9} $M^{-1}s^{-1}$, $k_{Cl\cdot/R}$ ranges from 4×10^{7} $M^{-1}s^{-1}$ to 2×10^{9} $M^{-1}s^{-1}$, $k_{Cl_2^{-}\cdot/R}$ ranges 1×10^{4} $M^{-1}s^{-1}$ to 6×10^{4} $M^{-1}s^{-1}$, and, $k_{ClO\cdot/R}$ ranges from 4×10^{5} $M^{-1}s^{-1}$ to 2×10^{6} $M^{-1}s^{-1}$.

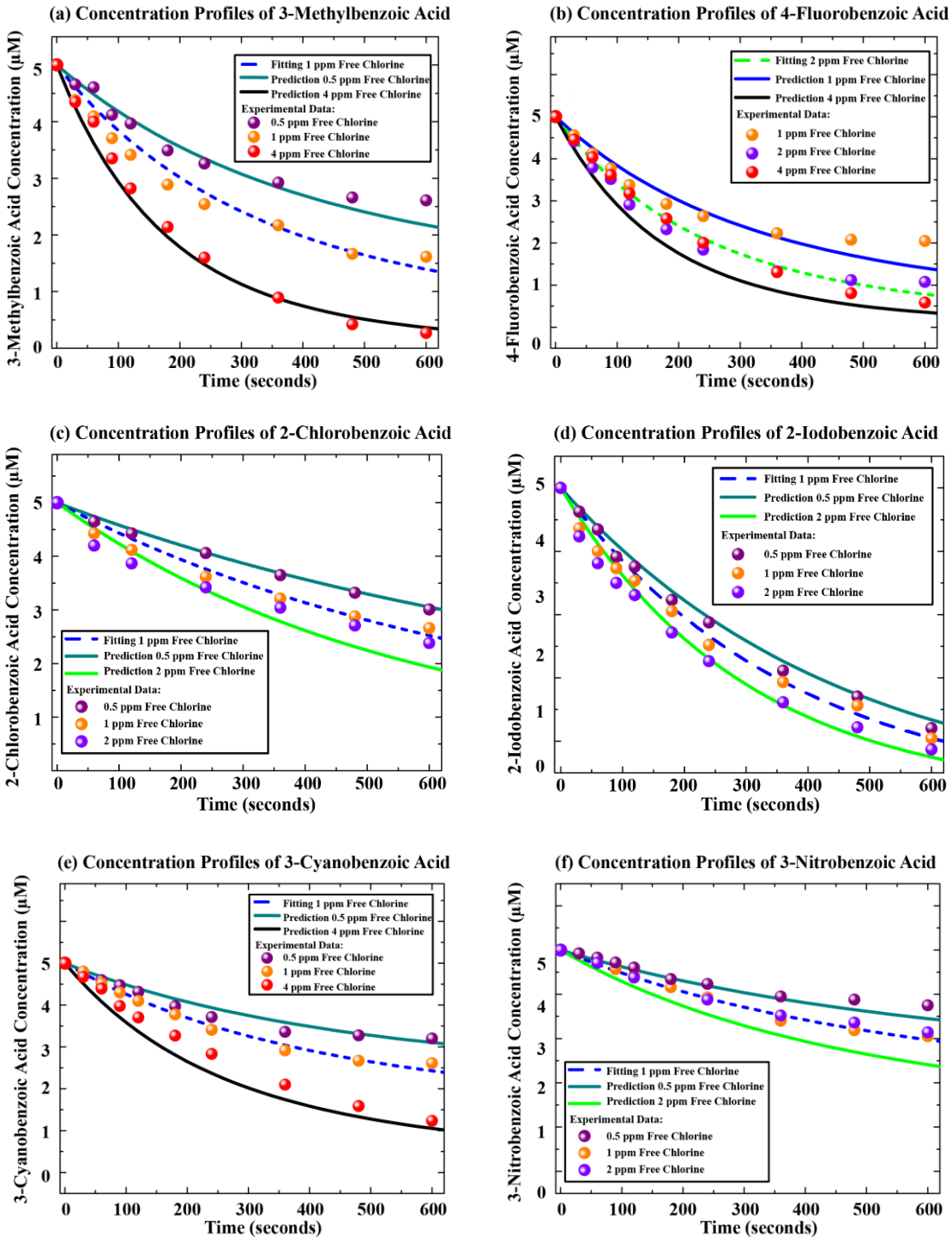

Figure 3.6. First-principles-based kinetic model fits and prediction results for SBACs degradation in the UV/free chlorine process. Experimental conditions: UV intensity = 1.97×10^{-6} Einstein/L · s ; free chlorine dosage range, 0.5 ppm to 4 ppm; initial concentration of SBAC = 5×10^{-6} M; pH was buffered at 7.2. The symbols represent the

experimental data, and the lines represent the model results. The dashed lines are the fitting results, and the solid lines are model predictions.

We determined the 75% confidence regions for these rate constants ($k_{Cl\cdot/R}$, $k_{Cl_2^-\cdot/R}$ and $k_{ClO\cdot/R}$) estimated from our kinetic model by fitting experimental data ($k_{HO\cdot/R}$ is not discussed at here because their values were estimated by GCM). The confidence contour is defined by eq 3.9:[125]

$$OF(\theta) = \hat{OF}(\theta)\left(1 + \frac{p}{n-p}F(p, n-p, 1-\alpha)\right) \tag{3.9}$$

where $\widehat{OF}(\theta)$ is the minimal OF; θ is rate constant; p is the number of fitted parameters; n is the number of experimental data; n−p is the degrees of freedom; α is 0.25; F(p, n-p, 1-α) comes from the F statistic table (**Text C.2, Table C. 1 in Appendix C**).[125] According to **Figure 3.7** and **Table C. 1**, the 75% confidence level for $k_{ClO\cdot/R}$ is narrow, whereas the 75% confidence level for $k_{Cl\cdot/R}$ and $k_{Cl_2^-\cdot/R}$ are wide. In another words, model prediction are not sensitive to $k_{Cl\cdot/R}$ and $k_{Cl_2^-\cdot/R}$ because they play a minor role for the SBACs oxidation. Consequently, $k_{Cl\cdot/R}$ and $k_{Cl_2^-\cdot/R}$ have large confidence intervals. The lower boundary for $k_{Cl\cdot/R}$ and $k_{Cl_2^-\cdot/R}$ cannot be determined because the degrees of freedom are not high enough (we would obtain their lower boundary if had more experimental data). It should be noted that the 75% level of confidence regions for $k_{Cl\cdot/R}$, $k_{Cl_2^-\cdot/R}$ and $k_{ClO\cdot/R}$ are 3-dimensional. Since $Cl_2^-\cdot$ contributes very little to the destruction of organic contaminants (as will be discussed later), we determined the 2-dimensional 75% level of confidence regions for the $k_{Cl\cdot/R}$ and $k_{ClO\cdot/R}$ in **Figure C.2 in Appendix C**. The shapes of the confidence regions were mapped out in details and were assumed to be trapezoidal.

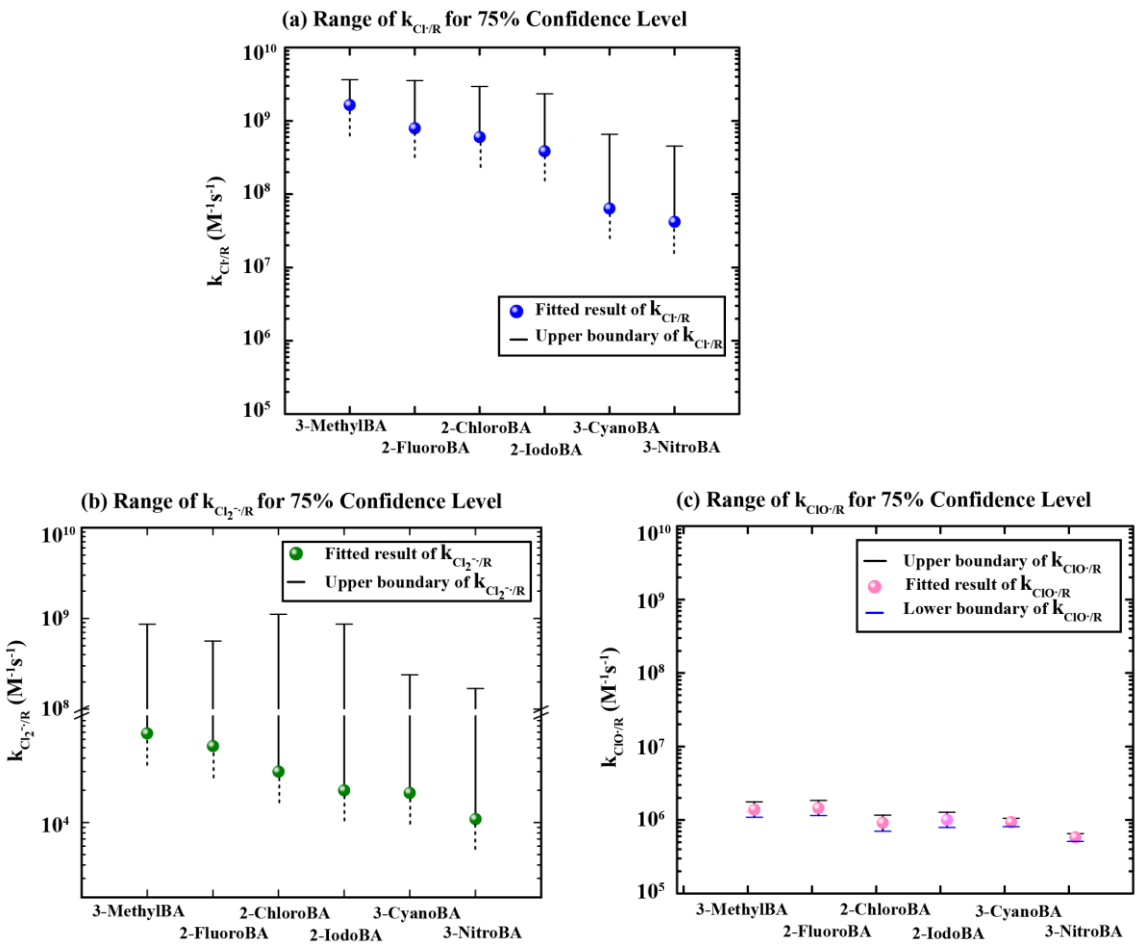

Figure 3.7. The range of the second-order constants for RCS with SBACs at the 75% confidence level. The symbols in each figure indicate the fitted results, and the upper and lower boundaries of each fitted rate constant are represented by bars. The dashed lines in (a) and (b) indicate that the lower boundaries of the reactivity of Cl· and $Cl_2^{\cdot-}$ cannot be determined. 3-MethylBA is 3-Methyl benzoic acid, 2-FluoroBA is 2-Fluorobenzoic acid, 2-ChloroBA is 2-Chlorobenzoic, 2-IodoBA is 2-Iodobenzoic acid, 3-CyanoBA is 3-Cyanobenzoic acid, 3-NitroBA is 3-Nitrobenzoic acid.

3.4.2 Model validation

After estimating the rate constants, we used our first-principles-based kinetic model to predict the concentration profiles of these SBACs for other initial free chlorine concentrations. The solid lines in **Figure 3.6** present the prediction results for these SBACs. As shown in **Figure 3.6(a)**, the degradation of 3-methylbenzoic acid was predicted

for 0.5 ppm and 4 ppm initial free chlorine. The objection function (OF) is 0.0666 and 0.167 for 0.5 ppm and 4 ppm free chlorine, respectively. As shown in **Figure 3.6(b)**, the degradation of 4-fluorobenzoic acid was predicted for 1 ppm and 4 ppm initial free chlorine. The OF is 0.129 and 0.256 for 1 ppm and 4 ppm free chlorine, respectively. As shown in **Figure 3.6(c)**, the degradation of 2-chlorobenzoic acid was predicted for 0.5 ppm and 2 ppm initial free chlorine. The OF is 0.0133 and 0.111 for 0.5 ppm and 2 ppm free chlorine, respectively. As shown in **Figure 3.6(d)**, the degradation of 2-iodobenzoic acid was predicted for 0.5 ppm and 2 ppm initial free chlorine. The OF is 0.0525 and 0.077 for 0.5 ppm and 2 ppm free chlorine, respectively. As shown in **Figure 3.6(e)**, the degradation of 3-cyanobenzoic acid was predicted for 0.5 ppm and 4 ppm initial free chlorine. The OF is 0.0376 and 0.126 for 0.5 ppm and 4 ppm free chlorine, respectively. As shown in **Figure 3.6(f)**, the degradation of 3-nitrobenzoic acid was predicted for 0.5 ppm and 2 ppm initial free chlorine. The OF is 0.0339 and 0.141 for 0.5 ppm and 2 ppm free chlorine, respectively. In general, our kinetic model adequately predicted the degradation of SBACs in the UV/free chlorine process for various operational conditions.

3.4.3 Contribution of radicals and photolysis to the destruction of SBACs

Once the second-order rate constants for SBACs are estimated and validated, they can be used to predict the time-dependent concentration profiles of reactive radicals during SBACs destruction as shown in **Figure 3.8**. **Appendix G** includes a MATLAB R2018b source code example of calculation of reactive radicals time-dependent concentration profiles.

(a) Radicals concentration profiles for 3-Methylbenzoic Acid deradation in UV/free chlorine

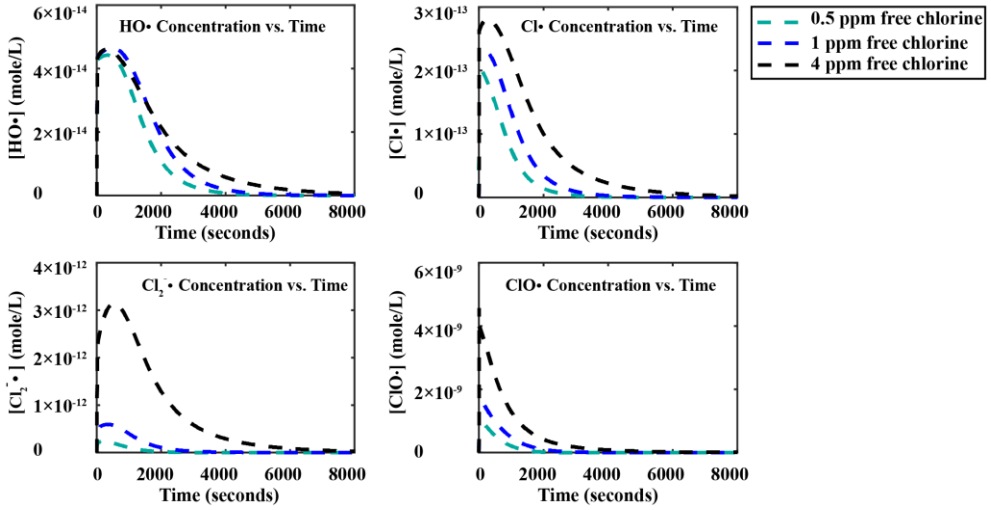

(b) Radicals concentration profiles for 4-Fluorobenzoic Acid deradation in UV/free chlorine

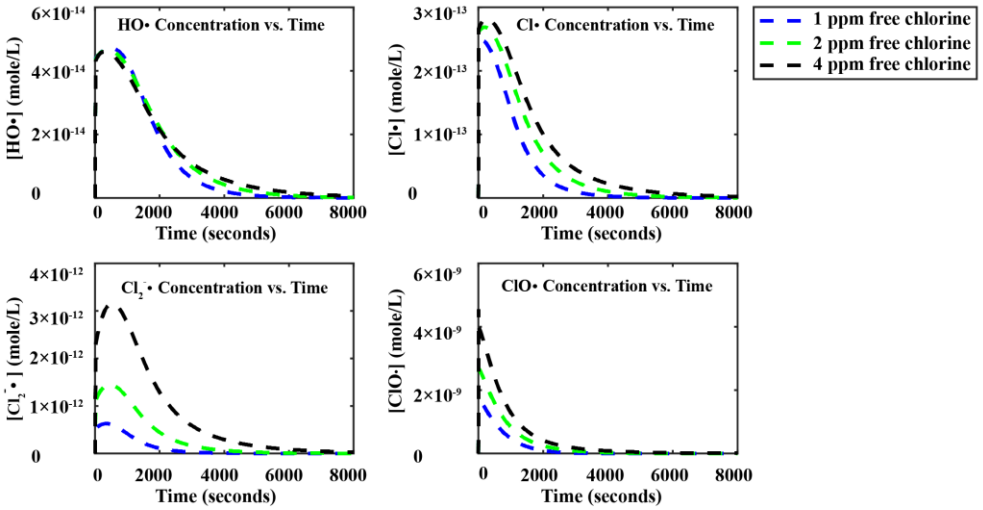

(c) Radicals concentration profiles for 2-Chlorobenzoic Acid deradation in UV/free chlorine

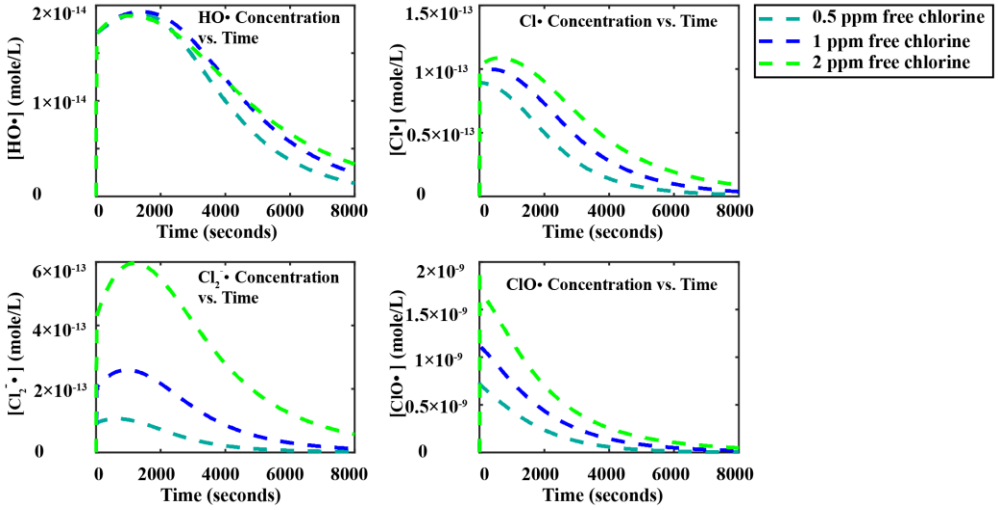

(d) Radicals concentration profiles for 2-Iodobenzoic Acid deradation in UV/free chlorine

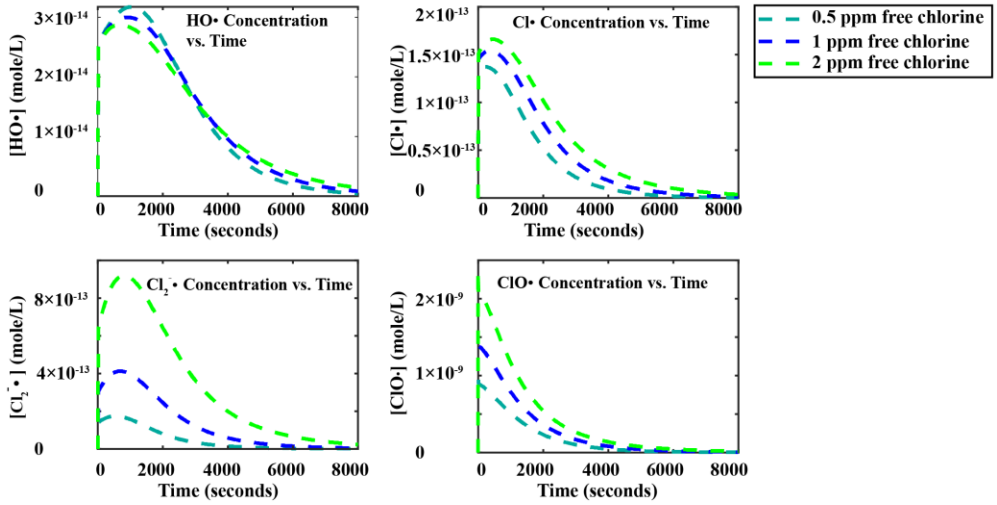

(e) Radicals concentration profiles for 3-Cyanobenzoic Acid deradation in UV/free chlorine

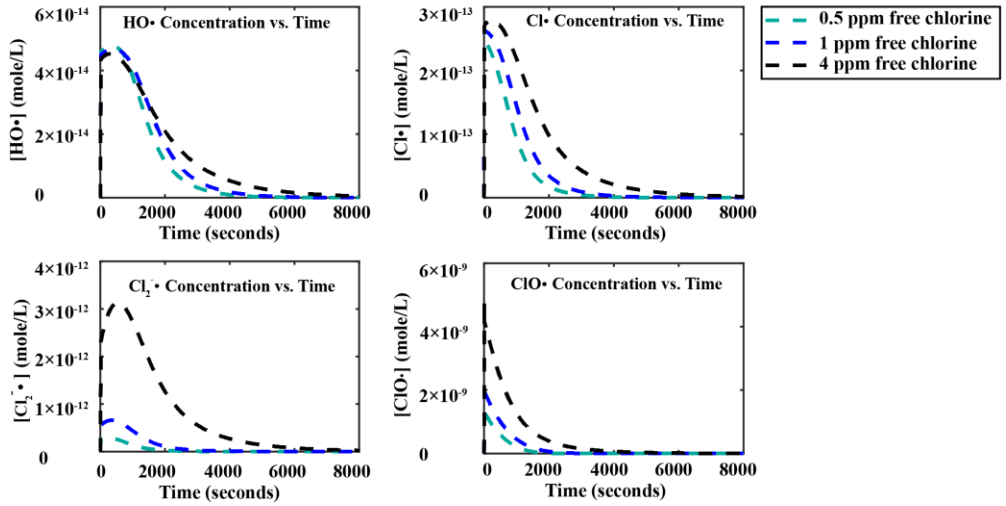

(f) Radicals concentration profiles for 3-Nitrobenzoic Acid deradation in UV/free chlorine

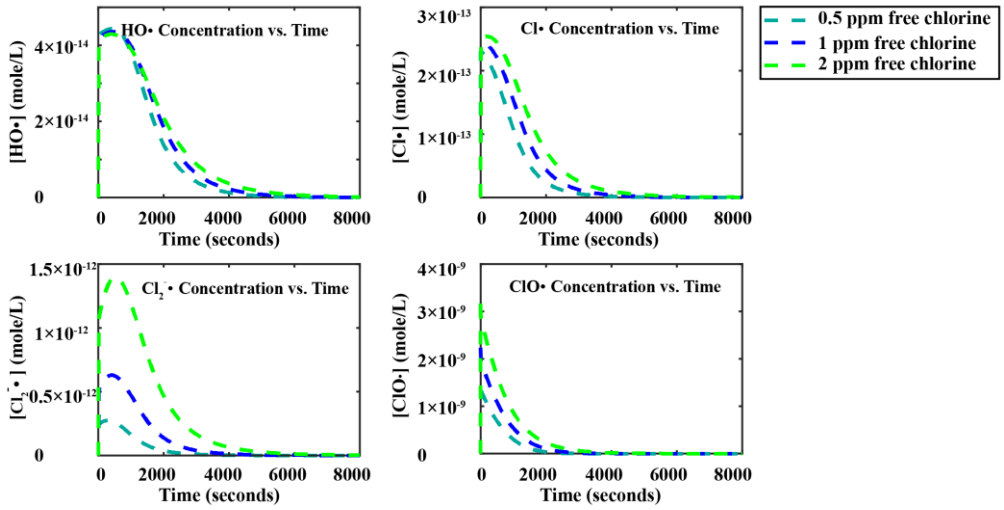

Figure 3.8. Time-dependent concentration profiles of HO·, Cl·, Cl_2^-· and ClO· during SBACs degradation in the UV/free chlorine process. Simulation Conditions: UV intensity =1.97 ×10^{-6} Einstein/L ·s ; free chlorine dosage range, 0.5 ppm to 4 ppm; initial concentration of SBACs = 5×10^{-6} M; pH was buffered at 7.2.

In addition, we calculated the integral average concentration of each reactive radicals using eq 3.10 and summarized the results in **Table 3.2**. **Appendix G** includes a MATLAB R2018b source code example of calculation of reactive radicals average concentration.

$$[\overline{C}]=\left(\int_{t_0}^{t_f}[C_t]dt\right)/\left(t_f-t_0\right) \tag{3.10}$$

where $\overline{C}$ is the integral average concentration of a species, in M; C_t is the concentration of a species at time t, in M; t_0 is the initial time, and t_f is the final time. For all of these SBACs, the integral average concentration of ClO· is typically 4 orders of magnitude larger than that of Cl· and 5 orders of magnitude larger than that of OH·. As the free chlorine dosage increases, the concentrations of HO· and Cl· slightly increase while the concentrations of Cl_2^-· and ClO· significantly increase. Therefore, although the second-order rate constants of ClO· with these SBACs are much lower than those of OH· and Cl·, ClO· may play a significant role for SBACs destruction in the UV/free chlorine process.

Table 3.2. Integral average concentrations of reactive radicals

(a) For 3-Methylbenzoic Acid Degradation

Reactive Radicals	Integral Average Concentration		
	0.5 ppm HOCl/OCl^-	1 ppm HOCl/OCl^-	4 ppm HOCl/OCl^-
HO·	4.37×10^{-14} M	4.56×10^{-14} M	4.52×10^{-14} M
Cl·	1.75×10^{-13} M	2.24×10^{-13} M	2.75×10^{-13} M
Cl_2^-·	2.16×10^{-13} M	5.69×10^{-13} M	2.87×10^{-12} M
ClO·	7.57×10^{-10} M	1.30×10^{-9} M	3.07×10^{-9} M

(b) For 4-Fluorobenzoic Acid Degradation

Reactive Radicals	Integral Average Concentration		
	1 ppm HOCl/OCl^-	2 ppm HOCl/OCl^-	4 ppm HOCl/OCl^-

HO•	4.62×10^{-14} M	4.58×10^{-14} M	4.53×10^{-14} M
Cl•	2.35×10^{-13} M	2.62×10^{-13} M	2.76×10^{-13} M
Cl_2^-•	6.01×10^{-13} M	1.36×10^{-12} M	2.89×10^{-12} M
ClO•	1.30×10^{-9} M	2.04×10^{-9} M	3.07×10^{-9} M

(c) For 2-Chlorobenzoic Acid Degradation

Reactive Radicals	Integral Average Concentration		
	0.5 ppm HOCl/OCl^-	1 ppm HOCl/OCl^-	2 ppm HOCl/OCl^-
HO•	1.78×10^{-14} M	1.79×10^{-14} M	1.79×10^{-14} M
Cl•	8.75×10^{-13} M	9.92×10^{-14} M	1.07×10^{-13} M
Cl_2^-•	1.01×10^{-13} M	2.31×10^{-13} M	4.99×10^{-13} M
ClO•	6.27×10^{-10} M	1.01×10^{-9} M	1.56×10^{-9} M

(d) For 2-Iodobenzoic Acid Degradation

Reactive Radicals	Integral Average Concentration		
	0.5 ppm HOCl/OCl^-	1 ppm HOCl/OCl^-	2 ppm HOCl/OCl^-
HO•	2.82×10^{-14} M	2.78×10^{-14} M	2.74×10^{-14} M
Cl•	1.35×10^{-13} M	1.52×10^{-13} M	1.62×10^{-13} M
Cl_2^-•	1.64×10^{-13} M	3.71×10^{-13} M	7.95×10^{-13} M
ClO•	7.96×10^{-10}M	1.24×10^{-9} M	1.86×10^{-9} M

(e) For 3-Cyanobenzoic Acid Degradation

Reactive Radicals	Integral Average Concentration		
	0.5 ppm HOCl/OCl^-	1 ppm HOCl/OCl^-	4 ppm HOCl/OCl^-
HO•	4.71×10^{-14} M	4.62×10^{-14} M	4.46×10^{-14} M
Cl•	2.14×10^{-13} M	2.44×10^{-13} M	2.74×10^{-13} M
Cl_2^-•	2.74×10^{-13} M	6.32×10^{-13} M	2.87×10^{-12} M
ClO•	8.60×10^{-10} M	1.36×10^{-9} M	3.08×10^{-9} M

(f) For 3-Nitrobenzoic Acid Degradation

Reactive Radicals	Integral Average Concentration		
	0.5 ppm HOCl/OCl^-	1 ppm HOCl/OCl^-	2 ppm HOCl/OCl^-
HO•	4.38×10^{-14} M	4.31×10^{-14} M	4.25×10^{-14} M
Cl•	2.06×10^{-13} M	2.32×10^{-13} M	2.49×10^{-13} M
Cl_2^-•	2.64×10^{-13} M	5.99×10^{-13} M	1.29×10^{-12} M
ClO•	9.32×10^{-10} M	1.42×10^{-9} M	2.11×10^{-9} M

To test the hypothesis that ClO• may be important for oxidizing SBACs , we quantified the relative contributions of each reactive radicals and photolysis for the SBACs

destruction in the UV/free chlorine process. Eq 3.11 – eq 3.15 represent the average relative contributions of reactive radicals (i.e. HO·, Cl· Cl_2^-· and ClO·**)** and photolysis. **Appendix G** includes a MATLAB R2018b source code example of calculation of average contribution of reactive radicals and photolysis.

Contribute of HO•

$$= \left[\int_{t_0}^{t_f}\left(\frac{k_{HO\bullet}[HO\bullet][R]}{k_{HO\bullet}[HO\bullet][R]+k_{Cl\bullet}[Cl\bullet][R]+k_{Cl_2^-\bullet}[Cl_2^-\bullet][R]+k_{ClO\bullet}[ClO\bullet][R]+r_{uv}+r_{Free\ Chlorine}}\right)\right] \quad (3.11)$$

Contribute of Cl•

$$= \left[\int_{t_0}^{t_f}\left(\frac{k_{Cl\bullet}[Cl\bullet][R]}{k_{HO\bullet}[HO\bullet][R]+k_{Cl\bullet}[Cl\bullet][R]+k_{Cl_2^-\bullet}[Cl_2^-\bullet][R]+k_{ClO\bullet}[ClO\bullet][R]+r_{uv}+r_{free\ chlorine}}\right)\right] \quad (3.12)$$

Contribute of Cl_2^-•

$$= \left[\int_{t_0}^{t_f}\left(\frac{k_{Cl_2^-\bullet}[Cl_2^-\bullet][R]}{k_{HO\bullet}[HO\bullet][R]+k_{Cl\bullet}[Cl\bullet][R]+k_{Cl_2^-\bullet}[Cl_2^-\bullet][R]+k_{ClO\bullet}[ClO\bullet][R]+r_{uv}+r_{free\ chlorine}}\right)\right] \quad (3.13)$$

Contribute of ClO•

$$= \left[\int_{t_0}^{t_f}\left(\frac{k_{ClO\bullet}[ClO\bullet][R]}{k_{HO\bullet}[HO\bullet][R]+k_{Cl\bullet}[Cl\bullet][R]+k_{Cl_2^-\bullet}[Cl_2^-\bullet][R]+k_{ClO\bullet}[ClO\bullet][R]+r_{uv}+r_{free\ chlorine}}\right)\right] \quad (3.14)$$

Contribute of UV

$$= \left[\int_{t_0}^{t_f}\left(\frac{r_{uv}}{k_{HO\bullet}[HO\bullet][R]+k_{Cl\bullet}[Cl\bullet][R]+k_{Cl_2^-\bullet}[Cl_2^-\bullet][R]+k_{ClO\bullet}[ClO\bullet][R]+r_{uv}+r_{free\ chlorine}}\right)\right] \quad (3.15)$$

Contribute of Free Chlorine

$$= \left[\int_{t_0}^{t_f}\left(\frac{r_{free\ chlorine}}{k_{HO\bullet}[HO\bullet][R]+k_{Cl\bullet}[Cl\bullet][R]+k_{Cl_2^-\bullet}[Cl_2^-\bullet][R]+k_{ClO\bullet}[ClO\bullet][R]+r_{uv}+r_{free\ chlorine}}\right)\right] \quad (3.16)$$

where [HO·], [Cl·], [Cl_2^-·], [ClO·] and [R] are the concentrations of reactive radicals and SBACs as a function of time; r_{UV} is the photolysis rate of SBACs at time t, in $M \cdot s^{-1}$; r_{HOCl} is the chlorination rate of SBACs at time t, in $M \cdot s^{-1}$. Since these six SBACs cannot be

oxidized by free chlorine alone, r_{HOCl} and contribution of free chlorine are both zero in this study; t_0 and t_f are initial and final time, respectively. **Figure 3.9** and **Table C.2 in Appendix C** show the average relative contributions of the SBACs destruction for various experimental conditions. It is obvious that ClO· plays a dominant role in the destruction of these SBACs except for 2-Iodobenzoic acid. For the 2-iodobenzoic acid, photolysis plays a more dominant role in its destruction than that of reactive radicals. (As shown and discussed in **Text C.1 and Figure C.1 in Appendix C**, UV alone significantly destroys 2-iodobenzoic acid). Nevertheless, ClO· still acts as the dominant contributor among the reactive radicals during the degradation 2-Iodobenzoic acid. Cl_2^-· contributes very little to the destruction of any of the SBAC due to its low concentration and low rate constant. Therefore, the relative contributions of Cl_2^-· are not apparent in **Figure 3.9**. The ranking of the relative contributions of reactive radicals and photolysis was summarized in **Table C.2**.

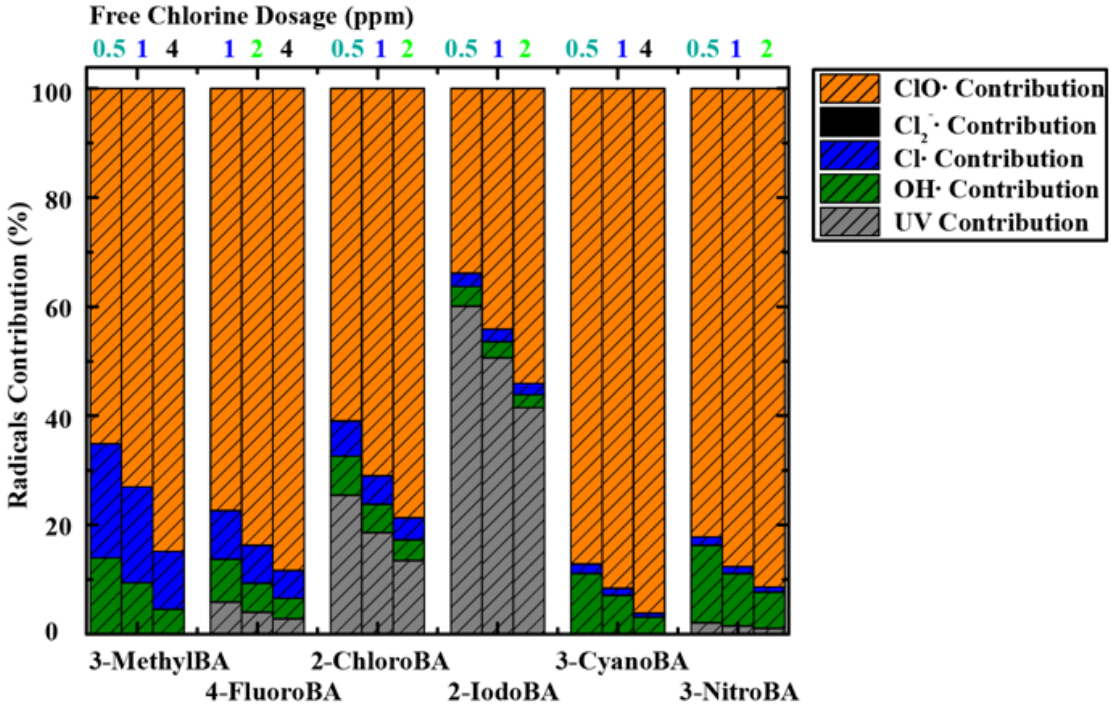

Figure 3.9. The average relative contributions (%) of each type reactive radicals and photolysis for the oxidation of the SBACs. The areas of the rectangles in green, navy, black,

orange and grey represent the average relative contributions of HO·, Cl·, Cl_2^-·, ClO· and photolysis, respectively. Simulation conditions: UV intensity = 1.97×10^{-6} Einstein/L· s; free chlorine dosage range, 0.5 ppm to 4 ppm; initial concentration of each SBAC = 5×10^{-6} M; pH was buffered at 7.2. 3-MethylBA is 3-Methyl benzoic acid, 2-FluoroBA is 2-Fluorobenzoic acid, 2-ChloroBA is 2-Chlorobenzoic, 2-IodoBA is 2-Iodobenzoic acid, 3-CyanoBA is 3-Cyanobenzoic acid, 3-NitroBA is 3-Nitrobenzoic acid.

Finally, to explore the reasons why ClO· is the dominant radicals contributor to the destruction of SBACs, it is critical to investigate the intrinsic mechanisms of organic contaminants oxidation. The simplified reaction network is shown in **Figure 3.10**. The UV/free chlorine process initially generates HO· and Cl· and, then: ***(1)*** the photolysis-generated HO· mainly reacts with (i) free chlorine (HOCl/OCl^-) ($k_5=2\times10^9$ $M^{-1}s^{-1}$ and $k_6=8.8\times10^{10}$ $M^{-1}s^{-1}$) and (ii) organic compounds ($k_{HO\cdot/R}$ ranges from 1×10^9 $M^{-1}s^{-1}$ to 5×10^9 $M^{-1}s^{-1}$). By comparing the rate of HO· reacting with free chlorine (k_5[HOCl][HO·]+k_6[OCl^-][HO·]) and the rate of HO· oxidizing SBACs ($k_{HO\cdot/R}$[R][HO·]), we found that HO· reacts with free chlorine (produces ClO·) much faster than it reacts with any of the SBACs for our experimental conditions (**Figure C. 3**, **Text C.3 in Appendix C**); ***(2)*** The photolysis-generated Cl· mainly react with (i) free chlorine (HOCl/OCl^-) ($k_{46}=3\times 10^9$ $M^{-1}s^{-1}$ and $k_{47}=8.2\times 10^9$ $M^{-1}s^{-1}$), (ii) SBACs ($k_{Cl\cdot/R}$ ranges from 4×10^7 $M^{-1}s^{-1}$ to 1×10^9 $M^{-1}s^{-1}$), (iii) H_2O (k_{20}[H_2O]=1.3×10^3 s^{-1}) and (iv) Cl^- ($k_{25}=8\times 10^9$ $M^{-1}s^{-1}$). Among these four reaction rates regarding Cl· (i.e., k_{46}[HOCl][Cl·]+k_{47}[OCl^-][Cl·], $k_{Cl\cdot/R}$[R][Cl·], k_{20}[H_2O][Cl·] and k_{25}[Cl^-][Cl·]) for our experimental conditions, Cl· reacts fastest with Cl^- (producing Cl_2^-·) and, then Cl· reacts with free chlorine to produce ClO· (**Figure C.4**, **Text C.3 in Appendix C**). The dominant pathway of Cl_2^-· is to dissociate and generate Cl· again (**Text C.3 in Appendix C**), resulting in a low concentration of Cl_2^-·. Overall, the initially generated HO· and Cl· are mostly converted to ClO·, and the

dominant pathway of ClO· is to react with SBACs. Moreover, as the free chlorine dosage increases, greater fractions of HO· and Cl· will react with free chlorine to generate ClO·, which significantly increases the ClO· concentration. Therefore, as shown in **Figure 3.9**, the free chlorine dosage enhanced the relative contribution of ClO· for destruction of all six SBACs. Therefore, free chlorine acts as an important HO· and Cl· scavenger, and then ClO· is generated. The average concentration of ClO· is higher for higher initial free chlorine dosages and the SBAC destruction rate is higher (**Table 3.2**). Furthermore, we plotted the free chlorine decay for these six SBACs in **Figure C. 5**. For the certain initial dosages of free chlorine (e.g. 1 ppm), we found if free chlorine decay was larger for a given SBAC, then average concentration of ClO· for this SBAC was higher. This can be attributed to the fact that more free chlorine was converted into ClO·.

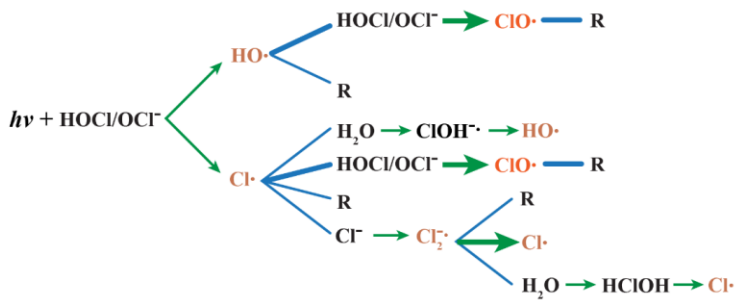

Figure 3.10. Reaction network of the oxidation of SBACs by the UV/free chlorine process. The blue lines represent reactions between two compounds, and the green arrows represent the generated reaction products. The bold blue lines and green arrows indicate the dominant reaction pathways under the experimental conditions: UV intensity = 1.97×10^{-6} Einstein/L·s; free chlorine dosage range, 0.5 ppm to 4 ppm; initial concentration of each SBAC = 5×10^{-6} M; pH was buffered at 7.2.

3.4.4 QSAR models for the second order rate constants for RCS and SBACs

In this study, four QSAR models were developed based on the linear correlation between the Hammett constants of SBACs and $k_{HO\cdot/R}$, $k_{Cl\cdot/R}$, $k_{Cl_2^-\cdot/R}$ and $k_{ClO\cdot/R}$, respectively. The linear relationship for Cl· , $Cl_2^-\cdot$, ClO· and HO· are shown in **Figure 3.11(a)**

($\log k_{Cl\cdot/R}$ = 9.11-2.13σ and R^2 = 0.976), **Figure 3.11(b)** ($\log k_{Cl_2^-\cdot/R}$ = 4.72-0.96σ and R^2 = 0.938), **Figure 3.11(c)** ($\log k_{ClO\cdot/R}$ = 6.08-0.45σ and R^2 = 0.821), and **Figure 3.11(d)** ($\log k_{OH\cdot/R}$ = 9.60-0.54σ and R^2 = 0.975), respectively. In general, the rate constants between reactive radicals and SBACs are linearly correlated with the Hammett constants, Cl· had the highest correlation coefficients. As shown in **Figure 3.11**, a certain SBAC with a larger Hammett constant typically has a smaller second-order rate constant with reactive radicals (the slopes of all four linear lines are negative). The following hypothesis was proposed to explain this phenomenon. For Cl· oxidizing SBACs, a previous study reported that the major mechanism is the addition of Cl· to the aromatic ring of the SBACs rather than H-abstraction from the aromatic ring or from the carboxylic group.[126] For a SBAC that has a larger value of the Hammett constant typically means the substituted functional group is more electron withdrawing.[43] In other words, electrons in the aromatic ring are attracted by the substituted functional group. As a result, it is more difficult for Cl· to oxidize SBACs since the electron cloud density in the aromatic ring is smaller. Some studies have hypothesized that the dominant mechanism by HO·, $Cl_2^-\cdot$ and ClO· oxidize SBACs are H-abstraction from the C-H bond on the aromatic ring.[72] Similarity, a SBAC with a larger Hammett constant contains functional groups that will attract more electrons from the aromatic ring. Hence, the reactivities of HO·, $Cl_2^-\cdot$ and ClO· are also less significant for SBACs with higher Hammett constants.

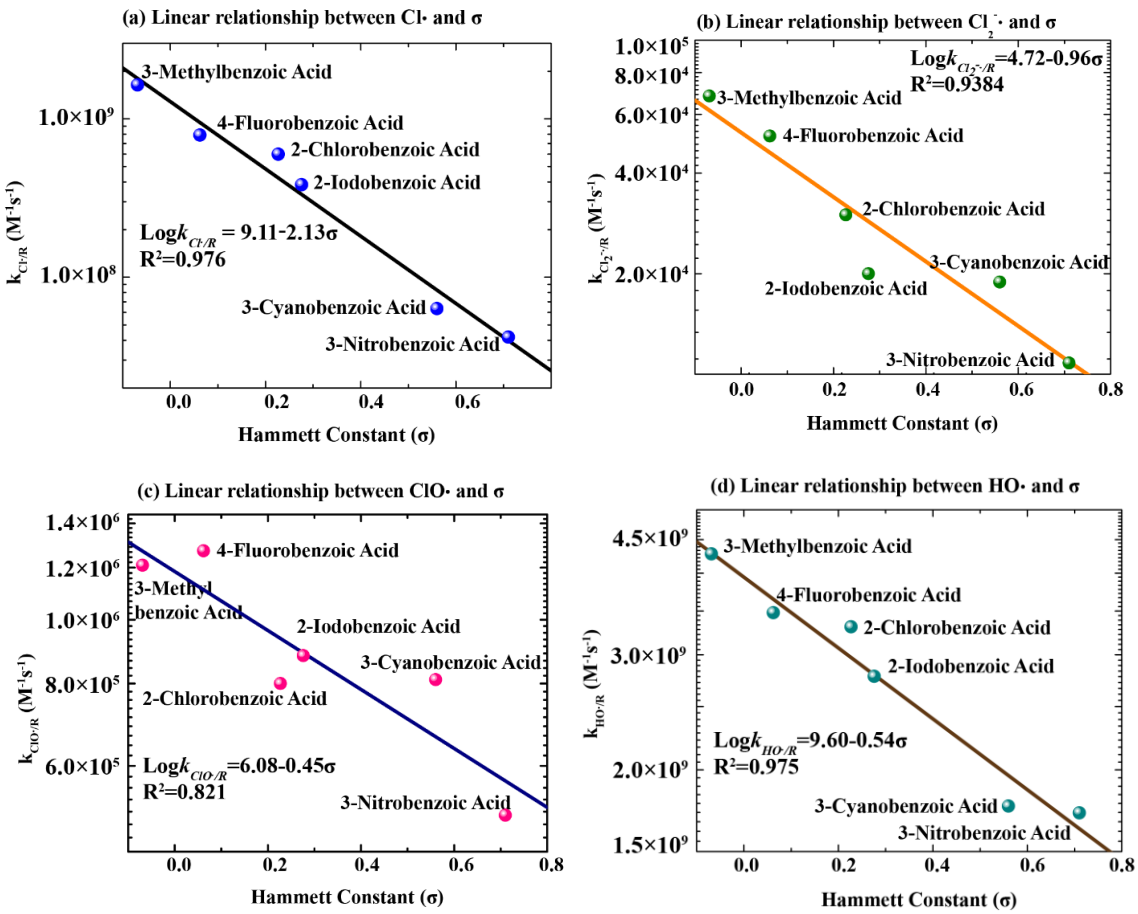

Figure 3.11. Correlations between the second-order rate constants of reactive radicals oxidizing SBACs and the Hammett constants of SBACs. The blue, green and pink symbols represent the kinetic data for Cl·, Cl_2^-·, and ClO· estimated from our dynamic kinetic model, respectively. The mint symbol represent the kinetic data for HO· estimated from GCM. The green, orange, navy and brown solid lines represent the linear equations obtained for Cl·, Cl_2^-·, ClO· and HO· in our QSARs models.

3.4.5 UV/free chlorine process optimization

UV-based photolytic reactions require a significant amount of electrical energy, and the associated energy costs are significant.[127] The electrical energy (in kWh) required to reduce the concentration of a pollutant by one order of magnitude is defined as (EE/O), and, EE/O is a useful way to evaluate energy associate cost in UV based AOPs. [10] In this study, we developed an energy efficiency estimator module as an extension of our first-principles-based kinetic model for the UV/free chlorine process. EE/O in a batch reactor

can be calculated according to eq 3.17, EE/O in a plug flow reactor is calculated using the same equation and t is the hydraulic detention time.[10]

$$EE/O=\frac{P\times t}{V\times\log(C_i/C_f)}+\frac{C\times E\times\frac{0.0022lb}{gram}}{\log(C_i/C_f)} \tag{3.17}$$

where, P is the total lamp power in kW, t is the irradiation time in s, V is the reactor volume in m^3, C_i is the target organic compound initial concentration in M, C_f is the target organic compound final concentration in M, C is the oxidant concentration in g/L, and E is the energy used to produce the oxidant in kWh/lb. **Appendix H** includes a source code example about the EE/O calculation.

Our energy efficiency estimator can be applied to evaluate the EE/O of any organic compound destruction in the UV/free chlorine process under various operational conditions. The objective of developing the energy efficiency estimator is to choose the light intensity and chlorine dosage that has the smallest EE/O. **Figure 3.12(a), (c), (e)** and **Figure C.6(a), (c), (e) in Appendix C** display six heat maps of EE/O for the these SBACs with UV intensity from 0 to 1×10^{-5} Einstein/L-s and free chlorine dosages from 0 to 0.7mM (water matrix is ultrapure). For example, the minimum EE/O of 2-iodobenzoic acid is 0.192 kWh/m^3 with optimal operation conditions of UV intensity as 2.13×10^{-7} Einstein/L-s and free chlorine as 0.104 mM . The minimum EE/O and optimal conditions for other SBACs in ultrapure water matrix were summarized in **Table C.4(a)**. It is important to note that these results are for organic free water, and, it would be possible to include scavenging of radicals and light absorption by NOM (the mass absorption coefficient of the NOM, ε_{NOM} can be measured), because we previously did this work for the UV/H_2O_2 process.[84] Since NOM can absorb UV light, we need include the absorptivity of NOM for the calculation

of A, f_{HOCl}, f_{OCl^-}, f_R if the water matrix contains NOM. According to our modeling results, the dominant species is ClO·. As a result, we can use just ClO· in the modeling analysis for the impact of NOM, and the rate constant between ClO· and NOM was reported as 4.5×10^4 L/mg-C-sec.[43] For example, we assumed ε_{NOM} as 0.107 L/mgC · cm and the initial concentration of NOM as 2mg/L,[10] then simulated six heatmaps of EE/O for these SBACs when NOM is present in **Figure 3.12(b), (d), (f)** and **Figure C.6(b), (d), (f)** (**Text S13**). The minimum EE/O and optimal conditions for other SBACs when NOM is present were summarized in **Table C.4(b)**. Accordingly, for each SBAC, the minimum EE/O when NOM is present typically ten times higher than the minimum EE/O when NOM is not present, and this is due to the fact that NOM not only absorbs UV light but also scavenges each type reactive radicals. We also found that when NOM is present the optimal UV intensity is ten times higher that of NOM is not present, and when NOM is present the optimal free chlorine initial dosage is ten times lower that of NOM is not present. This is because NOM absorbs most of input UV light of this system. Therefore, to achieve the optimal energy consumption, the UV intensity should be increased, and free chlorine dosage should be decreased. Overall, the above-mentioned method would be useful for preliminary design of the UV/free chlorine process.

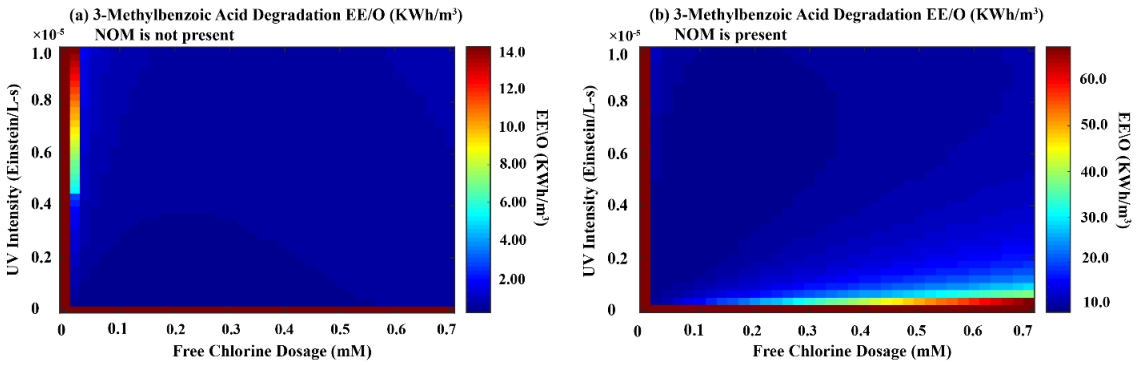

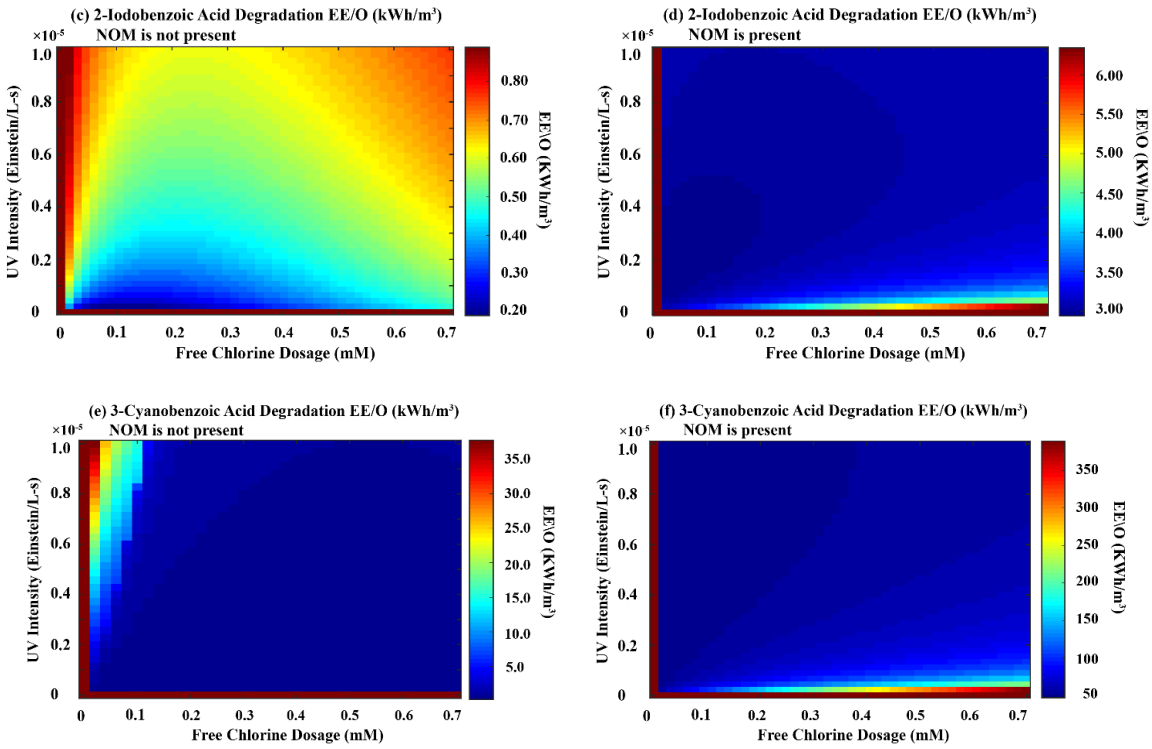

Figure 3.12. EE/O (in kWh·m^{-3}) estimation for SBACs degradation by the UV/free chlorine process with varying UV intensity and free chlorine dosage**.** Simulation conditions: UV intensity range, 0 to 1×10^{-5} Einstein/L·s ; free chlorine dosage range, 0 ppm to 50 ppm; initial concentration of each SBAC = 5×10^{-6} M; pH was buffered at 7.2. If NOM is present: initial concentration of NOM = 2 mg/L; mass absorption coefficient of NOM = 0.107 L/mgC · cm.

3.5 Environmental Implications

In this work, we successfully developed a first-principles-based kinetic model to investigate the degradation mechanisms of parent organic contaminants using the UV/free chlorine process in ultrapure water, and, our model can be used to determine the most cost-effective operation for this process (i.e., optimal light intensity and free chlorine dosage). For the practical applications, there are various ions (e.g., carbonate and bicarbonate ions, bromide ions, etc.) that may be present in the water matrix. These ions may impact on the effectiveness of the UV/free chlorine process in organic contaminants destruction. For example, ***(1)*** carbonate and bicarbonate ions (HCO_3^-/CO_3^{2-}) has been reported to inhibit the

UV/free chlorine process by some studies.[37,47,59] This is caused by the scavenging of reactive radicals by HCO_3^-/ CO_3^{2-}, and the generation of carbonate radicals ($CO_3^-\cdot$) that do not react very fast with most of organic compounds ($10^5 M^{-1}s^{-1}$ to $10^6 M^{-1}s^{-1}$).[12,85] However, according to our recent study, HCO_3^-/CO_3^{2-} only had a slight impact on the destruction rate of trimethoprim (TMP). This phenomena may be the result of a fast reaction between $CO_3^-\cdot$ and the organic compounds containing amine groups,[109] such as TMP. However, we did not investigate the impact of HCO_3^-/CO_3^{2-} on the destruction of SBACs and this will have to be examined in future work; ***(2)*** for bromide ions (Br^-), according the previous studies, HO· and reactive chlorine species (i.e. Cl·,$Cl_2^-\cdot$, ClO·) can be scavenged by bromide and then reactive bromine species (e.g. Br·,$Br_2^-\cdot$, BrO·, etc.) would be generated. As a result, the addition of Br^- will reduce the HO· and reactive chlorine species concentrations, but it would increase the concentration of reactive bromine species. Bromide has been shown to play multiple roles in the UV/free chlorine process for the Pharmaceuticals and Personal Care Products (PPCP) degradation.[128] For example, bromide decreased the degradation of ibuprofen and enhanced the degradation of carbamazepine and caffeine, respectively.[128] The multiple roles of bromide may depend on the rate constants of reactive bromine species oxidizing organic contaminants; consequently, further studies will have to investigate the relative contribution of each reactive bromine species as well as their reaction mechanisms.

For the future studies, there are two major issues that need to be resolved. First, many byproducts are generated during the degradation of parent organic compounds. Some byproducts are toxic and have smaller reaction rate constants with reactive radicals, thus they need extra time to be destroyed. The prediction in **Figure 3.6** under certain conditions

(e.g., 4-nitrobenzoic acid destruction under a free chlorine dosage of 4 ppm) are worse than others, which may be due to the impact of reaction with byproducts. Therefore, we are developing a pathway generator that will predict possible byproducts and reactions during the destruction of organic compounds in the UV/free chlorine process. Integrating the pathway generator into our model will help us evaluate the time-dependent overall toxicity of the UV/free chlorine system. Second, disinfection byproducts and their formation potential (DBPs) are major concerns for the practical application of the UV/free chlorine process. For example, free chlorine residual for one order magnitude of SBACs degradation under the optimal conditions typically ranged from 60% to 80% (**Figure C.7**, **Text C.6 in Appendix C**). In practical applications, natural organic matter can react with residual free chlorine to produce toxic DBPs. As a result, both the micropollutants and the formation potential of DBPs must be decreased (increasing in DBPFP has been found for other AOPs after some reaction time).[129] Consequently, we need to determine which of these two factors controls the design of the UV/free chlorine process. Some preliminary studies suggested that DBPs formation may not be a limiting factor for the UV/free chlorine process with careful management (e.g. avoid overdosing free chlorine),[130] but further investigations are still needed.

3.6 Acknowledgement

This work was supported by the Brook Byers Institute for Sustainable Systems, Hightower Chair and the Georgia Research Alliance at the Georgia Institute of Technology, the National Natural Science Foundation of China (51878257), the International Science and Technology Cooperation Program of China. W.Q. Zhang gratefully acknowledge the

support from the China Scholarship Council. The views and ideas expressed herein are solely the authors' and do not represent the ideas of the funding agencies in any form.

CHAPTER 4. FEASIBILE STUDY OF UV/FREE CHLORINE PROCESS FOR PRATICAL APPLICATION: OXIDATION MECHANISMS OF PHARMACEUTICALS AND FORMATION OF DISINFECTION BY-PRODUCTS

†*work from this chapter will be submitted in the following citation:*

Wang, Bing., Wang, Wei., **Zhang, Weiqiu**., Crittenden, John., Xiao, Xueting., Xu, Weijun., and Ran Zhilin., 2019. Degradation of Trimethoprim Using the UV/Free Chlorine Process: Kinetics and Influencing Factors.

Zhu, Shumin., **Zhang, Weiqiu**., Wu, Yangtao., Zhou, Shiqing., Bu, Lingjun., Dong, Bingzhi., and Crittenden, J.C., 2019. Insights into the comparison of UV/H_2O_2 and UV/chlorine processes: Kinetic Modeling, Energy Efficiency and DBPs Formation potential.

4.1 Abstract

Pharmaceuticals are emerging contaminants and have been detected worldwide in aqueous phase. UV/free chlorine process has gained attention for destroying pharmaceuticals in water matrix. To investigate the mechanisms of pharmaceuticals degradation, we developed a first-principles based kinetic model and determined the second-order rate constants between pharmaceuticals and reactive radicals (i.e. HO•, Cl•, Cl_2^-• and ClO•). We found that ClO• was the major reactant responsible for pharmaceuticals degradation. In practical application, the water matrix typically contains chloride ions (Cl^-), nature organic compound (NOM) and bicarbonate/carbonate (HCO_3^-/CO_3^{2-}). Therefore, we investigated the impact of water matrix components on the oxidation rate of pharmaceuticals in the UV/free chlorine process. We found that ***(1)*** higher pH had inhibition effect; ***(2)*** Cl^- (0.001M to 0.1M) had negligible effect; ***(3)*** HCO_3^-/CO_3^{2-} (1mM to 5mM) had slight inhibition effect; ***(4)*** NOM (1mg/L to 5 mg/L) had significant inhibition effect. Our model results agreed with our experimental data under various water matrix conditions. Furthermore, we determined the optimum operation conditions that result in the lowest energy use or EE/O. We found that the minimum EE/O required for the UV/free chlorine process to degrade pharmaceuticals was at least 3 times less than that of the UV/H_2O_2 process. Finally, we investigated disinfection byproducts (DBPs) formed during the pharmaceuticals degradation in the UV/free chlorine process, and we found DPBs did not significantly increase and less DBPs yields were observed than the UV/H_2O_2 process. Therefore, the controlling factor for UV/free chlorine process is the decreasing of micropollutants. Overall, this study revealed that the UV/free chlorine process is a promising technology for practical application at industrial scale.

4.2 Introduction

In recent years, many emerging contaminants including herbicides, odorous substances, pharmaceuticals and personal care products (PPCPs) have been found in water environment.[47] Antibiotics and antipain medications are common pharmaceuticals and widely applied in treatment and prevention of bacterial infections or pain relief. [131] For example, trimethoprim (TMP) is an antibiotic used mainly in the treatment of bladder infections. Carbamazepine (CBZ) is an antipain medication and primarily used in the treatment of neuropathic pain. The annual usage of antibiotics and antipain medications have been reported around 200 000 t globally.[131] However, once pharmaceuticals release into water matrix, there are adverse effects on human health and aquatic ecosystem. Therefore, it is necessary to remove pharmaceuticals from water environment. Nevertheless, pharmaceuticals (including TMP and CBZ) are persistent organic contaminants, and thus biological treatment process is insufficient to degrade antibiotics. Other conventional water treatment technologies (e.g. air stripping, absorption) are also unable to permanently remove pharmaceuticals.[10]

Advanced oxidation processes (AOPs) are alternative water treatment technologies. AOPs are effective to permanently destroy pharmaceuticals because the generation of various reactive radicals. For example, as the most common AOP, the UV/H_2O_2 process generates the non-selective hydroxyl radicals (HO•); Another promising AOP, the UV/free chlorine process generates HO• and chlorine radical (Cl•), Cl• is a selective oxidant that reacts fast with compounds containing aromatic rings and double bonds.[60] Subsequently, Cl_2^-• and ClO• are generated through complex radical chain reactions, Cl_2^-• and ClO• also oxide organic compounds. Many studies reported that the UV/free chlorine process

successfully destroyed some pharmaceuticals (e.g. sulfamethoxazole, diclofenac, etc.).[41] Furthermore, the UV/chlorine process has been reported more effective than the UV/H_2O_2 process (a common UV-based AOP) to destroy some micropollutants (e.g., iodoform).[59] These previous studies shed the light of some selected pharmaceuticals degradation in the UV/free chlorine process. However, the mechanisms of pharmaceuticals degradation in the UV/free chlorine process are not fully understood because complex radicals chain reactions are involved, and the second-order rate constants between pharmaceuticals and reactive radicals are lacking (i.e. HO•, Cl•, Cl_2^-• and ClO•). Previous experimental studies are difficulties to investigate the degradation mechanisms of all pharmaceuticals,[50,53] previous kinetic studies used lumped reactions or simplified pseudo steady state assumptions for simplicity,[44,45,51,56,57,58,59,60,61] and thus prevented us from obtaining a detailed insight into the degradation process.

To overcome the above-mentioned difficulties, we developed a first-principles based kinetic model for the UV/free chlorine process. Our model has been successfully used to investigate the degradation mechanisms of parent organic contaminants using the UV/free chlorine process in ultrapure water (e.g. estimating the second-order rate constants between reactive radicals and the target organic compounds, and predicting the concentration profiles of target organic compounds under various free chlorine dosage) (**Chapter 3**).[74] However, for the practical application of the UV/free chlorine to remove pharmaceuticals, the water matrix components are complex. Cl^- is one of the most common anions in water matrices; for example, Cl^- is 0.001 M in freshwater and 0.1 M in industrial wastewater.[22,23,24] Natural organic matter (NOM), bicarbonate (HCO_3^-) and carbonate (CO_3^{2-}) (HCO_3^-/CO_3^{2-}) are also commonly found in water matrices. The surface water or

ground water matrix contains typically 2 mg-C/L NOM (ranges from 1 mg-C/L to 3 mg-C/L),[10] 3 mM HCO_3^-/CO_3^{2-}.[93] Therefore, it is necessary to investigate the impact of water matrix components on the oxidation rate of pharmaceuticals in the UV/free chlorine process.

In this study, TMP and CBZ are chosen as the target pharmaceuticals. We developed a first-principles based kinetic mode to describe the kinetic behavior of pharmaceuticals (i.e. TMP and CBZ) oxidation in the UV/free chlorine process, and determine the second-order rate constants between pharmaceuticals and reactive radicals (i.e. HO•, Cl•, Cl_2^-• and ClO•). Then, we investigated the impacts of operational conditions and water matrix components (i.e. free chlorine dosage, pH, Cl^-, HCO_3^-/CO_3^{2-} and NOM) on the oxidation rate of pharmaceuticals in the UV/free chlorin process. Our model simulation results agreed with our experimental data for water matrix with various components. We explored the relative contributions of photolysis and each reactive species (i.e. HO•, Cl•, Cl_2^-• and ClO• and free chlorine). In addition, we optimized the operational conditions that result in the lowest energy consumption to degrade pharmaceuticals. Finally, since the disinfection byproducts (DBPs) and DBPs formation potential are major concerns for the practical application of the UV/free chlorine process, we investigated the DBPs formation and determined the controlling factor (e.g. micropollutants decreasing or DBPs formation potential decreasing) of this process. It is notable that we also compared the degradation efficiency, energy consumption and DBPs formation between UV/free chlorine process and the most common AOP (i.e. UV/H_2O_2 process). This study revealed that UV/free chlorine process is a more cost-effective AOPs than the UV/H_2O_2 process to degrade pharmaceuticals in the practical application.

4.3 Materials and Methods

4.3.1 Chemicals

Table 4.1. Basic properties of TMP and CBZ[132,133]

Compound	Structural formula	Molecular Weight	pKa1	pKa2
Trimethoprim (TMP) $C_{14}H_{18}N_4O_3$	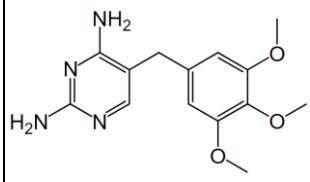	290.32 (g/mol)	3.2	7.1
Carbamazepine (CBZ) $C_{15}H_{12}N_2O$	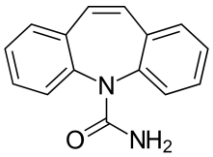	236.269(g/mol)	-3.8	15.96

4.3.1.1 Chemicals used for the degradation of TMP

These chemicals were purchased from Sigma Chemical Co., Ltd: chromatographically pure methanol; trimethoprim (98%); Suwannee River NOM (Cat. No. 2R101N); nitrobenzene (NB) (99%); sodium hypochlorite (effective free chlorine concentration 10%) and sodium thiosulfate. The solutions were buffered using phosphate. **Table 4.1** indicates the basic properties of TMP.

4.3.1.2 Chemicals used for the degradation of CBZ

All chemicals were at least analytical grade except as noted. All chemicals were used as purchased without further purification. Carbamazepine (99.0%) was obtained from Aladdin Industrial Corporation (Shanghai, China). The analyzed DBPs include THMs (i.e., chloroform ($CHCl_3$), chlorodibromomethane ($CHBr_2Cl$), bromodichloromethane ($CHBrCl_2$), and bromoform ($CHBr_3$)) and HANs (i.e., dichloroacetonitrile (DCAN), trichloroacetonitrile (TCAN), dibromoacetonitrile (DBAN), bromochloroacetonitrile

(BCAN)), they were provided by Sigma-Aldrich (MO, USA). A stock solution of free chlorine was prepared from sodium hypochlorite (5%, Sinopharm Chemical Reagent Co., Ltd., China) and standardized by the diethyl-p-phenylene diamine (DPD) colorimetric method. A stock solution of free chlorine was prepared from sodium hypochlorite (5%, Sinopharm Chemical Reagent Co., Ltd., China) and standardized by the diethyl-p-phenylene diamine (DPD) colorimetric method. All chemical solutions were prepared with ultrapure water (18.2 MΩ cm) produced by a Milli-Q academic water purification system. Then we added Cl^-, NOM (purchased from International Humic Substances Society, USA) and HCO_3^-/CO_3^{2-} into solutions, respectively. **Table 4.1** indicates the basic properties of CBZ. Since pKa1 for CBZ is -3.7 and pKa2 is 15.96, CBZ is present as uncharged molecule.

4.3.2 Experimental Procedures

4.3.2.1 Experimental procedures for the degradation of TMP

Our UV reactor is consisted of three parts (shown in **Figure 4.1**): ***(1)*** closed cardboard large container, ***(2)*** 2 UV 40 W low pressure mercury lamps that produced 254 nm UV light and ***(3)*** a magnetic stirrer. The temperature was maintained at 25°C.

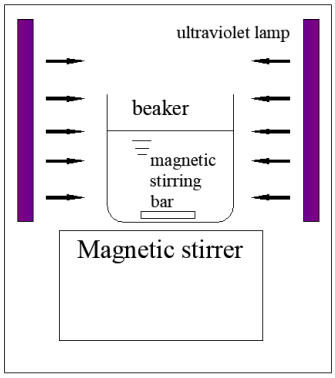

Figure 4.1. UV reactor for TMP degradation in the UV/free chlorine process

The UV photon flux (I_0) entering the solution was determined using iodide/iodate chemical actinometry in eq 4.1:

$$I_0 = C \times V \times 1/\Phi_{I_3^-} \times 1/t \quad (4.1)$$

where, I_0 is the photon flux (Es^{-1}), C is the concentration of I_3^- (M), V is the solution volume (L), and Φ is the apparent quantum yield of I_3^- (mol E^{-1}), t is the reaction time. As shown in **Figure 4.2(a)**, the slope is 0.699 and equals to $C \times 1/t$ in eq 4.1. The volume of UV reactor was 0.6 L, $\Phi_{I_3^-}$ is 0.738.[134] Hence, the UV intensity (P_{UV}) was determined to be 9.47×10^{-7} Einstein/L-s. The effective path length (L) was determined by measuring the kinetics of dilute H_2O_2 photolysis in eq 4.2:

$$dC_t/dt = (-2.303L \times I_0 \times \varepsilon_{H_2O_2} \times \Phi_{H_2O_2}/V) \times C_t = -k_{obs} \times C_t \quad (4.2)$$

where, C_t is the concentration of H_2O_2 (M) at time t, ε_{H2O2} is the molar absorption coefficient of H_2O_2 ($M^{-1}cm^{-1}$), L is the effective path length (cm), I_0 is the photon flux (Es^{-1}), V is the solution volume (L), k_{obs} is the slope of the regression line, and $\Phi_{H_2O_2}$ is the apparent quantum yield of H_2O_2 photolysis (mol E^{-1}). As shown in **Figure 4.2(b)**, the slope is 1.283×10^{-4} and equals to $-2.303L \times I_0 \times \varepsilon_{H_2O_2} \times f_{H_2O_2}/V$. At 254 nm, ε_{H2O2}=17.9 $M^{-1}cm^{-1}$-19.6 $M^{-1}cm^{-1}$, $\Phi_{H_2O_2}$=1.0 mol E^{-1},[37] I_0= 0.568 μEs^{-1}, and V=0.6 L. Therefore, the effective path length is 3.1cm.

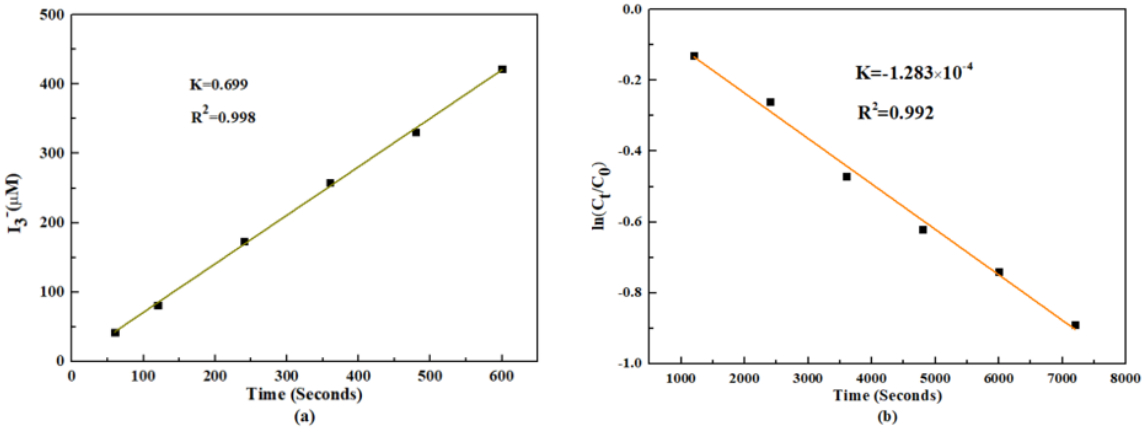

Figure 4.2. Determining UV intensity and effective path length. (a)Formation of I_3^- for KI/KIO_3 solution under irradiation at 254 nm. Conditions: 10mM Borate buffer solution; pH=9.1; 22° C; Solution volume 0.6 L; (b) Photolysis of dilute H_2O_2 under UV irradiation at 254 nm. Conditions: $[H_2O_2]_0$ = 300μM , 22 °C.

To prepare TMP stock solution, 0.01mM TMP was added to 1000 ml water. And the UV lamp was turned on for 60min before the start of the experiment. 100 mL TMP solution was added to the beaker next to the UV lamps, and then appropriate dosage of sodium hypochlorite solution was added to the test solution containing 2 mM phosphate buffer. The pH value was controlled with Phosphate buffer solution. The magnetic stirrer was set at a speed of 400r/min. The UV lamps irradiated the solution in the breaker for 20 minutes. At various time intervals within the 20 minutes, 1 mL solution sample was taken, then a few drops of 0.1 M of sodium thiosulfate was added into the solution sample to terminate the reactions among radicals and TMP. The experiments for UV alone, UV/hydrogen peroxide (H_2O_2), UV/free chlorine were conducted with the same experiment procedures, and the experiment for free chlorine alone was conducted similarity without UV light input.

4.3.2.2 Experimental procedures for the degradation of CBZ

The UV irradiation experiments were conducted in a photochemical reactor with a low-pressure mercury lamp (6 W, Heraeus Noblelight) emitting at 254 nm. The schematic schemes of UV reactor is shown in **Figure 3.1**. The UV light intensity (I_0) and effective

light path length (L) were calculated as 2.3 $\times 10^{-6}$ Einstein s^{-1} L^{-1} and 6.3 cm according to the method of our previous studies in **Chapter 3.3.2**. The experiment temperature (25±1 °C) was controlled by a recirculation water system. Solution pH was buffered with phosphate in the UV/H_2O_2 and UV/chlorine processes. The samples were quenched by excess sodium thiosulfate before analyzed.

The DBPs formation potential experiments were conducted in artificial natural water with the concentration of NOM around 2 mgC L^{-1}. After pretreatment of UV/H_2O_2 and UV/chlorine processes, residual solutions were chlorinated with 20 mg L^{-1} chlorine (in terms of Cl_2) and cultured in the dark for 24 h. Prior to DBPs analysis, the residual chlorine was quenched by excess ascorbic acid.

4.3.3 Analytical Methods

4.3.3.1 Analytical methods for the degradation of TMP

The concentrations of TMP were determined using high performance liquid chromatography. The column was a symmetry C18 column, and the mobile phase was 0.3% acetonitrile and acetic acid which had a V/V of 20:80 (Xiao et al., 2015). The detection wavelength was 280 nm, flow rate was 1.0 mL/min, and column temperature was 28°C.

4.3.3.2 Analytical methods for the degradation of CBZ

The concentration of CBZ was analyzed by a high-performance liquid chromatography (Agilent 1260, USA) equipped with a Symmetry C18 column (150 mm×4.6 mm×5 μm). The mobile phase consisted of methanol and ultrapure water at a ratio of 60:40. The injection volume and flow rate were set at 0.8 mL min^{-1} and 10 μL, respectively.

Purge-and-trap gas chromatography-mass spectrometry (PT-GC-MS) was applied to quantify the formed THMs and DCAN. The purge-and-trap sample concentrator (Tekmar Lumin, USA) used as a pretreatment can enrich volatile DBPs, which is then coupled to GC-MS (7890A-5975C, Agilent, USA) analysis. The instrumentation details are as follow: ***(1)*** purge and trap analysis: 5 mL of sample was injected into the U-tube chamber and purged at 20 ℃ for 11 min with helium at 40 mL min^{-1}; followed by the desorb mode, the trap was risen to 250 ℃ for 2 min at the flow rate of 300 mL min^{-1}; and finally baked at 280 ℃ for 2 min to clean up the trap; ***(2)*** GC–MS analysis (with a split ratio of 10:1): the initial temperature of the oven began at 30 ℃ for 9 min, increased to 40 ℃ at 2 ℃ min^{-1} and maintained for 1 min, and then raised up to 80 ℃ at 20 ℃ min^{-1}, then raised up to 160 ℃ at 40 ℃ min^{-1} and maintained for 2 min, and finally reached up to 250 ℃ at 50 ℃ and maintained for 1 min.

4.3.4 Equilibrium Calculation

4.3.4.1 Free chlorine equilibrium

pKa of free chlorine is 7.53, the free chlorine equilibrium concentrations at various pH were calculated by eq 4.3 and eq 4.4:

$$[\mathrm{HOCl}] = \frac{10^{-\mathrm{pH}}}{10^{-\mathrm{pH}} + 10^{-\mathrm{pKa}}}[\text{Total HOCl}] \tag{4.3}$$

$$[\mathrm{OCl^-}] = \frac{10^{-\mathrm{pKa}}}{10^{-\mathrm{pH}} + 10^{-\mathrm{pKa}}}[\text{Total HOCl}] \tag{4.4}$$

4.3.4.2 TMP Equilibrium

pKa1 of TMP is 3.2 and pKa2 of TPM is 7.1, the TMP equilibrium concentration at various pH are calculated by eq 4.5, eq 4.6 and eq 4.7:

$$[\mathrm{TMP^{2+}}] = \frac{(10^{-\mathrm{pH}})^2}{(10^{-\mathrm{pH}})^2 + (10^{-\mathrm{pH}})(10^{-\mathrm{pKa_1}}) + (10^{-\mathrm{pKa_1}})(10^{-\mathrm{pKa_2}})}[\text{Total TMP}] \tag{4.5}$$

$$[TMP^+] = \frac{(10^{-pH})(10^{-pKa_1})}{(10^{-pH})^2 + (10^{-pH})(10^{-pKa_1}) + (10^{-pKa_1})(10^{-pKa_2})}[\text{Total TMP}] \quad (4.6)$$

$$[TMP] = \frac{(10^{-pKa_1})(10^{-pKa_2})}{(10^{-pH})^2 + (10^{-pH})(10^{-pKa_1}) + (10^{-pKa_1})(10^{-pKa_2})}[\text{Total TMP}] \quad (4.7)$$

4.3.5 Kinetic Model Development

The details of kinetic model development approach have been described in **Chapter 3.3.4**. Briefly, we developed a first-principles based kinetic model for the UV/free chlorine process based on the elementary reactions in **Table B.1 in Appendix B** and the mass balance of involved species (eq B.1 to eq B.40). **Table B.1** includes the elementary reactions for various water matrix conditions, for example No.65 - No.70 reactions are included in our model if NOM (1mg/L to 5 mg/L) is present, No.71 – No.82 reaction are included in our model if HCO_3^-/CO_3^{2-} (1mM to 5mM) are present, etc.. It is notable that we considered the ionic strength and activity coefficients (eq 2.1) for charged species if Cl^- or HCO_3^-/CO_3^{2-} are present. We estimated unknown rate constants by fitting our experimental data, we implemented genetic algorithm to minimize the objective function in eq 3.6. **Appendix D** includes a source code of objective function and **Appendix F** includes a source code of genetic algorithm developed in MATLAB R2018b. To describe the kinetic behavior of pharmaceuticals degradation in UV/free chlorine process, we implemented the gear's algorithm to solve the ODEs system and obtain the time-dependent concentration profiles of pharmaceuticals and reactive radicals. **Appendix F** includes a source code of gear's method. Similarity, the first-principles based kinetic model for the UV/H_2O_2 process was developed based on the elementary reactions in **Table I.1 in Appendix I**.

4.4 Results and Discussion

4.4.1 Degradation of Pharmaceuticals by UV, H_2O_2, Free Chlorine, UV/H_2O_2 and UV/Free Chlorine Processes

We first compared the destruction of TMP and CBZ using UV alone, free chlorine alone, H_2O_2 alone, UV/free chlorine and UV/H_2O_2 processes. According to **Figure 4.3**, the TMP degradations by various oxidation processes follow a pseudo first-order reaction. The pseudo-first-order rate constants for UV/H_2O_2, free chlorine oxidation alone and UV/free chlorine processes are $1.2\times10^{-3}s^{-1}$, $3.5\times10^{-3}s^{-1}$, $9.8\times10^{-3}s^{-1}$, respectively. UV alone does not oxidize TMP because the TMP quantum yields are small, for example the quantum yield of TMP has been reported as 0.00149.[135] According to **Figure 4.4**, the degradation of CBZ was negligible (less than 5%) within 10 min using UV irradiation alone, which indicates that CBZ cannot be oxidized by UV directly and this phenomenon is consistent with previous studies.[136] After treated by H_2O_2 or chlorination in dark, the CBZ concentrations remained almost the same as CBZ initial concentration, and thus the direct contribution of oxidants (i.e. H_2O_2 or free chlorine) for CBZ degradation was negligible. In contrast, when adding the equivalent dosage of oxidants (100 μM H_2O_2 or free chlorine) into UV system respectively, the efficiency of CBZ degradation significantly enhanced. Within 4 minutes, the UV/H_2O_2 achieved 88.0% removal efficiency and the UV/free chlorine process achieved 92.6% removal efficiency. Since CBZ cannot be degraded by either UV irradiation alone or oxidants (H_2O_2 or free chlorine) alone, the high removal efficiency of CBZ could be attributed to the radicals generated from the UV/free chlorine and UV/H_2O_2 processes. Overall, UV/free chlorine is the most efficient process to oxidize both of TMP and CBZ.

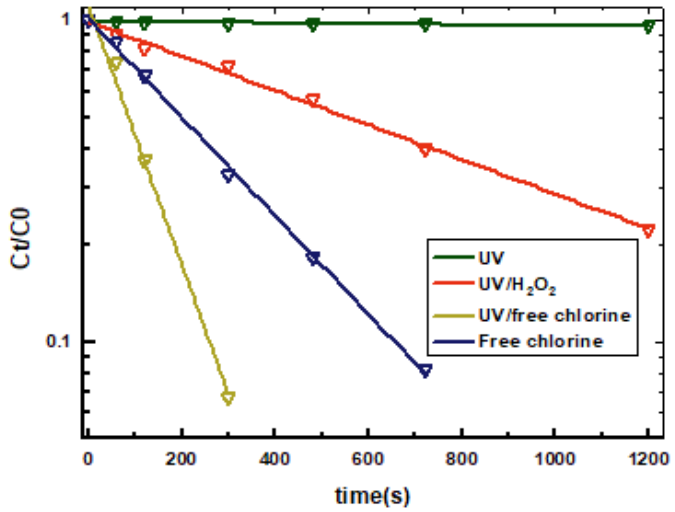

Figure 4.3. Degradation of TMP under different processes. Conditions: $[TMP]_0$=0.01mM, $[H_2O_2]_0$= [free chlorine]$_0$=0.05mM, UV light intensity=9.47×10^{-7} Einstein/L·s, pH=7.2.

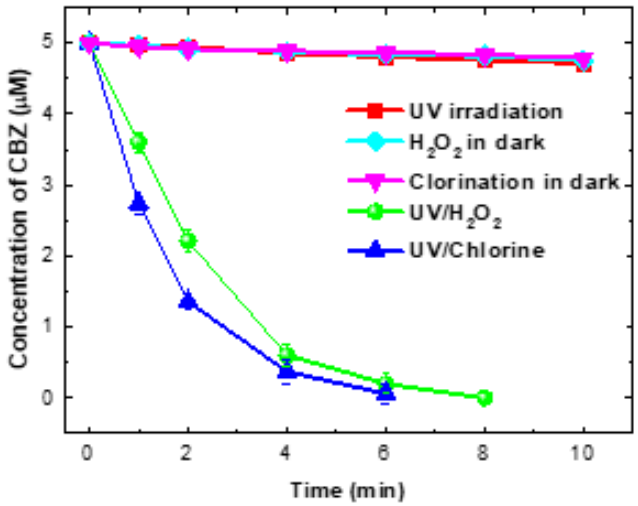

Figure 4.4. Degradation of CBZ under different processes. Experimental conditions: $[CBZ]_0$=5.0 μM, $[H_2O_2]_0$=[chlorine]$_0$= 100 μM, UV intensity= 2.3×10^{-6} Einstein/L·s .

4.4.2 Estimation of Rate Constants for Pharmaceuticals Oxidation

According to **Figure 4.3**, TMP can be oxidized by free chlorine alone. Therefore, we first estimated the rarely reported rate constants between HOCl/OCl^- and TMP^{2+}/TMP^+/TMP ($k_{HOCl/TMP^{2+}}$, k_{HOCl/TMP^+} , $k_{HOCl/TMP}$, $k_{OCl^-/TMP^{2+}}$, k_{OCl^-/TMP^+} and $k_{OCl^-/TMP}$). As shown in **Figure 4.5**, we simultaneously fitted all experimental data of free

chlorine alone oxidizing TMP under various pH conditions. We used the GA to achieve the minimum objective function (OF_{min}, eq 3.6), and the value of OF_{min} is 0.124. The estimated values of rate constants between HOCl/OCl^- and TMP^{2+}/TMP^+/TMP are shown in **Table 4.2**. Then, we estimated the rarely reported rate constants between reactive chlorine species (i.e. Cl•, Cl_2^-• and ClO•) and TMP^{2+}/TMP^+/TMP. As shown in **Figure 4.6**, we simultaneously fitted all experimental data of UV/free chlorine oxidizing TMP under various pH conditions. The estimated rate constants between Cl•, Cl_2^-• and ClO• and TMP^{2+}/TMP^+/TMP are summarized in **Table 4.2**, and the minimum objective function value is 0.506. The second-order rate constant between HO• and TMP has been reported as $(6.9\pm0.2)\times10^9 M^{-1}s^{-1}$.[137]

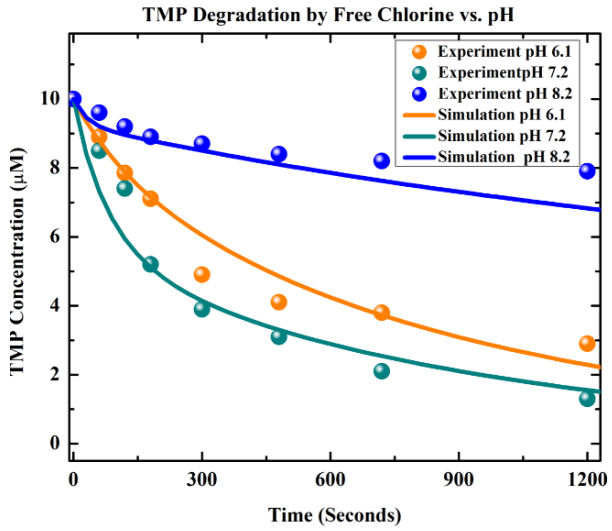

Figure 4.5. Degradation of TMP by free chlorine alone under various pH conditions. Conditions: $[TMP]_0$=0.01mM, $[\text{free chlorine}]_0$=0.05mM, pH 6.1, 7.2, 8.2.

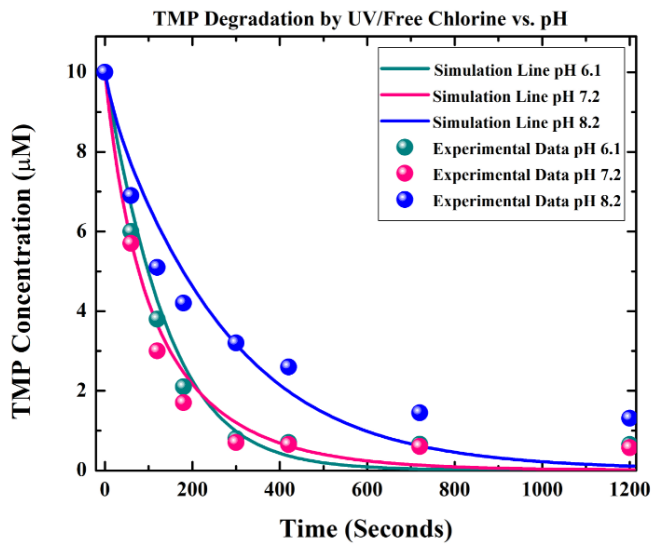

Figure 4.6. Degradation of TMP in UV/free chlorine process under various pH. Conditions: $[TMP]_0$=0.01mM, [free chlorine]$_0$=0.05mM, UV light intensity=9.47×10^{-7} Einstein/L·s.

Table 4.2. Estimated rate constants for TMP degradation in the UV/free chlorine process

1	$TMP^{2+} + OH\bullet \rightarrow \text{byproducts}$	$k_{HO\bullet/TMP^{2+}} = 7.10\times10^{9}$
2	$TMP^{2+} + Cl\bullet \rightarrow \text{byproducts}$	$k_{Cl\bullet/TMP^{2+}} = 6.52\times10^{9}$ (Fitted)
3	$TMP^{2+} + Cl_2^-\bullet \rightarrow \text{byproducts}$	$k_{Cl_2^-\bullet/TMP^{2+}} = 8.52\times10^{4}$ (Fitted)
4	$TMP^{2+} + ClO\bullet \rightarrow \text{byproducts}$	$k_{ClO\bullet/TMP^{2+}} = 9.20\times10^{6}$ (Fitted)
5	$TMP^{+} + OH\bullet \rightarrow \text{byproducts}$	$k_{HO\bullet/TMP^{+}} = 6.90\times10^{9}$
6	$TMP^{+} + Cl\bullet \rightarrow \text{byproducts}$	$k_{Cl\bullet/TMP^{+}} = 3.09\times10^{9}$ (Fitted)
7	$TMP^{+} + Cl_2^-\bullet \rightarrow \text{byproducts}$	$k_{Cl_2^-\bullet/TMP^{+}} = 4.75\times10^{4}$ (Fitted)
8	$TMP^{+} + ClO\bullet \rightarrow \text{byproducts}$	$k_{ClO\bullet/TMP^{+}} = 2.77\times10^{6}$ (Fitted)
9	$TMP + OH\bullet \rightarrow \text{byproducts}$	$k_{HO\bullet/TMP} = 6.70\times10^{9}$
10	$TMP + Cl\bullet \rightarrow \text{byproducts}$	$k_{Cl\bullet/TMP} = 7.76\times10^{9}$ (Fitted)
11	$TMP + Cl_2^-\bullet \rightarrow \text{byproducts}$	$k_{Cl_2^-\bullet/TMP} = 1.05\times10^{4}$ (Fitted)
12	$TMP + ClO\bullet \rightarrow \text{byproducts}$	$k_{ClO\bullet/TMP} = 1.93\times10^{6}$ (Fitted)
13	$TMP^{2+} + HOCl \rightarrow \text{byproducts}$	$k_{TMP^{2+}/HOCl} = 2.16\times10^{2}$ (Fitted)
14	$TMP^{+} + HOCl \rightarrow \text{byproducts}$	$k_{TMP^{+}/HOCl} = 2.20\times10^{1}$ (Fitted)
15	$TMP + HOCl \rightarrow \text{byproducts}$	$k_{TMP/HOCl} = 3.40\times10^{1}$ (Fitted)
16	$TMP^{2+} + OCl^- \rightarrow \text{byproducts}$	$k_{TMP^{2+}/OCl^-} = 5.00\times10^{1}$ (Fitted)

17	$TMP^{+} + OCl^{-} \rightarrow$ byproducts	$k_{TMP^{+}/OCl^{-}} = 7.90\times10^{2}$ (Fitted)
18	$TMP + OCl^{-} \rightarrow$ byproducts	$k_{TMP/OCl^{-}} = 1.00\times10^{-2}$ (Fitted)

According to **Figure 4.4**, CBZ cannot be oxidized by UV or free chlorine alone. Therefore, we first estimated the rate constant between HO· and CBZ. As shown in **Figure 4.7**, we simultaneously fitted all experimental data of CBZ degradation in the UV/H_2O_2 process with various H_2O_2 dosage (OF_{min} is 0.155). Then, we estimated the rarely reported rate constant between CBZ and Cl·, Cl_2^-· and ClO·. As shown in **Figure 4.8**, we simultaneously fitted all experimental data of UV/free chlorine oxidizing CBZ under various free chlorine dosage. The estimated rate constants between CBZ and HO·, Cl·, Cl_2^-· and ClO· are summarized in **Table 4.3**.

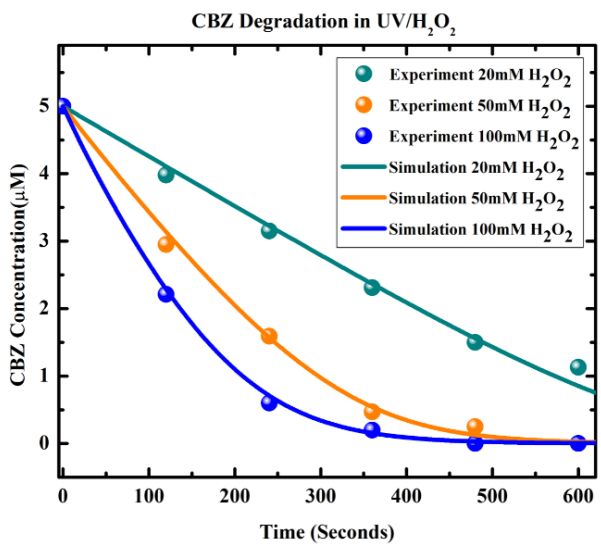

Figure 4.7. Degradation of CBZ under different oxidant dosages in the UV/H_2O_2 Experimental conditions: $[CBZ]_0$= 5.0 μM, $[H_2O_2]_0$= 20~100 μM, UV intensity= 2.3×10^{-6} Einstein/L·s.

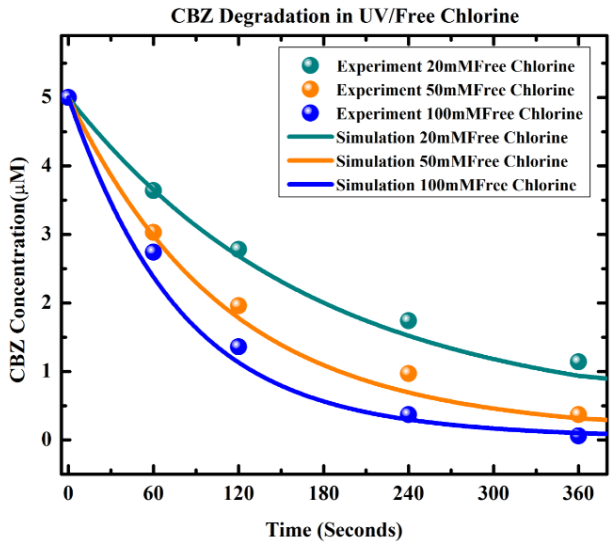

Figure 4.8. Degradation of CBZ under different oxidant dosages in the UV/Free Chlorine. Experimental conditions: $[CBZ]_0$= 5.0 μM, $[\text{Free Chlorine}]_0$= 20~100 μM, UV intensity= 2.3×10^{-6} Einstein/L·s.

Table 4.3. Estimated rate constants for CBZ degradation in the UV/free chlorine process

1	$CBZ + OH\bullet \rightarrow \text{byproducts}$	$k_{HO\bullet/CBZ} = 1.28\times10^{9}$ (Fitted)
2	$CBZ + Cl\bullet \rightarrow \text{byproducts}$	$k_{Cl\bullet/CBZ} = 1.84\times10^{9}$ (Fitted)
3	$CBZ + Cl_2^-\bullet \rightarrow \text{byproducts}$	$k_{Cl_2^-\bullet/CBZ} = 1.03\times10^{5}$ (Fitted)
4	$CBZ + ClO\bullet \rightarrow \text{byproducts}$	$k_{ClO\bullet/CBZ} = 1.78\times10^{6}$ (Fitted)

4.4.3 Contribution of Reactive Radicals, Free Chlorine and UV Photolysis

From **Figure 4.3** and **Figure 4.4**: ***(1)*** both of TMP and CBZ cannot be degraded by UV alone, and hence the contributions of UV degrading TMP and CBZ are negligible; ***(2)*** CBZ cannot be degraded by free chlorine alone, and hence the contribution of free chlorine oxidizing CBZ is also negligible. However, free chlorine is effective to oxidize TMP, and hence the contribution of free chlorine oxidizing TMP cannot be ignored. We calculated the average contribution of reactive radicals and free chlorine oxidizing TMP or CBZ using eq 3.11 – eq 3.16. **Appendix G** includes a source code example for the calculations of contributions of reactive radicals, free chlorine and UV photolysis. **Figure 4.9** indicates

the average contribution of reactive radicals and free chlorine oxidizing TMP under various pH conditions. **Figure 4.10** indicates the average contribution of reactive radicals oxidizing CBZ under various free chlorine dosage. Accordingly, ClO· makes the most dominant contributions to oxidize both TMP under various pH and CBZ under various free chlorine dosage. As we have discussed in **Chapter 3.4.3**, ClO· makes the most contributions because the initially generated HO· and Cl· are mostly converted to ClO·, and the dominant pathway of ClO· is to react with SBACs. For TMP oxidation in the UV/free chlorine process, as pH is 6.1 or 7.2 the relative average contributions follow the order of ClO· >free chlorine> Cl· >HO· >Cl_2^-· ; as pH is 8.2, the relative average contributions follow the order of ClO· > Cl· >free chlorine>HO· >Cl_2^-·; For CBZ oxidation in the UV/free chlorine process under various free chlorine dosage, the relative average contributions of different RCS radicals follow the order of ClO· > Cl· >HO· > Cl_2^-·. Moreover, as the chlorine dosage increases in **Figure 4.10**, the contribution of ClO· increases while the contribution of HO· and Cl· decreased gradually, which because more HO· and Cl· are converted into ClO·.

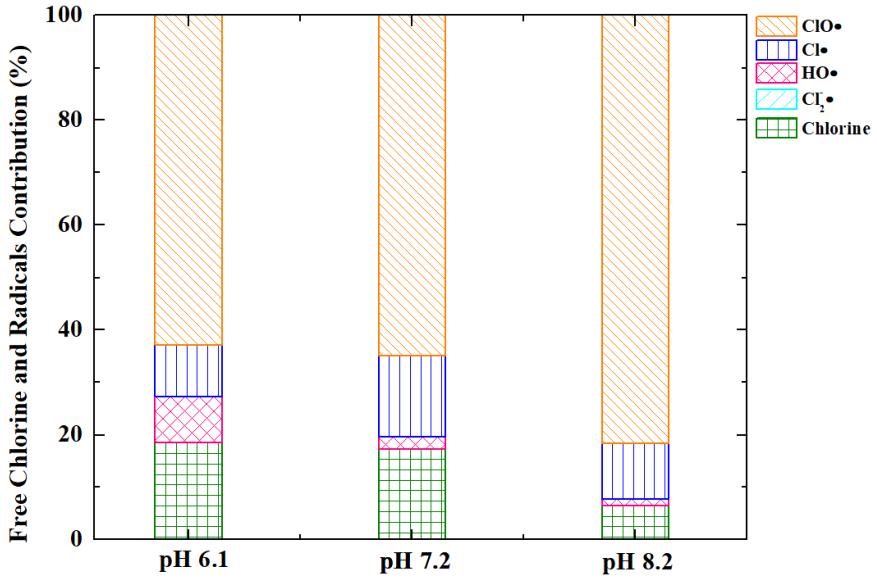

Figure 4.9. Relative average contribution of reactive radicals and free chlorine oxidizing TMP under various pH. [TMP] $_0$ = 0.01 mM, [free chlorine] $_0$ = 0.05 mM, UV light intensity=9.47×10^{-7} Einstein/L·s.

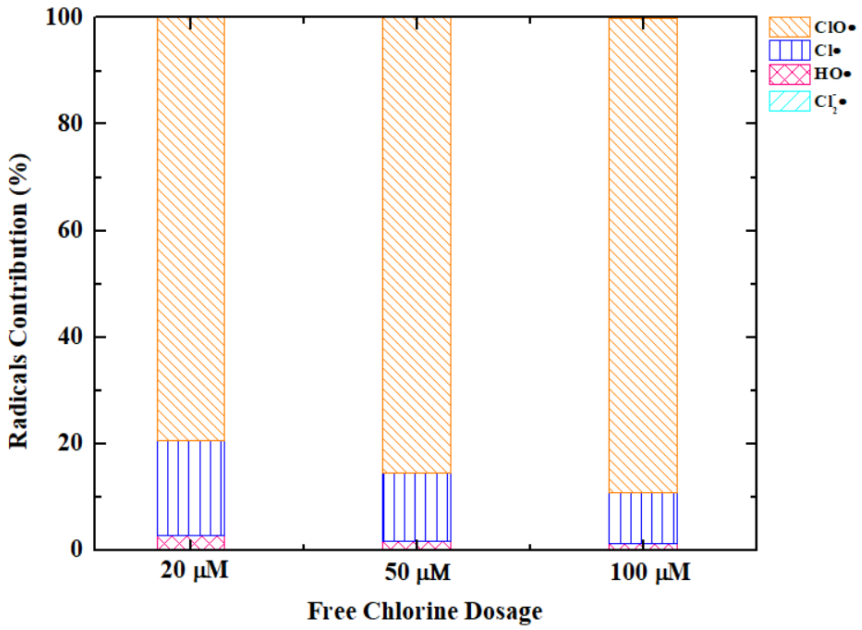

Figure 4.10. Relative average contribution of reactive radicals and free chlorine oxidizing CBZ under various free chlorine dosage. [CBZ] $_0$ = 0.005 mM, [free chlorine] $_0$ = 0.02 mM – 0.1 mM, UV light intensity=2.3×10^{-6} Einstein/L·s.

4.4.4 Impact of pH

The degradation of TMP in the UV/free chlorine process under various pH is shown in **Figure 4.6**. Accordingly, higher pH (e.g. pH >8) inhibits the TMP degradation rate

because ***(1)*** free chlorine exists as HOCl in acidic or weakly basic conditions (pH<7.35), and free chlorine exists as OCl^- in alkaline conditions (e.g. pH >8). HOCl has higher quantum yield and molar absorption coefficient than OCl^-, which results in generating more HO• and Cl•; ***(2)*** free chlorine alone destroys TMP slower at high pH than low pH as shown in **Figure 4.5**. It is notable that the difference between model simulation and experimental data are large when time exceeds 1000 seconds in **Figure 4.6**. After 1000s, the experimental data show TMP is almost not degraded under various pH conditions, in another word, the residual free chlorine is small. However, the model simulation results show TMP is still degraded after 1000s, and the model predicted that residual free chlorine ranges from 30% to 40% at 1200s for pH values from 6.1 to 8.2. The large difference between model results and experimental data can be attribute to the fact that TMP is large molecule, and thus many byproducts are generated during the TMP degradation, some of byproducts may react rapidly with free chlorine. However, the current version of our kinetic model does not include byproducts and relevant reactions.

4.4.5 Impact of Chloride Ions

Chloride ion (Cl^-) is ubiquitous in surface waters. **Figure 4.11** indicates the oxidation of TMP by the UV/free chlorine process under various Cl^- concentrations (1mM – 5mM) in the water matrix. **Figure 4.12(a)** and **Figure 4.12(b)** indicate the oxidation of CBZ by the UV/H_2O_2 and UV/free chlorine processes under various Cl^- concentrations (1mM – 0.1 M) in the water matrix. Our model prediction results agree with our experimental data in **Figure 4.11** and **Figure 4.12**. Accordingly, Cl^- has negligible effect on the oxidation rate of CBZ in the UV/H_2O_2 process. This finding is consist with our previous work in **Chapter 2**.[39] Cl^- (1mM – 0.1M) also slightly reduces the oxidation rate of both TMP and CBZ

degradation in the UV/free chlorine process. This phenomenon comes from the fact that ***(1)*** HO· reacts Cl^- to generate $ClOH^-$· (HO·+Cl^-→ $ClOH^-$·) but $ClOH^-$· rapidly dissociates into HO· ($ClOH^-$· →HO·+Cl^-; ***(2)*** Cl^- rapidly reacts with Cl· to form Cl_2·$^-$ (Cl·+Cl^-→ Cl_2·$^-$). However, Cl_2·$^-$ dissociates fast to generate Cl· again (Cl_2·$^-$→ Cl·+Cl^-) rather than reacts fast with TMP or CBZ; ***(3)*** ClO· makes the dominant contribution to oxidize TMP and CBZ, and ClO· is not scavenged by Cl^- . Many previous studies also reported that Cl^- slightly impacts on the effectiveness of the UV/free chlorine destroying other organic compounds (e.g. benzoic acid, clofibric acid, ibuprofen, etc.).[37,44,45]

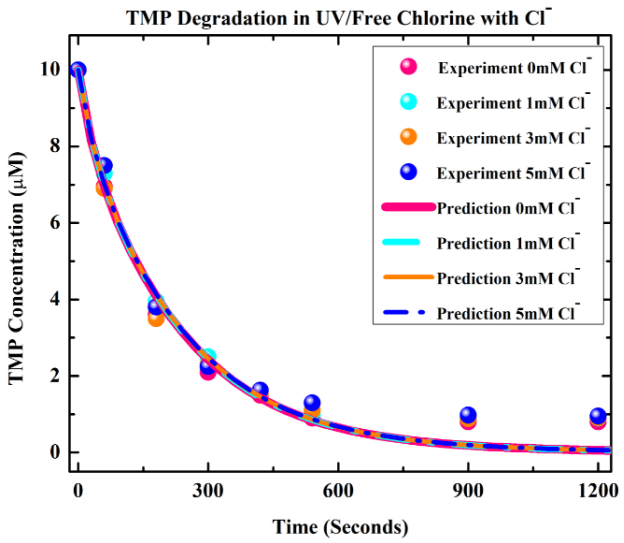

Figure 4.11. Impact of Cl^- on the degradation of TMP in the UV/free chlorine process. Experimental condition: $[TMP]_0$=0.01mM, [free chlorine]$_0$=0.05mM, $[Cl^-]_0$=1 mM to 5 mM, UV light intensity=9.47×10^{-7} Einstein/L·s.

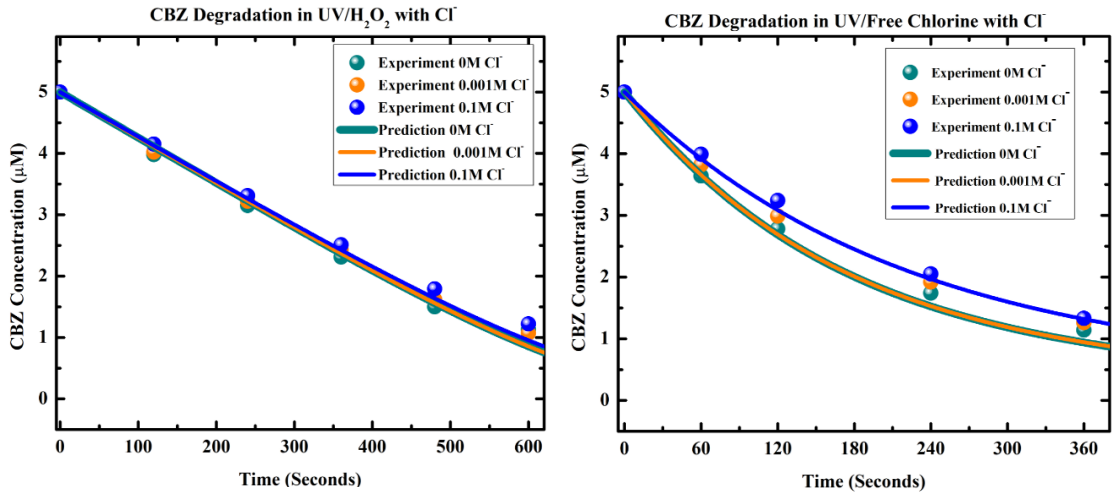

(a) **(b)**

Figure 4.12. Impact of Cl^- on the degradation of CBZ degradation in (a) UV/H_2O_2 process and (b) UV/free chlorine process. Experimental conditions: $[CBZ]_0$ = 5.0 μM, $[H_2O_2]_0$ = $[chlorine]_0$ = 20 μM, $[Cl^-]_0$=1 mM to 0.1 M, UV intensity= 2.3×10^{-6} Einstein/L·s .

4.4.6 Impact of Alkalinity

Bicarbonate and carbonate ions (HCO_3^-/CO_3^{2-}) are common components in water matrix. **Figure 4.13** indicates the oxidation of TMP by the UV/free chlorine process under various HCO_3^-/CO_3^{2-} concentrations (1mM – 5mM) in the water matrix. **Figure 4.14(a)** and **Figure 4.14(b)** indicate the oxidation of CBZ by the UV/H_2O_2 and UV/free chlorine processes under various HCO_3^-/CO_3^{2-}concentrations (1mM – 2mM) in the water matrix. Our model results agree with our experimental data in **Figure 4.13** and **Figure 4.14**. Accordingly, HCO_3^-/CO_3^{2-} reduce the oxidation rate of CBZ in the UV/H_2O_2 process. This phenomenon may because HO• can be scavenged by HCO_3^-/CO_3^{2-} (rate constants: 8.5×10^6 $M^{-1}s^{-1}$/3.9×10^9 $M^{-1}s^{-1}$) and generate CO_3^-• . We fitted all experimental data in **Figure 4.14(a)** simultaneously to estimate the rate constants between CO_3^-• and CBZ as 4.51×10^6 $M^{-1}s^{-1}$ (OF_{min} = 0.0768). However, the we found HCO_3^-/CO_3^{2-} slightly reduce the oxidation rate of both TMP and CBZ in the UV/free chlorine process. This phenomenon can be attributed to the fact that ***(1)*** ClO• makes the dominant contribution to oxidize TMP and CBZ. The

scavenge of ClO· by HCO_3^- is negligible, and the scavenge of ClO· by CO_3^{2-} with very slow rate constants (<600 $M^{-1}s^{-1}$); ***(2)*** HO·, Cl·, $Cl_2^{\cdot-}$ and ClO· are scavenged by HCO_3^-/CO_3^{2-} and generate $CO_3^{\cdot-}$. Previous study has reported that $CO_3^{\cdot-}$ has fast reaction with organic compounds containing amine groups including TMP and CBZ.[109] For example, the rate constants between $CO_3^{\cdot-}$ and TMP or CBZ are 3.47×10^7 $M^{-1}s^{-1}$ and 4.51×10^6 $M^{-1}s^{-1}$, respectively.[138]

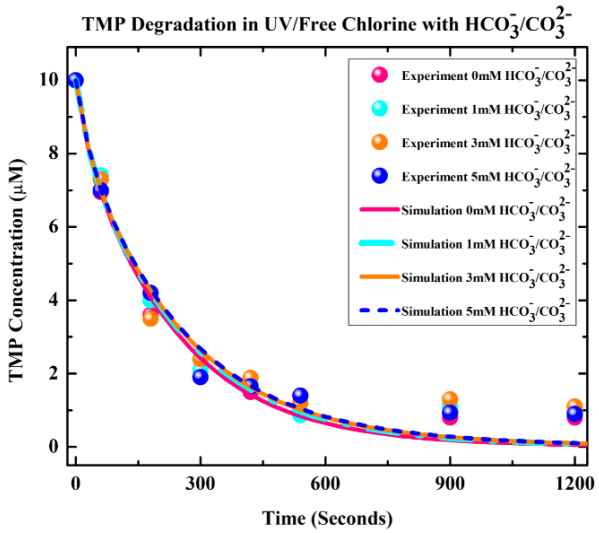

Figure 4.13. Impact of HCO_3^-/CO_3^{2-} on the degradation of TMP in the UV/free chlorine process. Experimental condition: $[TMP]_0$=0.01mM, $[\text{free chlorine}]_0$=0.05mM, $[HCO_3^-/CO_3^{2-}]_0$=1 mM to 5 mM, UV light intensity=9.47×10^{-7} Einstein/L·s .

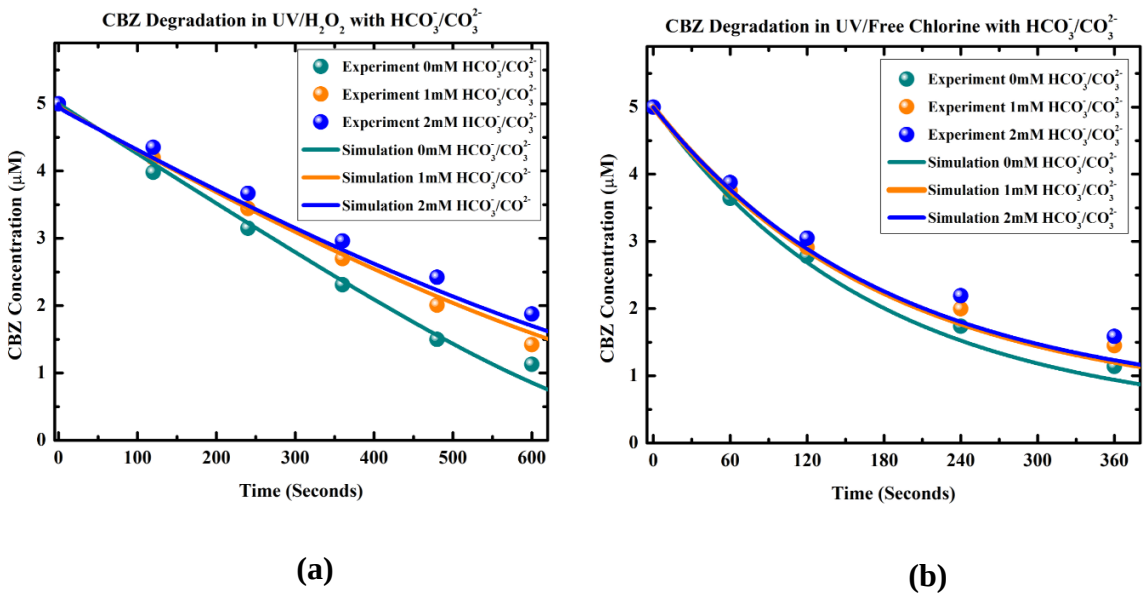

(a) **(b)**

Figure 4.14.Impact of HCO_3^-/CO_3^{2-} on the degradation of CBZ degradation in (a) UV/H_2O_2 process and (b) UV/free chlorine process. Experimental conditions: $[CBZ]_0$ = 5.0 μM, $[H_2O_2]_0$ = $[chlorine]_0$ = 20 μM, $[HCO_3^-/CO_3^{2-}]_0$=1 mM to 2 mM, UV intensity= 2.3×10^{-6} Einstein/L·s.

4.4.7 Impact of NOM

NOM is commonly found in water matrix. **Figure 4.15** indicates the oxidation of TMP by the UV/free chlorine process under various NOM concentrations (1 mgC/L – 5 mgC/L) in the water matrix. **Figure 4.16(a)** and **Figure 4.16(b)** indicate the oxidation of CBZ by the UV/H_2O_2 and UV/free chlorine processes under various NOM concentrations (2 mg-C/L – 4 mg-C/L) in the water matrix. Our model results agree with our experimental data in **Figure 4.15** and **Figure 4.16**. Accordingly, NOM significantly reduces the oxidation rate of CBZ in the UV/H_2O_2 process. In addition, NOM also significantly reduces the oxidation rate of both TMP and CBZ in the UV/free chlorine process. These phenomena come from the fact ***(1)*** NOM is known as a typical photosensitizer, and hence NOM is able to absorb UV light. Since NOM is a complex mixture of different compounds with varying chemical properties, the absorption coefficient of various NOM (ε_{NOM}) is different.[10] For example, ε_{NOM} is 0.041 $(mg\text{-}C/L)^{-1}s^{-1}$ for the NOM used in the

degradation of TMP, and ε_{NOM} is 0.0065 $(mg\text{-}C/L)^{-1}s^{-1}$ for the NOM used in the degradation of CBZ; ***(2)*** NOM scavenges reactive radicals (i.e. HO•, Cl•, Cl_2^-• and ClO•) and free chlorine. Various NOM has different rate constants with reactive radicals and free chlorine ($k_{HO\cdot/NOM}$, $k_{Cl\cdot/NOM}$, $k_{Cl_2^-\cdot/NOM}$, $k_{ClO\cdot/NOM}$, $k_{HOCl/NOM}$ and $k_{OCl^-/NOM}$). For example, we fitted all experimental data in **Figure 4.15** simultaneously, then for the NOM used in the degradation of TMP: $k_{HO\cdot/NOM}$ is 2.5×10^4 $(mg\text{-}C/L)^{-1}s^{-1}$, $k_{Cl\cdot/NOM}$ is 1.3×10^4 $(mg\text{-}C/L)^{-1}s^{-1}$, $k_{Cl_2^-\cdot/NOM}$ is 1×10^2 $(mg\text{-}C/L)^{-1}s^{-1}$, $k_{ClO\cdot/NOM}$ is 8.66×10^1 $(mg\text{-}C/L)^{-1}s^{-1}$, $k_{HOCl/NOM}$ is 1.5×10^{-5} $(mg\text{-}C/L)^{-1}s^{-1}$ and $k_{OCl^-/NOM}$ is 1.2×10^{-5} $(mg\text{-}C/L)^{-1}s^{-1}$. We fitted all experimental data in **Figure 4.16(a)** and **Figure 4.16(b)** simultaneously, then for the NOM used in the degradation of CBZ: $k_{HO\cdot/NOM}$ is 1.98×10^2 $(mg\text{-}C/L)^{-1}s^{-1}$, $k_{Cl\cdot/NOM}$ is 1.87×10^1 $(mg\text{-}C/L)^{-1}s^{-1}$, $k_{Cl_2^-\cdot/NOM}$ is 2.13×10^1 $(mg\text{-}C/L)^{-1}s^{-1}$, $k_{ClO\cdot/NOM}$ is 5.34 $(mg\text{-}C/L)^{-1}s^{-1}$, $k_{HOCl/NOM}$ is 1.46×10^{-5} $(mg\text{-}C/L)^{-1}s^{-1}$ and $k_{OCl^-/NOM}$ is 1.33×10^{-5} $(mg\text{-}C/L)^{-1}s^{-1}$.

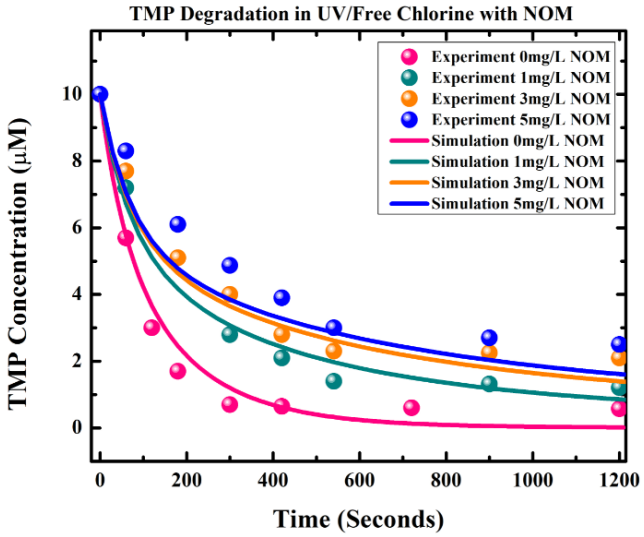

Figure 4.15. Impact of NOM on the degradation of TMP in the UV/free chlorine process. Experimental condition: $[TMP]_0$=0.01mM, $[\text{free chlorine}]_0$=0.05mM, $[NOM]_0$=1 mg/L to 5 mg/L, UV light intensity=9.47×10^{-7} Einstein/L·s.

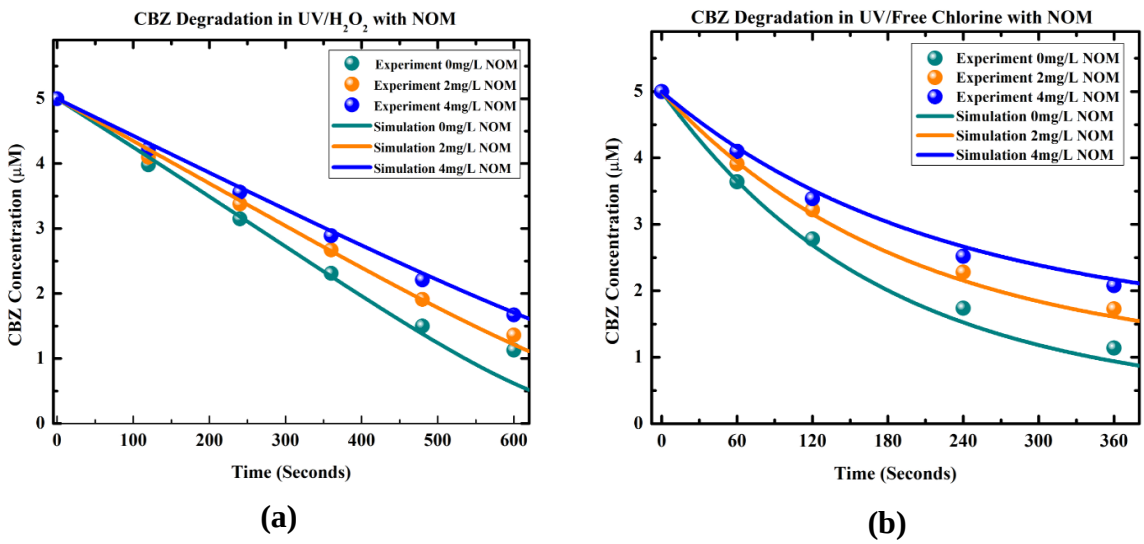

(a) **(b)**

Figure 4.16. Impact of NOM on the degradation of CBZ degradation in (a) UV/H_2O_2 process and (b) UV/free chlorine process. Experimental conditions: $[CBZ]_0$ = 5.0 μM, $[H_2O_2]_0$ = $[chlorine]_0$ = 20 μM, $[NOM]_0$=2 mg/L to 4 mg/L, UV intensity= 2.3×10^{-6} Einstein/L·s.

4.4.8 Comparison of EE/O in the UV/Free Chlorine and UV/H_2O_2 processes

At current stage, the UV/H_2O_2 process is most common AOP at industrial scale. To investigate the feasibility of the UV/free chlorine process for practical application, it is necessary to compare the electrical energy required for the UV/free chlorine process and the UV/ H_2O_2 process to reduce the concentration of a pollutant by one order of magnitude. Therefore, we developed the energy efficiency estimator to calculate the minimum EE/O for the UV/free chlorine and the UV/H_2O_2 processes by using eq 3.17. To simulate the water matrix in practical application, we chose Cl^- initial concentration as 0.01 M, NOM initial concentration as 2 mg/L and HCO_3^-/CO_3^{2-} concentration as 2mM for the EE/O calculation. **Appendix H** includes a source code example of EE/O calculation developed in MATLAB R2018b. As shown in figure X(a), the minimum EE/O for the UV/H_2O_2 process to degrade CBZ is 0.44 kWh/m^3-s, and the optimal H_2O_2 dosage is 0.303 mM and the optimal UV intensity 2.02×10^{-7} Einstein/L-s. As shown in figure X(a), the minimum

EE/O for the UV/free chlorine process to degrade CBZ is 0.126 kWh/m^3-s, and the optimal free chlorine dosage is 0.101 mM and the optimal UV intensity 1.01×10^{-7} Einstein/L-s. Overall, the UV/free chlorine saves at least 3 times energy than the UV/H_2O_2 process under the optimal operational conditions.

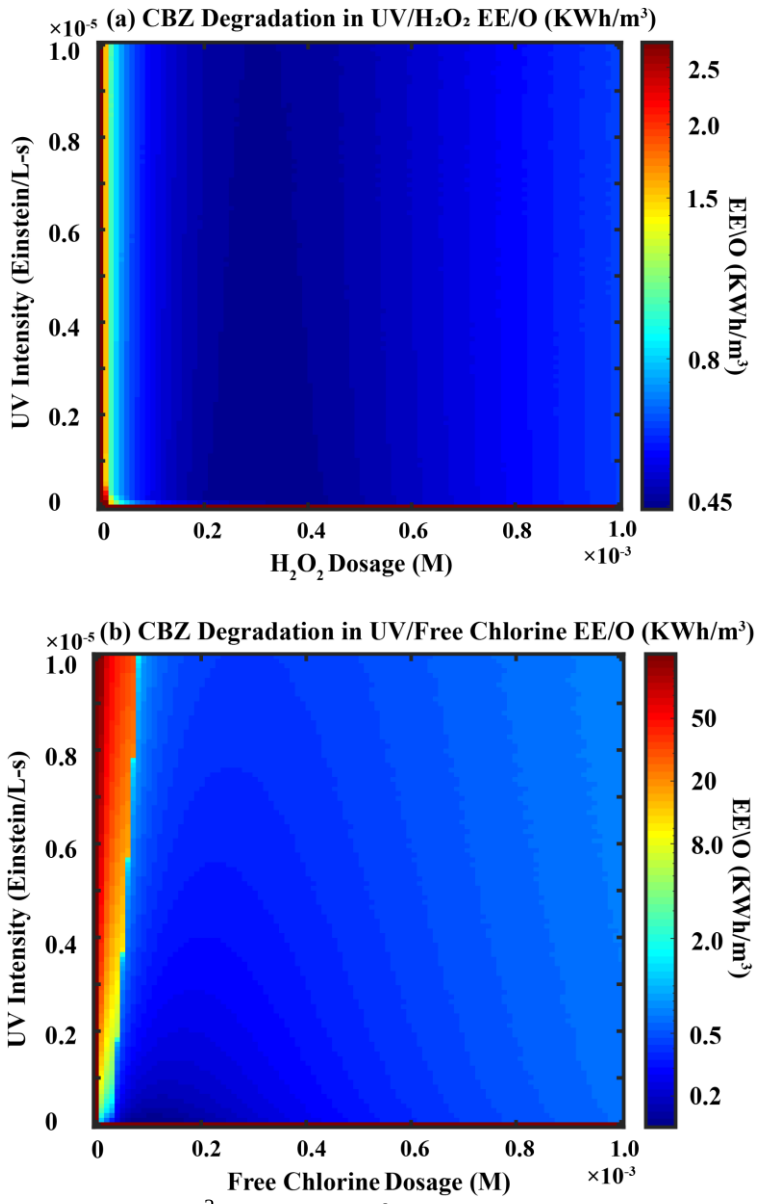

Figure 4.17. EE/O (in kWh m^{-3}) estimation for CBZ degradation in (a) UV/H_2O_2 and (b) UV/chlorine processes with varying UV intensity and H_2O_2/chlorine dosage. Experimental conditions: $[CBZ]_0$ = 5.0 µM, $[H_2O_2]_0$ = $[chlorine]_0$ = 0-1mM, [NOM]=2.0 mg L^{-1}, $[HCO_3^-]$=2 mM, $[Cl^-]$=0.01 M, UV intensity= 0 - 10^{-5} Einstein/L·s .

4.4.9 DBPs formation potential in the UV/chlorine and UV/H_2O_2 processes

In the practical application of UV/chlorine process or UV/H_2O_2 process, nature organic matters (NOM) typically exist in the raw water with the concentration around 2 mg-C/L. Based on the previous literatures, NOM will react with free chlorine to generate various DBPs. Therefore, it is necessary to investigate the DBPs formation potentials during the organic destruction of UV/H_2O_2 and UV/chlorine processes. Figure X indicates the DBPs varied with pretreatment time of UV/H_2O_2 and UV/chlorine processes. And the formation of trichloromethane (TCM) and dichloroacetonitrile (DCAN) were observed after 24 h post-chlorination. The formation potential of TCM and DCAN can be calculated by eq 4.8 and eq 4.9:

$$\text{THM Formation Potential} = \frac{\text{THM Yield Concentration (M)}}{\text{Initial CBZ Concentration (M)}} \times 100\% \tag{4.8}$$

$$\text{DCAN Formation Potential} = \frac{\text{DCAN Yield Concentration (M)}}{\text{Initial CBZ Concentration (M)}} \times 100\% \tag{4.9}$$

According to **Figure 4.18(a)**, the TCM formation during the CBZ destruction in the UV/H_2O_2 process keeps increasing, and after 30 min UV/H_2O_2 pretreatment, the TCM formation potentials increase by 28%; the TCM formation during the CBZ destruction in the UV/chlorine process slightly increases. In another word, after 30 min UV/chlorine pretreatment, the TCM formation potential only increases 9%. According to **Figure 4.18(b)**, the DCAN formation during the CBZ destruction in both of UV/H_2O_2 and UV/chlorine processes significantly decrease. After 30 min UV/H_2O_2 pretreatment, the DCAN formation potential decrease by 67.4%; the DCAN formation during the CBZ destruction in the UV/ chlorine process decrease by 100%. Overall, less DBPs yield were observed during the organic contaminants destruction in the UV/chlorine process than in the UV/H_2O_2 process. This may because the UV/chlorine process is more effective to

destroy the precursors of DBPs than that of the UV/ H_2O_2 process. These results further confirmed that the UV/chlorine process may be promising AOPs compared to the UV/H_2O_2 process. In addition, since DBPs do not significantly increase during the organic compounds destruction in the UV/free chlorine, the micropollutants decreasing is the controlling factor of the UV/free chlorine process in practical application.

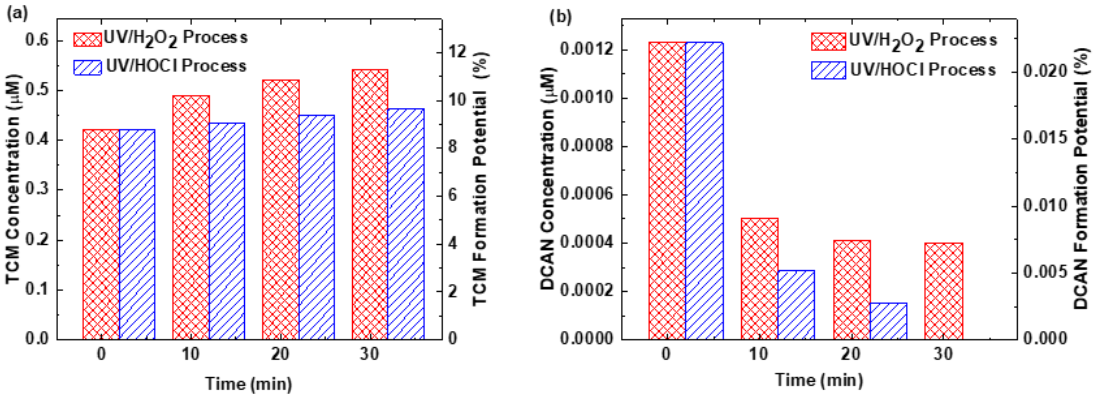

Figure 4.18. DBPs formation of CBZ degradation in UV/H_2O_2 and UV/Free Chlorine processes. (a) TCM yields; (b) DCAN yields.

4.5 Environmental Implications

In this study, we investigated the mechanisms of pharmaceuticals degradation by developing a first-principles based kinetic model. We successfully determined the second-order rate constants between pharmaceuticals and reactive radicals (i.e. HO•, Cl•, Cl_2^-• and ClO•). We found that ClO• was the major reactant responsible for pharmaceuticals degradation. Then, to investigate the feasibility of the UV/free chlorine process for practical application, we studied the impact of water matrix components on the degradation of pharmaceuticals under various water matrix , and our model successfully simulate the oxidation of TMP and CBZ in the UV/free chlorine process under various pH, various Cl^- concentration (0.1 mM - 0.1M), various NOM concentration (1 mg/L - 5mg/L) and various HCO_3^-/CO_3^{2-} (1 mM - 5 mM). In addition, we found that the minimum EE/O required for

UV/free chlorine process to degrade pharmaceuticals was at least 3 times less than the UV/H_2O_2 process. Finally, we found DPBs did not significantly increase and less DBPs yields were observed than the UV/H_2O_2 process. Therefore, the controlling factor for UV/free chlorine process is the decreasing of micropollutants. Overall, this study revealed that the UV/free chlorine process is a promising technology for practical application at industrial scale.

4.6 Acknowledgement

This work was supported by the Brook Byers Institute for Sustainable Systems, Hightower Chair and the Georgia Research Alliance at the Georgia Institute of Technology, the National Natural Science Foundation of China No. 1115073 and No. 51878257, Innovation and enhancing college project of Guangdong Province, China (2017GKTSCX065), Hunan Science & Technology Innovation Program (2018RS3038), the Natural Science Foundation of Hunan Province (2018JJ3059) and the Fund of State Key Laboratory of Pollution Control and Resource Reuse (PCRRF17023). W.Q. Zhang gratefully acknowledge the support from the China Scholarship Council. The views and ideas expressed herein are solely the authors' and do not represent the ideas of the funding agencies in any form.

CHAPTER 5. COMPUTERIZED PATHWAY GENERATOR FOR UV/FREE CHLORINE PROCESS: PREDICTION OF BYPRODUCTS AND REACTIONS

†*work from this chapter will be submitted in the following citation:*

Zhang, Weiqiu., Zhou, Shiqing., Wu, Yangtao., Zhu, Shumin., Shi, Zhou., Crittenden, John., 2019. Computerized Pathway Generator for UV/Free Chlorine Process: Prediction of Byproducts and Reactions.

5.1 Abstract

UV/free chlorine process is a very promising water treatment technology to remove persistent organic contaminants (POCs, e.g. pharmaceutical and personal care products). The radical chain reactions involved in the UV/free chlorine process are very complicated, and hence prevents us from attaining a fundamental understanding the mechanisms of organic contaminant degradation. Therefore, we developed a computerized pathway generator based on graph theory and predefined reactions rules for the UV/free chlorine process. Our pathway generator aims to automatically predict all possible intermediates, byproducts and elementary reactions that are involved in the oxidation of organic contaminants. For example, the degradation of TCE produces 497 species (i.e. intermediates and byproducts) and 6,608 elementary reactions. The predicted species from our pathway generator not only cover the major and stable byproducts observed in our experiments (e.g. $CHCl_2COOH$, CHCl(OCl)COOH, etc.) but also include many other minor and toxic byproducts that are reactive and are not measured. Overall, our pathway generator is very helpful to significantly improve our insight into the oxidation mechanisms that are involved in the UV/free chlorine process.

5.2 Introduction

Advanced oxidation processes (AOPs) have been applied to oxidize persistent organic contaminants (POCs) from water.[139,140,141,142,143] AOPs can generate various highly reactive radicals that degrade and eventually mineralize POCs. Conventional AOPs are the hydroxyl radical (HO•) based (e.g. UV/H_2O_2, H_2O_2/O_3 processes, etc.) and sulfate radical (SO_4^{-}•) based (e.g. UV/persulfate, peroxymonosulfate/ascorbic acid processes, etc.). According to our previous studies and literature review,[51] we found that the UV/free

chlorine process is a more cost-effective AOP than conventional AOPs because: ***(1)*** the UV/free chlorine process is more efficient than the UV/H_2O_2 process to oxidize pharmaceuticals (e.g. carbamazepine, trimethoprim, etc.);[46] ***(2)*** the UV/free chlorine process requires less energy than the UV/ H_2O_2 process to remove organic contaminant by one order of magnitude (EE/O). For example, as the degradation of carbamazepine (initial concentration is 5.0 μM), the minimum EE/O required for the UV/H_2O_2 process is 0.440 kWh/m^3-order and for the UV/free chlorine process is only 0.126 kWh/m^3-order; ***(3)*** the effectiveness of the UV/free chlorine process is only slightly impacted by common components in water matrix (e.g. Cl^-, HCO_3^-/CO_3^{2-}) .[37,44,45,46] However, we found Cl^- significantly reduced the oxidation rate of target compounds by $SO_4^{-}\cdot$ based AOPs (e.g. UV/persulfate process),[39] and HCO_3^-/CO_3^{2-} inhibit both of UV/H_2O_2 and UV/persulfate processes.[39] Furthermore, the disinfection byproducts (DBPs) formation is a concern for the practical application of the UV/free chlorine process.[144,145,146,147,148] Recently we found that the DPBs formation potential in the UV/free chlorine process was less than the DPBs formation potential in the UV/H_2O_2 process. Overall, the UV/free chlorine process is very promising for practical applications.

For wide scale applications, it is critical to design the UV/free chlorine process that consumes lowest amount of energy consumption and significantly reduces the water's toxicity. Therefore, it is necessary to understand the detailed mechanisms of UV/free chlorine process. However, previous studies about the UV/free chlorine process focus mainly on the theoretical or laboratory studies, because the radical chain reactions are very complex. Many experimental studies have investigated the degradation mechanisms of some selected organic compounds (e.g. atrazine, [50] desethylatrazine,[41]

sulfamethoxazole[41], etc.)[44,56,149,150] under various water matrix conditions, and hence they have laid the foundation for kinetic studies. Most of previous kinetic studies are insufficient to fully elucidate the mechanisms because of using lumped reactions or simplified steady-state assumption (SPSS). According, we developed a first-principles kinetic model to overcome these difficulties. In general, our kinetic model allows us to have a much deeper understanding about the oxidation mechanisms of the UV/free chlorine process. For example, our kinetic model successfully estimated the unknown second-order rate constants between target organic compounds and reactive radicals (i.e. HO•, Cl•, Cl_2^-• and ClO•), and predicted the time-dependent concentration profiles of target organic compounds for various water matrix conditions.[74] However, under certain conditions, we found there were some discrepancies between our model prediction results and our experimental data. For example, in our previous study, the prediction result of 3-nitrobenzoic acid destruction was faster than our experimental data under a free chlorine dosage of 2 ppm.[74] These discrepancies may come from the fact that many byproducts and intermediates were generated in the UV/free chlorine process, and these byproducts/intermediates reacted with reactive radicals (i.e. HO•, Cl•, Cl_2^-• and ClO•) faster than the 4-nitrobenzoic acid.

Accordingly, it is necessary to investigate the byproducts/intermediates and elementary reactions involved in the UV/free chlorine process to improve our current kinetic model; and, hence, improve our insight into the degradation mechanisms. Some experimental studies already reported the major and stable byproducts of certain organic compounds (e.g. atrazine, naproxen).[50,53,56,57,60,61] However, these experimental studies did not investigate the detailed reaction pathways that fully described the organic contaminant

mineralization. Furthermore, Chemical Abstracts Service lists more than 147 million compounds, and it would be impossible conduct experimental studies to reveal the oxidation for all these compounds. An attractive method is to develop a computerized pathway generator to automatically predict the detailed oxidation pathways and the fate of byproducts/intermediates in the UV/free chlorine process. Ke Li et al.[68] successfully developed a pathway generator to predict the degradation of organic compounds induced by HO· only (e.g. UV/H_2O_2 process, UV/TiO_2 process, etc.). However, the UV/free chlorine process is much more complicated pathways because HO·, Cl·, Cl_2^-· and ClO· are radicals are involved. Therefore, in study, we developed a new pathway generator specific for the UV/free chlorine process based on the graph theory and the reaction rules we uncovered from experimental observations. To check the validity of the pathway generator, we carefully compared our pathway generator results to the experimentally observed byproducts that were generated from the degradation of trichloroethylene (TCE), because the degradation of TCE includes all major reaction rules discussed in the following sections.

5.3 Material and Methods

5.3.1 Reaction Rules

According to literature review, the predefined reaction rules for reactive radicals involved in the UV/free chlorine process is shown in **Figure 5.1**:[68,151,152,153,154,155,156] HO·, Cl·, Cl_2^-· and ClO· mainly targets organic contaminant by (i) hydrogen atom abstraction, (ii) addition to an unsaturated bond, (iii) electron transfer. However, Daisuke et al.[72] reported that the electron transfer is not a major mechanism of these reactive radicals (i.e. HO·, Cl·, Cl_2^-· and ClO·). Hence, electron transfer is not included in our pathway generator.

After carbon centered radicals are formed from hydrogen abstraction and double bond addition, they mainly react with oxygen to generate peroxyl radical or recombine with Cl•/Cl_2^-•. Peroxyl radicals will undergo bi-molecular decay or uni-molecular decay to produce aldehydes and alcohols. Alkoxyl radical that is formed from peroxyl radical bi-molecular decay will become aldehyde/alcohol by β-scission or 1,2-H shift. Aldehydes and alcohols will hydrolyze to form carboxylic acids. And carboxylic acids mineralize to form CO_2 and mineral acids.

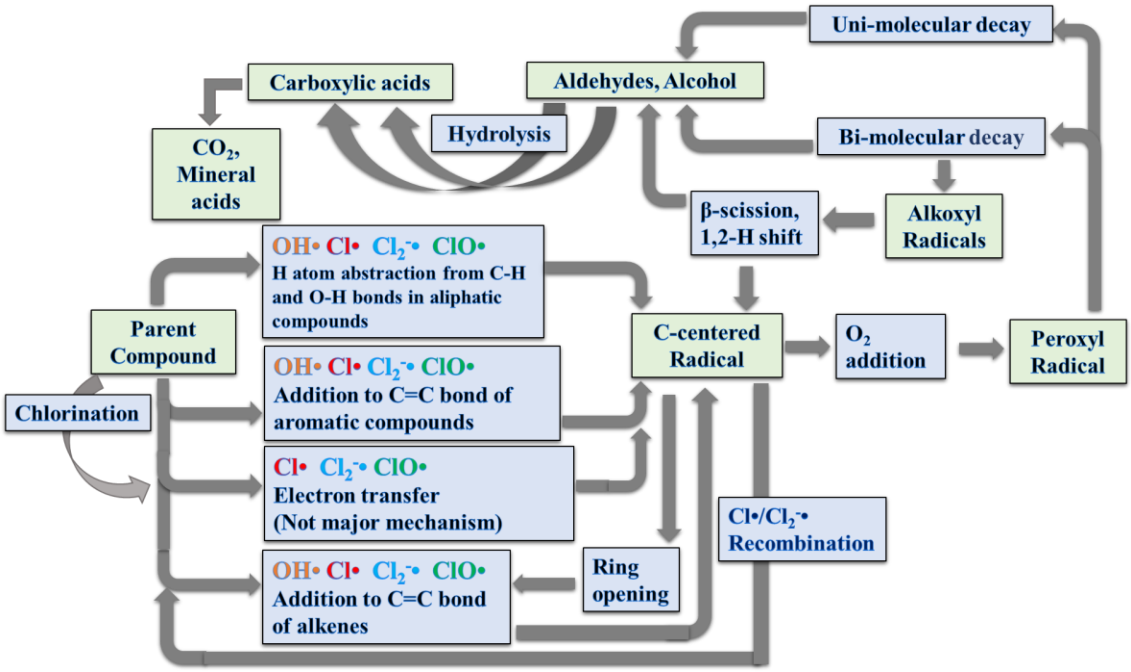

Figure 5.1. General reaction rules of reactive radicals involved in the UV/free chlorine process.

5.3.2 Graph Theory

The general flow diagram of our pathway generator is shown in **Figure 5.2** and was developed in Visual Studio using C++ programing language (~15,000 lines of code). We first input the parent target organic compound as the simplified molecular input line entry system (SMILES). SMILES is a short ASCII string used to describe the structure of

chemical species as a specification form of line notation. The encoding rules of SMILES have been reported in previous studies.[157] For example, SMILES of TCE is C([Cl])([Cl])=C([Cl]) and "=" indicates the double bond.

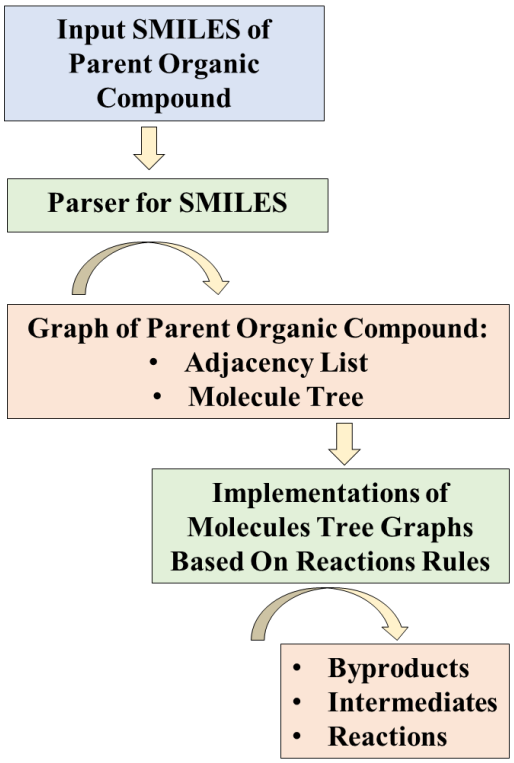

Figure 5.2. General flow of pathway generator

Then, we developed a parser to map the chemical structure and atom information of the parent organic compound inputted as the form of SMILES. The routine of parsing the input SMLES string follows three main steps: ***(1)*** a lexical analyzer is first used to analysis each character of the input SMILES string and return each token unit of the SMILES. A token unit consists of lexeme (substring of input SMILEs), token and attribute value. The major tokens units generate from our lexical analyzer include: (i) if the lexeme (substring of SMILES string) is a digit from 0 to 9, then the token represents digit, and the attribute value of the token is the numeric value of the digit; (ii) if the lexeme is any alphabetic character, *, or any characters between "[" and "]", then the token represents atom, and the attribute

value of the token is none; (iii) if the lexeme is "-", "=", "#" or ":", then the token represents single bond, double bond, triple bond and quadruple bond, respectively. The attribute value of the token is 1, 2, 3 and 4, representatively; ***(2)*** each token unit is stored in a singly linked list; and if any token unit in the list represents atom then we will implement a method named AtomParser; ***(3)*** the AtomParser will first analyze the chemical information of an atom as **Figure 5.3(a)** displays, and then it will insert this atom with its chemical information into a adjacency list; ***(4)*** after traversing all token units of the input SMILES string, the final adjacency list will be generated to map all chemical structure and information of the parent organic compound. For example, **Figure 5.3(b)** indicates the adjacency list for TCE.

(a)

ATOM ID
ATOM NAME
ATOM VALENCE
EXPLICIT HYDROGEN ATOM NUMBER
SP2 HYBRIDIZATION?
BOND LINKED ATOMS (SINGLY LINKED LIST)

(b)

```
Adjacency List for Molecule:
C(ID: 0 Valence: 0 Explicit H: -1 SP2: 1) Bond Linked List: -(1) -(2) =(3)

Cl(ID: 1 Valence: 0 Explicit H: -1 SP2: 0) Bond Linked List: -(0)

Cl(ID: 2 Valence: 0 Explicit H: -1 SP2: 0) Bond Linked List: -(0)

C(ID: 3 Valence: 0 Explicit H: -1 SP2: 1) Bond Linked List: -(4) =(0) -(5)

Cl(ID: 4 Valence: 0 Explicit H: -1 SP2: 0) Bond Linked List: -(3)

H(ID: 5 Valence: 0 Explicit H: 0 SP2: 0) Bond Linked List: -(3)
```

Figure 5.3. Parser for input SMILES string.

Based on the chemical structure and information of each atom in the adjacency list, we generated a molecule tree graph for the parent organic compound. Each atom is represented

as a tree node of the molecule tree, and each tree node not only stores the corresponding chemical information (**Figure 5.3 (a)**) but also includes the pointers that point to its parent node and children nodes. For example, **Figure 5.4** displays the molecule tree graph for TCE based on the adjacency list in **Figure 5.3(b)**.

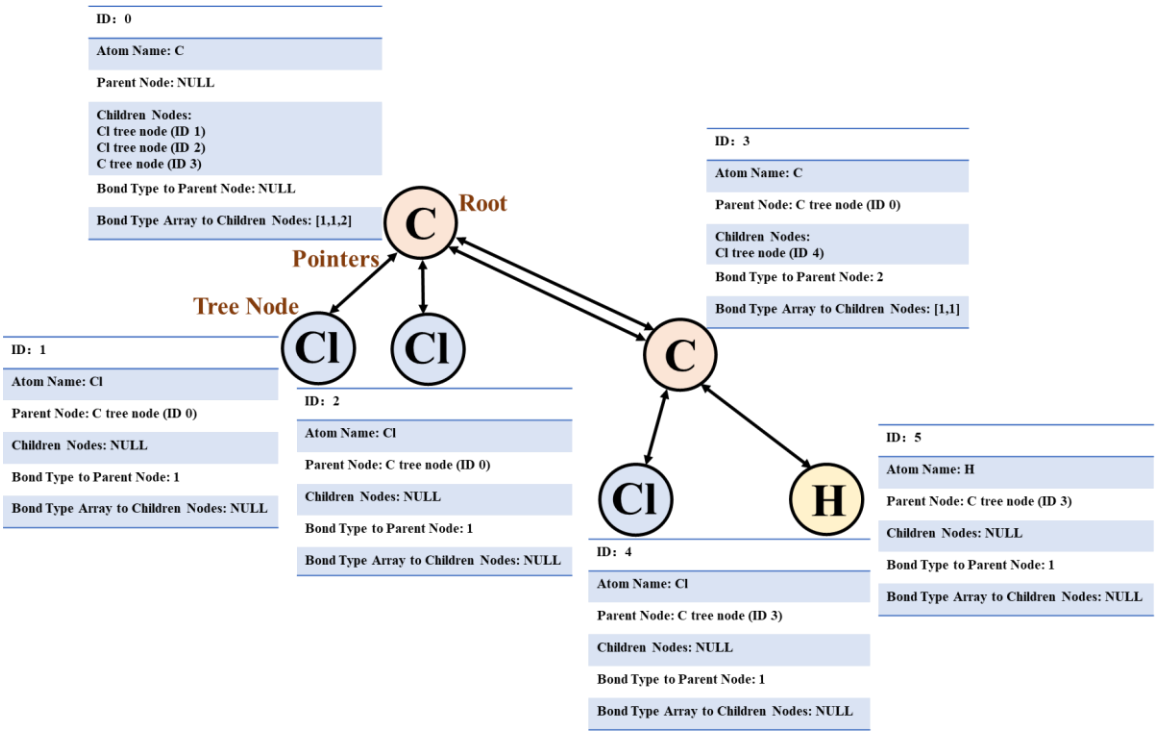

Figure 5.4. Molecule Tree Graph Example.

After generating the graph for parent organic compound as the first reactant graph, we recursively implemented the following steps to generate subsequent products graph and reactions:[68] ***(1)*** we first traverse the reactant graph in order to determine if there are any tree nodes that matched the reaction patterns in **Figure 5.1**; ***(2)*** if we found a matched tree node, we operated the reactant graph to modify all atom and bonds involved in the reaction but other parts of the molecule tree remain unchanged, and hence a product graph was generated. For example, **Figure 5.5** displays the implementation of reactant graph for ClO· addition into the double bond of TCE. **Appendix K** includes a source code of hydrogen

abstraction by ClO·; ***(3)*** we ensured one to one mapping between the generated product graph and the molecule structure by implementing the canonicity check for each tree node in the product molecule tree graph. The canonicity check is based on the weight and number of atoms in the subtree of the tree node. Each tree node has at most four children tree nodes, we checked the weight and atoms numbers of the subtree rooted at each child tree node, then we arranged each child tree node from left to right in order of its weight and atoms numbers of subtree decreasing. For example, **Figure 5.5** displays the canonicity check for the product graph of ClO· addition into the double bond of TCE; ***(4)*** we compared the product graph with existing species that stored in a singly linked list to determine if there any new byproduct/intermediate is generated; ***(5)*** if new species is generated, then the new product is the reactant for the next byproduct generator iteration.

To overcome the huge redundancy of generated byproducts/intermediates and reactions, the termination conditions used in our pathway included: ***(1)*** we limited the longest carbon length of new byproduct to be less than two times of the parent organic compound carbon length;[68] ***(2)*** we set single carbon species as terminate molecules to generate inorganic species directly (e.g. (OCl)COOH = CO_2 + HOCl, COHCl = HCl + CO, etc.).[68]

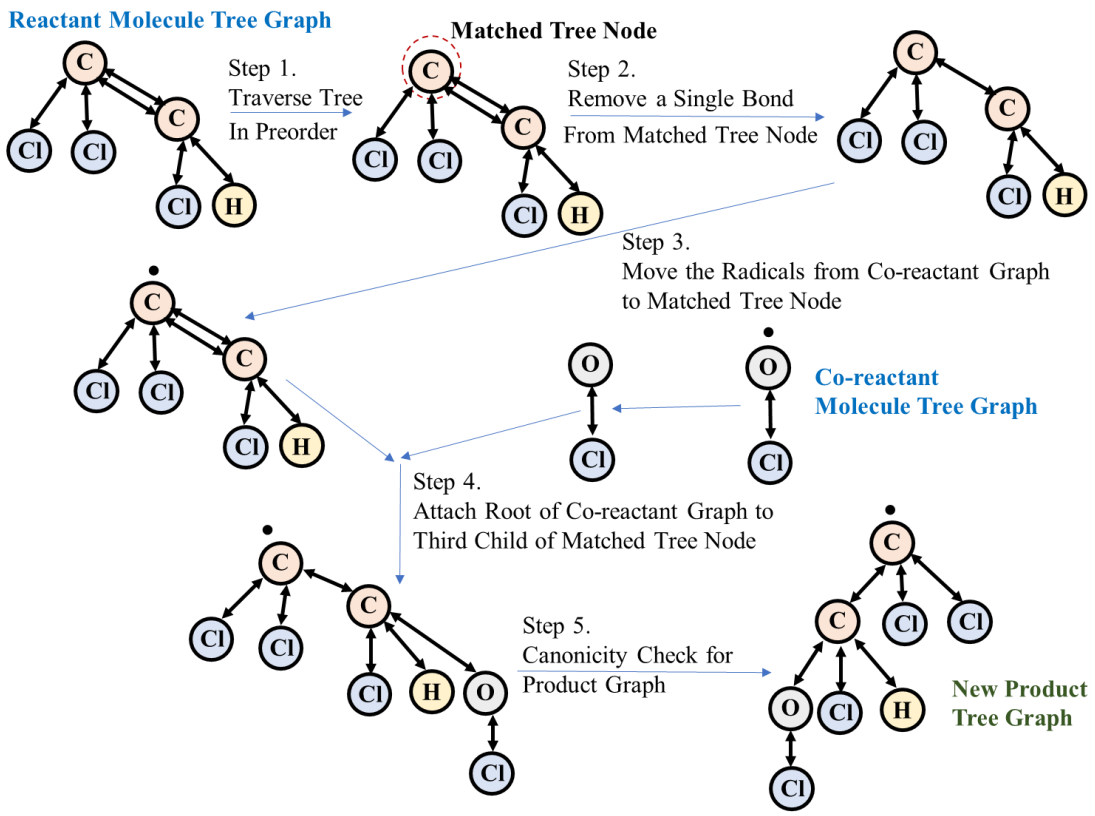

Figure 5.5. Implementation of reactant graph for ClO· addition into double bond of TCE and canonicity check for product graph.

5.3.3 Experimental Procedures

HPLC-MS/MS (Agilent 1290/6460 Triple Quad) equipped with a Symmetry C18 column (50 mm × 2.1 mm × 5 mm, Agilent, USA) in negative electrospray ionization (ESI) mode was used to identify the transformation products of TCE. The mobile phase consisted of ultrapure water as solvent A (1‰ formic acid) and acetonitrile as solvent B at a flow rate of 0.2 mL min^{-1}, with a gradient elution program as follows: 5% to 70% B from 0 to 18 min; 70% to 95% B from 18 to 20 min; 95% to 5% B from 20 to 23 min; 5% B from 23 to 25 min. The injection volume was 10 μL.

Purge-and-trap gas chromatography-mass spectrometry (PT-GC-MS) was used to determine the transformation products of TCE. The purge-and-trap sample concentrator

(Tekmar Lumin, USA) used as a pretreatment step because it increases the concentration of volatile DBPs. The concentrator was connected to a GC-MS ((7890A-5975C, Agilent, USA) for analysis. The instrumentation details are as follows: ***(1)*** purge and trap analysis: 5 mL of sample was injected into the U-tube chamber and purged at 20 °C for 11 min with a helium flow rate of 40 mL min^{-1}; followed by the desorption mode, in which the trap temperature was increased to 250 °C for 2 min at the flow rate of 300 mL min^{-1}; and finally the trap was heated to 280 °C for 2 min to clean up the trap; ***(2)*** GC–MS analysis: the initial temperature of the oven was 30 °C for 3 min, then increased to 50 °C at a rate of 5 °C min^{-1} and maintained for 1 min, and then raised up to 180 °C at 20 °C min^{-1} and maintained for 1 min; with a split ratio of 10:1.

5.4 Results and Discussion

5.4.1 Predefined Reaction Mechanisms

As shown in **Figure 5.1**, the UV/free chlorine process generates HO·, Cl· Cl_2^-· and ClO· radicals, and the major reaction mechanisms of these reactive radicals include hydrogen abstraction and addition into double bond, and carbonate centered radicals are generated. The propagation mechanism among subsequent radicals have been reported in previous studies.[68] We enumerated the major reaction rules included in our pathway generator as: ***(1)*** addition to double bonds (e.g. CCl_2=CClH + ClO· → ·CCl_2CHCl(OCl)); ***(2)*** hydrogen abstraction (e.g. CHR_3 + ClO· → ·CR_3 + HOCl); ***(3)*** oxygen addition into carbon centered radicals (e.g. ·CR_3+ O_2 → ·$OOCR_3$); ***(4)*** β scission of oxyl radicals or carbon centered radicals (e.g. ·OCR_3 → COR_2 + ·R); ***(5)*** 1,2-shift of oxyl radicals when the oxyl radicals have a hydroxy group (-OH) (e.g. ·$OCHR_2$ → ·C(OH)R_2); ***(6)*** elimination of HO_2· from peroxyl radicals when the peroxyl radicals has hydroxy group (-OH) (e.g. ·OOC(OH)R_2 →

$R_2CO + HO_2\cdot$); ***(7)*** bi-molecular decay of peroxyl radicals (e.g. $2\cdot OOCHR_2 \rightarrow R_2C(=O) + R_2CHOH + O_2$; $2\cdot OOCHR_2 \rightarrow 2R_2C(=O) + H_2O_2$; $2\cdot OOCHR_2 \rightarrow 2R_2CHO\cdot + O_2$; $2\cdot OOCHR_2 \rightarrow R_2CHOOCHR_2 + O_2$); ***(8)*** $Cl\cdot$ recombination with carbon centered radicals (e.g. $Cl\cdot + \cdot CHCl_2 \rightarrow CHCl_3$); ***(9)*** hydrolysis of carbonyl chloride group (e.g. $RC(=O)Cl + H_2O \rightarrow RCOOH + HCl$); ***(10)*** hydrolysis of carbonyl group (e.g. $RC(=O)H + H_2O \rightarrow RCH(OH)_2$; $RC(=O)H + H_2O \rightarrow RCOOH$); ***(11)*** elimination of HCl from alcohol or carbon centered radicals (e.g. $CR_2ClOH \rightarrow RC(=O)R + HCl$), etc. In addition, according to our previous studies and many other literatures,[64,68] the preference of reaction occurrence for molecules and carbon centered radicals follow this order: ***(1)*** for molecules: the hydrolysis rate of carbonyl chloride group > the hydrolysis of carbonyl group > radicals addition into double bond > other reaction rules; ***(2)*** for carbon centered radicals: hydrolysis of carbonyl group > elimination of HCl > oxygen addition > β scission > other reaction rules.

5.4.2 Complexity Setting

In this study, we set two kinds of complexity settings were used in our pathway generator. **Table 5.1** indicates the mechanisms differences between the simple complexity (complexity =1) and complex complexity (complexity 2). Other mechanisms that are not included in **Table 5.1** are the same for both of complexity settings. For example, the hydrogen abstraction is induced by $HO\cdot$, $Cl\cdot$ $Cl_2^-\cdot$,$ClO\cdot$ and carbon centered radicals for both complexity settings.

Table 5.1. Complexity setting for pathway generator

Mechanisms	Complexity = 1	Complexity = 2
Hydrolysis of carbonyl molecule	$RC(=O)H + H_2O \rightarrow RCH(OH)_2$	$RC(=O)H + H_2O \rightarrow RCOOH$
Bi-molecular decay of peroxyl radicals	(1) $2\cdot OOCHR_2 \rightarrow R_2C(=O) + R_2CHOH + O_2$;	(1) $2\cdot OOCHR_2 \rightarrow R_2C(=O) + R_2CHOH + O_2$;

	(2) 2· $OOCHR_2$ → $2R_2C(=O) + H_2O_2$; (3) 2• $OOCHR_2$ → $2R_2CHO• + O_2$;	(2) 2·$OOCHR_2$ → $2R_2C(=O) + H_2O_2$; (3) 2·$OOCHR_2$ → $2R_2CHO· + O_2$; (4) 2·$OOCHR_2$ → $R_2CHOOCHR_2 + O_2$
Preference of Reactions Occurrence for Peroxyl Radicals	Elimination of $HO_2·$ from peroxyl radicals > Bi-molecular decay of peroxyl radicals	No exclusions for peroxyl radicals

5.4.3 Case study for TCE

In this study, we first chose TCE as the input parent organic compound. For TCE degradation in the UV/free chlorine process, our pathway generator predicted 479 byproducts and intermediates, 6,608 elementary reactions for complexity level 2, and the results are shown in **Text L.2 in Appendix L**; our pathway generator also predicted 112 byproducts/intermediates and 305 reactions under complexity 1, and we listed species in **Table L.1**, and reactions in **Table L.2**. Accordingly, all intermediates/byproducts are eventually oxidized into inorganic compounds including H_2O, CO_2, HCl and HOCl, etc. It is notable that complexity setting 2 included the recombination of peroxyl radicals ($2·OOC(OH)R_2 = R_2CHOOCHR_2 + O_2$), and hence generated molecules with the carbon chain 1 time longer than that of parent organic compound. Therefore, many more species and reactions were generated for TCE degradation under complexity level 2 than complexity level 1.

Based on the **Table L.1** and **Table L.2**, we plotted the simplified pathway for TCE degradation in the UV/free chlorine process. As shown in **Figure 5.6**, the pathways for UV photolysis of TCE have been reported in previous studies (reaction #284 - #302 in **Table L.2**);[107] the pathway for free chlorination of TCE (reaction #304 and #305 in **Table L.2**) was generated based on our experimental observation (**Appendix J**); other reactions are

generated based on the above-mentioned reaction rules (**Figure 5.1**). Our pathway generator predicted all major by-products that were observed from our experiments (**Appendix J**), which are highlighted as blue in **Figure 5.6**. As shown in **Table 5.2**, major by-products for TCE degradation by the UV/free chlorine process include: ***(1)*** $CHCl_2CHCl(OH)$ and $CCl \equiv CH$ come from the direct photolysis of TCE,[107] ***(2)*** $CHCl_2CHO$ comes from HCl elimination of $CHCl_2CHCl(OH)$; ***(3)*** CH_3COOH come from the hydrolysis of $CCl{\equiv}CH$; ***(4)*** $CHCl_2CClO$ comes from the reaction path initiated by $Cl\cdot/Cl_2^-\cdot$ addition into double bound of TCE, and subsequent reactions involves oxygen addition into $\cdot CHCl_2CCl_2$, bi-molecular decay of $\cdot OOCHCl_2CCl_2$ and β scission of $\cdot OCHCl_2CCl_2$; ***(5)*** $CHCl_2COOH$ comes from (i) hydrolysis of $CHCl_2CHO$; (ii) chlorination of CH_3COOH or $CH_2ClCOOH$; (iii) hydrolysis of $CHCl_2CClO$ that generated from the direct chlorination of TCE; ***(6)*** $CHCl(OCl)COOH$ comes from the reaction path initiated by $ClO\cdot$ addition into double bond of TCE, and subsequent reactions involves oxygen addition into $\cdot CCl_2CHCl(OCl)$, bi-molecular decay of $\cdot OOCCl_2CHCl(OCl)$, β scission of $\cdot OCCl_2CHCl(OCl)$ and hydrolysis of $CHCl(OCl)COCl$; ***(7)*** $CHCl_3$ comes from the recombination of $Cl\cdot / Cl_2^-\cdot$ with $\cdot CHCl_2$, and $\cdot CHCl_2$ can be generated from direct photolysis of $CHCl_2CHO$, β scission of $\cdot OCHCl_2CCl_2$ or $\cdot OCOCHCl_2$. Most of stable byproducts are organic acids or aldehydes because they typically have much lower reaction rate constants (around the magnitude of 10^6 $M^{-1}s^{-1}$-10^7 $M^{-1}s^{-1}$) with reactive radicals than other byproducts/intermediates (around the magnitude of 10^9 $M^{-1}s^{-1}$ - 10^{10} $M^{-1}s^{-1}$).[10] Eventually, all of these major byproducts can be mineralized into inorganic compounds. Furthermore, our pathway generator also predict some minor but acute toxic byproducts, such as $CHCl_2CHCl_2$, CH_2Cl_2, etc.

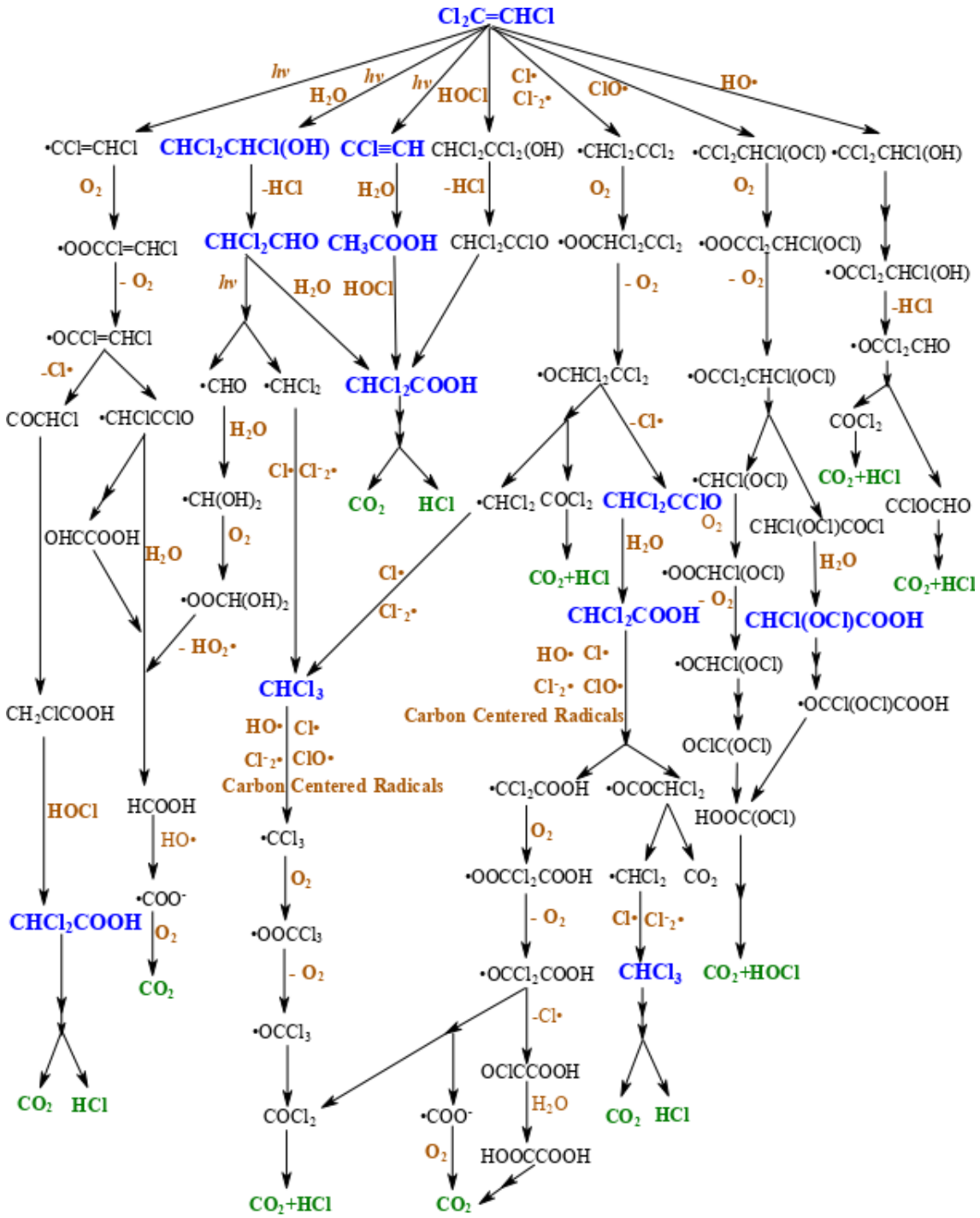

Figure 5.6. Degradation pathways of TCE oxidation in the UV/free chlorine process.

Table 5.2. Predicted reactions for major byproducts generated for TCE degradation in the UV/free chlorine process

Predicted Reactions	Mechanisms Type
1. Generation of $CHCl_2CHCl(OH)$	
$CCl_2{=}CClH + UV + H_2O \rightarrow CHCl_2CHCl(OH)$	UV
2. Generation of $CHCl_2CHO$	
$CHCl_2CHCl(OH) \rightarrow CHCl_2CHO + HCl$	XE
3. Generation of $CCl{\equiv}CH$	
$CCl_2{=}CClH + UV \rightarrow\rightarrow CCl{\equiv}CH$	UV
4. Generation of CH_3COOH	
$CCl{\equiv}CH + H_2O \rightarrow CH_3COCl$	HC
$CH_3COCl + H_2O \rightarrow CH_3COOH + HCl$	HX
5. Generation of $CHCl_2CClO$	
$CCl_2{=}CClH + Cl\bullet \rightarrow \bullet CCl_2CHCl_2$	HA
$CCl_2{=}CClH + Cl_2^-\bullet \rightarrow \bullet CCl_2CHCl_2 + Cl^-$	HA
$\bullet CCl_2CHCl_2 + O_2 \rightarrow \bullet OOCCl_2CHCl_2$	OA
$2\ \bullet OOCCl_2CHCl_2 \rightarrow 2\ \bullet OCCl_2CHCl_2 + O_2$	PB3
$\bullet OCCl_2CHCl_2 \rightarrow CHCl_2CClO + Cl\bullet$	BS
6. Generation of $CHCl_2COOH$	
(1) First Pathway:	
$CHCl_2CClO + H_2O \rightarrow CHCl_2COOH + HCl$	HX
(2) Second Pathway:	
$CH_3COOH + HOCl \rightarrow CH_2ClCOOH + H_2O$	ClR
$CH_2ClCOOH + HOCl \rightarrow CHCl_2COOH + H_2O$	ClR
(3) Third Pathway:	
$CCl_2{=}CClH + HOCl \rightarrow CHCl_2CCl_2(OH)$	ClR
$CHCl_2CCl_2(OH) \rightarrow CHCl_2CClO + HCl$	XE
$CHCl_2CClO + H_2O \rightarrow CHCl_2COOH + HCl$	HX
7. Generation of $CHCl(OCl)COOH$	
$CCl_2{=}CClH + ClO\bullet \rightarrow \bullet CCl_2CHCl(OCl)$	DA
$\bullet CCl_2CHCl(OCl) + O_2 \rightarrow \bullet OOCCl_2CHCl(OCl)$	OA
$2\ \bullet OOCCl_2CHCl(OCl) \rightarrow 2\ \bullet OCCl_2CHCl(OCl) + O_2$	PB3

•$OCCl_2CHCl(OCl)$ → $CHCl(OCl)COCl$ + Cl•	BS
$CHCl(OCl)COCl + H_2O$ → $CHCl(OCl)COOH$ + HCl	HX
8. Generation of $CHCl_3$	
(1) First Pathway:	
$CHCl_2CHO$ + UV + → •CHO + •$CHCl_2$	UV
•$CHCl_2$ + Cl• → $CHCl_3$	XR
(2) Second Pathway:	
$CHCl_2COOH$ + HO• → •$OCOCHCl_2$ + H_2O	HA
$CHCl_2COOH$ + •CCl_2CHCl_2 → •$OCOCHCl_2$ + $CHCl_2CHCl_2$	HA
$CHCl_2COOH$ + •$CCl_2CHCl(OCl)$ → •$OCOCHCl_2$ + $CHCl(OCl)CHCl_2$	HA
$CHCl_2COOH$ + •CCl_2CHO → •$OCOCHCl_2$ + $CHCl_2CHO$	HA
$CHCl_2COOH$ + •$CHCl_2$ → •$OCOCHCl_2$ + CH_2Cl_2	HA
$CHCl_2COOH$ + •$CHCl(OCl)$ → •$OCOCHCl_2$ + $CH_2Cl(OCl)$	HA
$CHCl_2COOH$ + Cl• → •$OCOCHCl_2$ + HCl	HA
$CHCl_2COOH$ + ClO• → •$OCOCHCl_2$ + HOCl	HA
$CHCl_2COOH$ + Cl_2^-• → •$OCOCHCl_2$ + Cl^- + HCl	HA
•$OCOCHCl_2$ → CO_2 + •$CHCl_2$	BS
•$CHCl_2$ + Cl• → $CHCl_3$	XR

5.5 Environmental Implications

In this study, we successfully developed a pathway generator to automatically predict the detailed degradation mechanisms of the UV/free chlorine process. We validate the approach by comparing the predicted pathway for TCE degradation to experiments with the UV/free chlorine process. The predicted species from our pathway generator not only cover the major and stable byproducts observed in our experiments (e.g. $CHCl_2COOH$, $CHCl(OCl)COOH$, etc.) but also include many other minor and toxic byproducts. Furthermore, our pathway generator is a powerful tool that can be used to predict the

degradation of various organic compounds. We listed the predicted results for other five kinds of parent organic compounds (i.e. Methane, Methanol, Acetone, IPA and MTBE) in **Table 5.3** and **Text L.2 in Appendix L**. Overall, our pathway generator is very helpful to significantly improve our insight into the detailed mechanisms of the UV/free chlorine process.

Table 5.3. Predicated oxidation mechanisms of various parent organic compounds in the UV/free chlorine process.

#	Target Organic Compound	SMILES	Complexity = 1		Complexity =2	
			Species Numbers	Reactions Numbers	Species Numbers	Reactions Numbers
1	Methane CH_4	C	32	65	120	808
2	Methanol CH_3OH	CO	29	55	95	430
3	Acetone $CH_3C(=O)CH_3$	CC(=O)C	76	251	346	6,558
4	Isopropyl Alcohol (IPA) $(CH_3)_2CHOH$	CC(O)C	136	981	617	14,660
5	Methyl tert-butyl ether (MTBE) $(CH_3)_3COCH_3$	CC(C)(C)OC	197	1,986	702	16,222

CHAPTER 6. CONCLUSIONS AND FUTURE WORK

Overall this study developed a first-principles based kinetic model to systematically investigated the oxidation mechanisms of organic compound degradation in the UV/free chlorine process. From the big picture, our kinetic model is advanced to ***(1)*** describe the kinetic behaviors of various target organic compounds degradation in the UV/free chlorine; ***(2)*** estimate rarely reported rate constants of various target organic compounds reacting with reactive radicals; ***(3)*** determine the radicals that make the most contribution to oxidizing organic compounds; ***(4)*** evaluate the impact of water matrix components on the effectiveness of the UV/free chlorine process; ***(5)*** determine the optimal operation conditions (i.e. UV intensity and free chlorine dosage) that results in the minimum EE/O. In addition, we investigated the DBPs formation during the micropollutants degradation in the UV/free chlorine process, and determined the controlling factor of the UV/free chlorine was the micropollutants decreasing. Therefore, our kinetic model is helpful for researchers to appropriately design the UV/free chlorine with lowest energy consumption for practical application.

Furthermore, we developed a pathway generator to automatically predict all possible byproducts/intermediates and reactions generated during the treatment of the UV/free chlorine process (e.g. the degradation of TCE involves more than 400 byproducts /intermediates and more than 6,600 reactions). Our pathway generator not only predict major byproducts but also many minor and toxic byproducts. Therefore, the pathway generator significantly advances our understanding about the degradation pathways. However, we have noticed that it is difficult to estimate the rate constants of all possible involved reactions among various intermediate radicals at current stage, because we only

have very limited amount of experimental data (e.g., we do not have data on peroxyl radicals reactions) to develop a GCM, and, the estimation of thousands unknown rate constants by fitting very limited experimental data will cause the overfitting problem. Therefore, future work will mainly focus on developing new methods (for example, linear free energy relationships or reaction class transition state theory using computation quantum chemistry) to estimate the rate constants of all the reactions.[71,72,73] Then, we can predict the time-dependent concentration profiles of byproducts, and predict the time-dependent toxicity of the UV/free chlorine process by using the computation toxicology tools from EPA.[64] Consequently, it is possible to design the UV/free chlorine that would have the lowest toxicity for practical application.

APPENDIX A. SUPPORTING INFORMATION FOR CHAPTER 2

A.1 Elementary Reactions

All elementary reactions were selected from the literature. The UV/Persulfate (PS) elementary reactions are reported in **Table A.1** and the UV/H_2O_2 elementary reactions are reported in

Table A.2.[15,20] Some elementary reactions between two radicals were not considered because they have a very slow reaction rate, and these reactions will not impact our conclusions. The second order rate constants for organic compound are reported in **Table A.3**.[85] In addition, the second rate constants between NOM and radicals depend on the NOM source, and their values typically range from 10^4 (mg-C/L)$^{-1}$/s to 4.5×10^4 (mg-C/L)$^{-1}$/s.[158] We choose feasible literature reported second order rate constants for the NOM reacting with $SO_4^{-}\cdot$, HO·, and Cl· in **Table A.3**.[20,37]

Figure A.1 is the elementary reaction network for UV/PS process where organic compounds only react with sulfate radical ($SO_4^{-}\cdot$). **Figure A.2** is the elementary reaction network for UV/H_2O_2 processes.

A.2 Representative Organic Compounds

28 organic contaminants that have reported rate constants with $SO_4^{-}\cdot$, HO· and Cl· were listed at **Table A.3**. Since their values cover the entire rate constant range, these organics can be used to represent almost all organic compounds. They are: PFOA, PFHpA, PFHeA, PFPeA, PFPBA, PFPrA for UV/PS case 1 that organic compounds only react with $SO_4^{-}\cdot$; chlorobenzene, 1,2-Dichlorobenzene, methane, fluorobenzene, acetonitrile, toluene, acetic acid, 2-methyl-2-propanol, 1-propanol, 1-octanol, 1-butanol, ethanol, methanol, 2-methyl-1-propanol, 2-propanol, methyl acrylate, acrylonitrile, dimethyl sulfoxide, 1-pentanol,

cyclohexene, benzene, and pyridine for UV/PS case 2 that organic compounds can react with $SO_4^-\cdot$, HO· and Cl· and for UV/H_2O_2 process. **Table A.3** includes their rate constants data from NDRL/NIST solution kinetics database.

A.3 Supplementary Calculation for UV/PS: Organic Compounds Only React with Sulfate Radicals

A.3.1 Chloride is not present

When Cl^- is not present, the quenching ratio Q_{A1} (eq A.1 is equal to the rate of $SO_4^-\cdot$ oxidizing target organic compound (R) divided by the rate of $SO_4^-\cdot$ reacting with all components in the water matrix (R, PS and H_2O) (**Figure A.1(a)**). In other words, Q_{A1} is the fraction of $SO_4^-\cdot$ reacting with organic compound.

$$Q_{A1} = \frac{k_{SO_4^-\cdot/R}[R]_0[SO_4^-\cdot]_{ss,0}}{k_{SO_4^-\cdot/R}[R]_0[SO_4^-\cdot]_{ss,0} + k_3[PS]_0[SO_4^-\cdot]_{ss,0} + k_1[H_2O][SO_4^-\cdot]_{ss,0} - k_4[PS]_0[HO\cdot]_{ss,0}} \quad (A.1)$$

The denominator includes the negative term $k_4[PS]_0[HO\cdot]_{ss,0}$,because $SO_4^-\cdot$ reacts with H_2O to generate HO· and HO· continues to react with PS to form $SO_4^-\cdot$. The consumption rate of $SO_4^-\cdot$ from the reaction between $SO_4^-\cdot$ and H_2O can be compensated by the production rate of $SO_4^-\cdot$ from the reaction between HO· and PS.

The HO· reaction rate is given by eq A.2:

$$r_{HO\cdot} = k_1[H_2O][SO_4^-\cdot]_{ss,0} - k_4[PS]_0[HO\cdot]_{ss,0} = 0 \quad (A.2)$$

Hence, Q_{A1} can be simplified as eq A.3:

$$Q_{S1} = \frac{k_{SO_4^-\cdot/R}[R]_0[SO_4^-\cdot]_{ss,0}}{k_{SO_4^-\cdot/R}[R]_0[SO_4^-\cdot]_{ss,0} + k_3[PS]_0[SO_4^-\cdot]_{ss,0}} \quad (A.3)$$

where k_1,k_3, k_4 and $k_{SO_4^-\cdot/R}$ are the second-order rate constants between H_2O and $SO_4^-\cdot$, PS and $SO_4^-\cdot$, PS and HO·, R and $SO_4^-\cdot$, respectively. k_1-k_4 have known values and have the

units as $M^{-1}\cdot s^{-1}$. $k_{SO_4^-\cdot/R}$ depends structure of the organic compound, and $k_{SO_4^-\cdot/R}$ ranges from 10^5 $M^{-1}\cdot s^{-1}$ to $10^8 M^{-1}\cdot s^{-1}$. $[R]_0$ is 0.1 mM; $[PS]_0$ is 0.01 M. As a result, for this case, Q_{A1} is close to 100% (around 99.9%), which means almost all $SO_4^-\cdot$ reacts with organic compound (other cases with different [R] and [PS] can be evaluated by our algorithm).

A.3.2 Chloride is present

When Cl^- is present, the quenching ratio Q_{A2} (eq A.4) is equal to the rate of $SO_4^-\cdot$ oxidizing target organic compound divided by the rate of $SO_4^-\cdot$ reacting with all components in water matrix (R, PS, H_2O, Cl^-) (**Figure A.1(a)**):

$$Q_{A2} = \frac{k_{SO_4^-\cdot/R}[R]_0[SO_4^-\cdot]_{ss,0}^{Cl^-}}{\left(k_{SO_4^-\cdot/R}[R]_0 + k_1[H_2O] + k_2[Cl^-]_0 + k_3[PS]_0\right)[SO_4^-\cdot]_{ss,0}^{Cl^-} - k_4[PS]_0[HO\cdot]_{ss,0}^{Cl^-}} \quad (A.4)$$

The denominator includes the negative term $k_4[PS]_0[HO\cdot]_{ss,0}^{Cl^-}$,because $SO_4^-\cdot$ reacts with H_2O to generate HO· and HO· continues to react with PS to form $SO_4^-\cdot$. The consumption rate of $SO_4^-\cdot$ from the reaction between $SO_4^-\cdot$ and H_2O can be compensated by the production rate of $SO_4^-\cdot$ from the reaction between HO· and PS.

The HO· reaction rate is given by eq A.5:

$$r_{HO\cdot} = k_1[H_2O][SO_4^-\cdot]_{ss,0}^{Cl^-} - k_4[PS]_0[HO\cdot]_{ss,0}^{Cl^-} = 0 \quad (A.5)$$

Hence, Q_{A2} is simplified as below:

$$Q_{A2} = \frac{k_{SO_4^-\cdot/R}[R]_0[SO_4^-\cdot]_{ss,0}^{Cl^-}}{k_{SO_4^-\cdot/R}[R]_0[SO_4^-\cdot]_{ss,0}^{Cl^-} + k_2[Cl^-]_0[SO_4^-\cdot]_{ss,0}^{Cl^-} + k_3[PS]_0[SO_4^-\cdot]_{ss,0}^{Cl^-}} \quad (A.6)$$

where k_1,k_2,k_3,k_4 and $k_{SO_4^-\cdot/R}$ are the second-order rate constants between H_2O and $SO_4^-\cdot$, Cl^- and $SO_4^-\cdot$, PS and $SO_4^-\cdot$, PS and HO·, R and $SO_4^-\cdot$, respectively. k_1-k_4 have known values and have the units as $M^{-1}\cdot s^{-1}$. $k_{SO_4^-\cdot/R}$ depends structure of the organic compound,

and $k_{SO_4^{-}\cdot/R}$ ranges from 10^5 $M^{-1}\cdot s^{-1}$ to 10^8 $M^{-1}\cdot s^{-1}$. $[Cl^-]/[R]$ is ranging from 10 to 1000; $[R]_0$ is 0.1 mM; and, $[PS]_0$ is 0.01 M. Therefore, for this case, the maximum value of Q_{S2} is 19.42% (other cases can be evaluated by our algorithm).

A.3.3 NOM is present

When NOM is present, the rate of PS photolysis to produce $SO_4^{-}\cdot$ is $2\emptyset_{PS}P_{UV}f_{PS}^{NOM}(1-e^{-A^{NOM}})$. While, when no NOM is present, the rate of PS photolysis to produce $SO_4^{-}\cdot$ is $2\emptyset_{PS}P_{UV}f_{PS}(1-e^{-A})$. We compared the rate of PS photolysis to produce $SO_4^{-}\cdot$ when NOM is presents to the case when NOM is not present as *RatioA1*. *RatioA1* is 0.529, which means $SO_4^{-}\cdot$ photolysis production rate decreases 47.1% because NOM absorbs UV light.

$$\text{RatioA1} = \frac{2\phi_{PS}P_{UV}f_{PS}^{NOM}(1-e^{-A^{NOM}})}{2\phi_{PS}P_{UV}f_{PS}(1-e^{-A})} = \frac{f_{PS}^{NOM}(1-e^{-A^{NOM}})}{f_{PS}(1-e^{-A})} \tag{A.7}$$

where,

$\emptyset_{PS}$ is PS quantum yield; P_{UV} is UV light intensity, Einstein·$L^{-1}\cdot s^{-1}$;

$$f_{PS}^{NOM} = \frac{\varepsilon_{PS}C_{PS}}{\varepsilon_R C_R + \varepsilon_{PS}C_{PS} + \varepsilon_{NOM}C_{NOM} + \varepsilon_{bac}C_{bac}}; \; f_{PS} = \frac{\varepsilon_{PS}C_{PS}}{\varepsilon_R C_R + \varepsilon_{PS}C_{PS} + \varepsilon_{bac}C_{bac}};$$

ε_{PS} is PS extinction coefficient, 20.07 L/mole·cm; [20]

ε_R is organic compound extinction coefficient, assumed as 180 L/mole·cm;[159]

ε_{NOM} is NOM extinction coefficient, assumed as 0.107 L/mg C·cm;[10]

ε_{bac} is water matrix background extinction coefficient, assumed 0 L/mole·cm;

L is reactor pathway, assumed as 6 cm.[20]

$$A = 2.303(\varepsilon_R C_R + \varepsilon_{PS}C_{PS} + \varepsilon_{bac}C_{bac})L;$$

$$A^{NOM} = 2.303(\varepsilon_R C_R + \varepsilon_{PS}C_{PS} + \varepsilon_{NOM}C_{NOM} + \varepsilon_{bac}C_{bac})L;$$

A^{NOM} and A can also be measured by UV spectrum. A NOM stock solution was prepared by dissolving a certain amount of Suwannee River NOM in ultrapure water, and then the solution was filtered through a 0.45-μm membrane to remove the insoluble fraction. The dissolved organic carbon content of the NOM stock solution was quantified and standardized using a total organic carbon analyzer (TOC-V, Shimadzu, Japan).

When NOM is present, the quenching ratio Q_{A3} (eq A.8) is equal to the rate of $SO_4^-\cdot$ oxidizing target organic compound (R) divided by the rate of $SO_4^-\cdot$ reacting with all components in water matrix (R, PS, H_2O, NOM) (**Figure A.1(c)**).

$$Q_{A3} = \frac{k_{SO_4^-\cdot/R}[R]_0[SO_4^-\cdot]_{ss,0}^{NOM}}{\left(\sum_{NOM}^{SO_4^-\cdot} k_i S_i\right)[SO_4^-\cdot]_{ss,0}^{NOM} - k_4[PS]_0[HO\cdot]_{ss,0}^{NOM}} \tag{A.8}$$

The denominator includes the negative term $k_4[PS]_0[HO\cdot]_{ss,0}^{NOM}$,because $SO_4^-\cdot$ reacts with H_2O to generate HO· and HO· continues to react with PS to form $SO_4^-\cdot$. The consumption rate of $SO_4^-\cdot$ from the reaction between $SO_4^-\cdot$ and H_2O can be compensated by the production rate of $SO_4^-\cdot$ from the reaction between HO· and PS.

The HO· reaction rate is given by eq A.9,

$$r_{HO\cdot} = k_1[H_2O][SO_4^-\cdot]_{ss,0}^{NOM} - k_4[PS]_0[HO\cdot]_{ss,0}^{NOM} - k_{HO\cdot/NOM}[NOM]_0[HO\cdot]_{ss,0}^{NOM} = 0 \tag{A.9}$$

Hence, Q_{A3} is simplified as below:

$$Q_{A3} = \frac{k_{SO_4^-\cdot/R}[R]_0}{\sum_{NOM}^{SO_4^-\cdot} k_i S_i - \frac{k_1 k_4[H_2O][PS]_0}{k_4[PS]_0 + k_{HO\cdot/NOM}[NOM]_0}} \tag{A.10}$$

where,

$$\sum_{NOM}^{SO_4^-\cdot} k_i S_i = k_{SO_4^-\cdot/R}[R]_0 + k_3[PS]_0 + k_{SO_4^-\cdot/NOM}[NOM]_0 + k_1[H_2O]_0$$

where, k_i is the second order rate constant between compound i and $SO_4^-\cdot$, $M^{-1}\cdot s^{-1}$;$k_{SO_4^-\cdot/NOM}$ is the second-order rate constant between NOM and $SO_4^-\cdot$, $M^{-1}\cdot s^{-1}$; $k_{HO\cdot/NOM}$ is the second-order rate constant between NOM and HO·, $M^{-1}\cdot s^{-1}$; $k_{SO_4^-\cdot/R}$ is the second-order rate constant between R and $SO_4^-\cdot$, $M^{-1}\cdot s^{-1}$. k_1-k_4, $k_{SO_4^-\cdot/NOM}$ and $k_{HO\cdot/NOM}$ have known values. $k_{SO_4^-\cdot/R}$ depends structure of the organic compound, and $k_{SO_4^-\cdot/R}$ ranges from 10^5 $M^{-1}\cdot s^{-1}$ to 10^8 $M^{-1}\cdot s^{-1}$. For our analysis, $[R]_0$ is 0.1mM, $[PS]_0$ is 0.01 M, $[NOM]_0$ is 2 $mg\cdot L^{-1}$. For this case, in this case Q_{A3} must be less than 16.4% (other cases can be evaluated by our algorithm.) Overall, when NOM is present, the fraction of $SO_4^-\cdot$ reacting with target organic compound is determined by two factors: ***(1)*** NOM absorbs UV light, $SO_4^-\cdot$ production rate decreases 47.1% in this case; ***(2)*** the quenching ratio Q_{A3} is no more than 16.4%. As a result, in this case at most 8.68% of the (0.164×(1-0.471) ×100%) $SO_4^-\cdot$ reacts with organic compound (other cases with different [PS], [R] and [NOM] can be evaluated by our algorithm). We reported the $k_{SO_4^-\cdot/R}$ for 6 organic compounds that only react with $SO_4^-\cdot$. The fraction of $SO_4^-\cdot$ reacting with these 6 organic compounds is summarized in **Table A.4**.

A.3.4 Chloride and NOM is not present

When Cl^- and NOM both are present, the quenching ratio Q_{A4} (eq A.11) is equal to the rate of $SO_4^-\cdot$ oxidizing the target organic compound (R) divided by the rate of $SO_4^-\cdot$ reacting with all components in water matrix (R, PS, H_2O, NOM, Cl^-) (**Figure A.1(c)**) :

$$Q_{A4} = \frac{k_{SO_4^-\cdot/R}[R]_0[SO_4^-\cdot]_{ss,0}^{Cl^-,NOM}}{\left(\sum_{Cl^-,NOM}^{SO_4^-\cdot} k_i S_i\right)[SO_4^-\cdot]_{ss,0}^{Cl^-,NOM} - k_4[PS]_0[HO\cdot]_{ss,0}^{Cl^-,NOM}} \quad (A.11)$$

The denominator includes the negative term $k_4[PS]_0[HO\cdot]_{ss,0}^{Cl^-,NOM}$,because $SO_4^-\cdot$ reacts with H_2O to generate HO· and HO· continues to react with PS to form $SO_4^-\cdot$. The consumption rate of $SO_4^-\cdot$ from the reaction between $SO_4^-\cdot$ and H_2O can be compensated by the production rate of $SO_4^-\cdot$ from the reaction between HO· and PS.

The HO· reaction rate is given at here:

$$r_{HO\cdot} = k_1[H_2O][SO_4^-\cdot]_{ss,0}^{Cl^-,NOM} - k_4[PS]_0[HO\cdot]_{ss,0}^{Cl^-,NOM} - k_{HO\cdot/NOM}[NOM]_0[HO\cdot]_{ss,0}^{Cl^-,NOM} = 0 \qquad (A.12)$$

Hence, Q_{A4} is simplified as below:

$$Q_{A4} = \frac{k_{SO_4^-\cdot/R}[R]_0}{\sum_{Cl^-,NOM}^{SO_4^-\cdot} k_i S_i - \frac{k_1 k_4 [H_2O][PS]_0}{k_4[PS]_0 + k_{HO\cdot/NOM}[NOM]_0}} \qquad (A.13)$$

where,

$$\sum_{Cl^-,NOM}^{SO_4^-\cdot} k_i S_i = k_{SO_4^-\cdot/R}[R]_0 + k_2[Cl^-]_0 + k_3[PS]_0 + k_{SO_4^-\cdot/NOM}[NOM]_0 + k_1[H_2O]_0$$

where, k_i is the second order rate constant between compound i and $SO_4^-\cdot$, $M^{-1}\cdot s^{-1}$;$k_{SO_4^-\cdot/NOM}$ is the second-order rate constant between NOM and $SO_4^-\cdot$, $M^{-1}\cdot s^{-1}$; $k_{HO\cdot/NOM}$ is the second-order rate constant between NOM and HO·, $M^{-1}\cdot s^{-1}$; $k_{SO_4^-\cdot/R}$ is the second-order rate constant between R and $SO_4^-\cdot$. k_1-k_4, $k_{SO_4^-\cdot/NOM}$ and $k_{HO\cdot/NOM}$ have known values and have the units as $M^{-1}\cdot s^{-1}$. $k_{SO_4^-\cdot/R}$ depends structure of the organic compound, and $k_{SO_4^-\cdot/R}$ ranges from 10^5 $M^{-1}\cdot s^{-1}$ to $10^8 M^{-1}\cdot s^{-1}$. $[Cl^-]/[R]$ ranges from 10 to 1000; $[R]_0$ is 0.1 mM; $[PS]_0$ is 0.01 M; and, $[NOM]_0$ is 2 $mg\cdot L^{-1}$. For this case, Q_{A4} must be less than 1.769%. Overall, when NOM and Cl^- are present, the fraction of $SO_4^-\cdot$ reacting with target organic compound is determined by two factors: ***(1)*** NOM absorbs UV light, $SO_4^-\cdot$ production rate decreases 47.1% in this case; ***(2)*** the quenching ratio Q_{A4} is no more than 1.769%. As a result, in this

case at most 0.936% (1.769×(1-0.471) ×100%) $SO_4^-\cdot$ will oxidize the target organic compound (other cases with different [Cl^-], [R], [PS], [NOM] can be evaluated by our algorithm). And as the [Cl^-]/[R] increases, the fraction of $SO_4^-\cdot$ reacting with target organic compound decreases (the quenching rate Q_{S4} decreases). We reported the $k_{SO_4^-\cdot/R}$ for 6 organic compounds that only react with $SO_4^-\cdot$. The fraction of $SO_4^-\cdot$ reacting with these 6 organic compounds is summarized in **Table A.4**.

A.3.5 Bicarbonate and Carbonate are not present

When HCO_3^- and CO_3^{2-} (HCO_3^-/CO_3^{2-}) are present, the quenching ratio Q_{A5} (eq A.14) is equal to the rate of $SO_4^-\cdot$ oxidizing the target organic compound (R) divided by the rate of $SO_4^-\cdot$ reacting with all components in water matrix (R, PS, H_2O, HCO_3^-, CO_3^{2-}) (**Figure A.1(d)**):

$$Q_{A5} = \frac{k_{SO_4^-\cdot/R}[R]_0[SO_4^-\cdot]^C_{ss,0}}{\left(\sum_C^{SO_4^-\cdot} k_i S_i\right)[SO_4^-\cdot]^C_{ss,0} - k_4[PS]_0[HO\cdot]^C_{ss,0}} \tag{A.14}$$

The denominator includes the negative term $k_4[PS]_0[HO\cdot]^C_{ss,0}$, because $SO_4^-\cdot$ reacts with H_2O to generate HO· and HO· continues to react with PS to form $SO_4^-\cdot$. The consumption rate of $SO_4^-\cdot$ from the reaction between $SO_4^-\cdot$ and H_2O can be compensated by the production rate of $SO_4^-\cdot$ from the reaction between HO· and PS.

The HO· reaction rate is given by eq A.15,

$$\begin{aligned} r_{HO\cdot} &= k_1[H_2O][SO_4^-\cdot]^C_{ss,0} - k_4[PS]_0[HO\cdot]^C_{ss,0} - k_{13}[HCO_3^-]_0[HO\cdot]^C_{ss,0} \\ &- k_{14}[CO_3^{2-}]_0[HO\cdot]^C_{ss,0} = 0 \end{aligned} \tag{A.15}$$

Hence, Q_{A5} can be simplified to：

$$Q_{A5} = \frac{k_{SO_4^-\cdot/R}[R]_0}{\sum_{C}^{SO_4^-\cdot} k_i S_i - \frac{k_1 k_4 [H_2O][PS]_0}{k_4[PS]_0 + k_{13}[HCO_3^-]_0 + k_{14}[CO_3^{2-}]_0}} \quad (A.16)$$

where,

$$\sum_{C}^{SO_4^-\cdot} k_i S_i = k_{SO_4^-\cdot/R}[R]_0 + k_3[PS]_0 + k_{11}[HCO_3^-]_0 + k_{12}[CO_3^{2-}]_0 + k_1[H_2O]$$

where, k_i is the second order rate constant between compound i and $SO_4^-\cdot$, $M^{-1}s^{-1}$; k_{12}, k_{13} and $k_{SO_4^-\cdot/R}$ are the second-order rate constants between HCO_3^- and HO·, CO_3^{2-} and HO·, R and $SO_4^-\cdot$, respectively. k_1-k_{13} have known values and have the units as $M^{-1}\cdot s^{-1}$. $k_{SO_4^-\cdot/R}$ depends structure of the organic compound, and $k_{SO_4^-\cdot/R}$ ranges from 10^5 $M^{-1}\cdot s^{-1}$ to $10^8 M^{-1}\cdot s^{-1}$. $[R]_0$ is 0.1 mM; $[PS]_0$ is 0.01 M; $[HCO_3^-]_0$ is 3 mM; and, $[CO_3^{2-}]_0$ is 14 μM. Therefore, in this case, Q_{A5} must be less than 45.57%, which means no more than 45.57% $SO_4^-\cdot$ will oxidize the target organic compound (other cases with different [R], [PS], $[HCO_3^-]$ and $[CO_3^{2-}]$ can be evaluated by our algorithm). We reported the $k_{SO_4^-\cdot/R}$ for 6 organic compounds that only react with $SO_4^-\cdot$. The fraction of $SO_4^-\cdot$ reacting with these 6 organic compounds is summarized in **Table A.5**.

A.3.6 Chloride, Bicarbonate and Carbonate are present

When Cl^- and HCO_3^-/CO_3^{2-} are present, the quenching ratio Q_{A6} (eq A.17) is equal to the rate of $SO_4^-\cdot$ oxidizing the target organic compound (R) divided by the rate of $SO_4^-\cdot$ reacting with all components in water matrix (R, PS, H_2O, HCO_3^-, CO_3^{2-}, Cl^-).

$$Q_{A6} = \frac{k_{SO_4^-\cdot/R}[R]_0[SO_4^-\cdot]_{ss,0}^{Cl^-,C}}{\left(\sum_{Cl^-,C}^{SO_4^-\cdot} k_i S_i\right)[SO_4^-\cdot]_{ss,0}^{Cl^-,C} - k_4[PS]_0[HO\cdot]_{ss,0}^{Cl^-,C}} \quad (A.17)$$

The denominator includes the negative term $k_4[PS]_0[HO\cdot]_{ss,0}^{Cl^-,C}$,because $SO_4^-\cdot$ reacts with H_2O to generate HO· and HO· continues to react with PS to form $SO_4^-\cdot$. The consumption rate of $SO_4^-\cdot$ from the reaction between $SO_4^-\cdot$ and H_2O can be compensated by the production rate of $SO_4^-\cdot$ from the reaction between HO· and PS.

The HO· reaction rate is given by eq A.18

$$r_{HO\cdot} = k_1[H_2O][SO_4^-\cdot]_{ss,0}^{Cl^-,C} - k_4[PS]_0[HO\cdot]_{ss,0}^{Cl^-,C} - k_{13}[HCO_3^-]_0[HO\cdot]_{ss,0}^{Cl^-,C} - k_{14}[CO_3^{2-}]_0[HO\cdot]_{ss,0}^{Cl^-,C} = 0 \quad \text{(A.18)}$$

Hence, Q_{A6} can be simplified to:

$$Q_{A6} = \frac{k_{SO_4^-\cdot/R}[R]_0}{\sum_{Cl^-,C}^{SO_4^-\cdot} k_i S_i - \frac{k_1 k_4 [H_2O][PS]_0}{k_4[PS]_0 + k_{13}[HCO_3^-]_0 + k_{14}[CO_3^{2-}]_0}} \quad \text{(A.19)}$$

where,

$$\sum_{Cl^-,C}^{SO_4^-\cdot} k_i S_i = k_{SO_4^-\cdot/R}[R]_0 + k_2[Cl^-]_0 + k_3[PS]_0 + k_{11}[HCO_3^-]_0 + k_{12}[CO_3^{2-}]_0 + k_1[H_2O]$$

where, k_i is the second order rate constant between compound i and $SO_4^-\cdot$ ($M^{-1}s^{-1}$). k_{12}, k_{13} and $k_{SO_4^-\cdot/R}$ are the second-order rate constants between HCO_3^- and HO·, CO_3^{2-} and HO·, R and $SO_4^-\cdot$, respectively. k_1-k_{13}have known values and have the units as $M^{-1}\cdot s^{-1}$. $k_{SO_4^-\cdot/R}$ depends structure of the organic compound, and $k_{SO_4^-\cdot/R}$ ranges from 10^5 $M^{-1}\cdot s^{-1}$ to $10^8 M^{-1}\cdot s^{-1}$. $[Cl^-]/[R]$ is ranges from 10 to 1000; $[R]_0$ is 0.1 mM; $[PS]_0$ is 0.01 M; $[HCO_3^-]_0$ is 3 mM; and,$[CO_3^{2-}]_0$ is 1 mM. Therefore, in this case, Q_{A6} must be less than 1.89%, which means no more than 1.89% $SO_4^-\cdot$ will destruct organic compound (other cases with different [R], [PS], $[HCO_3^-]$, $[CO_3^{2-}]$ and $[Cl^-]$ can be evaluated by our algorithm). And as the $[Cl^-]/[R]$ increases, the fraction of $SO_4^-\cdot$ reacting with target organic compound

decreases (the quenching rate Q_{A6} decreases). We reported the $k_{SO_4^-\cdot/R}$ for 6 organic compounds that only react with $SO_4^-\cdot$. The fraction of $SO_4^-\cdot$ reacting with these 6 organic compounds is summarized in **Table A.5**.

A.4 Supplementary Calculation for UV/PS Case 2: Organic Compounds React with Sulfate Radicals, Hydroxyl Radicals and Chlorine Radicals

A.4.1 Chloride is not present

When Cl^- is not present, the quenching ratio Q_{A7} (eq A.20) and is equal to the rate of $SO_4^-\cdot$ oxidizing the target organic compound (R) divided by the rate of $SO_4^-\cdot$ reacting with all components in the water matrix (R, PS and H_2O) (**Figure 2.1(a)**). In other words, Q_{A7} is the fraction of $SO_4^-\cdot$ reacting with organic compound.

$$Q_{A7} = \frac{k_{SO_4^-\cdot/R}[R]_0[SO_4^-\cdot]_{ss,0}}{k_{SO_4^-\cdot/R}[R]_0[SO_4^-\cdot]_{ss,0} + k_3[PS]_0[SO_4^-\cdot]_{ss,0} + k_1[H_2O][SO_4^-\cdot]_{ss,0} - k_4[PS]_0[HO\cdot]_{ss,0}} \quad (A.20)$$

The denominator includes the negative term $k_4[PS]_0[HO\cdot]_{ss,0}$, because $SO_4^-\cdot$ reacts with H_2O to generate HO· and HO· continues to react with PS to form $SO_4^-\cdot$. The consumption rate of $SO_4^-\cdot$ from the reaction between $SO_4^-\cdot$ and H_2O can be compensated by the production rate of $SO_4^-\cdot$ from the reaction between HO· and PS.

The HO· reaction rate is given by eq A.21:

$$r_{HO\cdot} = k_1[H_2O][SO_4^-\cdot]_{ss,0} - k_4[PS]_0[HO\cdot]_{ss,0} - k_{HO\cdot/R}[R]_0[HO\cdot]_{ss,0} = 0 \quad (A.21)$$

Hence, Q_{A7} can be simplified to eq A.22:

$$Q_{A7} = \frac{k_{SO_4^-\cdot/R}[R]_0}{k_{SO_4^-\cdot/R}[R]_0 + k_1[H_2O] + k_3[PS]_0 - \dfrac{k_1k_4[H_2O][PS]_0}{k_4[PS]_0 + k_{HO\cdot/R}[R]_0}} \quad (A.22)$$

where k_1,k_3, k_4, $k_{SO_4^-\cdot/R}$, $k_{HO\cdot/R}$ are the second-order rate constants between reactions of (i) H_2O and $SO_4^-\cdot$, (ii) PS and $SO_4^-\cdot$, (iii) PS and HO·, (iv) R and $SO_4^-\cdot$, (v) R and HO·, respectively. k_1-k_4 have known values and have the units as $M^{-1}\cdot s^{-1}$. $k_{SO_4^-\cdot/R}$ and $k_{HO\cdot/R}$ depends structure of the organic compound. $k_{SO_4^-\cdot/R}$ typically ranges from 10^2 $M^{-1}\cdot s^{-1}$ to 3.0×10^9 $M^{-1}\cdot s^{-1}$, and $k_{HO\cdot/R}$ typically ranges from 10^7 $M^{-1}\cdot s^{-1}$ to 1.2×10^{10} $M^{-1}\cdot s^{-1}$. $[R]_0$ is 0.1 mM; $[PS]_0$ is 0.01 M. Therefore, for this case, the maximum value of Q_{A7} is 99.99% (other cases with different [R] and [PS] can be evaluated by our algorithm). We reported rate constants for 22 organic compounds with $SO_4^-\cdot$, HO·, and Cl·. The fraction of $SO_4^-\cdot$ reacting with these organic compounds is summarized in **Table A.6**.

When Cl^- is not present, the quenching ratio Q_{A8} (eq A.23) is equal to the rate of HO· oxidizing the target organic compound (R) divided by the rate of HO· reacting with all components in the water matrix (R, PS) (**Figure 2.1 (a)**). In other words, Q_{S8} is the fraction of HO· reacting with organic compound.

$$Q_{A8} = \frac{k_{HO\cdot/R}[R]_0[HO\cdot]_{ss,0}}{k_{HO\cdot/R}[R]_0[HO\cdot]_{ss,0} + k_4[PS]_0[HO\cdot]_{ss,0}} \tag{A.23}$$

where k_4, $k_{HO\cdot/R}$ (in $M^{-1}\cdot s^{-1}$)are the second-order rate constants between reactions of (i) PS and HO·, (ii) R and HO·, respectively. k_4 has known value. $k_{HO\cdot/R}$ depends structure of the organic compound and $k_{HO\cdot/R}$ typically ranges from 10^7 $M^{-1}\cdot s^{-1}$ to 1.2×10^{10} $M^{-1}\cdot s^{-1}$. $[R]_0$ is 0.1 mM; $[PS]_0$ is 0.01 M. Therefore, in this case, the maximum value of Q_{A8} is 90.91%. We reported rate constants for 22 organic compounds with $SO_4^-\cdot$, HO·, and Cl· (other cases with different [R] and [PS] can be evaluated by our algorithm). The fraction of HO· reacting with 22 organic compounds is summarized in **Table A.7**.

A.4.2 Chloride is present

When Cl^- is present, the quenching ratio Q_{A9} (eq A.24) is equal to the rate of $SO_4^-\cdot$ oxidizing the target organic compound (R) divided by the rate of $SO_4^-\cdot$ reacting with all components in the water matrix (R, PS, Cl^- H_2O) (Figure 1(b)). In other words, Q_{A9} is the fraction of $SO_4^-\cdot$ reacting with organic compound.

$$Q_{A9} = \frac{k_{SO_4^-\cdot/R}[R]_0[SO_4^-\cdot]_{ss,0}^{Cl^-}}{\left(\sum_{Cl^-}^{SO_4^-\cdot} k_i S_i\right)[SO_4^-\cdot]_{ss,0}^{Cl^-} - k_4[PS]_0[HO\cdot]_{ss,0}^{Cl^-}} \tag{A.24}$$

where, $\sum_{Cl^-}^{SO_4^-\cdot} k_i S_i = k_{SO_4^-\cdot/R}[R]_0 + k_1[H_2O]_0 + k_2[Cl^-] + k_3[PS]_0$

The denominator includes the negative term $k_4[PS]_0[HO\cdot]_{ss,0}^{Cl^-}$,because $SO_4^-\cdot$ reacts with H_2O to generate HO· and HO· continues to react with PS to form $SO_4^-\cdot$. The consumption rate of $SO_4^-\cdot$ reacting with H_2O can be compensated by the production rate of $SO_4^-\cdot$ from the reaction between HO· and PS.

The initial steady state HO· concentration is given by eq A.99. Hence, Q_{A9} can be simplified as eq A.25:

$$Q_{A9} = \frac{k_{SO_4^-\cdot/R}[R]_0}{k_{SO_4^-\cdot/R}[R]_0 + k_1[H_2O]_0 + k_2[Cl^-] + k_3[PS]_0 - \dfrac{k_4[PS]_0\left(k_1[H_2O] + k_7[H_2O]A_3\right)}{k_4[PS]_0 + k_{HO\cdot/R}[R]_0}} \tag{A.25}$$

where, $A_3 = \dfrac{k_2[Cl^-]_0}{k_6[PS]_0 + k_7[H_2O] + k_{Cl\cdot/R}[R]_0 + \left(k_5 - \dfrac{k_9 k_5}{k_9 + k_{10}[PS]_0}\right)[Cl^-]_0}$

k_1, k_2, k_3, k_4, k_5, k_6, k_7, k_{10}, $k_{SO_4^-\cdot/R}$, $k_{HO\cdot/R}$ are the second-order rate constants between reactions of (i) H_2O and $SO_4^-\cdot$, (ii) Cl^- and $SO_4^-\cdot$, (iii) PS and $SO_4^-\cdot$, (iv) PS and HO·, (v) Cl- and Cl·, (vi) PS and Cl·, (vii) H_2O and Cl·, (viii) PS and $Cl_2^-\cdot$ (ix) R and $SO_4^-\cdot$, (x) R and HO·, respectively. k_1-k_4 have known values and have the units as $M^{-1}\cdot s^{-1}$. k_9 is the first-

order rate constant for $Cl_2^-\cdot$ producing Cl·, s^{-1}. $k_{SO_4^-\cdot/R}$ and $k_{HO\cdot/R}$ depends structure of the organic compound. $k_{SO_4^-\cdot/R}$ typically ranges from 10^2 $M^{-1}\cdot s^{-1}$ to 3.0×10^9 $M^{-1}\cdot s^{-1}$, and $k_{HO\cdot/R}$ typically ranges from 10^7 $M^{-1}\cdot s^{-1}$ to 1.2×10^{10} $M^{-1}\cdot s^{-1}$. $[Cl^-]/[R]$ ranges from 10 to 100; $[R]_0$ is 0.1 mM; and, $[PS]_0$ is 0.01 M. Therefore, in this case, the maximum value of Q_{A9} is 39.67% (other cases with different [R], [PS], $[Cl^-]$ can be evaluated by our algorithm). We reported rate constants for 22 organic compounds with $SO_4^-\cdot$, HO·, and Cl·. The fraction of $SO_4^-\cdot$ reacting with these organic compounds is summarized in **Table A.6**.

When Cl^- is present, HO· can be generated from ***(1)*** $SO_4^-\cdot$ reacts with H_2O; ***(2)*** $SO_4^-\cdot$ reacts with Cl^- to generate Cl·, Cl· reacts with H_2O to generate $ClOH^-\cdot$, then $ClOH^-\cdot$ produce HO·. We compared the HO· production rate when Cl^- is present to the rate when Cl^- is not present, which is given by Ratio A2 (eq A.26).

$$\text{RatioA2} = \frac{k_1[H_2O][SO_4^-\cdot]_{ss,0}^{Cl^-} + k_8[ClOH^-\cdot]_{ss,0}^{Cl^-}}{k_1[H_2O][SO_4^-\cdot]_{ss,0}} \tag{A.26}$$

According to eq A.96, $[ClOH^-\cdot]_{ss,0}^{Cl^-} = \frac{k_7[H_2O]A_3}{k_8}[SO_4^-\cdot]_{ss,0}^{Cl^-}$. Hence, Ratio A2 can be simplified as eq A.27:

$$\text{RatioA2} = \frac{\left(k_1[H_2O] + k_7[H_2O]A_3\right)}{k_1[H_2O]}\frac{[SO_4^-\cdot]_{ss,0}^{Cl^-}}{[SO_4^-\cdot]_{ss,0}} \tag{A.27}$$

where, $[SO_4^-\cdot]_{ss,0}$ equals to eq A.87, $[SO_4^-\cdot]_{ss,0}^{Cl^-}$ equals to eq A.98.

$$A_3 = \frac{k_2[Cl^-]_0}{k_6[PS]_0 + k_7[H_2O] + k_{Cl\cdot/R}[R]_0 + \left(k_5 - \frac{k_9k_5}{k_9 + k_{10}[PS]_0}\right)[Cl^-]_0}$$

k_1, k_2, k_3, k_4, k_5, k_6, k_7, k_{10}, $k_{SO_4^-\cdot/R}$, $k_{HO\cdot/R}$ are the second-order rate constants between reactions of (i) H_2O and $SO_4^-\cdot$, (ii) Cl^- and $SO_4^-\cdot$, (iii) PS and $SO_4^-\cdot$, (iv) PS and HO·, (v) Cl-

and Cl·, (vi) PS and Cl·, (vii) H_2O and Cl·, (viii) PS and Cl_2^-· (ix) R and SO_4^-·, (x) R and HO·, respectively.k_1-k_4 have known values and have the units as $M^{-1}\cdot s^{-1}$. k_9 is the first-order rate constant for Cl_2^-· producing Cl·, s^{-1}. $k_{SO_4^-\cdot/R}$ and $k_{HO\cdot/R}$ depends structure of the organic compound. $k_{SO_4^-\cdot/R}$ typically ranges from 10^2 $M^{-1}\cdot s^{-1}$ to 3.0×10^9 $M^{-1}\cdot s^{-1}$, and $k_{HO\cdot/R}$ typically ranges from 10^7 $M^{-1}\cdot s^{-1}$ to 1.2×10^{10} $M^{-1}\cdot s^{-1}$. $[Cl^-]/[R]$ ranges from 10 to 100; $[R]_0$ is 0.1 mM; and, $[PS]_0$ is 0.01 M. Therefore, in this case, the maximum value of *RatioA2* is 42.15% (other cases with different [R], [PS], $[Cl^-]$ can be evaluated by our algorithm). As a result, the generation rate of HO· decreases when Cl^- is present.

The quenching ratio Q_{A10} (eq A.28) is equal to the rate of HO· oxidizing organic compound (R) divided by the rate of HO· reacting with all components in the water matrix (R, PS) (**Figure 2.1(b)**).

$$Q_{A10} = \frac{k_{HO\cdot/R}[R]_0[HO\cdot]_{ss,0}^{Cl^-}}{k_{HO\cdot/R}[R]_0[HO\cdot]_{ss,0}^{Cl^-} + k_4[PS]_0[HO\cdot]_{ss,0}^{Cl^-}} \tag{A.28}$$

where k_4, $k_{HO\cdot/R}$ are the second-order rate constants between reactions of (i) PS and HO·, (ii) R and HO·, respectively. k_4 has known value and the unit is $M^{-1}\cdot s^{-1}$. $k_{HO\cdot/R}$ depends structure of the organic compound. $k_{HO\cdot/R}$ typically ranges from 10^7 $M^{-1}\cdot s^{-1}$ to 1.2×10^{10} $M^{-1}\cdot s^{-1}$ $[R]_0$ is 0.1 mM, $[PS]_0$ is 0.01 M. Overall, when Cl^- is present the fraction of HO· reacting with organic compound is equal to *Ratio A2* times Q_{A10}. Hence, in this case, at most 36.59% of HO· oxidizing the target organic compound (other cases with different [PS], [R], $[Cl^-]$ can be evaluated by our algorithm). We reported rate constants for 22 organic compounds with SO_4^-·, HO·, and Cl·. The fraction of SO_4^-· reacting with these organic compounds is summarized in **Table A.7**.

When Cl^- is present, the quenching ratio Q_{A11} (eq A.29) is equal to the rate of Cl· oxidizing organic compound (R) divided by the rate of Cl· reacting with all components in the water matrix (R, Cl^-, PS, H2O) (**Figure 2.1(b)**).

$$Q_{A11} = \frac{k_{Cl\cdot/R}[R]_0[Cl\cdot]_{ss,0}^{Cl^-}}{k_{Cl\cdot/R}[R]_0[Cl\cdot]_{ss,0}^{Cl^-} + k_5[Cl^-]_0[Cl\cdot]_{ss,0}^{Cl^-} + k_6[PS]_0[Cl\cdot]_{ss,0}^{Cl^-} + k_7[H_2O][Cl\cdot]_{ss,0}^{Cl^-} - k_8[Cl_2^-\cdot]_{ss,0}^{Cl^-}} \quad (A.29)$$

The denominator includes the negative term $k_8[Cl_2^-\cdot]_{ss,0}^{Cl^-}$,because Cl· reacts with Cl^- to generate $Cl_2^-\cdot$ and $Cl_2^-\cdot$ continues to dissociate to form Cl·. The consumption rate of Cl· from the reaction between Cl· and Cl^- can be compensated by the production rate of $Cl_2^-\cdot$ from the $Cl_2^-\cdot$ dissociate reaction.

The $Cl_2^-\cdot$ reaction rate is given by eq A.94. Hence, Q_{A11} can be simplified as eq A.30:

$$Q_{A11} = \frac{k_{Cl\cdot/R}[R]_0}{k_{Cl\cdot/R}[R]_0 + k_6[PS]_0 + k_7[H_2O] + \left(k_5 - \frac{k_5k_9}{k_9 + k_{10}[PS]_0}\right)[Cl^-]_0} \quad (A.30)$$

where k_5,k_6, k_7, k_9 and $k_{Cl\cdot/R}$ are the second-order rate constants between reactions of (i) Cl^- and Cl·, (ii) PS and Cl·, (iii) H_2O and Cl·, (iv) PS and $Cl_2^-\cdot$, (v) R and Cl·, respectively. k_8 is the first-order rate constant for $Cl_2^-\cdot$ producing Cl·, s^{-1}. k_5,k_6, k_7, k_9 have known values and have the units as $M^{-1}\cdot s^{-1}$. $k_{Cl\cdot/R}$ depends structure of the organic compound, and it typically ranges from $10^5 M^{-1}\cdot s^{-1}$ to 1.5×10^{10} $M^{-1}\cdot s^{-1}$. Three lines for 10%, 50% and 90% quenching ratio Q_{A11} in **Figure 2.3** were developed as following: ***(1)*** for a quenching ratio of Q_{A11} =0.1, (a line for 10% quenching could be obtained by substituting k_5-k_9 and $[PS]_0$ =0.01M in eq A.30 and the yellow dashed line, $k_{Cl\cdot/R}=6.36\times10^6\frac{[Cl^-]}{[R]}+3.26\times10^9$); ***(2)*** for a quenching ratio of Q_{A11} =0.5, (a line for 50% quenching can be obtained with the same values of k_5-k_9 and $[PS]_0$ and is shown as the blue dashed line,

$k_{Cl\cdot/R}=5.72\times10^{7}\frac{[Cl^-]}{[R]}+2.93\times10^{10}$); ***(3)*** similarly, for a quenching rate of Q_{A11} =0.9, a line for 90% quenching can be obtained (the green dashed line, $k_{Cl\cdot/R}=4.74\times10^{8}\frac{[Cl^-]}{[R]}+2.63\times10^{11}$); $[Cl^-]/[R]$ is ranging from 10 to 1000; $[R]_0$ is 0.1 mM; and, $[PS]_0$ is 0.01 M. Therefore, in this case, Q_{A11} must be less than 33.42% (other cases with different [R], [PS] and $[Cl^-]$ can be evaluated using our algorithm). We reported rate constants for 22 organic compounds with $SO_4^-\cdot$, HO·, and Cl·. The fraction of Cl· reacting with these organic compounds is summarized in **Table A.8**. Since Eq. 30 is monotone decreasing function in terms of $[Cl^-]/[R]$, the fraction of Cl· reacting with the target organic compound decrease with $[Cl^-]/[R]$ increase (**Table A.8**). This because higher $[Cl^-]/[R]$ cause more fraction of Cl· is scavenged by Cl^-.

Overall, for these 22 organic compounds, the ratio of organic destruction rate when Cl^- is present to the rate when Cl^- is not present is summarized in **Table A.9**.

A.4.3 NOM is present

When NOM is present, the quenching ratio Q_{A12} (eq A.31) is equal to the rate of $SO_4^-\cdot$ oxidizing organic compound (R) divided by the rate of $SO_4^-\cdot$ reacting with all components in the water matrix (R, PS, NOM, H_2O) (**Figure 2.1 (c)**). In other words, Q_{A12} is the fraction of $SO_4^-\cdot$ reacting with organic compound.

$$Q_{A12}=\frac{k_{SO_4^-\cdot/R}[R]_0[SO_4^-\cdot]_{ss,0}^{NOM}}{\left(\sum_{NOM}^{SO_4^-\cdot}k_iS_i\right)[SO_4^-\cdot]_{ss,0}^{NOM}-k_4[PS]_0[HO\cdot]_{ss,0}^{NOM}} \tag{A.31}$$

where,

$$\sum_{NOM}^{SO_4^-\cdot}k_iS_i=k_{SO_4^-\cdot/R}[R]_0+k_1[H_2O]_0+k_{SO_4^-\cdot/NOM}[NOM]_0+k_3[PS]_0$$

The denominator includes the negative term $k_4[PS]_0[HO\cdot]_{ss,0}^{NOM}$,because $SO_4^-\cdot$ reacts with H_2O to generate HO· and HO· continues to react with PS to form $SO_4^-\cdot$.

The initial steady state HO· concentration is given by eq A.110. Hence, Q_{A12} can be simplified as eq A.32:

$$Q_{A12} = \frac{k_{SO_4^-\cdot/R}[R]_0}{\sum_{NOM}^{SO_4^-\cdot} k_i S_i - \frac{k_1 k_4 [H_2O][PS]_0}{k_4[PS]_0 + k_{HO\cdot/NOM}[NOM]_0 + k_{HO\cdot/R}[R]_0}} \quad (A.32)$$

where, $\sum_{NOM}^{SO_4^-\cdot} k_i S_i = k_{SO_4^-\cdot/R}[R]_0 + k_1[H_2O]_0 + k_{SO_4^-\cdot/NOM}[NOM]_0 + k_3[PS]_0$

where k_1,k_3, k_4, $k_{SO_4^-\cdot/NOM}$, $k_{HO\cdot/NOM}$, $k_{SO_4^-\cdot/R}$, $k_{HO\cdot/R}$ are the second-order rate constants between reactions of (i) H_2O and $SO_4^-\cdot$, (ii) PS and $SO_4^-\cdot$, (iii) PS and HO·, (iv) NOM and $SO_4^-\cdot$, (v) NOM and HO·, (v) R and $SO_4^-\cdot$, (vi) R and HO·, respectively. k_1-k_4 have known values and have the units as $M^{-1}\cdot s^{-1}$. $k_{SO_4^-\cdot/R}$ and $k_{HO\cdot/R}$ depends structure of the organic compound. $k_{SO_4^-\cdot/R}$ typically ranges from 10^2 $M^{-1}\cdot s^{-1}$ to 3.0×10^9 $M^{-1}\cdot s^{-1}$, and $k_{HO\cdot/R}$ typically ranges from 10^7 $M^{-1}\cdot s^{-1}$ to 1.2×10^{10} $M^{-1}\cdot s^{-1}$. $[R]_0$ is 0.1 mM; $[PS]_0$ is 0.01 M; and, $[NOM]_0$ is 2 $mg\cdot L^{-1}$. Therefore, in this case, the maximum value of Q_{A12} is 86.58% (other cases with different [R], [PS], [NOM] can be evaluated using our algorithm). As the previous discussion, when NOM is present, the fraction of $SO_4^-\cdot$ oxidizing target organic compound is determined by two factors: ***(1)*** NOM absorbs UV light, $SO_4^-\cdot$ production rate decreases 47.1%; ***(2)*** quenching ratio Q_{A12} is no more than 86.58%. Consequently, in this case, at most 45.8% (0.8658×(1-0.471) ×100%) $SO_4^-\cdot$ reacts with organic compound (other cases with different [R], [PS], [NOM] can be evaluated using our algorithm). When

NOM is present, the fraction of $SO_4^-\cdot$ reacting with previously discussed 22 organic compounds is summarized in **Table A.10**.

When NOM is present, NOM absorbs UV light which can decrease the $SO_4^-\cdot$ photolysis production rate. Therefore, the HO· production rate from $SO_4^-\cdot$ reacting with H_2O will be decreased in the presence of NOM. Ratio S3 in eq is the HO· production rate from $SO_4^-\cdot$ reacting with H_2O when NOM is present to the rate when NOM is not present.

$$\text{RatioA3} = \frac{k_1[H_2O][SO_4^-\cdot]_{ss,0}^{NOM}}{k_1[H_2O][SO_4^-\cdot]_{ss,0}} = \frac{[SO_4^-\cdot]_{ss,0}^{NOM}}{[SO_4^-\cdot]_{ss,0}} \tag{A.33}$$

where, $[SO_4^-\cdot]_{ss,0}$ equals to eq A.87, $[SO_4^-\cdot]_{ss,0}^{NOM}$ equals to eq A.111 if $[Cl^-]$ is 0M.

The quenching ratio Q_{A13} in eq A.34 is equal to the rate of HO· oxidizing organic compound (R) divided by the rate of HO· reacting with all components in the water matrix (R, PS) (**Figure 2.1(c)**).

$$Q_{A13} = \frac{k_{HO\cdot/R}[R]_0[HO\cdot]_{ss,0}^{NOM}}{k_{HO\cdot/R}[R]_0[HO\cdot]_{ss,0}^{NOM} + k_4[PS]_0[HO\cdot]_{ss,0}^{NOM} + k_{HO\cdot/NOM}[NOM]_0[HO\cdot]_{ss,0}^{NOM}} \tag{A.34}$$

where k_4, $k_{HO\cdot/NOM}$, $k_{HO\cdot/R}$ are the second-order rate constants between reactions of (i) PS and HO·, (ii) NOM and HO·, (iii) R and HO·, respectively. k_4 has known value and have the units as $M^{-1}\cdot s^{-1}$. $k_{HO\cdot/R}$ depends structure of the organic compound. $k_{HO\cdot/R}$ typically ranges from 10^7 $M^{-1}\cdot s^{-1}$ to 1.2×10^{10} $M^{-1}\cdot s^{-1}$. $[R]_0$ is 0.1 mM; $[PS]_0$ is 0.01 M. Consequently, the fraction of HO· reacting with organic compound is Ratio A3 times Q_{A13}. We reported rate constants for 22 organic compounds with $SO_4^-\cdot$, HO·, and Cl·. When NOM is present, the fraction of HO· reacting with these organic compounds is summarized in **Table A.11**. For this case, at most 39.8% of HO· reacting with these organic compounds (other cases with different [R], [PS], and [NOM] can be evaluated using our algorithm).

Overall, for these 22 organic compounds, the ratio of organic destruction rate when NOM is present to the rate when NOM is not present is summarized in **Table A.13**.

A.4.4 Chloride and NOM are present

When NOM and Cl^- are present, the quenching ratio Q_{A14} (eq A.35) is equal to the rate of $SO_4^-\cdot$ oxidizing organic compound (R) divided by the rate of $SO_4^-\cdot$ reacting with all components in the water matrix (R, PS, Cl^-, NOM, H_2O) (**Figure 2.1(c)**). In other words, Q_{A14} is the fraction of $SO_4^-\cdot$ reacting with organic compound.

$$Q_{A14} = \frac{k_{SO_4^-\cdot/R}[R]_0[SO_4^-\cdot]_{ss,0}^{NOM,Cl^-}}{\left(\sum_{NOM,Cl^-}^{SO_4^-\cdot} k_i S_i\right)[SO_4^-\cdot]_{ss,0}^{NOM,Cl^-} - k_4[PS]_0[HO\cdot]_{ss,0}^{NOM,Cl^-}} \tag{A.35}$$

where,

$$\sum_{NOM,Cl^-}^{SO_4^-\cdot} k_i S_i = k_{SO_4^-\cdot/R}[R]_0 + k_1[H_2O]_0 + k_2[Cl^-]_0 + k_{SO_4^-\cdot/NOM}[NOM]_0 + k_3[PS]_0$$

The denominator includes the negative term $k_4[PS]_0[HO\cdot]_{ss,0}^{NOM,Cl^-}$,because $SO_4^-\cdot$ reacts with H_2O to generate HO· and HO· continues to react with PS to form $SO_4^-\cdot$. The consumption rate of $SO_4^-\cdot$ from the reaction between $SO_4^-\cdot$ and H_2O can be compensated by the production rate of $SO_4^-\cdot$ from the reaction between HO· and PS.

The initial steady state HO· concentration is given by eq A.110. Hence, Q_{A14} can be simplified as eq A.36:

$$Q_{A14} = \frac{k_{SO_4^-\cdot/R}[R]_0}{\sum_{NOM,Cl^-}^{SO_4^-\cdot} k_i S_i - \frac{k_4[PS]_0\left(k_1[H_2O] + k_7[H_2O]A_7\right)}{k_4[PS]_0 + k_{HO\cdot/NOM}[NOM]_0 + k_{HO\cdot/R}[R]_0}} \tag{A.36}$$

where, $\sum_{NOM,Cl^-}^{SO_4^-\cdot} k_i S_i = k_{SO_4^-\cdot/R}[R]_0 + k_1[H_2O]_0 + k_2[Cl^-]_0 + k_{SO_4^-\cdot/NOM}[NOM]_0 + k_3[PS]_0$

where k_1,k_2,k_3, k_4, $k_{SO_4^-\cdot/NOM}$, $k_{HO\cdot/NOM}$, $k_{SO_4^-\cdot/R}$, $k_{HO\cdot/R}$ are the second-order rate constants between reactions of (i) H_2O and $SO_4^-\cdot$, (ii) Cl^- and $SO_4^-\cdot$, (iii) PS and $SO_4^-\cdot$, (iv) PS and $HO\cdot$, (v) NOM and $SO_4^-\cdot$, (vi) NOM and $HO\cdot$, (vii) R and $SO_4^-\cdot$, (viii) R and $HO\cdot$, respectively. k_1-k_4 have known values and have the units as $M^{-1}\cdot s^{-1}$. $k_{SO_4^-\cdot/R}$ and $k_{HO\cdot/R}$ depends structure of the organic compound. $k_{SO_4^-\cdot/R}$ typically ranges from 10^2 $M^{-1}\cdot s^{-1}$ to 3.0×10^9 $M^{-1}\cdot s^{-1}$, and $k_{HO\cdot/R}$ typically ranges from 10^7 $M^{-1}\cdot s^{-1}$ to 1.2×10^{10} $M^{-1}\cdot s^{-1}$. $[R]_0$ is 0.1 mM; $[PS]_0$ is 0.01 M; $[NOM]_0$ is 2 $mg\cdot L^{-1}$; and, $[Cl^-]_0$ ranges from 0.001 M to 0.1 M. Therefore, in this case, the maximum value of Q_{A14} is 36.71% (other cases with different [R], [PS], [NOM], $[Cl^-]$ can be evaluated by our algorithm). As the previous discussion, when NOM is present, the fraction of $SO_4^-\cdot$ oxidizing target organic compound is determined by two factors: ***(1)*** NOM absorbs UV light, $SO_4^-\cdot$ production rate decreases 47.1%; ***(2)*** quenching ratio Q_{A12} is no more than 37.41%. Consequently, for this case, at most 19.79% (0.3741×(1-0.471) ×100%) $SO_4^-\cdot$ reacts with organic compound in the presence of NOM and Cl^- (other case with different [R], [PS], [NOM], $[Cl^-]$ can be evaluated using our algorithm). When NOM and Cl^- are present, the fraction of $SO_4^-\cdot$ reacting with previously discussed 22 organic compounds is summarized in **Table A.10**.

When NOM and Cl^- are present, we compared the $HO\cdot$ production rate when NOM and Cl^- is present to the rate when NOM and Cl^- are not present, which is given by Ratio A4 (eq A.37).

$$\text{RatioA4} = \frac{k_1[H_2O][SO_4^-\cdot]_{ss,0}^{NOM,Cl^-} + k_8[ClOH^-\cdot]_{ss,0}^{NOM,Cl^-}}{k_1[H_2O][SO_4^-\cdot]_{ss,0}} \quad \text{(A.37)}$$

According to eq A.109, $[ClOH^{-}\cdot]_{ss,0}^{NOM,\ Cl^{-}} = \frac{k_7[H_2O]A_7}{k_8}[SO_4^{-}\cdot]_{ss,0}^{NOM,\ Cl^{-}}$. Hence, Ratio A4 can be simplified as eq A.38:

$$\text{RatioA4} = \frac{k_1[H_2O][SO_4^{-}\cdot]_{ss,0}^{NOM,Cl^{-}} + k_8[ClOH^{-}\cdot]_{ss,0}^{NOM,Cl^{-}}}{k_1[H_2O][SO_4^{-}\cdot]_{ss,0}} \tag{A.38}$$

where, $[SO_4^{-}\cdot]_{ss,0}$ equals to eq A.87, $[SO_4^{-}\cdot]_{ss,0}^{Cl^{-}}$ equals to eq A.111.

$$A_3 = \frac{k_2[Cl^{-}]_0}{k_6[PS]_0 + k_7[H_2O] + k_{Cl\cdot/R}[R]_0 + \left(k_5 - \frac{k_9 k_5}{k_9 + k_{10}[PS]_0}\right)[Cl^{-}]_0}$$

where, k_1, k_2, k_3, k_4, k_5, k_6, k_7, k_{10}, $k_{SO_4^{-}\cdot/R}$, $k_{HO\cdot/R}$ are the second-order rate constants between reactions of (i) H_2O and $SO_4^{-}\cdot$, (ii) Cl^{-} and $SO_4^{-}\cdot$, (iii) PS and $SO_4^{-}\cdot$, (iv) PS and HO·, (v) Cl^{-} and Cl·, (vi) PS and Cl·, (vii) H_2O and Cl·, (viii) PS and $Cl_2^{-}\cdot$ (ix) R and $SO_4^{-}\cdot$, (x) R and HO·, respectively.k_1-k_4 have known values and have the units as $M^{-1}\cdot s^{-1}$. k_9 is the first-order rate constant for $Cl_2^{-}\cdot$ producing Cl·, s^{-1}. $k_{SO_4^{-}\cdot/R}$ and $k_{HO\cdot/R}$ depends structure of the organic compound. $k_{SO_4^{-}\cdot/R}$ typically ranges from 10^2 $M^{-1}\cdot s^{-1}$ to 3.0×10^9 $M^{-1}\cdot s^{-1}$, and $k_{HO\cdot/R}$ typically ranges from 10^7 $M^{-1}\cdot s^{-1}$ to 1.2×10^{10} $M^{-1}\cdot s^{-1}$. $[Cl^{-}]/[R]$ ranges from 10 to 100; $[R]_0$ is 0.1 mM; and, $[PS]_0$ is 0.01 M. Therefore, in this case, the maximum value of RatioA4 is 20.52% (other cases with different [R], [PS], $[Cl^{-}]$ can be evaluated by our algorithm). As a result, the generation rate of HO· decreases when Cl^{-} is present. The quenching ratio Q_{A15} in eq is equal to the rate of HO· oxidizing organic compound (R) divided by the rate of HO· reacting with all components in the water matrix (R, PS, NOM) (**Figure 2.1(c)**).

$$Q_{A15} = \frac{k_{HO\cdot/R}[R]_0[HO\cdot]_{ss,0}^{NOM,Cl^-}}{k_{HO\cdot/R}[R]_0[HO\cdot]_{ss,0}^{NOM,Cl^-} + k_4[PS]_0[HO\cdot]_{ss,0}^{NOM,Cl^-} + k_{HO\cdot/NOM}[NOM]_0[HO\cdot]_{ss,0}^{NOM,Cl^-}} \quad (A.39)$$

where k_4, $k_{HO\cdot/NOM}$, $k_{HO\cdot/R}$ are the second-order rate constants between reactions of (i) PS and HO·, (ii) NOM and HO·, (iii) R and HO·, respectively. k_4 has known value and has the unit as $M^{-1}\cdot s^{-1}$. $k_{HO\cdot/R}$ depends structure of the organic compound. $k_{HO\cdot/R}$ typically ranges from 10^7 $M^{-1}\cdot s^{-1}$ to 1.2×10^{10} $M^{-1}\cdot s^{-1}$ $[R]_0$ is 0.1 mM, $[PS]_0$ is 0.01 M. Consequently, the fraction of HO· reacting with organic compound is Ratio A4 times Q_{A15}. We reported rate constants for 22 organic compounds with $SO_4^-\cdot$, HO·, and Cl·. When NOM and Cl^- are present, the fraction of HO· reacting with these organic compounds is summarized in **Table A.11**. For this case, at most 17.81% of HO· reacting with these organic compounds (other cases with different [R], [PS], [NOM], $[Cl^-]$ can be evaluated using our algorithm).

When NOM and Cl^- is present, the quenching ratio Q_{A16} (eq A.40) is equal to the rate of Cl· oxidizing organic compound (R) divided by the rate of Cl· reacting with all components in the water matrix (R, Cl^-, PS, H_2O, NOM) (**Figure 2.1(c)**).

$$Q_{A16} = \frac{k_{Cl\cdot/R}[R]_0[Cl\cdot]_{ss,0}^{Cl^-,NOM}}{\left(\sum_{Cl^-,NOM}^{Cl\cdot} k_i S_i\right)[Cl\cdot]_{ss,0}^{Cl^-,NOM} - k_9[Cl_2^-\cdot]_{ss,0}^{Cl^-,NOM}} \quad (A.40)$$

The denominator includes the negative term $k_8[Cl_2^-\cdot]_{ss,0}^{Cl^-,NOM}$,because Cl· reacts with Cl^- to generate $Cl_2^-\cdot$ and $Cl_2^-\cdot$ continues to dissociate to form Cl·. The consumption rate of Cl· from the reaction between Cl· and Cl^- can be compensated by the production rate of $Cl_2^-\cdot$ from the $Cl_2^-\cdot$ dissociate reaction.

The $Cl_2^-\cdot$ reaction rate is given by eq A.108. Hence, Q_{A16} is simplified as eq A.41:

$$Q_{A16} = \frac{k_{Cl\cdot/R}[R]_0}{\left(\sum_{Cl^-,NOM}^{Cl\cdot} k_i S_i\right) - \frac{k_5 k_9 [Cl^-]_0}{k_9 + k_{10}[PS]_0 + k_{Cl_2^-\cdot/NOM}[NOM]_0}} \quad (A.41)$$

where,

$$\sum_{Cl^-,NOM}^{Cl\cdot} k_i S_i = k_5[Cl^-]_0 + k_6[PS]_0 + k_7[H_2O] + k_{Cl\cdot/NOM}[NOM]_0 + k_{Cl\cdot/R}[R]_0$$

where, k_i is the second order rate constant between compound i and Cl·, $M^{-1}\cdot s^{-1}$;k_9, $k_{Cl\cdot/NOM}$ and $k_{Cl_2^-\cdot/NOM}$ are the second order rate constants between PS and $Cl_2^-\cdot$, NOM and Cl·, NOM and $Cl_2^-\cdot$, respectively. k_5-k_9 and $k_{Cl\cdot/NOM}$ and $k_{Cl_2^-\cdot/NOM}$have known values, they have the units $M^{-1}\cdot s^{-1}$. $k_{Cl\cdot/R}$ depends structure of the organic compound, and it ranges from 10^5 $M^{-1}\cdot s^{-1}$ to 1.5×10^{10} $M^{-1}\cdot s^{-1}$. $[Cl^-]/[R]$ is ranging from 10 to 1000, $[R]_0$ is 0.1 mM; $[PS]_0$ is 0.01 M; and, $[NOM]_0$ is 2 mg/L. Therefore, in this case, Q_{A16} has the maximum value as 0.331 (other cases with different [R], [PS], [NOM], $[Cl^-]$ can be evaluated by our algorithm). As the previous discussion, when NOM and $Cl^-$are present, the fraction of $SO_4^-\cdot$ oxidizing target organic compound is determined by two factors: ***(1)*** NOM absorbs UV light, $SO_4^-\cdot$ production rate decreases 47.1%, the rate of $SO_4^-\cdot$ reacting Cl^- to produce Cl· will also decrease 47.1%; ***(2)*** quenching ratio Q_{S16} is no more than 86.58%. As a result, in this case, no more than 17.512 ($0.331\times(1\text{-}0.471)\times100\%$) Cl· will destruct organic compound (other cases with different [R], [PS], [NOM], $[Cl^-]$ can be evaluated by our algorithm). When NOM and Cl^- are present, the fraction of Cl· reacting with organic compound is summarized in **Table A.12**. Overall, for these 22 organic compounds, the ratio of organic destruction rate when NOM and Cl^- are present to the rate when NOM and Cl^- are not present is summarized in **Table A.13**.

A.4.5 Bicarbonate and Carbonate are present

When HCO_3^-/CO_3^{2-} is present, the quenching ratio Q_{A17} (eq A.42) is equal to the rate of $SO_4^-\cdot$ oxidizing organic compound (R) divided by the rate of $SO_4^-\cdot$ reacting with all components in the water matrix (R, PS, HCO_3^-, CO_3^{2-}, H_2O) (**Figure 2.1(d)**). In other words, Q_{A17} is the fraction of $SO_4^-\cdot$ reacting with organic compound.

$$Q_{A17} = \frac{k_{SO_4^-\cdot/R}[R]_0[SO_4^-\cdot]^C_{ss,0}}{\left(\sum_C^{SO_4^-\cdot} k_i S_i\right)[SO_4^-\cdot]^C_{ss,0} - k_4[PS]_0[HO\cdot]^C_{ss,0}} \tag{A.42}$$

where,

$$\sum_C^{SO_4^-\cdot} k_i S_i = k_{SO_4^-\cdot/R}[R]_0 + k_1[H_2O]_0 + k_3[PS]_0 + k_{10}[HCO_3^-]_0 + k_{11}[CO_3^{2-}]_0$$

The denominator includes the negative term $k_4[PS]_0[HO\cdot]^C_{ss,0}$,because $SO_4^-\cdot$ reacts with H_2O to generate HO· and HO· continues to react with PS to form $SO_4^-\cdot$. The consumption rate of $SO_4^-\cdot$ from the reaction between $SO_4^-\cdot$ and H_2O can be compensated by the production rate of $SO_4^-\cdot$ from the reaction between HO· and PS.

The HO· reaction rate is given at eq A.120. Hence, Q_{A17} can be simplified as eq A.43:

$$Q_{A17} = \frac{k_{SO_4^-\cdot/R}[R]_0}{\sum_C^{SO_4^-\cdot} k_i S_i - \dfrac{k_1 k_4 [H_2O][PS]_0}{k_4[PS]_0 + k_{13}[HCO_3^-]_0 + k_{14}[CO_3^{2-}]_0 + k_{HO\cdot/R}[R]_0}} \tag{A.43}$$

where,

$$\sum_C^{SO_4^-\cdot} k_i S_i = k_{SO_4^-\cdot/R}[R]_0 + k_1[H_2O]_0 + k_3[PS]_0 + k_{11}[HCO_3^-]_0 + k_{12}[CO_3^{2-}]_0$$

where k_1, k_3, k_4, k_{10}, k_{11}, k_{13}, k_{14} $k_{SO_4^-\cdot/R}$, $k_{HO\cdot/R}$ are the second-order rate constants between reactions of (i) H_2O and $SO_4^-\cdot$, (ii) PS and $SO_4^-\cdot$, (iii) PS and HO·, (iv) HCO_3^- and $SO_4^-\cdot$, (v) CO_3^{2-} and $SO_4^-\cdot$, (vi) HCO_3^- and HO·, (vii) CO_3^{2-} and HO·, (ix) R and $SO_4^-\cdot$, (x) R

and HO·, respectively,.k_1-k_{13} have known values and have the units as $M^{-1}\cdot s^{-1}$. $k_{SO_4^-\cdot/R}$ and $k_{HO\cdot/R}$ depends structure of the organic compound. $k_{SO_4^-\cdot/R}$ typically ranges from 10^2 $M^{-1}\cdot s^{-1}$ to 3.0×10^9 $M^{-1}\cdot s^{-1}$, and $k_{HO\cdot/R}$ typically ranges from 10^7 $M^{-1}\cdot s^{-1}$ to 1.2×10^{10} $M^{-1}\cdot s^{-1}$. $[R]_0$ is 0.1 mM; $[PS]_0$ is 0.01 M; $[HCO_3^-]_0$ is 0.1 mM; and, $[CO_3^{2-}]_0$ is 1.4 μM. Therefore, in this case, the maximum value of Q_{A17} is 96.19% (other cases with different [R], [PS], $[HCO_3^-]$, $[CO_3^{2-}]$ can be evaluated using our algorithm). When HCO_3^-/CO_3^{2-} is present, the fraction of $SO_4^-\cdot$ reacting with previously discussed 22 organic compounds is summarized in **Table A.14**.

When HCO_3^-/CO_3^{2-} is present, we compared the HO· production rate when HCO_3^-/CO_3^{2-} are present to the rate when HCO_3^-/CO_3^{2-} are not present as Ratio A5 (eq A.44).

$$\text{RatioA5} = \frac{k_1[H_2O][SO_4^-\cdot]^C_{ss,0}}{k_1[H_2O][SO_4^-\cdot]_{ss,0}} = \frac{[SO_4^-\cdot]^C_{ss,0}}{[SO_4^-\cdot]_{ss,0}} \tag{A.44}$$

where, $[SO_4^-\cdot]_{ss,0}$ equals to eq A.87, $[SO_4^-\cdot]^C_{ss,0}$ equals to eq A.127 if $[Cl^-]$ is 0M.

The quenching ratio Q_{A18} (eq A.45) is equal to the rate of HO· oxidizing organic compound (R) divided by the rate of HO· reacting with all components in the water matrix (R, PS, HCO_3^-/CO_3^{2-}) (**Figure 2.1(d)**).

$$Q_{A18} = \frac{k_{HO\cdot/R}[R]_0[HO\cdot]^C_{ss,0}}{k_{HO\cdot/R}[R]_0[HO\cdot]^C_{ss,0} + k_4[PS]_0[HO\cdot]^C_{ss,0} + k_{13}[HCO_3^-]_0[HO\cdot]^C_{ss,0} +_{14}[CO_3^{2-}]_0[HO\cdot]^C_{ss,0}} \tag{A.45}$$

where k_4, k_{13}, k_{14} are the second-order rate constants between reactions of (i) PS and HO·, (ii) HCO_3^- and HO·, (iii) CO_3^{2-} and HO·, (iii) R and HO·, respectively.k_4-k_{13} have known values and have the units as $M^{-1}\cdot s^{-1}$. $k_{HO\cdot/R}$ depends structure of the organic compound. $k_{HO\cdot/R}$ typically ranges from 10^7 $M^{-1}\cdot s^{-1}$ to 1.2×10^{10} $M^{-1}\cdot s^{-1}$. $[R]_0$ is 0.1 mM; $[PS]_0$ is 0.01

M; $[HCO_3^-]_0$ is 0.1 mM; and, $[CO_3^{2-}]_0$ is 1.4 μM. As previous discussion, HO· production rate decreases because of HCO_3^-/CO_3^{2-} scavenging SO_4^-·. Consequently, the fraction of HO· reacting with organic compound is Ratio A5 times Q_{A18}. When HCO_3^-/CO_3^{2-} is present, the fraction of HO· reacting with previously discussed 22 organic compounds is summarized in Table S15. In this case, at most 83.81% of HO· reacting with these organic compounds (other cases with different [R], [PS], $[HCO_3^-]$, $[CO_3^{2-}]$ can be evaluated using our algorithm). Overall, for these 22 organic compounds, the ratio of organic destruction rate when HCO_3^-/CO_3^{2-} is present to the rate when HCO_3^-/CO_3^{2-} is not present is summarized in **Table A.17**.

A.4.6 Chloride, Bicarbonate and Carbonate are present

When HCO_3^-/CO_3^{2-} and Cl^- are present, the quenching ratio Q_{A19} (eq A.46) is equal to the rate of SO_4^-· oxidizing organic compound (R) divided by the rate of SO_4^-· reacting with all components in the water matrix (R, PS, Cl^-, HCO_3^-, CO_3^{2-}, H_2O) (**Figure 2.1(d)**). In other words, Q_{A19} is the fraction of SO_4^-· reacting with organic compound.

$$Q_{A19} = \frac{k_{SO_4^-\cdot/R}[R]_0[SO_4^-\cdot]_{ss,0}^{C,Cl^-}}{\left(\sum_{C,Cl^-}^{SO_4^-\cdot} k_i S_i\right)[SO_4^-\cdot]_{ss,0}^{C,Cl^-} - k_4[PS]_0[HO\cdot]_{ss,0}^{C,Cl^-}} \tag{A.46}$$

where,

$$\sum_{NOM,Cl^-}^{SO_4^-\cdot} k_i S_i = k_{SO_4^-\cdot/R}[R]_0 + k_1[H_2O]_0 + k_2[Cl^-]_0 + k_{11}[HCO_3^-]_0 + k_{12}[CO_3^{2-}]_0 + k_3[PS]_0$$

The denominator includes the negative term $k_4[PS]_0[HO\cdot]_{ss,0}^{C,Cl^-}$,because SO_4^-· reacts with H_2O to generate HO· and HO· continues to react with PS to form SO_4^-·. The consumption

rate of $SO_4^-\cdot$ from the reaction between $SO_4^-\cdot$ and H_2O can be compensated by the production rate of $SO_4^-\cdot$ from the reaction between HO· and PS.

The initial steady state HO· concentration is given by eq A.122. Hence, Q_{A19} can be simplified as eq A.47:

$$Q_{A19} = \frac{k_{SO_4^-\cdot/R}[R]_0}{\sum_{C,Cl^-}^{SO_4^-\cdot} k_i S_i - \frac{k_4[PS]_0(k_1[H_2O]+k_7[H_2O]A_9)}{k_4[PS]_0 + k_{13}[HCO_3^-]_0 + k_{14}[CO_3^{2-}]_0 + k_{HO\cdot/R}[R]_0}} \quad \text{(A.47)}$$

where,

$$\sum_{C,Cl^-}^{SO_4^-\cdot} k_i S_i = k_{SO_4^-\cdot/R}[R]_0 + k_1[H_2O]_0 + k_2[Cl^-]_0 + k_3[PS]_0 + k_{10}[HCO_3^-]_0 + k_{11}[CO_3^{2-}]_0$$

where k_1,k_2,k_3, k_4, k_{10}, k_{11}, k_{13}, k_{14}, $k_{SO_4^-\cdot/R}$, $k_{HO\cdot/R}$ are the second-order rate constants between reactions of (i) H_2O and $SO_4^-\cdot$, (ii) Cl- and $SO_4^-\cdot$, (iii) PS and $SO_4^-\cdot$, (iv) PS and HO·, (v) HCO_3^- and $SO_4^-\cdot$, (vi) CO_3^{2-} and $SO_4^-\cdot$, (vii) HCO_3^- and HO·, (ix) CO_3^{2-} and HO·, (x) R and $SO_4^-\cdot$, (xi) R and HO·, respectively.k_1-k_{13} have known values and have the units as $M^{-1}\cdot s^{-1}$. $k_{SO_4^-\cdot/R}$ and $k_{HO\cdot/R}$ depends structure of the organic compound. $k_{SO_4^-\cdot/R}$ typically ranges from 10^2 $M^{-1}\cdot s^{-1}$ to 3.0×10^9 $M^{-1}\cdot s^{-1}$, and $k_{HO\cdot/R}$ typically ranges from 10^7 $M^{-1}\cdot s^{-1}$ to 1.2×10^{10} $M^{-1}\cdot s^{-1}$. $[R]_0$ is 0.1mM; $[PS]_0$ is 0.01 M; $[HCO_3^-]_0$ is 0.1 mM; $[CO_3^{2-}]_0$ is 1.4 μM; and, $[Cl^-]_0$ ranges from 0.001 M to 0.1 M. Therefore, in this case, the maximum value of Q_{S19} is 39.13% (other cases with different [R], [PS], $[Cl^-]$, $[HCO_3^-]$, $[CO_3^{2-}]$ can be evaluated using our algorithm). When HCO_3^-/ $CO_3^{2-}$and Cl^- are present, the fraction of $SO_4^-\cdot$ reacting with previously discussed 22 organic compounds is summarized in **Table A.14**.

When HCO_3^-/CO_3^{2-} and Cl^- are present, we compared the HO· production rate when Cl^- and HCO_3^-/CO_3^{2-} are present to the rate when Cl^- and HCO_3^-/CO_3^{2-} are not present as Ratio A6 (eq A.48).

$$\text{RatioA6} = \frac{(k_1[H_2O] + k_7[H_2O]A_9)\left(k_4[PS]_0 + k_{HO\cdot/R}[R]\right)}{\left(k_4[PS]_0 + k_{13}[HCO_3^-]_0 + k_{14}[CO_3^{2-}]_0 + k_{HO\cdot/R}[R]_0\right)k_1[H_2O]} \frac{[SO_4^-\cdot]_{ss,0}^{Cl^-,C}}{[SO_4^-\cdot]_{ss,0}^{no\ Cl^-}} \tag{A.48}$$

where, $[SO_4^-\cdot]_{ss,0}$ equals to eq A.87, $[SO_4^-\cdot]_{ss,0}^{C,\ Cl^-}$ equals to eq A.127.

The quenching ratio Q_{A20} (eq A.49) is equal to the rate of HO· oxidizing organic compound (R) divided by the rate of HO· reacting with all components in the water matrix (R, PS, HCO_3^-/CO_3^{2-}) (**Figure 2.1(d)**).

$$Q_{A20} = \frac{k_{HO\cdot/R}[R]_0[HO\cdot]_{ss,0}^{C,Cl^-}}{\left(\sum_{C,Cl^-}^{HO\cdot} k_j S_i\right)[HO\cdot]_{ss,0}^{C,Cl^-}} \tag{A.49}$$

where,

$$\sum_{C,Cl^-}^{HO\cdot} k_j S_j = k_{HO\cdot/R}[R]_0[HO\cdot]_{ss,0}^{C} + k_4[PS]_0[HO\cdot]_{ss,0}^{C} + k_{13}[HCO_3^-]_0[HO\cdot]_{ss,0}^{C} +_{14}[CO_3^{2-}]_0[HO\cdot]_{ss,0}^{C}$$

where k_4, k_{13}, k_{14} are the second-order rate constants between reactions of (i) PS and HO·, (ii) HCO_3^- and HO·, (iii) CO_3^{2-} and HO·, (iii) R and HO·, respectively.k_4-k_{14} have known values and have the units as $M^{-1}\cdot s^{-1}$. $k_{HO\cdot/R}$ depends structure of the organic compound. $k_{HO\cdot/R}$ typically ranges from 10^7 $M^{-1}\cdot s^{-1}$ to 1.2×10^{10} $M^{-1}\cdot s^{-1}$. $[R]_0$ is 0.1 mM; $[PS]_0$ is 0.01 M; $[HCO_3^-]_0$ is 0.1 mM; and, $[CO_3^{2-}]_0$ is 1.4 μM. As previous discussion, HO· production rate decreases because of HCO_3^-/CO_3^{2-} and Cl^- scavenging $SO_4^-\cdot$. Consequently, the fraction of HO· reacting with organic compound is Ratio A6 times Q_{S20}. When HCO_3^-/CO_3^{2-} and Cl^- are present, the fraction of HO· reacting with these organic compounds is summarized in **Table A.15**. For this case, at most 33.49% of HO· reacting with these organic compounds

(other cases with different [R], [PS], [Cl^-], [HCO_3^-], [CO_3^{2-}] can be evaluated using our algorithm).

When HCO_3^-/CO_3^{2-} and Cl^- is present, the quenching ratio Q_{A21} (eq A.50) is equal to the rate of Cl· destructing organic compound (R) divided by the rate of Cl· reacting with all components in the water matrix (R, Cl^-, PS, H_2O, HCO_3^-/CO_3^{2-}) (**Figure 2.1(d)**).

$$Q_{A21} = \frac{k_{Cl\cdot/R}[R]_0[Cl\cdot]_{ss,0}^{Cl^-,C}}{\left(\sum_{Cl^-,C}^{Cl\cdot} k_i S_i\right)[Cl\cdot]_{ss,0}^{Cl^-,C} - k_9[Cl_2^-\cdot]_{ss,0}^{Cl^-,C}} \tag{A.50}$$

The denominator includes the negative term $k_9[Cl_2^-\cdot]_{ss,0}^{Cl^-,C}$,because Cl· reacts with Cl^- to generate $Cl_2^-\cdot$ and $Cl_2^-\cdot$ continues to dissociate to form Cl·. The consumption rate of Cl· from the reaction between Cl· and Cl^- can be compensated by the production rate of $Cl_2^-\cdot$ from the $Cl_2^-\cdot$ dissociate reaction.

The $Cl_2^-\cdot$ reaction rate is given by eq A.123. Hence, Q_{A21} is simplified as eq A.51:

$$Q_{A21} = \frac{k_{Cl\cdot/R}[R]_0}{\left(\sum_{Cl^-,C}^{Cl\cdot} k_i S_i\right) - \frac{k_5 k_8 [Cl^-]_0}{k_8 + k_9[PS]_0 + k_{16}[HCO_3^-]_0 + k_{17}[CO_3^{2-}]_0}} \tag{A.51}$$

where,

$$\sum_{Cl^-,C}^{Cl\cdot} k_i S_i = k_5[Cl^-]_0 + k_6[PS]_0 + k_7[H_2O] + k_{15}[HCO_3^-]_0 + k_{16}[CO_3^{2-}]_0 + k_{Cl\cdot/R}[R]_0$$

where, k_i is the second order rate constant between compound i and Cl·, $M^{-1}\cdot s^{-1}$;k_9, k_{16} and k_{17} are the second order rate constants between reactions of (i) PS and $Cl_2^-\cdot$, (ii) HCO_3^- and $Cl_2^-\cdot$, (iii) CO_3^{2-} and $Cl_2^-\cdot$, respectively. k_5-k_{17} have known values and have the units as $M^{-1}\cdot s^{-1}$. $k_{Cl\cdot/R}$ depends structure of the organic compound, and it ranges from 10^5 $M^{-1}\cdot s^{-1}$ to 1.5×10^{10} $M^{-1}\cdot s^{-1}$. [Cl^-]/[R] is ranging from 10 to 1000; $[R]_0$ is 0.1 mM; $[PS]_0$ is 0.01 M;

$[HCO_3^-]_0$ is 0.1 mM; and, $[CO_3^{2-}]_0$ is 1.4 μM. Therefore, for this case, Q_{A21} has the maximum value as 0.128 (other cases with different [R], [PS], $[Cl^-]$, $[HCO_3^-]$, $[CO_3^{2-}]$ can be evaluated using our algorithm). When HCO_3^-/CO_3^{2-} and Cl^- are present, the fraction of Cl· reacting with organic compound is summarized in **Table A.16**. Overall, for these 22 organic compounds, the ratio of organic destruction rate when HCO_3^-/CO_3^{2-} and Cl^- is present to the rate when HCO_3^-/CO_3^{2-} and Cl^- is not present is summarized in **Table A.17**.

A.4.7 Dichloride anion radicals reacts with organic compound when chloride is present

When Cl^- is present, the quenching ratio Q_{A22} (eq A.52) is equal to the rate of $Cl_2^-\cdot$ oxidizing organic compound (R) divided by the rate of $Cl_2^-\cdot$ reacting with all components in the water matrix (R, Cl^-, PS, H_2O, HCO_3^-/CO_3^{2-}) (**Figure 2.1(b)**). In other words, Q_{A22} is the fraction of $Cl_2^-\cdot$ reacting with organic compound.

$$Q_{A22} = \frac{k_{Cl_2^-\cdot}[R]_0[Cl_2^-\cdot]_{ss,0}^{Cl^-}}{k_{Cl_2^-\cdot}[R]_0[Cl_2^-\cdot]_{ss,0}^{Cl^-} + k_8[Cl_2^-\cdot]_{ss,0}^{Cl^-} + k_9[PS]_0[Cl_2^-\cdot]_{ss,0}^{Cl^-}} \quad \text{(A.52)}$$

where, k_8 is the first order rate constant for $Cl_2^-\cdot$ producing Cl·, k_9 is the second order rate constant between $Cl_2^-\cdot$ and persulfate (PS), $k_{Cl_2^-\cdot/R}$ is the second order rate constant between $Cl_2^-\cdot$ and organic compound, the value is in the range from 10^4 $M^{-1}s^{-}1$ to 10^7 $M^{-1}s^{-1}$. $[R]_0$ is the organic concentration, 10^{-4} M; $[PS]_0$ is the persulfate concentration, 0.01 M. Therefore, in this case, the maximum value of Q_{S22} is 0.018, which indicates at most 1.8% $Cl_2^-\cdot$ reacts with organic compound (other cases with different [R], [PS] can be evaluated by our algorithm). Hence, very small portion of $Cl_2^-\cdot$ reacting with organic compound makes this reaction unimportant and negligible.

A.5 Supplementary Calculation for UV/H_2O_2: Organic Compounds React with Sulfate Radicals, Hydroxyl Radicals and Chlorine Radicals

A.5.1 Chloride is not present

When Cl^- is not present, the quenching ratio Q_{A23} (eq A.53) is equal to the rate of HO· oxidizing organic compound (R) divided by the rate of HO· reacting with all components in the water matrix (R, H_2O_2) (**Figure A.2(a)**).

$$Q_{A23} = \frac{k_{HO\cdot/R}[R]_0[HO\cdot]_{ss,0}^{no\,Cl^-}}{k_{HO\cdot/R}[R]_0[HO\cdot]_{ss,0}^{no\,Cl^-} + k_{19}[H_2O_2]_0[HO\cdot]_{ss,0}^{no\,Cl^-}} = \frac{k_{HO\cdot/R}[R]_0}{k_{HO\cdot/R}[R]_0 + k_{19}[H_2O_2]_0} \qquad (A.53)$$

where, k_{19} is the second-order rate constant between H_2O_2 and HO·, $M^{-1}\cdot s^{-1}$; $k_{HO\cdot/R}$ is the second-order rate constant between organic compound and HO·, $M^{-1}\cdot s^{-1}$; k_{18} has known value, $k_{HO\cdot/R}$ depends structure of the organic compound, and it ranges from 10^7 $M^{-1}\cdot s^{-1}$ to 1.2×10^{10} $M^{-1}\cdot s^{-1}$. $[R]_0$ is 0.1 mM; $[H_2O_2]_0$ is 0.01 M, Therefore, in this case, the maximum value of Q_{A23} is 81.6% (other cases with different $[H_2O_2]$, [R] can be evaluated using our algorithm). When Cl^- is not present, the fraction of HO· reacting with 22 organic compounds is summarized in **Table A.18**. Since H_2O_2 scavenges HO·, the fraction of HO· reacting with target organic compounds is not 100% when Cl^- is not present.

A.5.2 Chloride is present

When Cl^- is present, the quenching ratio Q_{A24} (eq A.54) is equal to the rate of HO· oxidizing organic compound (R) divided by the rate of HO· reacting with all components in the water matrix (R, H_2O_2, Cl^-) (**Figure A.2(a)**).

$$Q_{A24} = \frac{k_{HO\cdot/R}[R]_0[HO\cdot]_{ss,0}^{Cl^-}}{k_{HO\cdot/R}[R]_0[HO\cdot]_{ss,0}^{Cl^-} + k_{19}[H_2O_2][HO\cdot]_{ss,0}^{Cl^-} + k_{20}[Cl^-]_0[HO\cdot]_{ss,0}^{Cl^-} - k_8[ClOH^-\cdot]_{ss,0}^{Cl^-}} \qquad (A.54)$$

The denominator includes the negative term $k_8[ClOH^-\cdot]_{ss,0}^{Cl^-}$,because HO· reacts with Cl^- to generate $ClOH^-\cdot$ and $ClOH^-\cdot$ continues to dissociate to form HO·. The consumption rate of

HO· from the reaction between HO· and Cl^- can be compensated by the production rate of HO· from the $ClOH^-\cdot$ dissociate reaction.

The $ClOH^-\cdot$ reaction rate is given by eq A.55:

$$\begin{aligned} r_{ClOH^-\cdot}^{Cl^-} &= k_{20}[Cl^-]_0[HO\cdot]_{ss,0}^{Cl^-} - k_8[ClOH^-\cdot]_{ss,0}^{Cl^-} - k_{21}[Cl^-]_0[ClOH^-\cdot]_{ss,0}^{Cl^-} \\ &-k_{22}[H^+][ClOH^-\cdot]_{ss,0}^{Cl^-} + k_7[H_2O][Cl\cdot]_{ss,0}^{Cl^-} = 0 \end{aligned} \tag{A.55}$$

The Cl· reaction rate is given by eq A.56:

$$\begin{aligned} r_{Cl\cdot}^{Cl^-} &= k_{22}[H^+][ClOH^-\cdot]_{ss,0}^{Cl^-} - k_{23}[H_2O_2]_0[Cl\cdot]_{ss,0}^{Cl^-} - k_5[Cl^-]_0[Cl\cdot]_{ss,0}^{Cl^-} \\ &-k_7[H_2O][Cl\cdot]_{ss,0}^{Cl^-} - k_{Cl\cdot/R}[R]_0[Cl\cdot]_{ss,0}^{Cl^-} = 0 \end{aligned} \tag{A.56}$$

Hence, the $ClOH^-\cdot$ reaction rate at simplified steady state can be simplified as eq A.57:

$$\begin{aligned} r_{ClOH^-\cdot}^{Cl^-} &= k_{20}[Cl^-]_0[HO\cdot]_{ss,0}^{Cl^-} - k_8[ClOH^-\cdot]_{ss,0}^{Cl^-} - k_{21}[Cl^-]_0[ClOH^-\cdot]_{ss,0}^{Cl^-} \\ &-k_{22}[H^+][ClOH^-\cdot]_{ss,0}^{Cl^-} + \frac{k_7[H_2O]k_{22}[H^+]}{\sum_{Cl^-}^{Cl\cdot} k_i S_i}[ClOH^-\cdot]_{ss,0}^{Cl^-} = 0 \end{aligned} \tag{A.57}$$

where,

$$\sum_{Cl^-}^{Cl\cdot} k_i S_i = k_{23}[H_2O_2]_0 + k_5[Cl^-]_0 + k_7[H_2O] + k_{Cl\cdot/R}[R]_0$$

In the eq A.57, since the term $\frac{k_7[H_2O]k_{22}[H^+]}{\sum_{Cl^-}^{Cl\cdot} k_i S_i}[ClOH^-\cdot]_{ss,0}^{Cl^-}$ is much smaller than the term $k_8[ClOH^-\cdot]_{ss,0}^{Cl^-}$, the term $\frac{k_7[H_2O]k_{22}[H^+]}{\sum_{Cl^-}^{Cl\cdot} k_i S_i}[ClOH^-\cdot]_{ss,0}^{Cl^-}$ is negligible.

As a result, the $ClOH^-\cdot$ reaction rate at simplified steady state can be simplified as eq A.58:

$$\begin{aligned} r_{ClOH^-\cdot}^{Cl^-} &= k_{20}[Cl^-]_0[HO\cdot]_{ss,0}^{Cl^-} - k_8[ClOH^-\cdot]_{ss,0}^{Cl^-} - k_{21}[Cl^-]_0[ClOH^-\cdot]_{ss,0}^{Cl^-} \\ &-k_{22}[H^+][ClOH^-\cdot]_{ss,0}^{Cl^-} = 0 \end{aligned} \tag{A.58}$$

Hence, the quenching rate Q_{S24} can be simplified as eq A.59:

$$Q_{A24} = \frac{k_{HO\cdot/R}[R]}{k_{HO\cdot/R}[R] + k_{19}[H_2O_2] + \frac{k_{21}[Cl^-] + k_{22}[H^+]}{k_8 + k_{21}[Cl^-] + k_{22}[H^+]} k_{20}[Cl^-]} \quad (A.59)$$

where, k_{19} is the second-order rate constant between H_2O_2 and H_2O_2 and HO·, $M^{-1}\cdot s^{-1}$; k_{20} is the second-order rate constant between Cl^- and HO·, $M^{-1}\cdot s^{-1}$; k_8 is the first-order rate constant of $ClOH^-\cdot$ producing HO·, s^{-1}; k_{21} is the second-order rate constant between Cl^- and $ClOH^-\cdot$, $M^{-1}\cdot s^{-1}$; k_{22} is the second-order rate constant between H^+ and $ClOH^-\cdot$, $M^{-1}\cdot s^{-1}$; $k_{HO\cdot/R}$ is the second-order rate constant between organic compound and HO·, $M^{-1}S^{-1}$; k_{19}-k_{22} have known values, $k_{HO\cdot/R}$ depends structure of the organic compound, and it ranges from 10^7 $M^{-1}\cdot s^{-1}$ to 1.2×10^{10} $M^{-1}\cdot s^{-1}$. $[Cl^-]/[R]$ is ranging from 10 to 1000; $[R]_0$ is 0.1 mM; and, $[H_2O_2]_0$ is 0.01 M. Therefore, in this case, the maximum value of Q_{A24} is 81.6% (other cases with different $[H_2O_2]$, [R], $[Cl^-]$ can be evaluated using our algorithm). When Cl^- is present, the fraction of HO· reacting with 22 organic compounds is summarized in **Table A.18**.

A.5.3 NOM is present

When NOM is present, the rate of H_2O_2 photolysis to produce HO· is $2\emptyset_{H_2O_2}P_{UV}f^{NOM}_{H_2O_2}(1-e^{-A^{NOM}})$. While, when no NOM is present, the rate of H_2O_2 photolysis to produce HO· is $2\emptyset_{H_2O_2}P_{UV}f_{H_2O_2}(1-e^{-A})$. We compared the rate of H_2O_2 photolysis to produce HO· when NOM is presents to the rate when NOM is not present as RatioA7 (eq A.60). RatioA7 is 0.5086, which means HO· production decreases 49.14% when NOM is present.

$$\text{RatioA7} = \frac{2\phi_{H_2O_2}P_{UV}f^{NOM}_{H_2O_2}(1-e^{-A^{NOM}})}{2\phi_{H_2O_2}P_{UV}f_{H_2O_2}(1-e^{-A})} = \frac{f^{NOM}_{H_2O_2}(1-e^{-A^{NOM}})}{f_{H_2O_2}(1-e^{-A})} \quad (A.60)$$

where,

$\emptyset_{H_2O_2}$ is H_2O_2 quantum yield; P_{UV} is UV light intensity, Einstein·$L^{-1}\cdot s^{-1}$;

$$f_{H_2O_2}^{NOM} = \frac{\varepsilon_{H_2O_2} C_{H_2O_2}}{\varepsilon_R C_R + \varepsilon_{H_2O_2} C_{H_2O_2} + \varepsilon_{NOM} C_{NOM} + \varepsilon_{bac} C_{bac}}; \; f_{H_2O_2} = \frac{\varepsilon_{H_2O_2} C_{H_2O_2}}{\varepsilon_R C_R + \varepsilon_{H_2O_2} C_{H_2O_2} + \varepsilon_{bac} C_{bac}};$$

$$A^{NOM} = 2.303(\varepsilon_R C_R + \varepsilon_{H_2O_2} C_{H_2O_2} + \varepsilon_{NOM} C_{NOM} + \varepsilon_{bac} C_{bac})L;$$

$$A = 2.303(\varepsilon_R C_R + \varepsilon_{H_2O_2} C_{H_2O_2} + \varepsilon_{bac} C_{bac})L;$$

$\varepsilon_{H_2O_2}$ is H_2O_2 extinction coefficient, 17.9 L/mole·cm – 19.6 L/mole·cm;[20]

ε_R is organic compound extinction coefficient, assumed as 180 L/mole·cm;[159]

ε_{NOM} is NOM extinction coefficient, assumed as 0.107 L/mg-C·cm;[10]

ε_{bac} is water matrix background extinction coefficient, assumed 0 L/mole·cm;

L is reactor pathway, assumed as 6 cm.[20]

When NOM is present, the quenching ratio Q_{A25} (eq A.61) is equal to the rate of HO· oxidizing organic compound (R) divided by the rate of HO· reacting with all components in the water matrix (R, H_2O_2, NOM) (**Figure A.2(c)**).

$$\begin{aligned} Q_{A25} &= \frac{k_{HO\cdot/R}[R]_0[HO\cdot]_{ss,0}^{NOM}}{k_{HO\cdot/R}[R]_0[HO\cdot]_{ss,0}^{NOM} + k_{19}[H_2O_2]_0[HO\cdot]_{ss,0}^{NOM} + k_{HO\cdot/NOM}[NOM]_0[HO\cdot]_{ss,0}^{NOM}} \\ &= \frac{k_{HO\cdot/R}[R]_0}{k_{HO\cdot/R}[R]_0 + k_{19}[H_2O_2]_0 + k_{HO\cdot/NOM}[NOM]_0} \end{aligned} \quad (A.61)$$

where, k_{19} is the second-order rate constant between H_2O_2 and HO·, $M^{-1}\cdot s^{-1}$; where, $k_{HO\cdot/NOM}$ is the second-order rate constant between NOM and HO·, $M^{-1}\cdot s^{-1}$; k_{19} and $k_{HO\cdot/NOM}$ have known values, $k_{HO\cdot/R}$ depends structure of the organic compound, and it ranges from 10^7 $M^{-1}\cdot s^{-1}$ to 1.2×10^{10} $M^{-1}\cdot s^{-1}$. $[R]_0$ is 0.1 mM, $[H_2O_2]_0$ is 0.01 M, $[NOM]_0$ is 2 $mg\cdot L^{-1}$. Therefore, in this case, the maximum value of Q_{A25} is 78.95%. When NOM is present, the fraction of HO· oxidizing target organic compound is determined by two factors: ***(1)*** NOM absorbs UV light, HO· production rate decreases 49.14%; ***(2)*** the quenching ratio Q_{A25} is no more than 78.95% HO·. As a result, the fraction of HO·

oxidizing target organic compound is no more than 40.156% (0.7895×(1-0.4914) ×100%) (other cases with different $[H_2O_2]$, [R], [NOM] can be evaluated by our algorithm). When NOM is present, the fraction of HO· reacting with 22 organic compounds is summarized in **Table A.19**.

A.5.4 Bicarbonate and Carbonate are present

When HCO_3^-/CO_3^{2-} are present, the quenching ratio Q_{A26} (eq A.62) is equal to the rate of HO· oxidizing organic compound (R) divided by the rate of HO· reacting with all components in the water matrix (R, H_2O_2, HCO_3^-/CO_3^{2-}) (**Figure A.2(d)**).

$$Q_{A26} = \frac{k_{HO\cdot/R}[R]_0[HO\cdot]^C_{ss,0}}{k_{HO\cdot/R}[R]_0[HO\cdot]^C_{ss,0} + k_{19}[H_2O_2]_0[HO\cdot]^C_{ss,0} + k_{13}[HCO_3^-]_0[HO\cdot]^C_{ss,0} + k_{14}[CO_3^{2-}]_0[HO\cdot]^C_{ss,0}} = \frac{k_{HO\cdot/R}[R]_0}{k_{HO\cdot/R}[R]_0 + k_{19}[H_2O_2]_0 + k_{13}[HCO_3^-]_0 + k_{14}[CO_3^{2-}]_0} \quad (A.62)$$

where, k_{19} is the second-order rate constant between H_2O_2 and HO·, $M^{-1}\cdot s^{-1}$; k_{13} is the second-order rate constant between HCO_3^- and HO·, $M^{-1}\cdot s^{-1}$; k_{14} is the second-order rate constant between CO_3^{2-} and HO· , $M^{-1}S^{-1}$.k_{13}-k_{19} have known values, $k_{HO\cdot/R}$ depends structure of the organic compound, and it ranges from 10^7 $M^{-1}\cdot s^{-1}$ to 1.2×10^{10} $M^{-1}\cdot s^{-1}$. $[R]_0$ is 0.1 mM; $[H_2O_2]_0$ is 0.01 M; $[HCO_3^-]_0$ is 3 mM, $[CO_3^{2-}]_0$ is 14 μM. Therefore, in this case, the maximum value of Q_{A26} is 80.21%, which means no more than 80.21% HO· will destruct organic compound (other cases with different [H2O2], [R], $[HCO_3^-]$, $[CO_3^{2-}]$ can be evaluated by our algorithm). When HCO_3^-/CO_3^{2-} are present, the fraction of HO· reacting with 22 organic compounds is summarized in **Figure A.2**.

A.6 Mathematical Model Development for chloride ions effects on UV/PS and UV/H_2O_2 processes

A.6.1 Mathematical Development for UV/PS Case 1: Organic Compounds Only React with Sulfate Radicals

(1) When chloride is not present

When Cl^- is not present, $SO_4^-\cdot$ reaction rate is expressed as eq A.63:

$$\begin{aligned} r_{so_4^-\cdot} &= 2r_{UV,S_2O_8^{2-}} - k_1[H_2O][SO_4^-\cdot]_{ss,0}^{no\,Cl^-} - k_3[PS]_0[SO_4^-\cdot]_{ss,0}^{no\,Cl^-} \\ &-k_{SO_4^-\cdot/R}[R]_0[SO_4^-\cdot]_{ss,0}^{no\,Cl^-} + k_4[PS]_0[HO\cdot]_{ss,0}^{no\,Cl^-} = 0 \end{aligned} \tag{A.63}$$

$HO\cdot$ reaction rate is given by eq A.64:

$$r_{HO\cdot} = k_1[H_2O][SO_4^-\cdot]_{ss,0}^{no\,Cl^-} - k_4[PS]_0[SO_4^-\cdot]_{ss,0}^{no\,Cl^-} = 0 \tag{A.64}$$

Combining eq A.63 and eq A.64, the initial steady state $SO_4^-\cdot$ concentration is given as eq A.65:

$$\Rightarrow [SO_4^-\cdot]_{ss,0}^{no\,Cl^-} = \frac{2r_{UV,S_2O_8^{2-}}}{k_3[PS]_0 + k_{SO_4^-\cdot/R}[R]_0} \tag{A.65}$$

Hence, the organic compound (R) destruction rate is given by eq A.66:

$$r_R = k_{SO_4^-\cdot/R}[SO_4^-\cdot]_{ss,0}^{no\,Cl^-}[R] = \frac{2r_{UV,S_2O_8^{2-}}k_{SO_4^-\cdot/R}[R]}{k_3[PS]_0 + k_{SO_4^-\cdot/R}[R]_0} \tag{A.66}$$

(2) When chloride is present

If chloride is present, sulfate radical reaction rate is expressed as eq A.67:

$$\begin{aligned} r_{so_4^-\cdot}^{Cl^-} &= 2r_{UV,S_2O_8^{2-}} - k_1[H_2O][SO_4^-\cdot]_{ss,0}^{Cl^-} - k_2[Cl^-]_0[SO_4^-\cdot]_{ss,0}^{Cl^-} - k_3[PS]_0[SO_4^-\cdot]_{ss,0}^{Cl^-} \\ &-k_{SO_4^-\cdot/R}[R]_0[SO_4^-\cdot]_{ss,0}^{Cl^-} + k_4[PS]_0[HO\cdot]_{ss,0}^{Cl^-} = 0 \end{aligned} \tag{A.67}$$

If Cl^- is present, $HO\cdot$ reaction rate is expressed as eq A.68:

$$r_{HO\cdot}^{Cl^-} = k_1[H_2O][SO_4^-\cdot]_{ss,0}^{Cl^-} - k_4[PS]_0[HO\cdot]_{ss,0}^{Cl^-} = 0 \tag{A.68}$$

Combining eq A.67 and eq A.68, the initial steady state $SO_4^-\cdot$ concentration is given as eq A.69:

$$\Rightarrow [SO_4^-\cdot]_{ss,0}^{Cl^-} = \frac{2r_{UV,S_2O_8^{2-}}}{k_2[Cl^-]_0 + k_3[PS]_0 + k_{SO_4^-\cdot/R}[R]_0} \tag{A.69}$$

Hence, when Cl^- is present, the organic compound (R) destruction rate is expressed as eq A.70:

$$r_R^{Cl^-} = k_{SO_4^-\cdot/R}[SO_4^-\cdot]_{ss,0}^{Cl^-}[R] = \frac{2r_{UV,S_2O_8^{2-}} k_{SO_4^-\cdot/R}}{k_2[Cl^-]_0 + k_3[PS]_0 + k_{SO_4^-\cdot/R}[R]_0} \tag{A.70}$$

As a result, the ratio of organic compound's destruction rate when Cl^- is present to the rate when Cl^- is not present can be expressed as eq A.71:

$$\frac{r_R^{Cl^-}}{r_R} = \frac{k_{SO_4^-\cdot/R}[SO_4^-\cdot]_{ss,0}^{Cl^-}[R]}{k_{SO_4^-\cdot/R}[SO_4^-\cdot]_{ss,0}^{no\ Cl^-}[R]} = \frac{[SO_4^-\cdot]_{ss,0}^{Cl^-}}{[SO_4^-\cdot]_{ss,0}^{no\ Cl^-}} = \frac{k_3[PS]_0 + k_{SO_4^-\cdot/R}[R]_0}{k_2[Cl^-]_0 + k_3[PS]_0 + k_{SO_4^-\cdot/R}[R]_0} \tag{A.71}$$

(3) When chloride and NOM both present

If Cl^- and NOM are both present, $SO_4^-\cdot$ reaction rate is expressed as eq A.72:

$$\begin{aligned} r_{so_4^-\cdot}^{Cl^-,NOM} &= 2r_{UV,S_2O_8^{2-}} - k_1[H_2O][SO_4^-\cdot]_{ss,0}^{Cl^-} - k_2[Cl^-]_0[SO_4^-\cdot]_{ss,0}^{Cl^-} - k_3[PS]_0[SO_4^-\cdot]_{ss,0}^{Cl^-} \\ &- k_{SO_4^-\cdot/NOM}[NOM]_0[SO_4^-\cdot]_{ss,0}^{Cl^-} - k_{SO_4^-\cdot/R}[R]_0[SO_4^-\cdot]_{ss,0}^{Cl^-} + k_4[PS]_0[HO\cdot]_{ss,0}^{Cl^-} = 0 \end{aligned} \tag{A.72}$$

If Cl^- and NOM are both present, $HO\cdot$ reaction rate is expressed as eq A.73:

$$\begin{aligned} r_{HO\cdot}^{Cl^-,NOM} &= k_1[H_2O][SO_4^-\cdot]_{ss,0}^{Cl^-,NOM} - k_4[PS]_0[HO\cdot]_{ss,0}^{Cl^-,NOM} \\ &- k_{HO\cdot/NOM}[NOM]_0[HO\cdot]_{ss,0}^{Cl^-,NOM} = 0 \end{aligned} \tag{A.73}$$

Combining eq A.72 and eq A.73, the initial steady state $SO_4^-\cdot$ concentration is given as eq A.74:

$$[SO_4^-\cdot]_{ss,0}^{Cl^-,NOM} = \frac{2r_{UV,S_2O_8^{2-}}^{NOM}\left(k_4[PS]_0 + k_{HO\cdot/NOM}[NOM]_0\right)}{A_1\left(k_4[PS]_0 + k_{HO\cdot/NOM}[NOM]_0\right) - k_4k_1[PS]_0[H_2O]} \tag{A.74}$$

where,

$$A_1 = k_1[H_2O] + k_2[Cl^-]_0 + k_3[PS]_0 + k_{SO_4^-\cdot/NOM}[NOM]_0 + k_{SO_4^-\cdot/R}[R]_0$$

Hence, the organic compound (R) destruction rate is expressed as eq A.75:

$$r_R^{Cl^-,NOM} = k_{SO_4^-\cdot/R}[SO_4^-\cdot]_{ss,0}^{NOM}[R] = \frac{2r_{UV,S_2O_8^{2-}}^{NOM} k_{SO_4^-\cdot/R}\left(k_4[PS]_0 + k_{HO\cdot/NOM}[NOM]_0\right)[R]}{A_1\left(k_4[PS]_0 + k_{HO\cdot/NOM}[NOM]_0\right) - k_4k_1[PS]_0[H_2O]} \quad (A.75)$$

where,

$$A_1 = k_1[H_2O] + k_2[Cl^-]_0 + k_3[PS]_0 + k_{SO_4^-\cdot/NOM}[NOM]_0 + k_{SO_4^-\cdot/R}[R]_0$$

As a result, the ratio of organic compound's destruction rate when Cl^- and NOM are present to Cl^- and NOM are not present can be expressed as eq A.76:

$$\frac{r_R^{Cl^-,NOM}}{r_R} = \frac{r_{UV,PS}^{NOM}}{r_{UV,PS}} \cdot \frac{k_{SO_4^-\cdot/R}[SO_4^-\cdot]_{ss,0}^{Cl^-,NOM}[R]}{k_{SO_4^-\cdot/R}[SO_4^-\cdot]_{ss,0}[R]} = \frac{r_{UV,PS}^{NOM}}{r_{UV,PS}} \cdot \frac{[SO_4^-\cdot]_{ss,0}^{Cl^-,NOM}}{[SO_4^-\cdot]_{ss,0}} \quad (A.76)$$

$r_{UV,PS}^{NOM}$ is the rate of PS photolysis to produce sulfate radical when NOM is present, it is expressed as eq A.77:

$$r_{UV,PS}^{NOM} = 2\phi_{PS}P_{UV}f_{PS}^{NOM}(1 - e^{-A^{NOM}}) \quad (A.77)$$

$r_{UV,PS}$ is the rate of PS photolysis to produce sulfate radical when NOM is not present, it is expressed as eq A.78:

$$r_{UV,PS} = 2\phi_{PS}P_{UV}f_{PS}(1 - e^{-A}) \quad (A.78)$$

Hence, the ratio of organic compound's destruction rate when Cl^- and NOM are present to the rate Cl^- and NOM are not present can be expressed as eq A.79,

$$\frac{r_R^{Cl^-,NOM}}{r_R} = \left[\frac{f_{PS}^{NOM}\left(1 - e^{-A^{NOM}}\right)}{f_{PS}\left(1 - e^{-A}\right)}\right] \frac{\left(k_3[PS]_0 + k_{SO_4^-\cdot/R}[R]_0\right)\left(k_4[PS]_0 + k_{HO\cdot/NOM}[NOM]_0\right)}{A_1\left(k_4[PS]_0 + k_{HO\cdot/NOM}[NOM]_0\right) - k_4k_1[PS]_0[H_2O]} \quad (A.79)$$

where,

$$f_{PS}^{NOM} = \frac{\varepsilon_{PS}C_{PS}}{\varepsilon_R C_R + \varepsilon_{PS}C_{PS} + \varepsilon_{NOM}C_{NOM} + \varepsilon_{bac}C_{bac}};\ f_{PS} = \frac{\varepsilon_{PS}C_{PS}}{\varepsilon_R C_R + \varepsilon_{PS}C_{PS} + \varepsilon_{bac}C_{bac}}$$

$$A = 2.303(\varepsilon_R C_R + \varepsilon_{PS}C_{PS} + \varepsilon_{bac}C_{bac})L;$$

$$A^{NOM} = 2.303(\varepsilon_R C_R + \varepsilon_{PS}C_{PS} + \varepsilon_{NOM}C_{NOM} + \varepsilon_{bac}C_{bac})L;$$

$$A_1 = k_1[H_2O] + k_2[Cl^-]_0 + k_3[PS]_0 + k_{SO_4^-\cdot/NOM}[NOM]_0 + k_{SO_4^-\cdot/R}[R]_0$$

(4) When chloride and carbonate, bicarbonate are present

If Cl^- and HCO_3^-/CO_3^{2-} are present, $SO_4^-\cdot$ reaction rate is given as eq A.80:

$$\begin{aligned} r_{SO_4^-\cdot}^{Cl^-,C} &= 2r_{UV,S_2O_8^{2-}} - k_1[H_2O][SO_4^-\cdot]_{ss,0}^{Cl^-,C} - k_2[Cl^-]_0[SO_4^-\cdot]_{ss,0}^{Cl^-,C} - k_3[PS]_0[SO_4^-\cdot]_{ss,0}^{Cl^-,C} \\ &-k_{11}[HCO_3^-]_0[SO_4^-\cdot]_{ss,0}^{Cl^-,C} - k_{12}[CO_3^{2-}]_0[SO_4^-\cdot]_{ss,0}^{Cl^-,C} - k_{SO_4^-\cdot/R}[R]_0[SO_4^-\cdot]_{ss,0}^{Cl^-,C} \\ &+k_4[PS]_0[HO\cdot]_{ss,0}^{Cl^-,C} = 0 \end{aligned} \tag{A.80}$$

If Cl^- and HCO_3^-/CO_3^{2-} are present, $HO\cdot$ reaction rate is given as eq A.81:

$$\begin{aligned} r_{HO\cdot}^{Cl^-,C} &= k_1[H_2O][SO_4^-\cdot]_{ss,0}^{Cl^-,C} - k_4[PS]_0[HO\cdot]_{ss,0}^{Cl^-,C} - k_{13}[HCO_3^-]_0[HO\cdot]_{ss,0}^{Cl^-,C} \\ &-k_{14}[CO_3^{2-}]_0[HO\cdot]_{ss,0}^{Cl^-,C} = 0 \end{aligned} \tag{A.81}$$

Combining eq A.80 and eq A.81, when Cl^- and HCO_3^-/CO_3^{2-} are present, the initial steady state $SO_4^-\cdot$ concentration is expressed as eq A.82:

$$[SO_4^-\cdot]_{ss,0}^{Cl^-,C} = \frac{2r_{UV,S_2O_8^{2-}}\left(k_4[PS]_0 + k_{13}[HCO_3^-]_0 + k_{14}[CO_3^{2-}]_0\right)}{A_2\left(k_4[PS]_0 + k_{12}[HCO_3^-]_0 + k_{13}[CO_3^{2-}]_0\right) - k_4k_1[PS]_0[H_2O]} \tag{A.82}$$

where,

$$A_2 = k_1[H_2O] + k_2[Cl^-]_0 + k_3[PS]_0 + k_{11}[HCO_3^-]_0 + k_{12}[CO_3^{2-}]_0 + k_{SO_4^-\cdot/R}[R]_0$$

Hence, the organic compound (R) destruction rate is expressed as eq A.83:

$$r_R^{Cl^-,C} = k_{SO_4^-\cdot/R}[SO_4^-\cdot]_{ss,0}^{C}[R] = \frac{2r_{UV,S_2O_8^{2-}}k_{SO_4^-\cdot/R}\left(k_4[PS]_0 + k_{13}[HCO_3^-]_0 + k_{14}[CO_3^{2-}]_0\right)[R]}{A_2\left(k_4[PS]_0 + k_{13}[HCO_3^-]_0 + k_{14}[CO_3^{2-}]_0\right) - k_4k_1[PS]_0[H_2O]} \tag{A.83}$$

As a result, the ratio of organic compound's destruction rate when Cl^- and HCO_3^-/CO_3^{2-} are present to Cl^- and HCO_3^-/CO_3^{2-} are not presents can be expressed as eq A.84,

$$\frac{r_R^{Cl^-,C}}{r_R} = \frac{k_{SO_4^-\cdot/R}[SO_4^-\cdot]_{ss,0}^{Cl^-,C}[R]}{k_{SO_4^-\cdot/R}[SO_4^-\cdot]_{ss,0}^{no\,Cl^-}[R]} = \frac{[SO_4^-\cdot]_{ss,0}^{Cl^-,C}}{[SO_4^-\cdot]_{ss,0}}$$
$$= \frac{\left(k_3[PS]_0 + k_{SO_4^-\cdot/R}[PS]_0\right)\left(k_4[PS]_0 + k_{13}[HCO_3^-]_0 + k_{14}[CO_3^{2-}]_0\right)}{A_2\left(k_4[PS]_0 + k_{13}[HCO_3^-]_0 + k_{14}[CO_3^{2-}]_0\right) - k_4k_1[PS]_0[H_2O]} \quad (A.84)$$

where,

$$A_2 = k_1[H_2O] + k_2[Cl^-]_0 + k_3[PS]_0 + k_{11}[HCO_3^-]_0 + k_{12}[CO_3^{2-}]_0 + k_{SO_4^-\cdot/R}[R]_0$$

If we consider the ion strength, all species concentrations should be replaced into species activities for each equation from eq A.63 to eq A.84.

A.6.2 Mathematical Development for UV/PS Case 2: Organic Compounds React with Sulfate Radicals, hydroxyl radicals and chlorine radicals

(1) When chloride is not present

$SO_4^-\cdot$ reaction rate is given as eq A.85:

$$r_{SO_4^-\cdot} = 2r_{UV,S_2O_8^{2-}} - k_1[H_2O][SO_4^-\cdot]_{ss,0}^{no\,Cl^-} - k_3[PS]_0[SO_4^-\cdot]_{ss,0}^{no\,Cl^-}$$
$$-k_{SO_4^-\cdot/R}[R]_0[SO_4^-\cdot]_{ss,0}^{no\,Cl^-} + k_4[PS]_0[HO\cdot]_{ss,0}^{no\,Cl^-} = 0 \quad (A.85)$$

$HO\cdot$ reaction rate is given as eq A.86:

$$r_{HO\cdot} = k_1[H_2O][SO_4^-\cdot]_{ss,0}^{no\,Cl^-} - k_4[PS]_0[HO\cdot]_{ss,0}^{no\,Cl^-} - k_{HO\cdot/R}[R]_0[HO\cdot]_{ss,0}^{no\,Cl^-} = 0 \quad (A.86)$$

Combining eq A.85 and eq A.86, the initial steady state $SO_4^-\cdot$ concentration is given as eq A.87:

$$[SO_4^-\cdot]_{ss,0}^{no\,Cl^-} = \frac{2r_{UV,S_2O_8^{2-}}\left(k_4[PS]_0 + k_{HO\cdot/R}[R]_0\right)}{\left(k_1[H_2O] + k_3[PS]_0 + k_{SO_4^-\cdot/R}[R]_0\right)\left(k_4[PS]_0 + k_{HO\cdot/R}[R]_0\right) - k_4k_1[H_2O][PS]_0} \quad (A.87)$$

Combining eq A.85 and eq A.86, the initial steady state HO· concentration is given as eq A.88:

$$[HO\cdot]_{ss,0}^{no\ Cl^-} = \frac{2r_{UV,S_2O_8^{2-}} k_1[H_2O]}{\left(k_1[H_2O]+k_3[PS]_0+k_{SO_4^-\cdot/R}[R]_0\right)\left(k_4[PS]_0+k_{HO\cdot/R}[R]_0\right)-k_4k_1[H_2O][PS]_0} \quad (A.88)$$

Hence, the organic compound (R) destruction rate is expressed as eq A.89:

$$\begin{aligned} r_R &= k_{SO_4^-\cdot/R}[SO_4^-\cdot]_{ss,0}^{no\ Cl^-}[R]+k_{HO\cdot/R}[HO\cdot]_{ss,0}^{no\ Cl^-}[R] \\ &= \frac{2r_{UV,S_2O_8^{2-}}\left[k_{SO_4^-\cdot/R}\left(k_4[PS]_0+k_{HO\cdot/R}[R]_0\right)+k_{HO\cdot/R}k_1[H_2O]\right][R]}{\left(k_1[H_2O]+k_3[PS]_0+k_{SO_4^-\cdot/R}[R]_0\right)\left(k_4[PS]_0+k_{HO\cdot/R}[R]_0\right)-k_4k_1[H_2O][PS]_0} \end{aligned} \quad (A.89)$$

(2) When chloride is present

If Cl^- is present, $SO_4^-\cdot$ reaction rate is expressed as eq A.90:

$$\begin{aligned} r_{so_4^-\cdot}^{Cl^-} &= 2r_{UV,S_2O_8^{2-}} - k_1[H_2O][SO_4^-\cdot]_{ss,0}^{Cl^-} - k_2[Cl^-]_0[SO_4^-\cdot]_{ss,0}^{Cl^-} - k_3[PS]_0[SO_4^-\cdot]_{ss,0}^{Cl^-} \\ &-k_{SO_4^-\cdot/R}[R]_0[SO_4^-\cdot]_{ss,0}^{Cl^-} + k_4[PS]_0[HO\cdot]_{ss,0}^{Cl^-} = 0 \end{aligned} \quad (A.90)$$

If Cl^- is present, HO· reaction rate is given as eq A.91:

$$\begin{aligned} r_{HO\cdot}^{Cl^-} &= k_1[H_2O][SO_4^-\cdot]_{ss,0}^{Cl^-} - k_4[PS]_0[HO\cdot]_{ss,0}^{Cl^-} - k_{HO\cdot/R}[R]_0[HO\cdot]_{ss,0}^{Cl^-} \\ &+k_8[ClOH^-\cdot]_{ss,0}^{Cl^-} = 0 \end{aligned} \quad (A.91)$$

If Cl^- is present, $ClOH^-\cdot$ reaction rate is given by eq A.92:

$$r_{ClHO^-\cdot}^{Cl^-} = k_7[H_2O][Cl\cdot]_{ss,0}^{Cl^-} - k_8[ClOH\cdot]_{ss,0}^{Cl^-} = 0 \quad (A.92)$$

If Cl^- is present, Cl· reaction rate is expressed as eq A.93:

$$\begin{aligned} r_{Cl\cdot}^{Cl^-} &= k_2[Cl^-]_0[SO_4^-\cdot]_{ss,0}^{Cl^-} - k_5[Cl^-]_0[Cl\cdot]_{ss,0}^{Cl^-} - k_6[PS]_0[Cl\cdot]_{ss,0}^{Cl^-} - k_7[H_2O][Cl\cdot]_{ss,0}^{Cl^-} \\ &-k_{Cl\cdot/R}[R]_0[Cl\cdot]_{ss,0}^{Cl^-} + k_9[Cl_2^-\cdot]_{ss,0}^{Cl^-} = 0 \end{aligned} \quad (A.93)$$

If Cl^- is present, $Cl_2^-\cdot$ reaction rate is expressed as eq A.94:

$$r_{Cl_2^-\cdot}^{Cl^-} = k_5[Cl^-]_0[Cl\cdot]_{ss,0}^{Cl^-} - k_9[Cl_2^-\cdot]_{ss,0}^{Cl^-} - k_{10}[PS]_0[Cl_2^-\cdot]_{ss,0}^{Cl^-} = 0 \quad (A.94)$$

Combing eq A.93 and eq A.94, the initial steady state Cl· concentration is given as eq A.95:

$$[Cl\cdot]_{ss,0}^{Cl^-} = A_3[SO_4^-\cdot]_{ss,0}^{Cl^-} \tag{A.95}$$

where,

$$A_3 = \frac{k_2[Cl^-]_0}{k_6[PS]_0 + k_7[H_2O] + k_{Cl\cdot/R}[R]_0 + \left(k_5 - \frac{k_9 k_5}{k_9 + k_{10}[PS]_0}\right)[Cl^-]_0}$$

Combining eq A.92 and eq A.95 the initial steady state $ClOH^-\cdot$ concentration is given as eq A.96:

$$[ClOH^-\cdot]_{ss,0}^{Cl^-} = \frac{k_7[H_2O][Cl\cdot]_{ss,0}^{Cl^-}}{k_8} = \frac{k_7[H_2O]A_3}{k_8}[SO_4^-\cdot]_{ss,0}^{Cl^-} \tag{A.96}$$

Combing eq A.91 and eq A.96, the initial steady state Cl· concentration is given as eq A.97:

$$[HO\cdot]_{ss,0}^{Cl^-} = \frac{k_1[H_2O] + k_7[H_2O]A_3}{k_4[PS]_0 + k_{HO\cdot/R}[R]_0}[SO_4^-\cdot]_{ss,0}^{Cl^-} \tag{A.97}$$

Combining eq A.90 and eq A.97, the initial steady state $SO_4^-\cdot$ concentration is expressed as eq A.98:

$$[SO_4^-\cdot]_{ss,0}^{Cl^-} = \frac{2r_{UV,S_2O_8^{2-}}\left(k_4[PS]_0 + k_{HO\cdot/R}[R]_0\right)}{\left(k_4[PS]_0 + k_{HO\cdot/R}[R]_0\right)\sum_{Cl^-}^{SO_4^-\cdot} k_i S_i - k_4[PS]_0(k_1[H_2O] + k_7[H_2O]A_3)} \tag{A.98}$$

Combining eq A.96 and eq A.97, the initial steady state HO· concentration is expressed as eq A.99:

$$[HO\cdot]_{ss,0}^{Cl^-} = \frac{2r_{UV,S_2O_8^{2-}}(k_1[H_2O] + k_7[H_2O]A_3)}{\left(k_4[PS]_0 + k_{HO\cdot/R}[R]_0\right)\sum_{Cl^-}^{SO_4^-\cdot} k_i S_i - k_4[PS]_0(k_1[H_2O] + k_7[H_2O]A_3)} \tag{A.99}$$

Combining eq A.95 and eq A.98, the initial steady state Cl· concentration is expressed as eq A.100:

$$[Cl\cdot]_{ss,0}^{Cl^-} = \frac{2r_{UV,S_2O_8^{2-}}\left(k_4[PS]_0 + k_{HO\cdot/R}[R]_0\right)A_3}{\left(k_4[PS]_0 + k_{HO\cdot/R}[R]_0\right)\sum_{Cl^-}^{SO_4^-\cdot} k_i S_i - k_4[PS]_0(k_1[H_2O] + k_7[H_2O]A_3)} \tag{A.100}$$

Hence, when Cl^- the organic compound (R) destruction rate is expressed as eq :

$$\begin{aligned} r_R^{Cl^-} &= k_{SO_4^-\cdot/R}[SO_4^-\cdot]_{ss,0}^{Cl^-}[R]_0 + k_{HO\cdot/R}[HO\cdot]_{ss,0}^{Cl^-}[R]_0 + k_{Cl\cdot/R}[Cl\cdot]_{ss,0}^{Cl^-}[R]_0 \\ &= \frac{2r_{UV,S_2O_8^{2-}}\left[\left(k_{SO_4^-\cdot/R} + k_{Cl\cdot/R}A_3\right)\left(k_4[PS]_0 + k_{HO\cdot/R}[R]_0\right) + k_{HO\cdot/R}(k_1[H_2O] + k_7[H_2O]A_3)\right][R]_0}{\left(k_4[PS]_0 + k_{HO\cdot/R}[R]_0\right)\sum_{Cl^-}^{SO_4^-\cdot} k_i S_i - k_4[PS]_0(k_1[H_2O] + k_7[H_2O]A_3)} \end{aligned} \tag{A.101}$$

As a result, the ratio of organic compound's destruction rate when Cl^- is present to the rate when Cl^- is not present can be expressed as eq ,

$$\begin{aligned} \frac{r_R^{Cl^-}}{r_R} &= \frac{k_{SO_4^-\cdot/R}[SO_4^-\cdot]_{ss,0}^{Cl^-}[R] + k_{HO\cdot/R}[HO\cdot]_{ss,0}^{Cl^-}[R] + k_{Cl\cdot/R}[Cl\cdot]_{ss,0}^{Cl^-}[R]}{k_{SO_4^-\cdot/R}[SO_4^-\cdot]_{ss,0}[R] + k_{HO\cdot/R}[HO\cdot]_{ss,0}[R]} \\ &= \frac{k_{SO_4^-\cdot/R}[SO_4^-\cdot]_{ss,0}^{Cl^-} + k_{HO\cdot/R}[HO\cdot]_{ss,0}^{Cl^-} + k_{Cl\cdot/R}[Cl\cdot]_{ss,0}^{Cl^-}}{k_{SO_4^-\cdot/R}[SO_4^-\cdot]_{ss,0} + k_{HO\cdot/R}[HO\cdot]_{ss,0}} \\ &= \frac{A_5\left[\left(k_{SO_4^-\cdot/R} + k_{Cl\cdot/R}A_3\right)\left(k_4[PS]_0 + k_{HO\cdot/R}[R]_0\right) + k_{HO\cdot/R}(k_1[H_2O] + k_7[H_2O]A_3)\right]}{A_4\left[k_{SO_4^-\cdot/R}\left(k_4[PS]_0 + k_{HO\cdot/R}[R]_0\right) + k_{HO\cdot/R}k_1[H_2O]\right]} \end{aligned} \tag{A.102}$$

where,

$$A_3 = \frac{k_2[Cl^-]_0}{k_6[PS]_0 + k_7[H_2O] + k_{Cl\cdot/R}[R]_0 + \left(k_5 - \frac{k_9 k_5}{k_9 + k_{10}[PS]_0}\right)[Cl^-]_0}$$

$$A_4 = \left(k_1[H_2O] + k_2[Cl^-]_0 + k_3[PS]_0 + k_{SO_4^-\cdot/R}[R]_0\right)\left(k_4[PS]_0 + k_{HO\cdot/R}[R]_0\right) - k_4[PS]_0(k_1[H_2O] + k_7[H_2O]A_3)$$

$$A_5 = \left(k_1[H_2O] + k_3[PS]_0 + k_{SO_4^-\cdot/R}[R]_0\right)\left(k_4[PS]_0 + k_{HO\cdot/R}[R]_0\right) - k_4 k_1[H_2O][PS]_0$$

$$\sum_{Cl^-}^{SO_4^-\cdot} k_i S_i = k_{SO_4^-\cdot/R}[R]_0 + k_1[H_2O]_0 + k_2[Cl^-] + k_3[PS]_0$$

(3) When chloride and NOM are both present

If Cl^- and NOM are present, $SO_4^-\cdot$ reaction rate is given as eq A.103:

$$r_{so_4^-\cdot}^{Cl^-,NOM} = 2r_{UV,S_2O_8^{2-}} - k_1[H_2O][SO_4^-\cdot]_{ss,0}^{Cl^-,NOM} - k_2[Cl^-]_0[SO_4^-\cdot]_{ss,0}^{Cl^-,NOM}$$
$$-k_3[PS]_0[SO_4^-\cdot]_{ss,0}^{Cl^-,NOM} - k_{SO_4^-\cdot/NOM}[NOM]_0[SO_4^-\cdot]_{ss,0}^{Cl^-,NOM} \quad (A.103)$$
$$-k_{SO_4^-\cdot/R}[R]_0[SO_4^-\cdot]_{ss,0}^{Cl^-,NOM} + k_4[PS]_0[HO\cdot]_{ss,0}^{Cl^-,NOM} = 0$$

If Cl^- and NOM are present, HO· reaction rate is given as eq A.104:

$$r_{HO\cdot}^{Cl^-,NOM} = k_1[H_2O][SO_4^-\cdot]_{ss,0}^{Cl^-,NOM} - k_4[PS]_0[HO\cdot]_{ss,0}^{Cl^-,NOM}$$
$$-k_{HO\cdot/NOM}[NOM]_0[HO\cdot]_{ss,0}^{Cl^-,NOM} - k_{HO\cdot/R}[R]_0[HO\cdot]_{ss,0}^{Cl^-,NOM} \quad (A.104)$$
$$+k_8[ClOH^-\cdot]_{ss,0}^{Cl^-,NOM} = 0$$

If Cl^- and NOM are present, $ClOH^-\cdot$ reaction rate is given by eq A.105:

$$r_{ClHO^-\cdot}^{Cl^-,NOM} = k_7[H_2O][Cl\cdot]_{ss,0}^{Cl^-,NOM} - k_8[ClOH\cdot]_{ss,0}^{Cl^-,NOM} = 0 \quad (A.105)$$

If Cl^- and NOM are present, Cl· reaction rate is given as eq A.106:

$$r_{Cl\cdot}^{Cl^-,NOM} = k_2[Cl^-]_0[SO_4^-\cdot]_{ss,0}^{Cl^-,NOM} - k_5[Cl^-]_0[Cl\cdot]_{ss,0}^{Cl^-,NOM} - k_6[PS]_0[Cl\cdot]_{ss,0}^{Cl^-,NOM}$$
$$-k_7[H_2O][Cl\cdot]_{ss,0}^{Cl^-,NOM} - k_{Cl\cdot/NOM}[NOM]_0[Cl\cdot]_{ss,0}^{Cl^-,NOM} - k_{Cl\cdot/R}[R]_0[Cl\cdot]_{ss,0}^{Cl^-,NOM} \quad (A.106)$$
$$+k_9[Cl_2^-\cdot]_{ss,0}^{Cl^-,NOM} = 0$$

If Cl^- and NOM are both present, $Cl_2^-\cdot$ reaction rate is given as eq A.107:

$$r_{Cl_2^-\cdot}^{Cl^-,NOM} = k_5[Cl^-]_0[Cl\cdot]_{ss,0}^{Cl^-,NOM} - k_9[Cl_2^-\cdot]_{ss,0}^{Cl^-,NOM} - k_{10}[PS]_0[Cl_2^-\cdot]_{ss,0}^{Cl^-,NOM}$$
$$-k_{Cl_2^-\cdot/NOM}[NOM]_0[Cl_2^-\cdot]_{ss,0}^{Cl^-,NOM} = 0 \quad (A.107)$$

Combing eq A.106 and eq A.107, the initial steady state Cl· concentration is given as eq A.108:

$$[Cl\cdot]_{ss,0}^{Cl^-,NOM} = \frac{k_2[Cl^-]_0}{\sum_{Cl^-,NOM}^{Cl\cdot} k_i S_i - \left(\frac{k_5 k_9[Cl^-]_0}{k_9 + k_{10}[PS]_0 + k_{Cl_2^-\cdot/NOM}[NOM]_0}\right)}[SO_4^-\cdot]_{ss,0}^{Cl^-,NOM} \quad (A.108)$$

Combining eq A.105 and eq A.108, the initial steady state $ClOH^-\cdot$ concentration is given as eq A.109:

$$[ClOH^{-}\cdot]_{ss,0}^{Cl^{-},NOM} = \frac{k_7[H_2O][Cl\cdot]_{ss,0}^{Cl^{-},NOM}}{k_8} = \frac{k_7[H_2O]A_7}{k_8}[SO_4^{-}\cdot]_{ss,0}^{Cl^{-},NOM} \quad (A.109)$$

Combing eq A.104 and eq A.109, the initial steady state HO· concentration is given as eq A.110:

$$[HO\cdot]_{ss,0}^{Cl^{-},NOM} = \frac{k_1[H_2O] + k_7[H_2O]A_7}{k_4[PS]_0 + k_{HO\cdot/NOM}[NOM]_0 + k_{HO\cdot/R}[R]_0}[SO_4^{-}\cdot]_{ss,0}^{Cl^{-},NOM} \quad (A.110)$$

Combining eq A.103 and eq A.110, the initial steady state $SO_4^{-}\cdot$ concentration is expressed as eq :

$$[SO_4^{-}\cdot]_{ss,0}^{Cl^{-},NOM} = \frac{2r_{UV,S_2O_8^{2-}}^{NOM}\left(k_4[PS]_0 + k_{HO\cdot/NOM}[NOM]_0 + k_{HO\cdot/R}[R]_0\right)}{A_6} \quad (A.111)$$

Combining eq A.110 and eq A.111, the initial steady state HO· concentration is given as eq A.112A.112A.112:

$$[HO\cdot]_{ss,0}^{Cl^{-},NOM} = \frac{2r_{UV,S_2O_8^{2-}}^{NOM}(k_1[H_2O] + k_7[H_2O]A_7)}{A_6} \quad (A.112)$$

Combining eq A.108 and eq A.111, when Cl^{-} and NOM are present the initial steady state Cl· concentration is expressed as eq A.113:

$$[Cl\cdot]_{ss,0}^{Cl^{-},NOM} = \frac{2r_{UV,S_2O_8^{2-}}^{NOM}A_7\left(k_4[PS]_0 + k_{HO\cdot/NOM}[NOM]_0 + k_{HO\cdot/R}[R]_0\right)}{A_6} \quad (A.113)$$

Organic compound's destruction rate when Cl^{-} and NOM are both present is given as eq A.114:

$$r_R^{Cl^{-},NOM} = k_{SO_4^{-}\cdot/R}[SO_4^{-}\cdot]_{ss,0}^{Cl^{-},NOM} + k_{HO\cdot/R}[HO\cdot]_{ss,0}^{Cl^{-},NOM} + k_{Cl\cdot/R}[Cl\cdot]_{ss,0}^{Cl^{-},NOM}$$
$$= \frac{2r_{UV,S_2O_8^{2-}}\left[\left(k_{SO_4^{-}\cdot/R} + k_{Cl\cdot/R}A_7\right)\left(k_4[PS]_0 + k_{HO\cdot/NOM}[NOM]_0 + k_{HO\cdot/R}[R]_0\right) + k_{HO\cdot/R}\left(k_1[H_2O] + k_7[H_2O]A_7\right)\right][R]_0}{A_6} \quad (A.114)$$

As a result, the ratio of organic compound's destruction rate when Cl^{-} and NOM are present to the rate when Cl^{-} and NOM are not present can be expressed as eq A.115:

$$\frac{r_R^{Cl^-,NOM}}{r_R} = \frac{r_{UV,PS}^{NOM}}{r_{UV,PS}} \cdot \frac{k_{SO_4^-\cdot/R}[SO_4^-\cdot]_{ss,0}^{Cl^-,NOM}[R] + k_{HO\cdot/R}[HO\cdot]_{ss,0}^{Cl^-,NOM}[R] + k_{Cl\cdot/R}[Cl\cdot]_{ss,0}^{Cl^-,NOM}[R]}{k_{SO_4^-\cdot/R}[SO_4^-\cdot]_{ss,0}^{no\ Cl^-}[R] + k_{HO\cdot/R}[HO\cdot]_{ss,0}^{no\ Cl^-}[R]}$$

$$= \frac{r_{UV,PS}^{NOM}}{r_{UV,PS}} \cdot \frac{k_{SO_4^-\cdot/R}[SO_4^-\cdot]_{ss,0}^{Cl^-,NOM} + k_{HO\cdot/R}[HO\cdot]_{ss,0}^{Cl^-,NOM} + k_{Cl\cdot/R}[Cl\cdot]_{ss,0}^{Cl^-,NOM}}{k_{SO_4^-\cdot/R}[SO_4^-\cdot]_{ss,0}^{no\ Cl^-} + k_{HO\cdot/R}[HO\cdot]_{ss,0}^{no\ Cl^-}} \quad \text{(A.115)}$$

Since,

$$r_{UV,PS}^{NOM} = 2\phi_{PS}P_{UV}f_{PS}^{NOM}(1-e^{-A^{NOM}}) \quad \text{(A.116)}$$

$$r_{UV,PS} = 2\phi_{PS}P_{UV}f_{PS}(1-e^{-A}) \quad \text{(A.117)}$$

Hence, the ratio of organic compound's destruction rate when Cl^- and NOM are both present to chloride and NOM are not present is expressed as eq A.118:

$$\frac{r_R^{Cl^-,NOM}}{r_R} = \frac{f_{PS}^{NOM}\left(1-e^{-A^{NOM}}\right)}{f_{PS}\left(1-e^{-A}\right)} \cdot \frac{A_5\left[\left(k_{SO_4^-\cdot/R} + k_{Cl\cdot/R}A_7\right)\left(\sum_{Cl^-,NOM}^{HO\cdot} k_iS_i\right) + k_{HO\cdot/R}\left(k_1[H_2O] + k_7[H_2O]A_7\right)\right]}{A_6\left[k_{SO_4^-\cdot/R}\left(k_4[PS]_0 + k_{HO\cdot/R}[R]_0\right) + k_{HO\cdot/R}k_1[H_2O]\right]} \quad \text{(A.118)}$$

where,

$$\sum_{Cl^-,NOM}^{HO\cdot} k_iS_i = k_4[PS]_0 + k_{HO\cdot/NOM}[NOM]_0 + k_{HO\cdot/R}[R]_0$$

$$f_{PS}^{NOM} = \frac{\varepsilon_{PS}C_{PS}}{\varepsilon_RC_R + \varepsilon_{PS}C_{PS} + \varepsilon_{NOM}C_{NOM} + \varepsilon_{bac}C_{bac}}; f_{PS} = \frac{\varepsilon_{PS}C_{PS}}{\varepsilon_RC_R + \varepsilon_{PS}C_{PS} + \varepsilon_{bac}C_{bac}}$$

$$A^{NOM} = 2.303(\varepsilon_RC_R + \varepsilon_{PS}C_{PS} + \varepsilon_{NOM}C_{NOM} + \varepsilon_{bac}C_{bac})L$$

$$A = 2.303(\varepsilon_RC_R + \varepsilon_{PS}C_{PS} + \varepsilon_{bac}C_{bac})L$$

$$A_5 = \left(k_1[H_2O] + k_3[PS]_0 + k_{SO_4^-\cdot/R}[R]_0\right)\left(k_4[PS]_0 + k_{HO\cdot/R}[R]_0\right) - k_4k_1[H_2O][PS]_0$$

$$A_6 = \left(\sum_{Cl^-,NOM}^{SO_4^-\cdot} k_i S_i \right) \left(k_4[PS]_0 + k_{HO\cdot/NOM}[NOM]_0 + k_{HO\cdot/R}[R]_0 \right) - k_4[PS]_0 (k_1[H_2O] + k_7[H_2O]A_7)$$

$$A_7 = \frac{k_2[Cl^-]_0}{\sum_{Cl^-,NOM}^{Cl\cdot} k_i S_i - \left(\frac{k_5 k_9 [Cl^-]_0}{k_9 + k_{10}[PS]_0 + k_{Cl_2^-\cdot/NOM}[NOM]_0} \right)}$$

$$\sum_{Cl^-,NOM}^{SO_4^-\cdot} k_i S_i = k_1[H_2O] + k_2[Cl^-]_0 + k_3[PS]_0 + k_{SO_4^-\cdot/NOM}[NOM]_0 + k_{SO_4^-\cdot/R}[R]_0$$

$$\sum_{Cl^-,NOM}^{Cl\cdot} k_i S_i = k_5[Cl^-]_0 + k_6[PS]_0 + k_7[H_2O] + k_{Cl\cdot/NOM}[NOM]_0 + k_{Cl\cdot/R}[R]_0$$

(4) When chloride and carbonate, bicarbonate are present

If Cl^- and HCO_3^-/CO_3^{2-} are present, $SO_4^-\cdot$ reaction rate is expressed as eq A.119:

$$\begin{aligned} r_{so_4^-\cdot}^{Cl^-,C} &= 2r_{UV,S_2O_8^{2-}} - k_1[H_2O][SO_4^-\cdot]_{ss,0}^{Cl^-,C} - k_2[Cl^-]_0[SO_4^-\cdot]_{ss,0}^{Cl^-,C} - k_3[PS]_0[SO_4^-\cdot]_{ss,0}^{Cl^-,C} \\ &-k_{11}[HCO_3^-]_0[SO_4^-\cdot]_{ss,0}^{Cl^-,C} - k_{12}[CO_3^{2-}]_0[SO_4^-\cdot]_{ss,0}^{Cl^-,C} \\ &-k_{SO_4^-\cdot/R}[R]_0[SO_4^-\cdot]_{ss,0}^{Cl^-,C} + k_4[PS]_0[HO\cdot]_{ss,0}^{Cl^-,C} = 0 \end{aligned} \tag{A.119}$$

If Cl^- and HCO_3^-/CO_3^{2-} are present, $HO\cdot$ reaction rate is expressed as eq A.120:

$$\begin{aligned} r_{HO\cdot}^{Cl^-,C} &= k_1[H_2O][SO_4^-\cdot]_{ss,0}^{Cl^-,C} - k_4[PS]_0[HO\cdot]_{ss,0}^{Cl^-,C} - k_{13}[HCO_3^-]_0[HO\cdot]_{ss,0}^{Cl^-,C} \\ &-k_{14}[CO_3^{2-}]_0[HO\cdot]_{ss,0}^{Cl^-,C} - k_{HO\cdot/R}[R]_0[HO\cdot]_{ss,0}^{Cl^-,C} + k_8[ClOH^-\cdot]_{ss,0}^{Cl^-,C} = 0 \end{aligned} \tag{A.120}$$

If Cl^- and HCO_3^-/CO_3^{2-} are present, $ClOH^-\cdot$ reaction rate is given by eq A.121:

$$r_{ClHO^-\cdot}^{Cl^-,NOM} = k_7[H_2O][Cl\cdot]_{ss,0}^{Cl^-,NOM} - k_8[ClOH\cdot]_{ss,0}^{Cl^-,NOM} = 0 \tag{A.121}$$

If Cl^- and HCO_3^-/CO_3^{2-} are present, $Cl\cdot$ reaction rate is expressed as eq A.122:

$$\begin{aligned} r_{Cl\cdot}^{Cl^-,C} &= k_2[Cl^-]_0[SO_4^-\cdot]_{ss,0}^{Cl^-,C} - k_5[Cl^-]_0[Cl\cdot]_{ss,0}^{Cl^-,C} - k_6[PS]_0[Cl\cdot]_{ss,0}^{Cl^-,C} \\ &-k_7[H_2O][Cl\cdot]_{ss,0}^{Cl^-,C} - k_{15}[HCO_3^-]_0[Cl\cdot]_{ss,0}^{Cl^-,NOM} - k_{16}[CO_3^{2-}]_0[Cl\cdot]_{ss,0}^{Cl^-,NOM} \\ &-k_{Cl\cdot/R}[R]_0[Cl\cdot]_{ss,0}^{Cl^-,C} + k_9[Cl_2^-\cdot]_{ss,0}^{Cl^-,C} = 0 \end{aligned} \tag{A.122}$$

If Cl^- and HCO_3^-/CO_3^{2-} are present, $Cl_2^-\cdot$ reaction rate is expressed as eq A.123:

$$r_{Cl_2^-\cdot}^{Cl^-,C} = k_5[Cl^-]_0[Cl\cdot]_{ss,0}^{Cl^-,C} - k_9[Cl_2^-\cdot]_{ss,0}^{Cl^-,C} - k_{17}[HCO_3^-]_0[Cl_2^-\cdot]_{ss,0}^{Cl^-,C} - k_{18}[CO_3^{2-}]_0[Cl_2^-\cdot]_{ss,0}^{Cl^-,C} = 0 \quad \text{(A.123)}$$

Combing eq A.122 and eq A.123, the initial steady state Cl· concentration is given as eq A.124:

$$[Cl\cdot]_{ss,0}^{Cl^-,C} = \frac{k_2[Cl^-]_0[SO_4^-\cdot]_{ss,0}^{Cl^-,C}}{\left(\sum_{Cl^-,C}^{Cl\cdot} k_i S_i\right) - \frac{k_5 k_9[Cl^-]_0}{k_9 + k_{10}[PS]_0 + k_{17}[HCO_3^-]_0 + k_{18}[CO_3^{2-}]_0}} \quad \text{(A.124)}$$

Combining eq A.121 and eq A.124, the initial steady state $ClOH^-\cdot$ concentration is given as eq A.125:

$$[ClOH^-\cdot]_{ss,0}^{Cl^-,C} = \frac{k_7[H_2O][Cl\cdot]_{ss,0}^{Cl^-,C}}{k_8} = \frac{k_7[H_2O]A_9}{k_8}[SO_4^-\cdot]_{ss,0}^{Cl^-,C} \quad \text{(A.125)}$$

Combing eq A.120 and eq A.125, the initial steady state Cl· concentration is given as eq A.126:

$$[HO\cdot]_{ss,0}^{Cl^-,C} = \frac{k_1[H_2O] + k_7[H_2O]A_9}{k_4[PS]_0 + k_{13}[HCO_3^-]_0 + k_{14}[CO_3^{2-}]_0 + k_{HO\cdot/R}[R]_0}[SO_4^-\cdot]_{ss,0}^{Cl^-,C} \quad \text{(A.126)}$$

Combining eq A.119 and eq A.126, the initial steady state $SO_4^-\cdot$ concentration is expressed as eq A.127:

$$[SO_4^-\cdot]_{ss,0}^{Cl^-,C} = \frac{2r_{UV,S_2O_8^{2-}}\left(k_4[PS]_0 + k_{13}[HCO_3^-]_0 + k_{14}[CO_3^{2-}]_0 + k_{HO\cdot/R}[R]_0\right)}{A_8} \quad \text{(A.127)}$$

Combining eq A.126 and eq A.127, the initial steady state $SO_4^-\cdot$ concentration is expressed as eq A.128:

$$[HO\cdot]_{ss,0}^{Cl^-,C} = \frac{2r_{UV,S_2O_8^{2-}}\left(k_1[H_2O] + k_7[H_2O]A_9\right)}{A_8} \quad \text{(A.128)}$$

Combining eq A.124 and Eq. S127, the initial steady state Cl· concentration is expressed as eq A.129:

$$[Cl\cdot]_{ss,0}^{Cl^-,C} = \frac{2r_{UV,S_2O_8^{2-}} A_9 \left(k_4[PS]_0 + k_{13}[HCO_3^-]_0 + k_{14}[CO_3^{2-}]_0 + k_{HO\cdot/R}[R]_0\right)}{A_8} \tag{A.129}$$

Organic compound's destruction rate when Cl^- and HCO_3^-/CO_3^{2-} are present is expressed as eq:

$$\begin{aligned} r_R^{Cl^-,C} &= k_{SO_4^-\cdot/R}[SO_4^-\cdot]_{ss,0}^{Cl^-,C} + k_{HO\cdot/R}[HO\cdot]_{ss,0}^{Cl^-,C} + k_{Cl\cdot/R}[Cl\cdot]_{ss,0}^{Cl^-,C} \\ &= \frac{2r_{UV,S_2O_8^{2-}}\left[\left(k_{SO_4^-\cdot/R} + k_{Cl\cdot/R}A_9\right)\left(k_4[PS]_0 + k_{13}[HCO_3^-]_0 + k_{14}[CO_3^{2-}]_0 + k_{HO\cdot/R}[R]_0\right) + k_{HO\cdot/R}\left(k_1[H_2O] + k_7[H_2O]A_9\right)\right][R]}{A_8} \end{aligned} \tag{A.130}$$

As a result, the ratio of organic compound's destruction rate when Cl^- and HCO_3^-/CO_3^{2-} are present to the rate when Cl^- and HCO_3^-/CO_3^{2-} are not present is expressed as eq:

$$\begin{aligned} \frac{r_R^{Cl^-,C}}{r_R} &= \frac{k_{SO_4^-\cdot/R}[SO_4^-\cdot]_{ss,0}^{Cl^-,C}[R] + k_{HO\cdot/R}[HO\cdot]_{ss,0}^{Cl^-,C}[R] + k_{Cl\cdot/R}[Cl\cdot]_{ss,0}^{Cl^-,C}[R]}{k_{SO_4^-\cdot/R}[SO_4^-\cdot]_{ss,0}^{no\ Cl^-}[R] + k_{HO\cdot/R}[HO\cdot]_{ss,0}^{no\ Cl^-}[R]} \\ &= \frac{k_{SO_4^-\cdot/R}[SO_4^-\cdot]_{ss,0}^{Cl^-,C} + k_{HO\cdot/R}[HO\cdot]_{ss,0}^{Cl^-,C} + k_{Cl\cdot/R}[Cl\cdot]_{ss,0}^{Cl^-,C}}{k_{SO_4^-\cdot/R}[SO_4^-\cdot]_{ss,0}^{no\ Cl^-} + k_{HO\cdot/R}[HO\cdot]_{ss,0}^{no\ Cl^-}} \\ &= \frac{A_5\left[\left(k_{SO_4^-\cdot/R} + k_{Cl\cdot/R}A_9\right)\left(k_4[PS]_0 + k_{13}[HCO_3^-]_0 + k_{14}[CO_3^{2-}]_0 + k_{HO\cdot/R}[R]_0\right) + k_{HO\cdot/R}\left(k_1[H_2O] + k_7[H_2O]A_9\right)\right]}{A_8\left[k_{SO_4^-\cdot/R}\left(k_4[PS]_0 + k_{HO\cdot/R}[R]_0\right) + k_{HO\cdot/R}k_1[H_2O]\right]} \end{aligned} \tag{A.131}$$

where,

$$A_2 = k_1[H_2O] + k_2[Cl^-]_0 + k_3[PS]_0 + k_{11}[HCO_3^-]_0 + k_{12}[CO_3^{2-}]_0 + k_{SO_4^-\cdot/R}[R]_0$$

$$A_5 = \left(k_1[H_2O] + k_3[PS]_0 + k_{SO_4^-\cdot/R}[R]_0\right)\left(k_4[PS]_0 + k_{HO\cdot/R}[R]_0\right) - k_4k_1[H_2O][PS]_0$$

$$A_8 = A_2\left(k_4[PS]_0 + k_{13}[HCO_3^-]_0 + k_{14}[CO_3^{2-}]_0 + k_{HO\cdot/R}[R]_0\right) - k_4[PS]_0\left(k_1[H_2O] + k_7[H_2O]A_9\right)$$

$$A_9 = \frac{k_2[Cl^-]_0}{\left(\sum_{Cl^-,C}^{Cl\cdot} k_iS_i\right) - \frac{k_5k_9[Cl^-]_0}{k_9 + k_{10}[PS]_0 + k_{17}[HCO_3^-]_0 + k_{18}[CO_3^{2-}]_0}}$$

$$\sum_{Cl^-,C}^{Cl\cdot} k_iS_i = k_5[Cl^-]_0 + k_6[PS]_0 + k_7[H_2O] + k_{15}[HCO_3^-]_0 + k_{16}[CO_3^{2-}]_0 + k_{Cl\cdot/R}[R]_0$$

If we consider the ion strength, all species concentrations should be replaced into species activities for each equation from eq A.85 to eq A.131.

A.6.3 Mathematical Development for UV/H_2O_2: Organic Compounds React with Hydroxyl Radicals and Chlorine Radicals

(1) When chloride is not present

When Cl^- is not present, HO· reaction rate is expressed as eq A.132:

$$r_{HO\cdot} = 2r_{UV,H_2O_2} - k_{19}[H_2O_2]_0[HO\cdot]_{ss,0}^{no\ Cl^-} - k_{HO\cdot/R}[R]_0[HO\cdot]_{ss,0}^{no\ Cl^-} = 0 \quad \text{(A.132)}$$

The initial steady state HO· concentration is expressed as eq A.133:

$$[HO\cdot]_{ss,0}^{Cl^-} = \frac{2r_{UV,H_2O_2}}{k_{19}[H_2O_2]_0 + k_{HO\cdot/R}[R]_0} \quad \text{(A.133)}$$

Hence, the organic compound (R) destruction rate is expressed as eq A.134:

$$r_R = k_{HO\cdot/R}[HO\cdot]_{ss,0}^{no\ Cl^-}[R] = \frac{2r_{UV,H_2O_2}k_{HO\cdot/R}[R]}{k_{19}[H_2O_2]_0 + k_{HO\cdot/R}[R]_0} \quad \text{(A.134)}$$

(2) When chloride is present

If Cl^- is present, HO· reaction rate is expressed as eq A.135:

$$\begin{aligned} r_{HO\cdot}^{Cl^-} &= 2r_{UV,H_2O_2} - k_{19}[H_2O_2]_0[HO\cdot]_{ss,0}^{Cl^-} - k_{20}[Cl^-]_0[HO\cdot]_{ss,0}^{Cl^-} - k_{HO\cdot/R}[R]_0[HO\cdot]_{ss,0}^{Cl^-} \\ &+ k_8[ClOH^-\cdot]_{ss,0}^{Cl^-} = 0 \end{aligned} \quad \text{(A.135)}$$

If Cl^- is present, $ClOH^-\cdot$ reaction rate is expressed as eq A.136:

$$\begin{aligned} r_{ClOH^-\cdot}^{Cl^-} &= k_{20}[Cl^-]_0[HO\cdot]_{ss,0}^{Cl^-} - k_8[ClOH^-\cdot]_{ss,0}^{Cl^-} - k_{21}[Cl^-]_0[ClOH^-\cdot]_{ss,0}^{Cl^-} \\ &- k_{22}[H^+][ClOH^-\cdot]_{ss,0}^{Cl^-} + k_7[H_2O][Cl\cdot]_{ss,0}^{Cl^-} = 0 \end{aligned} \quad \text{(A.136)}$$

If Cl^- is present, Cl· reaction rate is expressed as eq A.137:

$$\begin{aligned} r_{Cl\cdot}^{Cl^-} &= k_{22}[H^+][ClOH^-\cdot]_{ss,0}^{Cl^-} - k_{23}[H_2O_2]_0[Cl\cdot]_{ss,0}^{Cl^-} - k_5[Cl^-]_0[Cl\cdot]_{ss,0}^{Cl^-} \\ &- k_7[H_2O][Cl\cdot]_{ss,0}^{Cl^-} - k_{Cl\cdot/R}[R]_0[Cl\cdot]_{ss,0}^{Cl^-} = 0 \end{aligned} \quad \text{(A.137)}$$

Combining eq A.132 – eq A.137, the initial steady state hydroxyl radical concentration is expressed as eq A.138:

$$[HO\cdot]_{ss,0}^{Cl^-} = \frac{2r_{UV,H_2O_2}}{k_{19}[H_2O_2]_0 + k_{20}[Cl^-]_0 + k_{HO\cdot/R}[R]_0 - k_8A_{11}} \tag{A.138}$$

Combining eq A.132 – eq A.137, the initial steady state Cl· concentration is expressed as eq A.139:

$$[Cl\cdot]_{ss,0}^{Cl^-} = A_{10}A_{11}\frac{2r_{UV,H_2O_2}}{k_{19}[H_2O_2]_0 + k_{20}[Cl^-]_0 + k_{HO\cdot/R}[R]_0 - k_8A_{11}} \tag{A.139}$$

Hence, when chloride the organic compound (R) destruction rate is expressed as eq A.140:

$$\begin{aligned} r_R^{Cl^-} &= k_{HO\cdot/R}[HO\cdot]_{ss,0}^{Cl^-}[R] + k_{Cl\cdot/R}[HO\cdot]_{ss,0}^{Cl^-}[R] \\ &= \frac{2r_{UV,H_2O_2}\left(k_{HO\cdot/R} + A_{10}A_{11}k_{Cl\cdot/R}\right)[R]}{k_{19}[H_2O_2]_0 + k_{20}[Cl^-]_0 + k_{HO\cdot/R}[R]_0 - k_8A_{11}} \end{aligned} \tag{A.140}$$

As a result, the ratio of organic compound's destruction rate when Cl^- is present to the rate when Cl^- is not present can be expressed as eq A.141:

$$\begin{aligned} \frac{r_R^{Cl^-}}{r_R} &= \frac{k_{HO\cdot/R}[HO\cdot]_{ss,0}^{Cl^-}[R] + k_{Cl\cdot/R}[Cl\cdot]_{ss,0}^{Cl^-}[R]}{k_{HO\cdot/R}[HO\cdot]_{ss,0}^{no\ Cl^-}[R]} = \frac{k_{HO\cdot/R}[HO\cdot]_{ss,0}^{Cl^-} + k_{Cl\cdot/R}[Cl\cdot]_{ss,0}^{Cl^-}}{k_{HO\cdot/R}[HO\cdot]_{ss,0}^{no\ Cl^-}} \\ &= \frac{\left(k_{19}[H_2O_2]_0 + k_{HO\cdot/R}[R]_0\right)\left(k_{HO\cdot/R} + A_{10}A_{11}k_{Cl\cdot/R}\right)}{k_{HO\cdot/R}\left(k_{19}[H_2O_2]_0 + k_{20}[Cl^-]_0 + k_{HO\cdot/R}[R]_0 - k_8A_{11}\right)} \end{aligned} \tag{A.141}$$

(3) When chloride and NOM are present

If Cl^- and NOM are present, HO· reaction rate is expressed as eq A.142:

$$\begin{aligned} r_{HO\cdot}^{Cl^-,NOM} &= 2r_{UV,H_2O_2}^{NOM} - k_{19}[H_2O_2]_0[HO\cdot]_{ss,0}^{Cl^-} - k_{20}[Cl^-]_0[HO\cdot]_{ss,0}^{Cl^-} \\ &-k_{HO\cdot/NOM}[NOM]_0[HO\cdot]_{ss,0}^{Cl^-} - k_{HO\cdot/R}[R]_0[HO\cdot]_{ss,0}^{Cl^-} + k_8[ClOH^-\cdot]_{ss,0}^{Cl^-} = 0 \end{aligned} \tag{A.142}$$

If Cl^- and NOM are both present, $ClOH^-\cdot$ reaction rate is expressed as eq A.143:

$$\begin{aligned} r_{ClOH^-\cdot}^{Cl^-,NOM} &= k_{20}[Cl^-]_0[HO\cdot]_{ss,0}^{Cl^-,NOM} - k_8[ClOH^-\cdot]_{ss,0}^{Cl^-,NOM} \\ &-k_{21}[Cl^-]_0[ClOH^-\cdot]_{ss,0}^{Cl^-,NOM} - k_{22}[H^+][ClOH^-\cdot]_{ss,0}^{Cl^-,NOM} \\ &+k_7[H_2O][Cl\cdot]_{ss,0}^{Cl^-,NOM} = 0 \end{aligned} \tag{A.143}$$

If Cl^- and NOM are present, Cl· reaction rate is expressed as eq A.144:

$$r_{Cl\cdot}^{Cl^-,NOM} = k_{22}[H^+][ClOH^-\cdot]_{ss,0}^{Cl^-,NOM} - k_{23}[H_2O_2]_0[Cl\cdot]_{ss,0}^{Cl^-,NOM} - k_5[Cl^-]_0[Cl\cdot]_{ss,0}^{Cl^-,NOM}$$
$$-k_7[H_2O][Cl\cdot]_{ss,0}^{Cl^-,NOM} - k_{Cl\cdot/NOM}[NOM]_0[Cl\cdot]_{ss,0}^{Cl^-,NOM} - k_{Cl\cdot/R}[R]_0[Cl\cdot]_{ss,0}^{Cl^-,NOM} = 0 \quad (A.144)$$

Combining eq A.142 – eq A.144, the initial steady state HO· concentration is expressed as eq A.145:

$$[HO\cdot]_{ss,0}^{Cl^-} = \frac{2r_{UV,H_2O_2}^{NOM}}{k_{19}[H_2O_2]_0 + k_{20}[Cl^-]_0 + k_{HO\cdot/NOM}[NOM]_0 + k_{HO\cdot/R}[R]_0 - k_8A_{13}} \quad (A.145)$$

Combining eq A.142 – eq A.144, the initial steady state Cl· concentration is expressed as eq A.146:

$$[Cl\cdot]_{ss,0}^{Cl^-} = A_{12}A_{13}\frac{2r_{UV,H_2O_2}^{NOM}}{k_{19}[H_2O_2]_0 + k_{20}[Cl^-]_0 + k_{HO\cdot/NOM}[NOM]_0 + k_{HO\cdot/R}[R]_0 - k_8A_{13}} \quad (A.146)$$

Hence, when Cl^- and NOM are present, the organic compound (R) destruction rate is expressed as eq A.147:

$$r_R^{Cl^-,NOM} = k_{HO\cdot/R}[HO\cdot]_{ss,0}^{Cl^-,NOM}[R] + k_{Cl\cdot/R}[HO\cdot]_{ss,0}^{Cl^-,NOM}[R]$$
$$= \frac{2r_{UV,H_2O_2}^{NOM}\left(k_{HO\cdot/R} + A_{12}A_{13}k_{Cl\cdot/R}\right)[R]}{k_{19}[H_2O_2]_0 + k_{20}[Cl^-]_0 + k_{HO\cdot/NOM}[NOM]_0 + k_{HO\cdot/R}[R]_0 - k_8A_{13}} \quad (A.147)$$

As a result, the ratio of organic compound's destruction rate when Cl^- and NOM are present to the rate when Cl^- and NOM are not present can be expressed as eq A.148:

$$\frac{r_R^{Cl^-,NOM}}{r_R} = \frac{r_{UV,H_2O_2}^{NOM}}{r_{UV,H_2O_2}} \cdot \frac{k_{HO\cdot/R}[HO\cdot]_{ss,0}^{Cl^-,NOM}[R] + k_{Cl\cdot/R}[Cl\cdot]_{ss,0}^{Cl^-,NOM}[R]}{k_{HO\cdot/R}[HO\cdot]_{ss,0}^{no\ Cl^-}[R]} \quad (A.148)$$

$r_{UV,H_2O_2}^{NOM}$ is the rate of H_2O_2 photolysis to produce hydroxyl radical when NOM is present, it is expressed as eq A.149:

$$r_{UV,H_2O_2}^{NOM} = 2\phi_{H_2O_2}P_{UV}f_{H_2O_2}^{NOM}(1-e^{-A^{NOM}}) \quad (A.149)$$

r_{UV,H_2O_2} is the rate of H_2O_2 photolysis to produce sulfate radical when NOM is not present, it is expressed as eq A.150:

$$r_{UV,H_2O_2} = 2\phi_{H_2O_2} P_{UV} f_{H_2O_2} (1-e^{-A}) \tag{A.150}$$

Hence, the ratio of organic compound's destruction rate when Cl^- and NOM are present to Cl^- and NOM are not present can be expressed as eq A.151:

$$\frac{r_R^{Cl^-,NOM}}{r_R} = \frac{f_{H_2O_2}^{NOM}\left(1-e^{-A^{NOM}}\right)}{f_{H_2O_2}\left(1-e^{-A}\right)} \cdot \frac{\left(k_{19}[H_2O_2]_0 + k_{HO\cdot/R}[R]_0\right)\left(k_{HO\cdot/R} + A_{12}A_{13}k_{Cl\cdot/R}\right)}{k_{HO\cdot/R}\left(k_{19}[H_2O_2]_0 + k_{20}[Cl^-]_0 + k_{HO\cdot/NOM}[NOM]_0 + k_{HO\cdot/R}[R]_0 - k_8 A_{13}\right)} \tag{A.151}$$

where,

$$f_{H_2O_2}^{NOM} = \frac{\varepsilon_{H_2O_2} C_{H_2O_2}}{\varepsilon_R C_R + \varepsilon_{H_2O_2} C_{H_2O_2} + \varepsilon_{NOM} C_{NOM} + \varepsilon_{bac} C_{bac}}$$

$$f_{H_2O_2} = \frac{\varepsilon_{H_2O_2} C_{H_2O_2}}{\varepsilon_R C_R + \varepsilon_{H_2O_2} C_{H_2O_2} + \varepsilon_{bac} C_{bac}}$$

$$A^{NOM} = 2.303(\varepsilon_R C_R + \varepsilon_{H_2O_2} C_{H_2O_2} + \varepsilon_{NOM} C_{NOM} + \varepsilon_{bac} C_{bac})L$$

$$A = 2.303(\varepsilon_R C_R + \varepsilon_{H_2O_2} C_{H_2O_2} + \varepsilon_{bac} C_{bac})L$$

$$A_{12} = \frac{k_{22}[H^+]}{k_{23}[H_2O_2]_0 + k_5[Cl^-]_0 + k_7[H_2O] + k_{Cl\cdot/NOM}[NOM]_0 + k_{Cl\cdot/R}[R]_0}$$

$$A_{13} = \frac{k_{20}[Cl^-]_0}{k_8 + k_{21}[Cl^-]_0 + k_{22}[H^+] - k_7[H_2O]A_{12}}$$

(4) When chloride and bicarbonate, carbonate are present

If Cl^- and HCO_3^-/CO_3^{2-} are present, HO· reaction rate is expressed as eq A.152:

$$\begin{aligned} r_{HO\cdot}^{Cl^-,C} &= 2r_{UV,H_2O_2} - k_{19}[H_2O_2]_0[HO\cdot]_{ss,0}^{Cl^-,C} - k_{20}[Cl^-]_0[HO\cdot]_{ss,0}^{Cl^-,C} - k_{13}[HCO_3^-]_0[HO\cdot]_{ss,0}^{Cl^-,C} \\ &k_{14}[CO_3^{2-}]_0[HO\cdot]_{ss,0}^{Cl^-,C} - k_{HO\cdot/R}[R]_0[HO\cdot]_{ss,0}^{Cl^-,C} + k_8[ClOH^-\cdot]_{ss,0}^{Cl^-,C} = 0 \end{aligned} \tag{A.152}$$

If Cl^- and HCO_3^-/CO_3^{2-} are present, $ClOH^-\cdot$ reaction rate is expressed as eq A.153:

$$\begin{aligned} r_{ClOH^-\cdot}^{Cl^-,C} &= k_{20}[Cl^-]_0[HO\cdot]_{ss,0}^{Cl^-,C} - k_8[ClOH^-\cdot]_{ss,0}^{Cl^-,C} - k_{21}[Cl^-]_0[ClOH^-\cdot]_{ss,0}^{Cl^-,C} \\ &-k_{22}[H^+][ClOH^-\cdot]_{ss,0}^{Cl^-,C} + k_7[H_2O][Cl\cdot]_{ss,0}^{Cl^-,C} = 0 \end{aligned} \tag{A.153}$$

If Cl^- and HCO_3^-/CO_3^{2-} are present, $Cl\cdot$ reaction rate is expressed as eq A.154:

$$\begin{aligned} r_{Cl\cdot}^{Cl^-,C} &= k_{22}[H^+][ClOH^-\cdot]_{ss,0}^{Cl^-,C} - k_{23}[H_2O_2]_0[Cl\cdot]_{ss,0}^{Cl^-,C} - k_5[Cl^-]_0[Cl\cdot]_{ss,0}^{Cl^-,C} \\ &-k_7[H_2O][Cl\cdot]_{ss,0}^{Cl^-,C} - k_{15}[HCO_3^-]_0[Cl\cdot]_{ss,0}^{Cl^-,NOM} - k_{16}[CO_3^{2-}]_0[Cl\cdot]_{ss,0}^{Cl^-,NOM} \\ &-k_{Cl\cdot/R}[R]_0[Cl\cdot]_{ss,0}^{Cl^-,NOM} = 0 \end{aligned} \tag{A.154}$$

Combining eq A.152 – eq A.154, the initial steady state $HO\cdot$ concentration is expressed as eq A.155:

$$[HO\cdot]_{ss,0}^{Cl^-} = \frac{2r_{UV,H_2O_2}}{k_{19}[H_2O_2]_0 + k_{20}[Cl^-]_0 + k_{13}[HCO_3^-]_0 + k_{14}[CO_3^{2-}]_0 + k_{HO\cdot/R}[R]_0 - k_8A_{15}} \tag{A.155}$$

Combining eq A.152 – eq A.154, the initial steady state $Cl\cdot$ concentration is expressed as eq A.156:

$$[Cl\cdot]_{ss,0}^{Cl^-} = A_{14}A_{15}\frac{2r_{UV,H_2O_2}}{k_{19}[H_2O_2]_0 + k_{20}[Cl^-]_0 + k_{13}[HCO_3^-]_0 + k_{14}[CO_3^{2-}]_0 + k_{HO\cdot/R}[R]_0 - k_8A_{15}} \tag{A.156}$$

Hence, the organic compound (R) destruction rate is expressed as eq A.157:

$$\begin{aligned} r_R^{Cl^-,C} &= k_{HO\cdot/R}[HO\cdot]_{ss,0}^{Cl^-,C}[R] + k_{Cl\cdot/R}[HO\cdot]_{ss,0}^{Cl^-,C}[R] \\ &= \frac{2r_{UV,H_2O_2}\left(k_{HO\cdot/R} + A_{14}A_{15}k_{Cl\cdot/R}\right)[R]}{k_{19}[H_2O_2]_0 + k_{20}[Cl^-]_0 + k_{13}[HCO_3^-]_0 + k_{14}[CO_3^{2-}]_0 + k_{HO\cdot/R}[R]_0 - k_8A_{15}} \end{aligned} \tag{A.157}$$

As a result, the ratio of organic compound's destruction rate when Cl^- and HCO_3^-/CO_3^{2-} are present to the rate when Cl^- and HCO_3^-/CO_3^{2-} are not present is expressed as eq A.158:

$$\frac{r_R^{Cl^-,C}}{r_R} = \frac{k_{HO\cdot/R}[HO\cdot]_{ss,0}^{Cl^-,C}[R] + k_{Cl\cdot/R}[Cl\cdot]_{ss,0}^{Cl^-,C}[R]}{k_{HO\cdot/R}[HO\cdot]_{ss,0}^{Cl^-}[R]}$$

$$= \frac{k_{HO\cdot/R}[HO\cdot]_{ss,0}^{Cl^-,C} + k_{Cl\cdot/R}[Cl\cdot]_{ss,0}^{Cl^-,C}}{k_{HO\cdot/R}[HO\cdot]_{ss,0}^{Cl^-}} \tag{A.158}$$

$$= \frac{\left(k_{19}[H_2O_2]_0 + k_{HO\cdot/R}[R]_0\right)\left(k_{HO\cdot/R} + A_{14}A_{15}k_{Cl\cdot/R}\right)}{k_{HO\cdot/R}\left(k_{19}[H_2O_2]_0 + k_{20}[Cl^-]_0 + k_{13}[HCO_3^-]_0 + k_{14}[CO_3^{2-}]_0 + k_{HO\cdot/R}[R]_0 - k_8A_{15}\right)}$$

A.7 Determining Oxidants Concentration

We prepared standard solutions with different concentrations of PS as the following procedure: add 0.125 g $NaHCO_3$ into 1 mL standard solution together with to avoid air-oxidation of iodide, and, add 2.5 g KI into 25 mL pure water in 25 mL-colorimetric tube. Then hand shook the solutions and allowed to equilibrate for 15 min. The analytical wavelength was fixed at 352 nm and calibration concentrations ranged from 0.0 mM up to 1.0 mM in this study. All sample solution analysis was conducted in accordance with the calibration preparation procedures.

The concentrations of H_2O_2 were measured according to the spectrophotometric method.[96]

A.8 Experimental Materials and Reagents

Benzoic acid (BZA, ≥99.5%), Sodium persulfate (PS, $Na_2S_2O_8$, ≥98%), Hydrogen peroxide (H_2O_2, ≥30%), Sodium chloride (NaCl, ≥99.5%), and Dipotassium hydrogen phosphate trihydrate ($K_2HPO_4 \cdot 3H_20$, ≥98.0%) were supplied by Sinopharm Chemical Reagent Co. (China). Monopotassium phosphate (KH_2PO_4, ≥99.5%) were obtained from Tianjin Kemiou Chemical Reagent Co. (China). Phosphoric acid (H_3PO_4, ≥85%) was obtained from Tianjin Damao Chemical Reagent Co. (China).Methanol (MeOH, HPLC grade, ≥99.9%) (HPLC grade, ≥99.9%) were purchased from Sigma–Aldrich Chemical Co.

Ltd. (USA). Ultrapure water was obtained from UP Water Purification System(18.5 MΩ cm, ELGA, UK).

A.9 Analytical Methods

The quantifications of the BZA were performed with an Agilent 1260 Series HPLC (CA, USA) at an UV wavelength of 270nm. The mobile phase was a mixture of MeOH/water in 50/50 (v/v) ratio. The flow rate was set at 1mL min^{-1} and the injection volume was 20 mL. The temperature of the column was set at 25℃

A.10 Notations for Model Development

$r_{SO_4^-\cdot}$	$SO_4^-\cdot$ reaction rate when Cl^- is present, s^{-1}
$r_{SO_4^-\cdot}^{Cl^-}$	$SO_4^-\cdot$ reaction rate when Cl^- is present, s^{-1}
$r_{SO_4^-\cdot}^{NOM}$	$SO_4^-\cdot$ reaction rate when NOM is present, s^{-1}
$r_{SO_4^-\cdot}^{Cl^-,NOM}$	$SO_4^-\cdot$ reaction rate when Cl^- and NOM are present, s^{-1}
$r_{SO_4^-\cdot}^{C}$	$SO_4^-\cdot$ reaction rate when HCO_3^-/CO_3^{2-} are present, s^{-1}
$r_{SO_4^-\cdot}^{Cl^-,C}$	$SO_4^-\cdot$ reaction rate when Cl^- and HCO_3^-/CO_3^{2-} are present, s^{-1}
$r_{HO\cdot}$	$HO\cdot$ reaction rate when Cl^- is not present, s^{-1}
$r_{HO\cdot}^{Cl^-}$	$HO\cdot$ reaction rate when Cl^- is present, s^{-1}
$r_{HO\cdot}^{NOM}$	$HO\cdot$ reaction rate when NOM is present, s^{-1}
$r_{HO\cdot}^{Cl^-,NOM}$	$HO\cdot$ reaction rate when Cl^- and NOM are present, s^{-1}
$r_{HO\cdot}^{C}$	$HO\cdot$ reaction rate when HCO_3^-/CO_3^{2-} are present, s^{-1}
$r_{HO\cdot}^{Cl^-,C}$	$HO\cdot$ reaction rate when Cl^- and HCO_3^-/CO_3^{2-} are present,s^{-1}
$r_{Cl\cdot}^{Cl^-}$	$Cl\cdot$ reaction rate when Cl^- is present, s^{-1}
$r_{Cl\cdot}^{Cl^-,NOM}$	$Cl\cdot$ reaction rate when Cl^- and NOM are present, s^{-1}
$r_{Cl\cdot}^{Cl^-,C}$	$Cl\cdot$ reaction rate when Cl^- and HCO_3^-/CO_3^{2-} are present, s^{-1}
$r_{Cl_2^-\cdot}^{Cl^-}$	$Cl_2^-\cdot$ reaction rate when Cl^- is present, s^{-1}
$r_{Cl_2^-\cdot}^{Cl^-,NOM}$	$Cl_2^-\cdot$ reaction rate when Cl^- and NOM are present, s^{-1}
$r_{Cl_2^-\cdot}^{Cl^-,C}$	$Cl_2^-\cdot$ reaction rate when Cl^- and HCO_3^-/CO_3^{2-} are present, s^{-1}
$r_{ClOH^-\cdot}$	$ClOH^-\cdot$ reaction rate when Cl^- not is present, s^{-1}
$r_{ClOH^-\cdot}^{Cl^-}$	$ClOH^-\cdot$ reaction rate when Cl^- is present, s^{-1}

$r_{ClOH^-\cdot}^{Cl^-,NOM}$	$ClOH^-\cdot$ reaction rate when Cl^- and NOM are present, s^{-1}
$r_{ClOH^-\cdot}^{Cl^-,C}$	$ClOH^-\cdot$ reaction rate when Cl^- and HCO_3^-/CO_3^{2-} are present, s^{-1}
r_R	organic compound's destruction rate when Cl^- is not present, s^{-1}
$r_R^{Cl^-}$	organic compound's destruction rate when Cl^- is present, s^{-1}
$r_R^{Cl^-,NOM}$	organic compound's destruction rate when Cl^- and NOM are present, s^{-1}
$r_R^{Cl^-,C}$	organic compound's destruction rate when Cl^- and HCO_3^-/CO_3^{2-} are present, s^{-1}
$[SO_4^-\cdot]_{ss,0}^{no\ Cl^-}$	initial steady state $SO_4^-\cdot$ concentration when Cl^- is not present, M
$[SO_4^-\cdot]_{ss,0}^{Cl^-}$	initial steady state $SO_4^-\cdot$ concentration when Cl^- is present, M
$[SO_4^-\cdot]_{ss,0}^{NOM}$	initial steady state $SO_4^-\cdot$ concentration when NOM is present, M
$[SO_4^-\cdot]_{ss,0}^{Cl^-,NOM}$	initial steady state $SO_4^-\cdot$ concentration when Cl^- and NOM are present, M
$[SO_4^-\cdot]_{ss,0}^{C}$	initial steady state $SO_4^-\cdot$ concentration when HCO_3^-/CO_3^{2-} are present, M
$[SO_4^-\cdot]_{ss,0}^{Cl^-,C}$	initial steady state $SO_4^-\cdot$ concentration when Cl^- and HCO_3^-/CO_3^{2-} are present, M
$[HO\cdot]_{ss,0}^{no\ Cl^-}$	initial steady state $HO\cdot$ concentration when Cl^- is not present, M
$[HO\cdot]_{ss,0}^{Cl^-}$	initial steady state $HO\cdot$ concentration when Cl^- is present, M
$[HO\cdot]_{ss,0}^{NOM}$	initial steady state $HO\cdot$ concentration when NOM is present, M
$[HO\cdot]_{ss,0}^{Cl^-,NOM}$	initial steady state $HO\cdot$ concentration when Cl^- and NOM are present, M
$[HO\cdot]_{ss,0}^{C}$	initial steady state $HO\cdot$ concentration when HCO_3^-/CO_3^{2-} are present, M
$[HO\cdot]_{ss,0}^{Cl^-,C}$	initial steady state $HO\cdot$ concentration when Cl^- and HCO_3^-/CO_3^{2-} are present, M
$[Cl\cdot]_{ss,0}^{Cl^-}$	initial steady state $Cl\cdot$ concentration when Cl^- is present, M
$[Cl\cdot]_{ss,0}^{Cl^-,NOM}$	initial steady state $Cl\cdot$ concentration when Cl^- and NOM are present, M
$[Cl\cdot]_{ss,0}^{Cl^-,C}$	initial steady state $Cl\cdot$ concentration when Cl^- and HCO_3^-/CO_3^{2-} are present, M
$[Cl_2^-\cdot]_{ss,0}^{Cl^-}$	initial steady state $Cl_2^-\cdot$ concentration when Cl^- is present, M
$[Cl_2^-\cdot]_{ss,0}^{Cl^-,NOM}$	initial stead state $Cl_2^-\cdot$ concentration when Cl^- and NOM are present, M
$[Cl_2^-\cdot]_{ss,0}^{Cl^-,C}$	initial steady state $Cl_2^-\cdot$ concentration when Cl^- and HCO_3^-/CO_3^{2-} are presents, M
$[ClOH^-\cdot]_{ss,0}^{no\ Cl^-}$	initial steady state $ClOH^-\cdot$ concentration when Cl^- is not present, M
$[ClOH^-\cdot]_{ss,0}^{Cl^-}$	initial steady state $ClOH^-\cdot$ concentration when Cl^- is present, M

$[ClOH^{-}\cdot]_{ss,0}^{Cl^{-},NOM}$	initial steady state $ClOH^{-}\cdot$ concentration when Cl^{-} and NOM both are present, M
$[ClOH^{-}\cdot]_{ss,0}^{Cl^{-},C}$	initial steady state $ClOH^{-}\cdot$ concentration when Cl^{-} and HCO_3^{-}/CO_3^{2-} are present, M
$[PS]_0$	initial persulfate concentration, M
$[H_2O_2]_0$	initial hydrogen peroxide concentration, M
$[Cl^{-}]_0$	initial Cl^{-} concentration, M
$[R]_0$	initial organic compound concentration, M
$[NOM]_0$	initial NOM concentration, $mg\cdot L^{-1}$
$[HCO_3^{-}]_0$	initial HCO_3^{-} concentration, M
$[CO_3^{2-}]_0$	initial CO_3^{2-} concentration, M

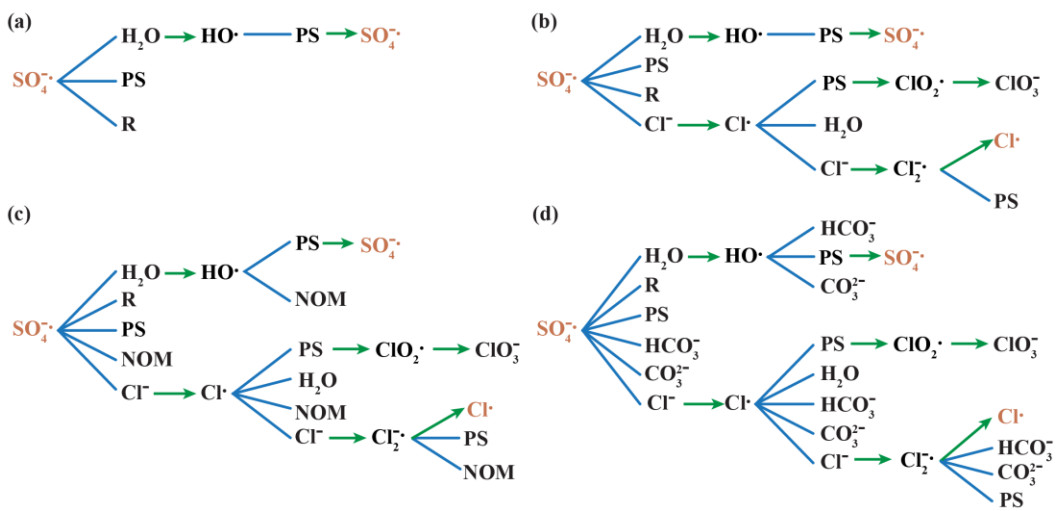

Figure A.1. UV/PS elementary reaction network (this is the case that organic compounds react only with , where (a) Cl^{-} is not present; (b) only Cl^{-} is present; (c) Cl^{-} and NOM are present; (d) Cl^{-}, HCO_3^{-} and CO_3^{2-} are present. The blue lines represent reaction between these two compounds, and green rows represent reaction products that are generated.

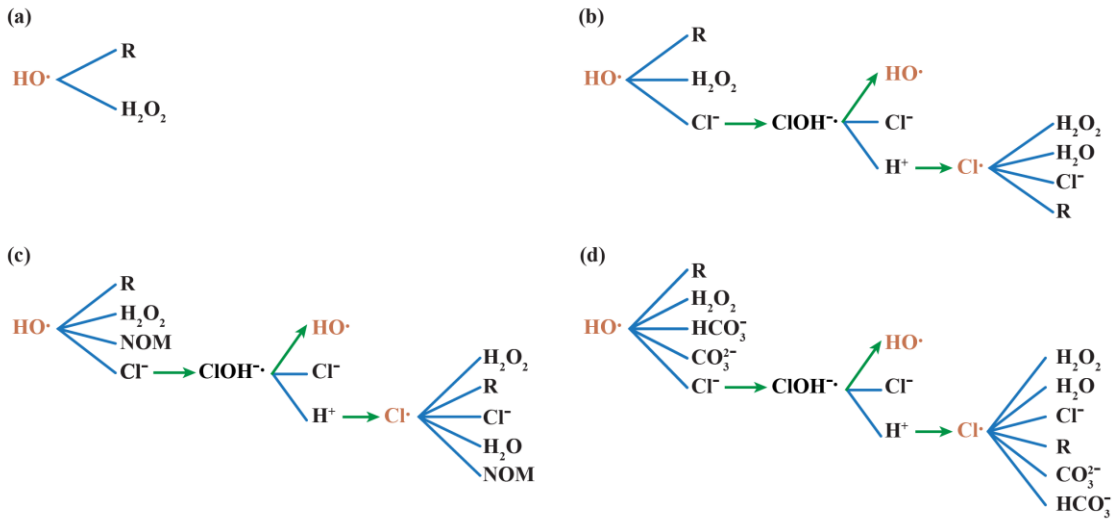

Figure A.2. UV/H_2O_2 elementary reaction network, where (a) Cl^- is not present; (b) only Cl^- is present; (c) Cl^- and NOM are present; (d) Cl^-, HCO_3^- and CO_3^{2-} are present. The blue lines represent reaction between these two compounds, and green rows represent reaction products that are generated.

Table A.1. Elementary reactions for UV/PS process [20]

#	Reaction	k($M^{-1}s^{-1}$)
1	$S_2O_8^{2-} + h\nu \rightarrow 2SO_4^{-}\bullet$	$r_{SO_4^-\bullet} = -2r_{UV,S_2O_8^{2-}} = 2\phi_{S_2O_8^{2-}} P_{UV} f_{S_2O_8^{2-}} \left[1-10^{(-A)}\right]$ $\phi_{S_2O_8^{2-},254nm} = 0.7$ $\varepsilon_{S_2O_8^{2-},254nm} = 20.07\,M^{-1}cm^{-1}$ $A = \left(\varepsilon_{S_2O_8^{2-}} C_{S_2O_8^{2-}} + \varepsilon_R C_R + \varepsilon_{Background} C_{Background}\right) L$ $f_{S_2O_8^{2-}} = \varepsilon_{S_2O_8^{2-}} C_{S_2O_8^{2-}} L / A$ L is effective length, cm
2	$SO_4^{-}\bullet + R \rightarrow$ byproduct	$k_{SO_4^-\bullet/R}$
3	$SO_4^{-}\bullet + H_2O \rightarrow HO\bullet + HSO_4^{-}$	$k_1[H_2O] = 1.817\times10^3 s^{-1}$
4	$SO_4^{-}\bullet + Cl^- \rightarrow Cl\bullet + SO_4^{2-}$	$k_2 = 4.7\times10^8$
5	$SO_4^{-}\bullet + S_2O_8^{2-} \rightarrow S_2O_8^{-}\bullet + SO_4^{2-}$	$k_3 = 0.095$
6	$HO\bullet + S_2O_8^{2-} \rightarrow SO_4^{-}\bullet + HSO_4^{-} + 0.5O_2$	$k_4 = 1.2\times10^7$
7	$Cl\bullet + Cl^- \rightarrow Cl_2^{-}\bullet$	$k_5 = 8\times10^9$
8	$Cl\bullet + S_2O_8^{2-} \rightarrow ClO_2\bullet \rightarrow ClO_3^-$	$k_6 = 2.93\times10^8$
9	$Cl\bullet + H_2O \rightarrow ClOH^-\bullet + H^+$	$k_7[H_2O] = 1.3\times10^3 s^{-1}$
10	$ClOH^-\bullet \rightarrow HO\bullet + Cl^-$	$k_8 = 6.1\times10^9$
11	$Cl_2^{-}\bullet \rightarrow Cl\bullet + Cl^-$	$k_9 = 5.3\times10^4$
12	$Cl_2^{-}\bullet + S_2O_8^{2-} \rightarrow ClO_2\bullet$ + byproduct	$k_{10} = 3.82\times10^4$
13	$SO_4^{-}\bullet$ + NOM $\rightarrow$ byproduct	$k_{SO_4^-\bullet/NOM} = 2.35\times10^4$ (mg-C/L)$^{-1}s^{-1}$
14	$HO\bullet$ + NOM $\rightarrow$ byproduct	$k_{HO\bullet/NOM} = 2.5\times10^4$ (mg-C/L)$^{-1}s^{-1}$
15	$Cl\bullet$ + NOM $\rightarrow$ byproduct	$k_{Cl\bullet/NOM} = 1.3\times10^4$ (mg-C/L)$^{-1}s^{-1}$ [37]
16	$Cl_2^{-}\bullet$ + NOM $\rightarrow$ byproduct	$k_{Cl_2^-\bullet/NOM} = 1\times10^2$ (mg-C/L)$^{-1}s^{-1}$ [160]
17	$SO_4^{-}\bullet + HCO_3^- \rightarrow CO_3^{-}\bullet + SO_4^{2-} + H^+$	$k_{11} = 3.6\times10^6$
18	$SO_4^{-}\bullet + CO_3^{2-} \rightarrow CO_3^{-}\bullet + SO_4^{2-}$	$k_{12} = 6.5\times10^6$
19	$HO\bullet + HCO_3^- \rightarrow CO_3^{-}\bullet + H_2O$	$k_{13} = 8.5\times10^6$
20	$HO\bullet + CO_3^{2-} \rightarrow CO_3^{-}\bullet + OH^-$	$k_{14} = 3.9\times10^9$
21	$Cl\bullet + HCO_3^- \rightarrow CO_3^{-}\bullet + H^+ + Cl^-$	$k_{15} = 2.2\times10^8$
22	$Cl\bullet + CO_3^{2-} \rightarrow CO_3^{-}\bullet + Cl^-$	$k_{16} = 5\times10^8$
23	$Cl_2^{-}\bullet + HCO_3^- \rightarrow CO_3^{-}\bullet + H^+ + 2Cl^-$	$k_{17} = 8\times10^7$

24	$Cl_2^-\bullet + CO_3^{2-} \rightarrow CO_3^-\bullet + 2Cl^-$	$k_{18} = 1.6\times10^8$
25	$HO\bullet + R \rightarrow$ byproduct	$k_{HO\bullet/R}$
26	$Cl\bullet + R \rightarrow$ byproduct	$k_{Cl\bullet/R}$

Table A.2. Elementary reactions for UV/H_2O_2 [15]

#	Reaction	k($M^{-1}s^{-1}$)
1	$H_2O_2 + hv \rightarrow 2HO\bullet$	$r_{HO\bullet} = -2r_{UV,H_2O_2} = 2\phi_{H_2O_2}P_{UV}f_{H_2O_2}\left[1-10^{(-A)}\right]$ $\phi_{H_2O_2,254nm} = 0.5$ $\varepsilon_{H_2O_2,254nm} = 19.6\,M^{-1}cm^{-1}$ $A = \left(\varepsilon_{H_2O_2}C_{H_2O_2} + \varepsilon_R C_R + \varepsilon_{Background}C_{Background}\right)L$ $f_{H_2O_2} = \varepsilon_{H_2O_2}C_{H_2O_2}L/A$ L is reactor depth, cm
2	$HO\bullet + R \rightarrow$ byproduct	$k_{HO\bullet/R}$
3	$HO\bullet + H_2O_2 \rightarrow HO_2\bullet + H_2O$	$k_{19} = 2.7\times10^7$
4	$HO\bullet + Cl^- \rightarrow ClOH^-\bullet$	$k_{20} = 4.3\times10^9$
5	$ClOH^-\bullet \rightarrow OH\bullet + Cl^-$	$k_8 = 6.1\times10^9 s^{-1}$
6	$ClOH^-\bullet + Cl^- \rightarrow Cl_2^-\bullet + OH^-$	$k_{21} = 1\times10^4$
7	$ClOH^-\bullet + H^+ \rightarrow Cl\bullet + H_2O$	$k_{22} = 2.1\times10^{10}$
8	$Cl\bullet + H_2O_2 \rightarrow H^+ + Cl^- + HO_2\bullet$	$k_{23} = 2\times10^9$
9	$Cl\bullet + Cl^- \rightarrow Cl_2^-\bullet$	$k_5 = 8\times10^9$
10	$Cl\bullet + H_2O \rightarrow ClOH^-\bullet + H^+$	$k_7[H_2O] = 1.3\times10^3$
11	$Cl\bullet + R \rightarrow$ byproduct	$k_{Cl\bullet/R}$
12	$HO\bullet + NOM \rightarrow$ byproduct	$k_{HO\bullet/NOM} = 2.5\times10^4$ (mg-C/L)$^{-1}s^{-1}$
13	$Cl\bullet + NOM \rightarrow$ byproduct	$k_{Cl\bullet/NOM} = 1.3\times10^4$ (mg-C/L)$^{-1}s^{-1}$ [37]
14	$HO\bullet + HCO_3^- \rightarrow CO_3^-\bullet + H_2O$	$k_{13} = 8.5\times10^6$
15	$HO\bullet + CO_3^{2-} \rightarrow CO_3^-\bullet + OH^-$	$k_{14} = 3.9\times10^9$
16	$Cl\bullet + HCO_3^- \rightarrow CO_3^-\bullet + H^+ + Cl^-$	$k_{15} = 2.2\times10^8$
17	$Cl\bullet + CO_3^{2-} \rightarrow CO_3^-\bullet + Cl^-$	$k_{16} = 5\times10^8$

Table A.3. Representative Organics Kinetic Data[85]

Name	$k_{SO_4^-\cdot/R}$($M^{-1}S^{-1}$)	$k_{HO\cdot/R}$($M^{-1}S^{-1}$)	$k_{Cl\cdot/R}$($M^{-1}S^{-1}$)
UV/PS case 1. Organic compound only reacts with $SO_4^-\cdot$			
PFOA	2.59×10^5	N/A	N/A

PFHpA	2.68×10^{5}	N/A	N/A
PFHeA	7.02×10^{5}	N/A	N/A
PFPeA	1.26×10^{6}	N/A	N/A
PFPBA	1.05×10^{7}	N/A	N/A
PFPrA	9.31×10^{7}	N/A	N/A
UV/PS Case 2. Organic compound reacts with $SO_4^{\cdot-}$, HO· and Cl· UV/H_2O_2. Organic compound reacts with HO· and Cl·			
Chlorobenzene	1.5×10^{9}	5.6×10^{9}	4×10^{5}
1,2-Dichlorobenzene	6×10^{8}	2.5×10^{9}	4×10^{5}
Methane	1×10^{6}	1.2×10^{8}	5×10^{5}
Fluorobenzene	9.8×10^{8}	5.7×10^{9}	8×10^{5}
Acetonitrile	5×10^{2}	2.2×10^{7}	2.8×10^{6}
Toluene	3.1×10^{9}	5.1×10^{9}	1.5×10^{7}
2-Methyl-2-Propanol	8.4×10^{5}	6×10^{8}	3×10^{8}
1-Propanol	5.9×10^{7}	2.8×10^{9}	4×10^{8}
1-Octanol	3.2×10^{8}	7.7×10^{9}	5×10^{8}
1-Butanol	8.1×10^{7}	4.2×10^{9}	5×10^{8}
Ethanol	5.6×10^{7}	1.9×10^{9}	1×10^{9}
Acetic Acid	1.4×10^{4}	1.2×10^{10}	4.1×10^{9}
Methanol	8.8×10^{6}	9.7×10^{8}	5.7×10^{9}
2-Methyl-1-Propanol	1.3×10^{8}	3.3×10^{9}	5.8×10^{9}
2-Propanol	4.7×10^{6}	1.9×10^{9}	6×10^{9}
Methyl Acrylate	5.7×10^{7}	5.3×10^{9}	6.7×10^{9}
Acrylonitrile	8.1×10^{7}	5.3×10^{9}	6.9×10^{9}
Dimethyl Sulfoxide	2.7×10^{9}	6.5×10^{9}	7×10^{9}
1-Pentanol	1.3×10^{8}	3.7×10^{9}	7.9×10^{9}
Cyclohexene	1.7×10^{9}	8.8×10^{9}	9.9×10^{9}
Benzene	3×10^{9}	7.9×10^{9}	1.3×10^{10}
Pyridine	2.2×10^{8}	3×10^{9}	1.5×10^{10}

Table A.4. Fraction of $SO_4^-\cdot$ reacting with the target organic compound when NOM and Cl^- are present for UV/PS (Organic compounds only react with $SO_4^-\cdot$)

Organic Compound	Fraction of $SO_4^-\cdot$ reacting with organic compound				
	NOM and Cl^- are not present	NOM is present	NOM and Cl^- are present		
			[Cl]/[R]=10	[Cl]/[R]=100	[Cl]/[R]=1000
PFOA	99.999%	0.0289%	0.00265%	0.000289%	0.0000292%
PFHpA	99.999%	0.0299%	0.00274%	0.000299%	0.0000302%
PFHeA	99.999%	0.0781%	0.00719%	0.000784%	0.0000791%
PFPeA	99.999%	0.140%	0.0129%	0.00141%	0.000142%
PFPBA	99.999%	1.14%	0.107%	0.0117%	0.00118%
PFPrA	99.999%	8.68%	0.936%	0.104%	0.0105%

Table A.5. Fraction of $SO_4^-\cdot$ reacting with the target organic compound when HCO_3^-/CO_3^{2-} and Cl^- are present for UV/PS (Organic compounds only react with $SO_4^-\cdot$)

Organic Compound	Fraction of $SO_4^-\cdot$ reacting with organic compound				
	HCO_3^-/CO_3^{2-} /Cl^- are not present	HCO_3^-/CO_3^{2-} is present	HCO_3^-/CO_3^{2-} /Cl^- are present		
			[Cl]/[R]= 10	[Cl]/[R]= 100	[Cl]/[R]= 1000
PFOA	99.999%	0.232%	0.00538 %	0.000549 %	0.0000551%
PFHpA	99.999%	0.240%	0.00557 %	0.000569 %	0.0000569%
PFHeA	99.999%	0.627%	0.0146%	0.00149%	0.000148%
PFPeA	99.999%	1.121%	0.0262	0.00267%	0.000267%
PFPBA	99.999%	8.629%	0.218%	0.0222%	0.00222%
PFPrA	99.999%	45.574%	1.89%	0.196%	0.0197%

Table A.6. Fraction of $SO_4^-\cdot$ reacting with the target organic compound when Cl^- is present for UV/PS (Organic compounds that can react with $SO_4^-\cdot$, HO·, and Cl·)

Organic Compound	Fraction of $SO_4^-\cdot$ reacting with organic compound			
	Cl^- is not present	Cl^- is present		
		$[Cl^-]/[R]=10$	$[Cl^-]/[R]=100$	$[Cl^-]/[R]=1000$
Chlorobenzene	99.012%	24.147%	3.092%	0.318%
1,2-Dichlorobenzene	97.995%	11.296%	1.260%	0.127%
Methane	37.710%	0.0213%	0.00213%	0.000213%
Fluorobenzene	98.491%	17.209%	2.042%	0.208%
Acetonitrile	0.153%	0.0000106 %	0.00000106%	0.000000106%
Toluene	99.528%	39.671%	6.186%	0.655%
2-Methyl-2-Propanol	12.180%	0.0178%	0.00179%	0.000178%
1-Propanol	82.265%	1.236%	0.125%	0.0126%

1-Octanol	95.317%	6.355%	0.676%	0.0680%
1-Butanol	85.145%	1.689%	0.172%	0.0172%
Ethanol	83.412%	1.175%	0.119%	0.0119%
Acetic Acid	0.0847%	0.000297%	0.0000297%	0.00000298%
Methanol	52.003%	0.187%	0.0187%	0.00187%
2-Methyl-1-Propanol	90.703%	2.684%	0.276%	0.0276%
2-Propanol	29.678%	0.0997%	0.0100%	0.00100%
Methyl Acrylate	79.370%	1.195%	0.121%	0.0121%
Acrylonitrile	84.537%	1.689%	0.172%	0.0172%
Dimethyl Sulfoxide	99.435%	36.412%	5.431%	0.571%
1-Pentanol	90.454%	2.684%	0.276%	0.0276%
Cyclohexene	99.068%	26.497%	3.489%	0.360%
Benzene	99.477%	38.882%	5.998%	0.634%
Pyridine	94.429%	4.460%	0.466%	0.0467%

Table A.7. Fraction of HO· reacting with the target organic compound when Cl^- is present for UV/PS. (Organic compounds can react with SO_4^-·, HO·, and Cl·)

Organic Compound	Fraction of HO· reacting with organic compound			
	Cl^- is not present	Cl^- is present		
		$[Cl^-]/[R]=10$	$[Cl^-]/[R]=100$	$[Cl^-]/[R]=1000$
Chlorobenzene	82.353%	22.334%	5.039%	1.292%
1,2-Dichlorobenzene	67.568%	8.665%	1.703%	0.429%
Methane	9.091%	0.00571%	0.00101%	0.000251%
Fluorobenzene	82.609%	16.058%	3.356%	0.852%
Acetonitrile	1.800%	0.000140%	0.0000246%	0.00000613%
Toluene	80.952%	35.896%	9.859%	2.603%
2-Methyl-2-Propanol	33.333%	0.0543%	0.00955%	0.00238%
1-Propanol	70.000%	1.169%	0.208%	0.0519%
1-Octanol	86.517%	6.41%	1.194%	0.300%
1-Butanol	77.778%	1.713%	0.306%	0.0765%
Ethanol	61.290%	0.957%	0.169%	0.0424%
Acetic Acid	90.909%	0.350%	0.0594%	0.0151%
Methanol	44.700%	0.175%	0.0294%	0.00748%
2-Methyl-1-Propanol	73.333%	2.375%	0.406%	0.104%
2-Propanol	61.290%	0.225%	0.0376%	0.00957%
Methyl Acrylate	81.538%	1.340%	0.225%	0.0574%
Acrylonitrile	81.538%	1.778%	0.299%	0.0764%
Dimethyl Sulfoxide	84.416%	33.730%	8.299%	2.228%

1-Pentanol	75.510%	2.440%	0.411%	0.105%
Cyclohexene	88.000%	25.526%	5.419%	1.436%
Benzene	86.813%	36.593%	8.899%	2.423%
Pyridine	71.429%	3.626%	0.589%	0.153%

Table A.8. Fraction of Cl· reacting with the target organic compound when Cl^- is present for UV/PS (Organic compounds can react with SO_4^-·, HO·, and Cl·)

Organic Compound	Fraction of Cl· reacting with organic compound			
	Cl^- is not present	Cl^- is present		
		$[Cl^-]/[R]=10$	[Cl]/[R]=100	[Cl]/[R]=1000
Chlorobenzene	0.000%	0.00134%	0.00114%	0.000462%
1,2-Dichlorobenzene	0.000%	0.00134%	0.00114%	0.000462%
Methane	0.000%	0.00167%	0.00143%	0.000578%
Fluorobenzene	0.000%	0.00268%	0.00228%	0.000924%
Acetonitrile	0.000%	0.00937%	0.00799%	0.00323%
Toluene	0.000%	0.0502%	0.0428%	0.0173%
2-Methyl-2-Propanol	0.000%	0.994%	0.849%	0.345%
1-Propanol	0.000%	1.321%	1.129%	0.459%
1-Octanol	0.000%	1.645%	1.407%	0.574%
1-Butanol	0.000%	1.645%	1.407%	0.574%
Ethanol	0.000%	3.238%	2.775%	1.142%
Acetic Acid	0.000%	12.064%	10.476%	4.522%
Methanol	0.000%	16.018%	13.992%	6.178%
2-Methyl-1-Propanol	0.000%	16.253%	14.202%	6.279%
2-Propanol	0.000%	16.719%	14.621%	6.482%
Methyl Acrylate	0.000%	18.313%	16.053%	7.184%
Acrylonitrile	0.000%	18.757%	16.453%	7.383%
Dimethyl Sulfoxide	0.000%	18.978%	16.652%	7.482%
1-Pentanol	0.000%	20.907%	18.399%	8.363%
Cyclohexene	0.000%	24.883%	22.030%	10.263%
Benzene	0.000%	30.313%	27.062%	13.057%
Pyridine	0.000%	33.418%	29.977%	14.769%

Table A.9. The ratio of organic destruction rate when Cl^- is present to the rate when Cl^- is not present for UV/PS (Organic compounds can react with SO_4^-·, HO·, and Cl·)

Organic Compound	The ratio of organic destruction rate when Cl^- is present to the rate when Cl^- is not present		
	$[Cl^-]/[R]=10$	$[Cl^-]/[R]=100$	$[Cl^-]/[R]=1000$
Chlorobenzene	24.405%	3.154%	0.334%
1,2Dichloro-benzene	11.554%	1.312%	0.141%
Methane	0.0620%	0.0104%	0.00251%
Fluorobenzene	17.504%	2.105%	0.224%

Acetonitrile	0.0171%	0.00936%	0.00358%
Toluene	39.910%	6.284%	0.687%
2-Methyl-2-Propanol	1.153%	0.876%	0.352%
1-Propanol	2.834%	1.305%	0.486%
1-Octanol	8.238%	2.137%	0.658%
1-Butanol	3.629%	1.613%	0.606%
Ethanol	4.627%	2.936%	1.165%
Acetic Acid	12.407%	10.538%	4.539%
Methanol	16.338%	14.039%	6.188%
2-Methyl-1-Propanol	18.759%	14.489%	6.319%
2-Propanol	17.024%	14.671%	6.494%
Methyl Acrylate	19.572%	16.207%	7.209%
Acrylonitrile	20.410%	16.649%	7.413%
Dimethyl Sulfoxide	48.667%	21.229%	8.025%
1-Pentanol	23.281%	18.671%	8.402%
Cyclohexene	44.996%	24.802%	10.602%
Benzene	57.568%	31.483%	13.623%
Pyridine	36.586%	30.343%	14.821%

Table A.10. Fraction of $SO_4^{-}\cdot$ reacting with the target organic compound when NOM and Cl^- are present for UV/PS (Organic compounds can react with $SO_4^{-}\cdot$, HO·, and Cl·)

Organic Compound	Fraction of $SO_4^{-}\cdot$ reacting with organic compound				
	NOM and Cl^- are not present	NOM is present	NOM and Cl^- are present		
			$[Cl^-]/[R]=10$	$[Cl^-]/[R]=100$	$[Cl^-]/[R]=1000$
Chlorobenzene	99.012%	40.044%	11.870%	1.620%	0.168%
1,2-Dichlorobenzene	97.995%	29.361%	5.489%	0.660%	0.0674%
Methane	37.710%	0.111%	0.0102%	0.00111%	0.000112%
Fluorobenzene	98.491%	35.446%	8.409%	1.070%	0.110%
Acetonitrile	0.153%	0.0000557 %	0.00000511 %	0.000000557%	0.0000000562%
Toluene	99.528%	45.827%	19.794%	3.242%	0.346%
2-Methyl-2-Propanol	12.180%	0.0928%	0.00858%	0.000936%	0.0000944%
1-Propanol	82.265%	5.766%	0.595%	0.0657%	0.00663%
1-Octanol	95.317%	21.045%	3.075%	0.354%	0.0359%
1-Butanol	85.145%	7.591%	0.814%	0.0901%	0.00911%
Ethanol	83.412%	5.515%	0.566%	0.0623%	0.00630%
Acetic Acid	0.0847%	0.0052%	0.000142%	0.0000156%	0.00000157%
Methanol	52.003%	0.954%	0.0897%	0.00980%	0.000989%
2-Methyl-1-Propanol	90.703%	11.224%	1.294%	0.144%	0.0146%
2-Propanol	29.678%	0.512%	0.0479%	0.00524%	0.000528%
Methyl Acrylate	79.370%	5.573%	0.575%	0.0634%	0.00641%
Acrylonitrile	84.537%	7.584%	0.814%	0.0901%	0.00911%

Dimethyl Sulfoxide	99.435%	44.919%	18.113%	2.846%	0.302%
1-Pentanol	90.454%	11.218%	1.294%	0.144%	0.0146%
Cyclohexene	99.068%	41.212%	13.059%	1.828%	0.190%
Benzene	99.477%	45.609%	19.387%	3.143%	0.335%
Pyridine	94.429%	16.572%	2.154%	0.244%	0.0247%

Table A.11. Fraction of HO· reacting with the target organic compound when NOM and Cl^- are present for UV/PS (Organic compounds can react with SO_4^-·, HO·, and Cl·)

Organic Compound	Fraction of HO· reacting with organic compound				
	NOM and Cl^- are not present	NOM is present	NOM and Cl^- are present		
			$[Cl^-]/[R]=10$	$[Cl^-]/[R]=100$	$[Cl^-]/[R]=1000$
Chlorobenzene	82.353%	33.306%	10.212%	2.358%	0.506%
1,2-Dichlorobenzene	67.568%	20.245%	3.702%	0.753%	0.159%
Methane	9.091%	0.0268%	0.00198%	0.000366%	0.0000764%
Fluorobenzene	82.609%	29.730%	7.303%	1.572%	0.334%
Acetonitrile	1.800%	0.000657%	0.0000475%	0.00000876%	0.00000183%
Toluene	80.952%	37.274%	16.564%	4.590%	1.014%
2-Methyl-2-Propanol	33.333%	0.254%	0.0204%	0.00377%	0.000786%
1-Propanol	70.000%	4.906%	0.500%	0.0933%	0.0195%
1-Octanol	86.517%	19.102%	2.934%	0.572%	0.120%
1-Butanol	77.778%	6.935%	0.756%	0.141%	0.0296%
Ethanol	61.290%	4.052%	0.397%	0.0741%	0.0155%
Acetic Acid	90.909%	1.637%	0.164%	0.0303%	0.00633%
Methanol	44.700%	0.820%	0.0696%	0.0129%	0.00269%
2-Methyl-1-Propanol	73.333%	9.075%	1.046%	0.197%	0.0413%
2-Propanol	61.290%	1.057%	0.0947%	0.0175%	0.00365%
Methyl Acrylate	81.538%	5.725%	0.609%	0.114%	0.0238%
Acrylonitrile	81.538%	7.315%	0.809%	0.152%	0.0317%
Dimethyl Sulfoxide	84.416%	38.134%	16.035%	4.263%	0.935%
1-Pentanol	75.510%	9.365%	1.089%	0.206%	0.0430%
Cyclohexene	88.000%	36.608%	12.269%	2.906%	0.626%
Benzene	86.813%	39.803%	17.810%	4.886%	1.078%
Pyridine	71.429%	12.536%	1.617%	0.310%	0.0650%

Table A.12. Fraction of Cl· reacting with the target organic compound when NOM and Cl^- are present for UV/PS (Organic compounds that can react with SO_4^-·, HO·, and Cl·)

Organic Compound	Fraction of Cl· reacting with organic compound			
	NOM and Cl^- are not present	NOM and Cl^- is present		
		$[Cl^-]/[R]=10$	$[Cl^-]/[R]=100$	$[Cl^-]/[R]=1000$
Chlorobenzene	0.000%	0.00698%	0.000555%	0.000182%

1,2-Dichlorobenzene	0.000%	0.00698%	0.000555%	0.000182%
Methane	0.000%	0.000872%	0.000694%	0.000228%
Fluorobenzene	0.000%	0.00139%	0.00111%	0.000364%
Acetonitrile	0.000%	0.00489%	0.00389%	0.00128%
Toluene	0.000%	0.0261%	0.0208%	0.00683%
2-Methyl-2-Propanol	0.000%	0.518%	0.413%	0.136%
1-Propanol	0.000%	0.689%	0.549%	0.181%
1-Octanol	0.000%	0.858%	0.685%	0.227%
1-Butanol	0.000%	0.858%	0.685%	0.227%
Ethanol	0.000%	1.689%	1.352%	0.451%
Acetic Acid	0.000%	6.301%	5.136%	1.803%
Methanol	0.000%	8.372%	6.881%	2.474%
2-Methyl-1-Propanol	0.000%	8.495%	6.985%	2.515%
2-Propanol	0.000%	8.740%	7.194%	2.598%
Methyl Acrylate	0.000%	9.575%	7.908%	2.884%
Acrylonitrile	0.000%	9.808%	8.108%	2.966%
Dimethyl Sulfoxide	0.000%	9.924%	8.207%	3.006%
1-Pentanol	0.000%	10.937%	9.081%	3.368%
Cyclohexene	0.000%	13.025%	10.907%	4.154%
Benzene	0.000%	15.881%	13.455%	5.324%
Pyridine	0.000%	17.517%	14.942%	6.049%

Table A.13. The ratio of organic destruction rate when NOM and Cl^- are present to the rate when NOM and Cl^- are not present for UV/PS (Organic compounds can react with $SO_4^{\cdot-}$, HO·, and Cl·)

Organic Compound	The ratio of organic destruction rate when NOM is present to the rate when NOM is not present	The ratio of organic destruction rate when NOM and Cl^- are present to the rate when NOM and Cl^- are not present		
		$[Cl^-]/[R]=10$	$[Cl^-]/[R]=100$	$[Cl^-]/[R]=1000$
Chlorobenzene	40.415%	12.015%	1.652%	0.175%
1,2Dichloro-benzene	29.891%	5.610%	0.684%	0.0724%
Methane	0.244%	0.0247%	0.00433%	0.000866%
Fluorobenzene	35.952%	8.559%	1.101%	0.117%
Acetonitrile	0.0259%	0.00711%	0.00435%	0.00138%
Toluene	46.028%	19.942%	3.294%	0.359%
2-Methyl-2-Propanol	0.617%	0.536%	0.0422%	0.0138%
1-Propanol	6.870%	1.345%	0.0635%	0.0193%
1-Octanol	22.023%	3.976%	1.062%	0.0269%

1-Butanol	8.803%	1.731%	0.797%	0.0242%
Ethanol	6.460%	2.199%	1.426%	0.0462%
Acetic Acid	1.735%	5.922%	5.140%	1.811%
Methanol	1.670%	7.790%	6.865%	2.479%
2-Methyl-1-Propanol	12.259%	8.984%	7.096%	2.536%
2-Propanol	1.556%	8.119%	7.178%	2.604%
Methyl Acrylate	6.917%	9.360%	7.943%	2.898%
Acrylonitrile	8.871%	9.768%	8.164%	2.982%
Dimethyl Sulfoxide	45.159%	24.199%	10.598%	3.299%
1-Pentanol	12.293%	11.156%	9.172%	3.389%
Cyclohexene	41.581%	22.145%	12.326%	4.338%
Benzene	45.836%	28.688%	15.751%	5.635%
Pyridine	17.446%	17.584%	15.043%	6.079%

Table A.14. Fraction of $SO_4^-\cdot$ reacting with organic compound when $HCO_3^-/CO_3^{2-}/Cl^-$ are present for UV/PS (Organic compounds can react with $SO_4^-\cdot$, HO·, and Cl·)

Organic Compound	Fraction of $SO_4^-\cdot$ reacting with organic compound				
	$HCO_3^-/CO_3^{2-}/Cl^-$ are not present	HCO_3^-/CO_3^{2-} is present	HCO_3^-/CO_3^{2-} and Cl^- are present		
			$[Cl^-]/[R]=10$	$[Cl^-]/[R]=100$	$[Cl^-]/[R]=1000$
Chlorobenzene	99.012%	92.416%	23.723%	3.085%	0.318%
1,2-Dichlorobenzene	97.995%	83.255%	11.069%	1.257%	0.127%
Methane	37.710%	0.882%	0.0208%	0.00212%	0.000213%
Fluorobenzene	98.491%	88.838%	16.888%	2.037%	0.208%
Acetonitrile	0.153%	0.000449%	0.0000104%	0.00000106 %	0.000000106%
Toluene	99.528%	96.188%	39.128%	6.172%	0.655%
2-Methyl-2-Propanol	12.180%	0.721%	0.0174%	0.00178%	0.000179%
1-Propanol	82.265%	32.767%	1.209%	0.125%	0.0125%
1-Octanol	95.317%	72.105%	6.221%	0.674%	0.0680%
1-Butanol	85.145%	39.837%	1.652%	0.172%	0.0172%
Ethanol	83.412%	31.874%	1.149%	0.119%	0.0119%
Acetic Acid	0.0847%	0.0112%	0.000290%	0.0000297%	0.00000298%
Methanol	52.003%	6.984%	0.182%	0.0186%	0.00187%
2-Methyl-1-Propanol	90.703%	51.670%	2.625%	0.275%	0.0276%
2-Propanol	29.678%	3.778%	0.0974%	0.00997%	0.000999%
Methyl Acrylate	79.370%	31.675%	1.168%	0.121%	0.0121%
Acrylonitrile	84.537%	39.715%	1.652%	0.172%	0.0172%
Dimethyl Sulfoxide	99.435%	95.628%	35.888%	5.419%	0.571%
1-Pentanol	90.454%	51.597%	2.625%	0.275%	0.0276%
Cyclohexene	99.068%	93.199%	26.058%	3.482%	0.360%
Benzene	99.477%	96.035%	38.345%	5.985%	0.634%
Pyridine	94.429%	64.461%	4.364%	0.465%	0.0467%

Table A.15. Fraction of HO· reacting with organic compound when $HCO_3^-/CO_3^{2-}/Cl^-$ are present for UV/PS. Organic compounds can react with $SO_4^-\cdot$, HO·, and Cl·.

Organic Compound	Fraction of HO· reacting with organic compound				
	$HCO_3^-/CO_3^{2-}/Cl^-$ are not present	HCO_3^-/CO_3^{2-} is present	HCO_3^-/CO_3^{2-} and Cl^- are present		
			$[Cl^-]/[R]=10$	$[Cl^-]/[R]=100$	$[Cl^-]/[R]=1000$
Chlorobenzene	82.353%	76.867%	19.633%	2.591%	0.268%
1,2-Dichlorobenzene	67.568%	57.405%	7.366%	0.849%	0.0863%
Methane	9.091%	0.213%	0.00432%	0.000448%	0.0000450%
Fluorobenzene	82.609%	74.512%	14.101%	1.727%	0.177%
Acetonitrile	1.800%	0.005529%	0.000104%	0.0000108%	0.0000011%
Toluene	80.952%	78.236%	31.574%	5.056%	0.538%
2-Methyl-2-Propanol	33.333%	1.974%	0.0431%	0.00447%	0.000449%
1-Propanol	70.000%	27.881%	0.998%	0.105%	0.0105%
1-Octanol	86.517%	65.447%	5.667%	0.624%	0.0630%
1-Butanol	77.778%	36.390%	1.487%	0.157%	0.0158%
Ethanol	61.290%	23.421%	0.804%	0.0844%	0.00848%
Acetic Acid	90.909%	12.065%	0.315%	0.0328%	0.00329%
Methanol	44.700%	6.003%	0.144%	0.0150%	0.00151%
2-Methyl-1-Propanol	73.333%	41.775%	2.0695%	0.220%	0.0222%
2-Propanol	61.290%	7.803%	0.191%	0.0199%	0.00200%
Methyl Acrylate	81.538%	32.540%	1.190%	0.125%	0.0126%
Acrylonitrile	81.538%	38.306%	1.579%	0.1668%	0.0168%
Dimethyl Sulfoxide	84.416%	81.184%	30.384%	4.664%	0.493%
1-Pentanol	75.510%	43.073%	2.145%	0.229%	0.0230%
Cyclohexene	88.000%	82.787%	23.240%	3.159%	0.328%
Benzene	86.813%	83.810%	33.488%	5.320%	0.565%
Pyridine	71.429%	48.760%	3.198%	0.347%	0.0350%

Table A.16. Fraction of Cl· reacting with organic compound when $HCO_3^-/CO_3^{2-}/Cl^-$ are present for UV/PS (Organic compounds can react with SO_4^-·, HO·, and Cl·)

Organic Compound	Fraction of Cl· reacting with organic compound			
	$HCO_3^-/CO_3^{2-}/Cl^-$ are not present	HCO_3^-/CO_3^{2-} and Cl^- are present		
		$[Cl^-]/[R]=10$	$[Cl^-]/[R]=100$	$[Cl^-]/[R]=1000$
Chlorobenzene	0.000%	0.000394%	0.0000578%	0.00000607%
1,2-Dichlorobenzene	0.000%	0.000394%	0.0000578%	0.00000607%
Methane	0.000%	0.000493%	0.0000732%	0.00000759%
Fluorobenzene	0.000%	0.000788%	0.000116%	0.0000121%
Acetonitrile	0.000%	0.00276%	0.000405%	0.0000425%
Toluene	0.000%	0.0148%	0.00217%	0.000227%
2-Methyl-2-Propanol	0.000%	0.295%	0.0434%	0.00455%
1-Propanol	0.000%	0.393%	0.0578%	0.00607%
1-Octanol	0.000%	0.490%	0.0723%	0.00759%
1-Butanol	0.000%	0.490%	0.0723%	0.00759%
Ethanol	0.000%	0.976%	0.144%	0.0152%
Acetic Acid	0.000%	3.884%	0.590%	0.0622%
Methanol	0.000%	5.319%	0.818%	0.0864%
2-Methyl-1-Propanol	0.000%	5.407%	0.832%	0.0879%
2-Propanol	0.000%	5.583%	0.860%	0.0910%

Methyl Acrylate	0.000%	6.194%	0.960%	0.102%
Acrylonitrile	0.000%	6.368%	0.988%	0.105%
Dimethyl Sulfoxide	0.000%	6.454%	1.002%	0.106%
1-Pentanol	0.000%	7.224%	1.130%	0.120%
Cyclohexene	0.000%	8.890%	1.412%	0.150%
Benzene	0.000%	11.357%	1.846%	0.197%
Pyridine	0.000%	12.880%	2.123%	0.227%

Table A.17. The ratio of organic destruction rate when HCO_3^-/ CO_3^{2-} and Cl^- are present to the rate when HCO_3^-/ CO_3^{2-} and Cl^- are not present for UV/PS. Organic compounds can react with SO_4^-·, HO·, and Cl·.

Organic Compound	The ratio of organic destruction rate when HCO_3^-/ CO_3^{2-} is present to the rate when HCO_3^-/ CO_3^{2-} is not present	The ratio of organic destruction rate when HCO_3^-/ CO_3^{2-} and Cl^- are present to the rate when HCO_3^-/ CO_3^{2-} and Cl^- are not present		
		[Cl^-]/[R]=10	[Cl^-]/[R]=100	[Cl^-]/[R]=1000
Chlorobenzene	93.304%	23.959%	3.116%	0.321%
1,2Dichloro-benzene	84.847%	11.288%	1.283%	0.130%
Methane	2.099%	0.0509%	0.00527%	0.000529%
Fluorobenzene	90.149%	17.150%	2.069%	0.211%
Acetonitrile	0.242%	0.00850%	0.00101%	0.000103%
Toluene	96.626%	39.321%	6.204%	0.658%
2-Methyl-2-Propanol	5.265%	0.411%	0.0550%	0.00571%
1-Propanol	39.398%	1.826%	0.206%	0.0209%
1-Octanol	75.546%	6.957%	0.775%	0.0785%
1-Butanol	46.468%	2.386%	0.269%	0.0273%
Ethanol	37.721%	2.230%	0.267%	0.0274%
Acetic Acid	13.014%	3.147%	0.407%	0.0419%
Methanol	12.738%	3.839%	0.485%	0.0498%
2-Methyl-1-Propanol	56.676%	6.338%	0.756%	0.0772%
2-Propanol	12.037%	3.935%	0.496%	0.0509%
Methyl Acrylate	39.590%	5.297%	0.642%	0.0656%
Acrylonitrile	46.699%	5.827%	0.699%	0.0714%
Dimethyl Sulfoxide	96.153%	38.639%	5.924%	0.625%
1-Pentanol	56.768%	7.048%	0.837%	0.0850%
Cyclohexene	94.053%	29.858%	4.081%	0.423%
Benzene	96.526%	41.917%	6.628%	0.703%
Pyridine	68.042%	10.171%	1.170%	0.119%

Table A.18. Fraction of HO· reacting with organic compound when Cl^- is present for UV/H_2O_2

Organic Compound	Fraction of HO· reacting with organic compound	
		Cl^- is present

	Cl^- is not present	$[Cl^-]/[R]=10$	$[Cl^-]/[R]=100$	$[Cl^-]/[R]=1000$
Acetonitrile	0.808%	0.808%	0.808%	0.804%
Methane	4.26%	4.255%	4.253%	4.232%
2-Methyl-2-Propanol	18.2%	18.181%	18.174%	18.097%
Methanol	26.431%	26.429%	26.420%	26.319%
Ethanol	41.304%	41.303%	41.291%	41.166%
2-Propanol	41.304%	41.303%	41.291%	41.166%
1,2-Dichlorobenzene	48.077%	48.076%	48.063%	47.934%
1-Propanol	50.909%	50.908%	50.895%	50.766%
Pyridine	52.632%	52.630%	52.618%	52.489%
2-Methyl-1-Propanol	55.000%	54.999%	54.986%	54.858%
1-Pentanol	57.813%	57.811%	57.799%	57.673%
1-Butanol	60.870%	60.868%	60.856%	60.733%
Toluene	65.385%	65.383%	65.372%	65.255%
Methyl Acrylate	66.250%	66.249%	66.238%	66.122%
Acrylonitrile	66.250%	66.249%	66.238%	66.122%
Chlorobenzene	67.470%	67.469%	67.458%	67.344%
Fluorobenzene	67.857%	67.856%	67.845%	67.732%
Dimethyl Sulfoxide	70.652%	70.651%	70.641%	70.533%
1-Octanol	74.038%	74.037%	74.028%	73.928%
Benzene	74.528%	74.527%	74.518%	74.419%
Cyclohexene	76.522%	76.521%	76.512%	76.419%
Acetic Acid	81.633%	81.632%	81.624%	81.547%

Table A.19. Fraction of HO· reacting with organic compound when NOM or HCO_3^-/CO_3^{2-} is present for UV/H_2O_2

Organic Compound	Fraction of HO· reacting with organic compound		
	NOM or HCO_3^-/CO_3^{2-} is not present	NOM is present	HCO_3^-/CO_3^{2-} is present
Acetonitrile	0.808%	0.347%	0.738%
Methane	4.26%	1.838%	3.895%
2-Methyl-2-Propanol	18.2%	8.031%	16.852%
Methanol	26.431%	11.832%	24.679%
Ethanol	41.304%	18.950%	39.091%
2-Propanol	41.304%	18.950%	39.091%
1,2-Dichlorobenzene	48.077%	22.309%	45.784%
1-Propanol	50.909%	23.737%	48.607%
Pyridine	52.632%	24.612%	50.332%
2-Methyl-1-Propanol	55.000%	25.824%	52.712%
1-Pentanol	57.813%	27.275%	55.552%

1-Butanol	60.870%	28.869%	58.655%
Toluene	65.385%	31.254%	63.272%
Methyl Acrylate	66.250%	31.716%	64.161%
Acrylonitrile	66.250%	31.716%	64.161%
Chlorobenzene	67.470%	32.368%	65.417%
Fluorobenzene	67.857%	32.576%	65.816%
Dimethyl Sulfoxide	70.652%	34.085%	68.707%
1-Octanol	74.038%	35.932%	72.230%
Benzene	74.528%	36.201%	72.741%
Cyclohexene	76.522%	37.301%	74.827%
Acetic Acid	81.633%	40.156%	80.211%

APPENDIX B. ELEMENTARY REACTIONS FOR THE UV/FREE CHLORINE PROCESS

Table B.1. Elementary reactions for the UV/free chlorine process.[37,43,47]

No.	REACTIONS	RATE CONSTANTS, $M^{-1}\ S^{-1}$
UV/Chlorine		
1	$HOCl + hv \rightarrow HO\bullet + Cl\bullet$	$\phi_{HOCl} = 0.9 - 1.45$ $\varepsilon_{HOCl} = 59\ M^{-1}cm^{-1}$ $r_{uv,HOCl} = \phi_{HOCl} P_{UV} f_{HOCl} (1 - 10^{-A})$ $r_{uv,HOCl}$ is defined in Chapter 3.3.4
2	$OCl^- + hv \rightarrow O^-\bullet + Cl\bullet$	$\phi_{HOCl} = 0.8 - 0.97$ $\varepsilon_{HOCl} = 66\ M^{-1}cm^{-1}$ $r_{uv,OCl^-} = \phi_{OCl^-} P_{UV} f_{OCl^-} (1 - 10^{-A})$ r_{uv,OCl^-} is defined in Chapter 3.3.4
3	$OCl^- + H^+ \rightarrow HOCl$	$k_1 = 5 \times 10^{10}$
4	$HOCl \rightarrow OCl^- + H^+$	$k_2 = 1.6 \times 10^3$
5	$O^-\bullet + H_2O \rightarrow HO\bullet + OH^-$	$k_3 = 1.8 \times 10^6$
6	$HO\bullet + OH^- \rightarrow O^-\bullet + H_2O$	$k_4 = 1.3 \times 10^{10}$
7	$HO\bullet + HOCl \rightarrow ClO\bullet + H_2O$	$k_5 = 2 \times 10^9$
8	$HO\bullet + OCl^- \rightarrow ClO\bullet + OH^-$	$k_6 = 8.8 \times 10^{10}$
9	$HO\bullet + HO\bullet \rightarrow H_2O_2$	$k_7 = 5.5 \times 10^9$
10	$H_2O_2 \rightarrow H^+ + HO_2^-$	$k_8 = 1.3 \times 10^{-1}\ s^{-1}$
11	$H^+ + HO_2^- \rightarrow H_2O_2$	$k_9 = 5 \times 10^{10}$
12	$H_2O_2 + HO\bullet \rightarrow HO_2\bullet + H_2O$	$k_{10} = 2.7 \times 10^7$
13	$HO_2^- + HO\bullet \rightarrow HO_2\bullet + OH^-$	$k_{11} = 7.5 \times 10^9$
14	$HO_2\bullet \rightarrow H^+ + O_2^-\bullet$	$k_{12} = 7 \times 10^5\ s^{-1}$
15	$H^+ + O_2^-\bullet \rightarrow HO_2\bullet$	$k_{13} = 5 \times 10^{10}$
16	$HO\bullet + HO_2\bullet \rightarrow H_2O + O_2$	$k_{14} = 6.6 \times 10^9$
17	$HO\bullet + O_2^-\bullet \rightarrow OH^- + O_2$	$k_{15} = 1 \times 10^{10}$

18	$H_2O_2 + O_2^-\bullet \rightarrow OH^- + O_2 + HO\bullet$	$k_{16} = 1.3\times10^{-1}$
19	$H_2O_2 + HO_2\bullet \rightarrow H_2O + O_2 + HO\bullet$	$k_{17} = 3$
20	$HO_2\bullet + HO_2\bullet \rightarrow H_2O_2 + O_2$	$k_{18} = 8.3\times10^{5}$
21	$HO_2\bullet + O_2^-\bullet \rightarrow HO_2^- + O_2$	$k_{19} = 9.7\times10^{7}$
22	$Cl\bullet + H_2O \rightarrow ClOH^-\bullet + H^+$	$k_{20}[H_2O] = 1.3\times10^{3}\ s^{-1}$
23	$ClOH^-\bullet + H^+ \rightarrow Cl\bullet + H_2O$	$k_{21} = 2.1\times10^{10}$
24	$ClOH^-\bullet \rightarrow OH\bullet + Cl^-$	$k_{22} = 6.1\times10^{9}\ s^{-1}$
25	$OH\bullet + Cl^- \rightarrow ClOH^-\bullet$	$k_{23} = 4.3\times10^{9}$
26	$ClOH^-\bullet + Cl^- \rightarrow Cl_2^-\bullet + OH^-$	$k_{24} = 1\times10^{4}$
27	$Cl\bullet + Cl^- \rightarrow Cl_2^-\bullet$	$k_{25} = 8\times10^{9}$
28	$Cl_2^-\bullet \rightarrow Cl\bullet + Cl^-$	$k_{26} = 5.3\times10^{4}\ s^{-1}$
29	$Cl\bullet + Cl\bullet \rightarrow Cl_2$	$k_{27} = 8.8\times10^{7}$
30	$Cl_2 + OH^- \rightarrow HOCl + Cl^-$	$k_{28} = 1.0\times10^{9}$
31	$Cl_2^-\bullet + Cl_2^-\bullet \rightarrow Cl_2 + 2Cl^-$	$k_{29} = 6.41\times10^{9}$
32	$Cl\bullet + Cl_2^-\bullet \rightarrow Cl_2 + Cl^-$	$k_{30} = 2.1\times10^{9}$
33	$Cl_2^-\bullet + H_2O_2 \rightarrow H^+ + 2Cl^- + HO_2\bullet$	$k_{31} = 1.4\times10^{5}$
34	$Cl_2^-\bullet + HO_2\bullet \rightarrow H^+ + 2Cl^- + O_2$	$k_{32} = 3\times10^{9}$
35	$Cl_2^-\bullet + O_2^-\bullet \rightarrow 2Cl^- + O_2$	$k_{33} = 1\times10^{9}$
36	$Cl_2^-\bullet + H_2O \rightarrow Cl^- + HClOH$	$k_{34}[H_2O] = 1.3\times10^{3}\ s^{-1}$
37	$Cl_2^-\bullet + OH^- \rightarrow Cl^- + ClOH^-\bullet$	$k_{35} = 4.5\times10^{7}$
38	$HClOH \rightarrow ClOH\bullet^- + H^+$	$k_{36} = 1.0\times10^{2}\ s^{-1}$
39	$HClOH \rightarrow Cl\bullet + H_2O$	$k_{37} = 5.0\times10^{9}\ s^{-1}$
40	$HClOH + Cl^- \rightarrow Cl_2^-\bullet + H_2O$	$k_{38} = 1.0\times10^{8}$
41	$Cl\bullet + H_2O_2 \rightarrow H^+ + Cl^- + HO_2\bullet$	$k_{39} = 2.0\times10^{9}$
42	$Cl_2^-\bullet + HO\bullet \rightarrow HOCl + Cl^-$	$k_{40} = 1.0\times10^{9}$
43	$Cl_2 + H_2O \rightarrow HOCl + Cl^- + H^+$	$k_{41}[H_2O] = 15\ s^{-1}$
44	$Cl_2 + O_2^-\bullet \rightarrow O_2 + Cl_2^-\bullet$	$k_{42} = 1.0\times10^{9}$
45	$Cl_2 + HO_2\bullet \rightarrow H^+ + O_2 + Cl_2^-\bullet$	$k_{43} = 1.0\times10^{9}$
46	$HOCl + O_2^-\bullet \rightarrow OH^- + O_2 + Cl\bullet$	$k_{44} = 7.5\times10^{6}$
47	$HOCl + HO_2\bullet \rightarrow H_2O + O_2 + Cl\bullet$	$k_{45} = 7.5\times10^{6}$
48	$Cl\bullet + HOCl \rightarrow H^+ + Cl^- + ClO\bullet$	$k_{46} = 3.0\times10^{9}$

49	$Cl\bullet + OCl^- \rightarrow Cl^- + ClO\bullet$	$k_{47} = 8.2\times10^9$
50	$Cl\bullet + OH^- \rightarrow ClOH\bullet^-$	$k_{48} = 1.8\times10^{10}$
51	$ClO\bullet + ClO\bullet \rightarrow Cl_2O_2$	$k_{49} = 2.5\times10^9$
52	$Cl_2O_2 + H_2O \rightarrow HOCl + H^+ + ClO_2^-$	$k_{50}[H_2O] = 2.5\times10^9\ s^{-1}$
53	$Cl_2O_2 + OH^- \rightarrow OCl^- + H^+ + ClO_2^-$	$k_{51} = 2.5\times10^9$
54	$ClO\bullet + HO\bullet \rightarrow ClO_2^- + H^+$	$k_{52} = 1.0\times10^9$
55	$ClO_2^- + HO\bullet \rightarrow ClO_2\bullet + OH^-$	$k_{53} = 6.3\times10^9$
56	$ClO_2\bullet + HO\bullet \rightarrow ClO_3^- + H^+$	$k_{54} = 4.0\times10^9$
57	$ClO_2^- + Cl_2^-\bullet \rightarrow ClO_2\bullet + 2Cl^-$	$k_{55} = 1.3\times10^8$
58	$ClO_2^- + ClO\bullet \rightarrow ClO_2\bullet + OCl^-$	$k_{56} = 9.4\times10^8$
Destruction of Target Organic Compound (R)		
59	$R + OH\bullet \rightarrow \text{byproducts}$	$k_{HO\bullet/R}$
60	$R + Cl\bullet \rightarrow \text{byproducts}$	$k_{Cl\bullet/R}$
61	$R + Cl_2^-\bullet \rightarrow \text{byproducts}$	$k_{Cl_2^-\bullet/R}$
62	$R + ClO\bullet \rightarrow \text{byproducts}$	$k_{ClO\bullet/R}$
63	If target organic compound can be destructed by UV alone: $R + h\nu \rightarrow \text{byproducts}$	$r_{UV,R} = \phi_R P_{UV} f_R (1-10^{-A})$ $f_R = \dfrac{\varepsilon_R C_R}{\varepsilon_{HOCl} C_{HOCl} + \varepsilon_{OCl^-} C_{OCl^-} + \sum_i \varepsilon_i C_i}$ A is defined in Chapter 3.3.4
64	If target organic compound can be oxidized by free chlorine alone: $R + HOCl / OCl^- \rightarrow \text{byproducts}$	$k_{HOCl/R}$ $k_{ClO^-/R}$
If NOM is present in water matrix		
65	$NOM + OH\bullet \rightarrow \text{byproducts}$	$k_{HO\bullet/NOM}$
66	$NOM + Cl\bullet \rightarrow \text{byproducts}$	$k_{Cl\bullet/NOM}$
67	$NOM + Cl_2^-\bullet \rightarrow \text{byproducts}$	$k_{Cl_2^-\bullet/NOM}$
68	$NOM + ClO\bullet \rightarrow \text{byproducts}$	$k_{ClO\bullet/NOM}$
69	$NOM + HOCl \rightarrow \text{byproducts}$	$k_{HOCl/NOM}$
70	$NOM + OCl^- \rightarrow \text{byproducts}$	$k_{HOCl/NOM}$
If Bicarbonate/Carbonate are present		
71	$HCO_3^- + OH\bullet \rightarrow CO_3^-\bullet + H_2O$	$k_{57} = 8.5\times10^6$
72	$CO_3^{2-} + OH\bullet \rightarrow CO_3^-\bullet + OH^-$	$k_{58} = 3.9\times10^9$
73	$HCO_3^- + Cl\bullet \rightarrow CO_3^-\bullet + H^+ + Cl^-$	$k_{59} = 2.2\times10^8$

74	$CO_3^{2-} + Cl\bullet \rightarrow CO_3^{-}\bullet + Cl^{-}$	$k_{60} = 5\times10^{8}$
75	$HCO_3^{-} + Cl_2^{-}\bullet \rightarrow CO_3^{-}\bullet + H^{+} + 2Cl^{-}$	$k_{61} = 8\times10^{7}$
76	$CO_3^{2-} + Cl_2^{-}\bullet \rightarrow CO_3^{-}\bullet + 2Cl^{-}$	$k_{62} = 1.6\times10^{8}$
77	$CO_3^{2-} + ClO\bullet \rightarrow CO_3^{-}\bullet + OCl^{-}$	$k_{63} = 6\times10^{2}$
78	$HOCl + CO_3^{-}\bullet \rightarrow OCl\bullet + CO_3^{2-} + H^{+}$	$k_{64} = 9.51\times10^{8}$ (Fitted)
79	$OCl^{-} + CO_3^{-}\bullet \rightarrow OCl\bullet + CO_3^{2-}$	$k_{65} = 5.7\times10^{5}$
80	$CO_3^{-}\bullet + R \rightarrow \text{byproduct}$	k_{66}
81	$HCO_3^{-} \rightarrow CO_3^{2-} + H^{+}$	$k_{67} = 2.5$
82	$CO_3^{2-} + H^{+} \rightarrow HCO_3^{-}$	$k_{68} = 5\times10^{10}$

B.1 Mass Balance for the UV/Free Chlorine Process

Based on the elementary reaction in **Table B.1**, eq B.1– eq B.40 express the mass balance equation for species involved in the oxidization of target organic compounds in the UV/free chlorine process (batch reactor).

(1) Mass balance for HOCl

$$\begin{aligned}\frac{d[HOCl]}{dt} &= -r_{uv,HOCl} + k_1[OCl^-][H^+] - k_2[HOCl] - k_5[HO\bullet][HOCl] \\ &+k_{28}[Cl_2][OH^-] + k_{40}[Cl_2^-\bullet][HO\bullet] + k_{41}[H_2O][Cl_2] - k_{44}[HOCl][O_2^-\bullet] \\ &-k_{45}[HOCl][HO_2\bullet] - k_{46}[HOCl][Cl\bullet] + k_{50}[H_2O][Cl_2O_2]\end{aligned} \tag{B.1}$$

(2) Mass balance for HO·

$$\begin{aligned}\frac{d[HO\bullet]}{dt} &= r_{uv,HOCl} + k_3[H_2O][O_2^-\bullet] - k_4[HO\bullet][OH^-] - k_5[HO\bullet][HOCl] \\ &-k_6[HO\bullet][OCl^-] - 2k_7[HO\bullet][HO\bullet] - k_{10}[HO\bullet][H_2O_2] - k_{11}[HO\bullet][HO_2^-] \\ &-k_{14}[HO\bullet][HO_2\bullet] - k_{15}[HO\bullet][O_2^-\bullet] + k_{16}[H_2O_2][O_2^-\bullet] + k_{17}[H_2O_2][HO_2\bullet] \\ &+k_{22}[ClOH^-\bullet] - k_{23}[HO\bullet][ClOH^-\bullet] - k_{40}[HO\bullet][Cl_2^-\bullet] - k_{52}[HO\bullet][Cl_2^-\bullet] \\ &-k_{53}[HO\bullet][ClO_2^-] - k_{54}[HO\bullet][ClO_2\bullet] - k_{HO\bullet/R}[HO\bullet][R]\end{aligned} \tag{B.2}$$

If NOM is present:

$$\frac{d[HO\bullet]}{dt} = r_{uv,HOCl} + k_3[H_2O][O_2^-\bullet] - k_4[HO\bullet][OH^-] - k_5[HO\bullet][HOCl]$$
$$-k_6[HO\bullet][OCl^-] - 2k_7[HO\bullet][HO\bullet] - k_{10}[HO\bullet][H_2O_2] - k_{11}[HO\bullet][HO_2^-]$$
$$-k_{14}[HO\bullet][HO_2\bullet] - k_{15}[HO\bullet][O_2^-\bullet] + k_{16}[H_2O_2][O_2^-\bullet] + k_{17}[H_2O_2][HO_2\bullet] \quad \text{(B.3)}$$
$$+k_{22}[ClOH^-\bullet] - k_{23}[HO\bullet][ClOH^-\bullet] - k_{40}[HO\bullet][Cl_2^-\bullet] - k_{52}[HO\bullet][Cl_2^-\bullet]$$
$$-k_{53}[HO\bullet][ClO_2^-] - k_{54}[HO\bullet][ClO_2\bullet] - k_{HO\bullet/R}[HO\bullet][R] - k_{HO\bullet/NOM}[HO\bullet][NOM]$$

If HCO_3^-/CO_3^{2-} are present:

$$\frac{d[HO\bullet]}{dt} = r_{uv,HOCl} + k_3[H_2O][O_2^-\bullet] - k_4[HO\bullet][OH^-] - k_5[HO\bullet][HOCl]$$
$$-k_6[HO\bullet][OCl^-] - 2k_7[HO\bullet][HO\bullet] - k_{10}[HO\bullet][H_2O_2] - k_{11}[HO\bullet][HO_2^-]$$
$$-k_{14}[HO\bullet][HO_2\bullet] - k_{15}[HO\bullet][O_2^-\bullet] + k_{16}[H_2O_2][O_2^-\bullet] + k_{17}[H_2O_2][HO_2\bullet] \quad \text{(B.4)}$$
$$+k_{22}[ClOH^-\bullet] - k_{23}[HO\bullet][ClOH^-\bullet] - k_{40}[HO\bullet][Cl_2^-\bullet] - k_{52}[HO\bullet][Cl_2^-\bullet]$$
$$-k_{53}[HO\bullet][ClO_2^-] - k_{54}[HO\bullet][ClO_2\bullet] - k_{HO\bullet/R}[HO\bullet][R] - k_{57}[HO\bullet][HCO_3^-]$$
$$-k_{58}[HO\bullet][CO_3^{2-}]$$

If NOM and HCO_3^-/CO_3^{2-} are present:

$$\frac{d[HO\bullet]}{dt} = r_{uv,HOCl} + k_3[H_2O][O_2^-\bullet] - k_4[HO\bullet][OH^-] - k_5[HO\bullet][HOCl]$$
$$-k_6[HO\bullet][OCl^-] - 2k_7[HO\bullet][HO\bullet] - k_{10}[HO\bullet][H_2O_2] - k_{11}[HO\bullet][HO_2^-]$$
$$-k_{14}[HO\bullet][HO_2\bullet] - k_{15}[HO\bullet][O_2^-\bullet] + k_{16}[H_2O_2][O_2^-\bullet] + k_{17}[H_2O_2][HO_2\bullet] \quad \text{(B.5)}$$
$$+k_{22}[ClOH^-\bullet] - k_{23}[HO\bullet][ClOH^-\bullet] - k_{40}[HO\bullet][Cl_2^-\bullet] - k_{52}[HO\bullet][Cl_2^-\bullet]$$
$$-k_{53}[HO\bullet][ClO_2^-] - k_{54}[HO\bullet][ClO_2\bullet] - k_{HO\bullet/R}[HO\bullet][R] - k_{HO\bullet/NOM}[HO\bullet][NOM]$$
$$-k_{57}[HO\bullet][HCO_3^-] - k_{58}[HO\bullet][CO_3^{2-}]$$

(3) Mass balance for Cl·

$$\frac{d[Cl\bullet]}{dt} = r_{uv,HOCl} + r_{uv,OCl^-} - k_{20}[H_2O][Cl\bullet] + k_{21}[ClOH^-\bullet][H^+] - k_{25}[Cl\bullet][Cl^-]$$
$$+k_{26}[Cl_2^-\bullet] - 2k_{27}[Cl\bullet][Cl\bullet] - k_{30}[Cl\bullet][Cl_2^-\bullet] + k_{37}[Cl_2^-\bullet] - k_{39}[Cl\bullet][H_2O_2] \quad \text{(B.6)}$$
$$+k_{44}[HOCl][O_2^-\bullet] + k_{45}[HOCl][HO_2\bullet] - k_{46}[Cl\bullet][HOCl] - k_{47}[Cl\bullet][OCl^-]$$
$$-k_{48}[Cl\bullet][OH^-] - k_{Cl\bullet/R}[Cl\bullet][R]$$

If NOM is present:

$$\frac{d[Cl\bullet]}{dt} = r_{uv,HOCl} + r_{uv,OCl^-} - k_{20}[H_2O][Cl\bullet] + k_{21}[ClOH^-\bullet][H^+] - k_{25}[Cl\bullet][Cl^-]$$
$$+k_{26}[Cl_2^-\bullet] - 2k_{27}[Cl\bullet][Cl\bullet] - k_{30}[Cl\bullet][Cl_2^-\bullet] + k_{37}[Cl_2^-\bullet] - k_{39}[Cl\bullet][H_2O_2] \quad \text{(B.7)}$$
$$+k_{44}[HOCl][O_2^-\bullet] + k_{45}[HOCl][HO_2\bullet] - k_{46}[Cl\bullet][HOCl] - k_{47}[Cl\bullet][OCl^-]$$
$$-k_{48}[Cl\bullet][OH^-] - k_{Cl\bullet/R}[Cl\bullet][R] - k_{Cl\bullet/NOM}[Cl\bullet][NOM]$$

If HCO_3^-/CO_3^{2-} are present

$$\frac{d[Cl\bullet]}{dt} = r_{uv,HOCl} + r_{uv,OCl^-} - k_{20}[H_2O][Cl\bullet] + k_{21}[ClOH^-\bullet][H^+] - k_{25}[Cl\bullet][Cl^-]$$
$$+k_{26}[Cl_2^-\bullet] - 2k_{27}[Cl\bullet][Cl\bullet] - k_{30}[Cl\bullet][Cl_2^-\bullet] + k_{37}[Cl_2^-\bullet] - k_{39}[Cl\bullet][H_2O_2] \quad \text{(B.8)}$$
$$+k_{44}[HOCl][O_2^-\bullet] + k_{45}[HOCl][HO_2\bullet] - k_{46}[Cl\bullet][HOCl] - k_{47}[Cl\bullet][OCl^-]$$
$$-k_{48}[Cl\bullet][OH^-] - k_{Cl\bullet/R}[Cl\bullet][R] - k_{59}[Cl\bullet][HCO_3^-] - k_{60}[Cl\bullet][CO_3^{2-}]$$

If NOM and HCO_3^-/CO_3^{2-} are present

$$\frac{d[Cl\bullet]}{dt} = r_{uv,HOCl} + r_{uv,OCl^-} - k_{20}[H_2O][Cl\bullet] + k_{21}[ClOH^-\bullet][H^+] - k_{25}[Cl\bullet][Cl^-]$$
$$+k_{26}[Cl_2^-\bullet] - 2k_{27}[Cl\bullet][Cl\bullet] - k_{30}[Cl\bullet][Cl_2^-\bullet] + k_{37}[Cl_2^-\bullet] - k_{39}[Cl\bullet][H_2O_2] \quad \text{(B.9)}$$
$$+k_{44}[HOCl][O_2^-\bullet] + k_{45}[HOCl][HO_2\bullet] - k_{46}[Cl\bullet][HOCl] - k_{47}[Cl\bullet][OCl^-]$$
$$-k_{48}[Cl\bullet][OH^-] - k_{Cl\bullet/R}[Cl\bullet][R] - k_{Cl\bullet/NOM}[Cl\bullet][NOM] - k_{59}[Cl\bullet][HCO_3^-]$$
$$-k_{60}[Cl\bullet][CO_3^{2-}]$$

(4) Mass balance for OCl^-

$$\frac{d[OCl^-]}{dt} = -r_{uv,OCl^-} - k_1[OCl^-][H^+] + k_2[HOCl] - k_6[OCl^-][HO\bullet] \quad \text{(B.10)}$$
$$-k_{47}[Cl\bullet][OCl^-] + k_{51}[Cl_2O_2][OH^-] + k_{56}[ClO_2^-][ClO\bullet]$$

(5) Mass balance for $O^-\bullet$

$$\frac{d[O^-\bullet]}{dt} = r_{uv,OCl^-} - k_3[H_2O][O^-\bullet] + k_4[OH^-][HO\bullet] \quad \text{(B.11)}$$

(6) Mass balance for $ClO\bullet$

$$\frac{d[ClO\bullet]}{dt} = k_5[HOCl][HO\bullet] + k_6[OCl^-][HO\bullet] + k_{46}[HOCl][Cl\bullet] + k_{47}[OCl^-][Cl\bullet] - 2k_{49}[ClO\bullet][ClO\bullet] - k_{52}[HO\bullet][ClO\bullet] - k_{56}[ClO_2^-][ClO\bullet] - k_{ClO\bullet/R}[R][ClO\bullet] \quad (B.12)$$

If NOM is present

$$\frac{d[ClO\bullet]}{dt} = k_5[HOCl][HO\bullet] + k_6[OCl^-][HO\bullet] + k_{46}[HOCl][Cl\bullet] + k_{47}[OCl^-][Cl\bullet] - 2k_{49}[ClO\bullet][ClO\bullet] - k_{52}[HO\bullet][ClO\bullet] - k_{56}[ClO_2^-][ClO\bullet] - k_{ClO\bullet/R}[R][ClO\bullet] - k_{ClO\bullet/NOM}[ClO\bullet][NOM] \quad (B.13)$$

If HCO_3^-/CO_3^{2-} are present

$$\frac{d[ClO\bullet]}{dt} = k_5[HOCl][HO\bullet] + k_6[OCl^-][HO\bullet] + k_{46}[HOCl][Cl\bullet] + k_{47}[OCl^-][Cl\bullet] - 2k_{49}[ClO\bullet][ClO\bullet] - k_{52}[HO\bullet][ClO\bullet] - k_{56}[ClO_2^-][ClO\bullet] - k_{ClO\bullet/R}[R][ClO\bullet] - k_{ClO\bullet/CO_3^{2-}}[ClO\bullet][CO_3^{2-}] \quad (B.14)$$

If NOM and HCO_3^-/CO_3^{2-} are present

$$\frac{d[ClO\bullet]}{dt} = k_5[HOCl][HO\bullet] + k_6[OCl^-][HO\bullet] + k_{46}[HOCl][Cl\bullet] + k_{47}[OCl^-][Cl\bullet] - 2k_{49}[ClO\bullet][ClO\bullet] - k_{52}[HO\bullet][ClO\bullet] - k_{56}[ClO_2^-][ClO\bullet] - k_{ClO\bullet/R}[R][ClO\bullet] - k_{ClO\bullet/NOM}[NOM][ClO\bullet] - k_{ClO\bullet/CO_3^{2-}}[ClO\bullet][CO_3^{2-}] \quad (B.15)$$

(7) Mass balance for H_2O_2

$$\frac{d[H_2O_2]}{dt} = k_7[HO\bullet][HO\bullet] - k_8[H_2O_2] + k_9[H^+][HO_2^-] - k_{10}[HO\bullet][H_2O_2] - k_{16}[H_2O_2][O_2^-\bullet] - k_{17}[H_2O_2][HO_2\bullet] + k_{18}[HO_2\bullet][HO_2\bullet] - k_{31}[H_2O_2][Cl_2^-\bullet] - k_{39}[H_2O_2][Cl\bullet] \quad (B.16)$$

(8) Mass balance for HO_2^-

$$\frac{d[HO_2^-]}{dt} = k_8[H_2O_2] - k_9[H^+][HO_2^-] - k_{11}[HO\bullet][HO_2^-] + k_{19}[HO_2\bullet][O_2^-\bullet] \quad (B.17)$$

(9) Mass balance for $HO_2\cdot$

$$\begin{aligned}\frac{d[HO_2\bullet]}{dt} &= k_{10}[H_2O_2][HO\bullet]+k_{11}[HO_2^-][HO\bullet]-k_{12}[HO_2\bullet]\\ &+k_{13}[H^+][O_2^-\bullet]-k_{14}[HO\bullet][HO_2\bullet]-k_{17}[H_2O_2][HO_2\bullet]\\ &-2k_{18}[HO_2\bullet][HO_2\bullet]-k_{19}[O_2^-\bullet][HO_2\bullet]+k_{31}[H_2O_2][Cl_2^-\bullet]\\ &-k_{32}[Cl_2^-\bullet][HO_2\bullet]+k_{39}[H_2O_2][Cl\bullet]-k_{43}[Cl_2][HO_2\bullet]\\ &-k_{45}[HOCl][HO_2\bullet]\end{aligned} \tag{B.18}$$

(10) Mass balance for $O_2^-\cdot$

$$\begin{aligned}\frac{d[O_2^-\bullet]}{dt} &= k_{12}[HO_2\bullet]-k_{13}[H^+][O_2^-\bullet]-k_{15}[HO\bullet][O_2^-\bullet]\\ &-k_{16}[H_2O_2][O_2^-\bullet]-k_{19}[HO_2\bullet][O_2^-\bullet]-k_{33}[Cl_2^-\bullet][O_2^-\bullet]\end{aligned} \tag{B.19}$$

(11) Mass balance for O_2

$$\begin{aligned}\frac{d[O_2]}{dt} &= k_{14}[HO\bullet][HO_2\bullet]+k_{15}[HO\bullet][O_2^-\bullet]+k_{16}[H_2O_2][O_2^-\bullet]+k_{17}[H_2O_2][HO_2\bullet]\\ &+k_{18}[HO_2\bullet][HO_2\bullet]+k_{19}[HO_2\bullet][O_2^-\bullet]+k_{32}[Cl_2^-\bullet][HO_2\bullet]+k_{33}[Cl_2^-\bullet][O_2^-\bullet]\\ &+k_{42}[Cl_2][O_2^-\bullet]+k_{43}[Cl_2][HO_2\bullet]+k_{44}[HOCl][O_2^-\bullet]+k_{45}[HOCl][HO_2\bullet]\end{aligned} \tag{B.20}$$

(12) Mass balance for $ClOH^-\cdot$

$$\begin{aligned}\frac{d[ClOH^-\bullet]}{dt} &= k_{20}[H_2O][Cl\bullet]-k_{21}[H^+][ClOH^-\bullet]-k_{22}[ClOH^-\bullet]\\ &+k_{23}[Cl^-][HO\bullet]-k_{24}[Cl^-][ClOH^-\bullet]+k_{35}[Cl_2^-\bullet][OH^-]\\ &+k_{36}[HClOH]+k_{48}[OH^-][Cl\bullet]\end{aligned} \tag{B.21}$$

(13) Mass balance for Cl^-

$$\frac{d[Cl^-]}{dt} = k_{22}[ClOH^-\bullet] - k_{23}[Cl^-][HO\bullet] - k_{24}[Cl^-][ClOH^-\bullet] - k_{25}[Cl^-][Cl\bullet]$$
$$+k_{26}[Cl_2^-\bullet] + k_{28}[Cl_2][OH^-] + 2k_{29}[Cl_2^-\bullet][Cl_2^-\bullet] + k_{30}[Cl\bullet][Cl_2^-\bullet]$$
$$+2k_{31}[H_2O_2][Cl_2^-\bullet] + 2k_{32}[HO_2\bullet][Cl_2^-\bullet] + 2k_{33}[O_2^-\bullet][Cl_2^-\bullet] + k_{34}[H_2O][Cl_2^-\bullet] \quad \text{(B.22)}$$
$$+k_{35}[OH^-][Cl_2^-\bullet] - k_{38}[HClOH][Cl^-] + k_{39}[Cl\bullet][H_2O_2] + k_{40}[Cl_2^-\bullet][HO\bullet]$$
$$+k_{41}[H_2O][Cl_2] + k_{46}[HOCl][Cl\bullet] + k_{47}[OCl^-][Cl\bullet] + 2k_{55}[ClO_2^-][Cl_2^-\bullet]$$

(14) Mass balance for $Cl_2^-\bullet$

$$\frac{d[Cl_2^-\bullet]}{dt} = k_{24}[Cl^-][ClOH^-\bullet] + k_{25}[Cl^-][Cl\bullet] - k_{26}[Cl_2^-\bullet] - 2k_{29}[Cl_2^-\bullet][Cl_2^-\bullet]$$
$$-k_{30}[Cl\bullet][Cl_2^-\bullet] - k_{31}[H_2O_2][Cl_2^-\bullet] - k_{32}[HO_2\bullet][Cl_2^-\bullet] - k_{33}[O_2^-\bullet][Cl_2^-\bullet] \quad \text{(B.23)}$$
$$-k_{34}[H_2O][Cl_2^-\bullet] - k_{35}[OH^-][Cl_2^-\bullet] + k_{38}[HClOH][Cl^-] - k_{40}[Cl_2^-\bullet][HO\bullet]$$
$$+k_{42}[Cl_2][O_2^-\bullet] + k_{43}[Cl_2][HO_2\bullet] - k_{55}[ClO_2^-][Cl_2^-\bullet] - k_{Cl_2^-\bullet/R}[R][Cl_2^-\bullet]$$

If NOM is present:

$$\frac{d[Cl_2^-\bullet]}{dt} = k_{24}[Cl^-][ClOH^-\bullet] + k_{25}[Cl^-][Cl\bullet] - k_{26}[Cl_2^-\bullet] - 2k_{29}[Cl_2^-\bullet][Cl_2^-\bullet]$$
$$-k_{30}[Cl\bullet][Cl_2^-\bullet] - k_{31}[H_2O_2][Cl_2^-\bullet] - k_{32}[HO_2\bullet][Cl_2^-\bullet] - k_{33}[O_2^-\bullet][Cl_2^-\bullet] \quad \text{(B.24)}$$
$$-k_{34}[H_2O][Cl_2^-\bullet] - k_{35}[OH^-][Cl_2^-\bullet] + k_{38}[HClOH][Cl^-] - k_{40}[Cl_2^-\bullet][HO\bullet]$$
$$+k_{42}[Cl_2][O_2^-\bullet] + k_{43}[Cl_2][HO_2\bullet] - k_{55}[ClO_2^-][Cl_2^-\bullet] - k_{Cl_2^-\bullet/R}[R][Cl_2^-\bullet]$$
$$-k_{Cl_2^-\bullet/NOM}[NOM][Cl_2^-\bullet]$$

If HCO_3^-/CO_3^{2-} are present:

$$\frac{d[Cl_2^-\bullet]}{dt} = k_{24}[Cl^-][ClOH^-\bullet] + k_{25}[Cl^-][Cl\bullet] - k_{26}[Cl_2^-\bullet] - 2k_{29}[Cl_2^-\bullet][Cl_2^-\bullet]$$
$$-k_{30}[Cl\bullet][Cl_2^-\bullet] - k_{31}[H_2O_2][Cl_2^-\bullet] - k_{32}[HO_2\bullet][Cl_2^-\bullet] - k_{33}[O_2^-\bullet][Cl_2^-\bullet] \quad \text{(B.25)}$$
$$-k_{34}[H_2O][Cl_2^-\bullet] - k_{35}[OH^-][Cl_2^-\bullet] + k_{38}[HClOH][Cl^-] - k_{40}[Cl_2^-\bullet][HO\bullet]$$
$$+k_{42}[Cl_2][O_2^-\bullet] + k_{43}[Cl_2][HO_2\bullet] - k_{55}[ClO_2^-][Cl_2^-\bullet] - k_{Cl_2^-\bullet/R}[R][Cl_2^-\bullet]$$

If NOM and HCO_3^-/CO_3^{2-} are present:

$$\frac{d[Cl_2^-\bullet]}{dt} = k_{24}[Cl^-][ClOH^-\bullet] + k_{25}[Cl^-][Cl\bullet] - k_{26}[Cl_2^-\bullet] - 2k_{29}[Cl_2^-\bullet][Cl_2^-\bullet]$$
$$-k_{30}[Cl\bullet][Cl_2^-\bullet] - k_{31}[H_2O_2][Cl_2^-\bullet] - k_{32}[HO_2\bullet][Cl_2^-\bullet] - k_{33}[O_2^-\bullet][Cl_2^-\bullet]$$
$$-k_{34}[H_2O][Cl_2^-\bullet] - k_{35}[OH^-][Cl_2^-\bullet] + k_{38}[HClOH][Cl^-] - k_{40}[Cl_2^-\bullet][HO\bullet]$$
$$+k_{42}[Cl_2][O_2^-\bullet] + k_{43}[Cl_2][HO_2\bullet] - k_{55}[ClO_2^-][Cl_2^-\bullet] - k_{Cl_2^-\bullet/R}[R][Cl_2^-\bullet]$$
$$-k_{Cl_2^-\bullet/NOM}[NOM][Cl_2^-\bullet] - k_{61}[Cl_2^-\bullet][HCO_3^-] - k_{62}[Cl_2^-\bullet][CO_3^{2-}] \quad \text{(B.26)}$$

(15) Mass balance for Cl_2

$$\frac{d[Cl_2]}{dt} = k_{27}[Cl\bullet][Cl\bullet] + k_{29}[Cl_2^-\bullet][Cl_2^-\bullet] + k_{30}[Cl\bullet][Cl_2^-\bullet]$$
$$-k_{41}[H_2O][Cl_2] - k_{42}[O_2^-\bullet][Cl_2] - k_{43}[HO_2^-\bullet][Cl_2] \quad \text{(B.27)}$$

(16) Mass balance for HClOH

$$\frac{d[HClOH]}{dt} = k_{34}[H_2O][Cl_2^-\bullet] - k_{36}[HClOH] - k_{37}[HClOH]$$
$$-k_{38}[HClOH][Cl^-] \quad \text{(B.28)}$$

(17) Mass balance for Cl_2O_2

$$\frac{d[Cl_2O_2]}{dt} = k_{49}[ClO\bullet][ClO\bullet] - k_{50}[H_2O][Cl_2O_2] - k_{51}[OH^-][Cl_2O_2] \quad \text{(B.29)}$$

(18) Mass balance for ClO_2^-

$$\frac{d[ClO_2^-]}{dt} = k_{50}[H_2O][Cl_2O_2] + k_{51}[OH^-][Cl_2O_2]$$
$$+k_{52}[ClO\bullet][HO\bullet] - k_{53}[ClO_2^-][HO\bullet] - k_{55}[ClO_2^-][Cl_2^-\bullet]$$
$$-k_{56}[ClO_2^-][ClO\bullet] \quad \text{(B.30)}$$

(19) Mass balance for $ClO_2\bullet$

$$\frac{d[ClO_2\bullet]}{dt} = k_{53}[ClO_2^-][HO\bullet] - k_{54}[ClO_2\bullet][HO\bullet] + k_{55}[ClO_2^-][Cl_2^-\bullet] + k_{56}[ClO_2^-][ClO\bullet] \quad \text{(B.31)}$$

(20) Mass balance for ClO_3^-

$$\frac{d[ClO_3^-]}{dt} = k_{54}[ClO_2\bullet][HO\bullet] \quad \text{(B.32)}$$

(21) Mass balance for target organic compound (R)

$$\frac{d[R]}{dt} = -r_{UV,R} - k_{HO\bullet/R}[R][HO\bullet] - k_{Cl\bullet/R}[R][Cl\bullet] - k_{Cl_2^-\bullet/R}[R][Cl_2^-\bullet] - k_{ClO\bullet/R}[R][ClO\bullet] - k_{HOCl/R}[R][HOCl] - k_{ClO^-/R}[R][ClO^-] \quad \text{(B.33)}$$

If HCO_3^-/CO_3^{2-} are present:

$$\frac{d[R]}{dt} = -r_{UV,R} - k_{HO\bullet/R}[R][HO\bullet] - k_{Cl\bullet/R}[R][Cl\bullet] - k_{Cl_2^-\bullet/R}[R][Cl_2^-\bullet] - k_{ClO\bullet/R}[R][ClO\bullet] - k_{HOCl/R}[R][HOCl] - k_{ClO^-/R}[R][ClO^-] - k_{CO_3^-\bullet/R}[R][CO_3^-\bullet] \quad \text{(B.34)}$$

(22) Mass balance for NOM if NOM is present in water matrix

$$\frac{d[NOM]}{dt} = -k_{HO\bullet/NOM}[HO\bullet][NOM] - k_{Cl\bullet/NOM}[Cl\bullet][NOM] - k_{Cl_2^-\bullet/NOM}[Cl_2^-\bullet][NOM] - k_{ClO\bullet/NOM}[ClO\bullet][NOM] - k_{HOCl/NOM}[HOCl][NOM] - k_{OCl^-/NOM}[OCl^-][NOM] \quad \text{(B.35)}$$

(23) Mass balance for HCO_3^-/CO_3^{2-} if HCO_3^-/CO_3^{2-} are present in water matrix

$$\frac{d[HCO_3^-]}{dt} = -k_{57}[HO\bullet][HCO_3^-] - k_{59}[Cl\bullet][HCO_3^-] - k_{61}[Cl_2^-\bullet][HCO_3^-] - k_{67}[HCO_3^-] + k_{68}[CO_3^{2-}][H^+] \quad \text{(B.36)}$$

$$\frac{d[CO_3^{2-}]}{dt} = -k_{58}[HO\bullet][CO_3^{2-}] - k_{60}[Cl\bullet][CO_3^{2-}] - k_{62}[Cl_2^-\bullet][CO_3^{2-}]$$
$$-k_{63}[ClO\bullet][CO_3^{2-}] + k_{64}[HOCl][CO_3^-\bullet] + k_{65}[OCl^-][CO_3^-\bullet]$$
$$+k_{67}[HCO_3^-] - k_{68}[H^+][CO_3^{2-}] \tag{B.37}$$

$$\frac{d[CO_3^-\bullet]}{dt} = k_{57}[HO\bullet][HCO_3^-] + k_{58}[HO\bullet][CO_3^{2-}] + k_{59}[Cl\bullet][HCO_3^-]$$
$$+k_{60}[Cl\bullet][CO_3^{2-}] + k_{61}[Cl_2^-\bullet][HCO_3^-] + k_{62}[Cl_2^-\bullet][CO_3^{2-}]$$
$$+k_{63}[ClO\bullet][CO_3^{2-}] - k_{64}[HOCl][CO_3^-\bullet] - k_{65}[OCl^-][CO_3^-\bullet]$$
$$-k_{CO_3^-\bullet/R}[R][CO_3^-\bullet] \tag{B.38}$$

$$\frac{d[OCl^-]}{dt} = -r_{uv,OCl^-} - k_1[OCl^-][H^+] + k_2[HOCl] - k_6[OCl^-][HO\bullet]$$
$$-k_{47}[Cl\bullet][OCl^-] + k_{51}[Cl_2O_2][OH^-] + k_{56}[ClO_2^-][ClO\bullet] + k_{63}[CO_3^{2-}][ClO\bullet] \tag{B.39}$$

$$\frac{d[Cl^-]}{dt} = k_{22}[ClOH^-\bullet] - k_{23}[Cl^-][HO\bullet] - k_{24}[Cl^-][ClOH^-\bullet] - k_{25}[Cl^-][Cl\bullet]$$
$$+k_{26}[Cl_2^-\bullet] + k_{28}[Cl_2][OH^-] + 2k_{29}[Cl_2^-\bullet][Cl_2^-\bullet] + k_{30}[Cl\bullet][Cl_2^-\bullet]$$
$$+2k_{31}[H_2O_2][Cl_2^-\bullet] + 2k_{32}[HO_2\bullet][Cl_2^-\bullet] + 2k_{33}[O_2^-\bullet][Cl_2^-\bullet] + k_{34}[H_2O][Cl_2^-\bullet]$$
$$+k_{35}[OH^-][Cl_2^-\bullet] - k_{38}[HClOH][Cl^-] + k_{39}[Cl\bullet][H_2O_2] + k_{40}[Cl_2^-\bullet][HO\bullet]$$
$$+k_{41}[H_2O][Cl_2] + k_{46}[HOCl][Cl\bullet] + k_{47}[OCl^-][Cl\bullet] + 2k_{55}[ClO_2^-][Cl_2^-\bullet]$$
$$+k_{59}[HCO_3^-][Cl\bullet] + k_{60}[CO_3^{2-}][Cl\bullet] + 2k_{61}[HCO_3^-][Cl_2^-\bullet] + 2k_{62}[CO_3^{2-}][Cl_2^-\bullet] \tag{B.40}$$

It is notable that if the target organic compound cannot be degraded by UV alone, then $r_{UV,R}$ equals to 0 in eq B.33 and eq B.34; if the target organic compound cannot be oxidized by free chlorine alone, then both of $k_{HOCl/R}[R][HOCl]$ and $k_{ClO^-/R}[R][ClO^-]$ equal to 0 in eq B.33 and eq B.34.

APPENDIX C. SUPPORTING INFORMATION FOR CHAPTER 3

C.1 Quantum Yields of Substituted Benzoic Acid Compounds (SBACs)

The experimental data indicated that four of these SBACs can be destructed by UV alone, they are 4-fluorobenzoic acid, 2-chlorobenzoic acid, 2-iodobenzoic acid and 3-nitrobenzoic acid. Based on the fit of the experimental data for degradation by UV alone in **Figure C.1,** the quantum yields are (i) 0.0014 for fluorobenzoic acid; (ii) 0.0028 for 2-chlorobenzoic acid; (iii) 0.0132 for 2-iodobenzoic acid; and (iv) 0.0005 for 3-nitrobenzoic acid.

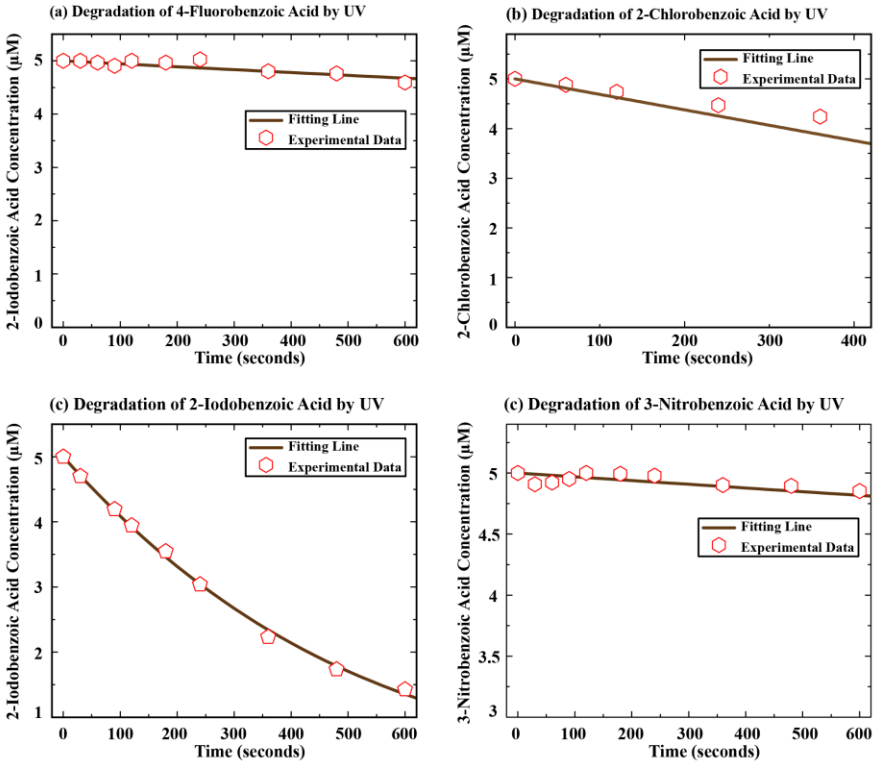

Figure C.1. Fitting results of 4-fluorobenzoic acid, 2-chlorobenzoic acid, 2-iodobenzoic acid and 3-nitrobenzoic acid by UV alone. Experimental conditions: UV intensity = 1.97×10^{-6} Einstein/L·s; initial concentration of SBACs = 5×10^{-6} M; pH was buffered at 7.2. The symbols represent experimental data and the lines represent model results.

C.2 Confidence Level of Estimated Rate Constants

To determine the 75% confidence level regions for the reactivity of RCS toward these SBACs, we calculated the corresponding objective function (OF(θ)) based on eq 3.9. The boundary of $k_{Cl\cdot/R}$ for each SBACs was determined by fixing $k_{Cl_2^-\cdot/R}$ and $k_{ClO\cdot/R}$ as their estimated values, then updated the value of $k_{Cl\cdot/R}$ to achieve the value of corresponding OF(θ). The boundary of $k_{Cl_2^-\cdot/R}$ and $k_{ClO\cdot/R}$ were determined by similar method. As a result, **Table C. 1** and **Figure 3.7** indicate the results of confidence range for the estimated $k_{Cl\cdot/R}$, $k_{Cl_2^-\cdot/R}$ and $k_{ClO\cdot/R}$.

Table C. 1. Range of the reactivity of RCS towards SBACs for 75% confidence level

(a) The range of $k_{Cl\cdot/R}$ for 75% Confidence

Organic Compounds	n	p	Degree of Freedom (n-p)	F (p, n-p,1-α)	$\hat{S}(\theta)$	S(θ)	$k_{Cl\bullet/R}$ ($M^{-1}s^{-1}$)		
							Lower bond	Fitted Results	Upper bond
3-MethylBA	10	3	7	1.72	0.0737	0.128	-	1.64×10^{9}	3.64×10^{9}
4-FluoroBA	10	3	7	1.72	0.121	0.211	-	7.92×10^{8}	3.54×10^{9}
2-ChloroBA	7	3	4	2.05	0.0400	0.075	-	6.00×10^{8}	2.94×10^{9}
2-IodoBA	10	3	7	1.72	0.0520	0.0903	-	3.85×10^{8}	2.34×10^{9}
3-CyanoBA	10	3	7	1.72	0.0294	0.0510	-	6.35×10^{7}	6.56×10^{8}
3-NitroBA	10	3	7	1.72	0.0189	0.0328	-	4.18×10^{7}	4.55×10^{8}

(b) The range of $k_{Cl_2^-\cdot/R}$ for 75% Confidence

Organic Compounds	n	p	Degree of Freedom (n-p)	F (p, n-p,1-α)	$\hat{S}(\theta)$	S(θ)	$k_{Cl_2^-\bullet/R}$ ($M^{-1}s^{-1}$)		
							Lower bond	Fitted Results	Upper bond
3-MethylBA	10	3	7	1.72	0.0737	0.128	-	6.81×10^{4}	8.62×10^{8}
4-FluoroBA	10	3	7	1.72	0.121	0.211	-	5.20×10^{4}	5.64×10^{8}
2-ChloroBA	7	3	4	2.05	0.0400	0.075	-	3.00×10^{4}	1.11×10^{9}
2-IodoBA	10	3	7	1.72	0.0520	0.0903	-	2.00×10^{4}	8.67×10^{8}
3-CyanoBA	10	3	7	1.72	0.0294	0.0510	-	1.89×10^{4}	2.40×10^{8}
3-NitroBA	10	3	7	1.72	0.0189	0.0328	-	1.08×10^{4}	1.69×10^{8}

(c) The range of $k_{ClO\cdot/R}$ for 75% Confidence

Organic Compounds	n	p	Degree of Freedom (n-p)	F (p, n-p,1-α)	$\hat{S}(\theta)$	$S(\theta)$	$k_{Cl\bullet/R}$ ($M^{-1}s^{-1}$)		
							Lower bond	Fitted Results	Upper bond
3-MethylBA	10	3	7	1.72	0.0737	0.128	9.482×10^5	1.21×10^6	1.532×10^6
4-FluoroBA	10	3	7	1.72	0.121	0.211	1.001×10^6	1.27×10^6	1.61×10^6
2-ChloroBA	7	3	4	2.05	0.0400	0.075	6.118×10^5	8.00×10^5	1.013×10^6
2-IodoBA	10	3	7	1.72	0.0520	0.0903	6.898×10^5	8.82×10^5	1.112×10^6
3-CyanoBA	10	3	7	1.72	0.0294	0.051	7.078×10^5	8.11×10^5	9.18×10^5
3-NitroBA	10	3	7	1.72	0.0189	0.0328	4.462×10^5	5.05×10^5	5.702×10^5

The 75% confidence level regions for $k_{Cl\cdot/R}$, $k_{Cl_2^-\cdot/R}$ and $k_{ClO\cdot/R}$ are 3-dimensional. Since $Cl_2^-\cdot$ contributes very little to the destruction of organic contaminants (as will be discussed later), we determined the 2-dimensional 75% confidence level regions for the $k_{Cl\cdot/R}$ and $k_{ClO\cdot/R}$ in **Figure C.2**. The shapes of the confidence regions were mapped out in details and were assumed to be trapezoidal.

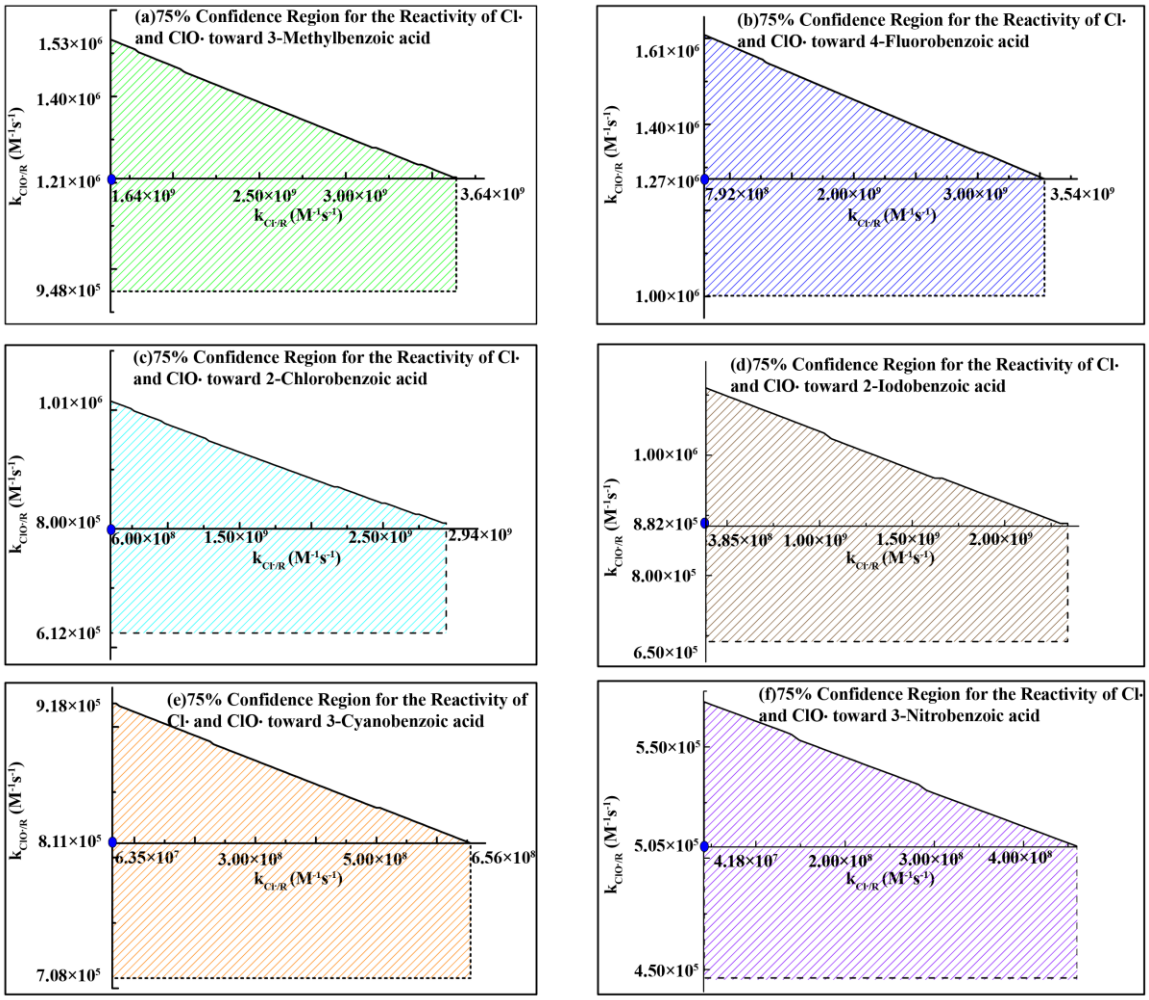

Figure C.2. Regions of 75% confidence level for the reactivity of Cl· and ClO· toward SBACs. The shadow in each figure indicates the 2-dimensional 75% level of confidence region.

C.3 Relative Contributions of Reactive Radicals and Photolysis Results

The relative contribution of reactive radicals (HO·, Cl·, Cl_2^-· and ClO·) and photolysis destroying each SBAC were calculated based on eq 3.11– eq 3.15. The calculation results of the average relative contribution of reactive radicals and photolysis were summarized in **Table C.2(a) – Table C.2(f)**. The ranking of average relative contributions of reactive radicals and photolysis for each SBAC was indicated in **Table C.3**.

Table C.2. Relative contribution of reactive radicals and photolysis for SBACs degradation in the UV/free chlorine process

(a)For 3-Methylbenzoic Acid Degradation

Reactive Radicals	Relative Contribution		
	0.5 ppm HOCl/OCl^-	1 ppm HOCl/OCl^-	4 ppm HOCl/OCl^-
HO•	14.0%	9.44%	4.56%
Cl•	20.9%	17.6%	10.6%
Cl_2^-•	Negligible	Negligible	Negligible
ClO•	65.1%	73.0%	84.9%
UV	NA	NA	NA

(b) For 4-Fluorobenzoic Acid Degradation

Reactive Radicals	Relative Contribution		
	1 ppm HOCl/OCl^-	2 ppm HOCl/OCl^-	4 ppm HOCl/OCl^-
HO•	7.85%	5.32%	3.68%
Cl•	8.97%	6.89%	5.11%
Cl_2^-•	Negligible	Negligible	Negligible
ClO•	77.3%	83.7%	88.3%
UV	5.86%	4.06%	2.86%

(c) For 2-Chlorobenzoic Acid Degradation

Reactive Radicals	Relative Contribution		
	0.5 ppm HOCl/OCl^-	1 ppm HOCl/OCl^-	2 ppm HOCl/OCl^-
HO•	7.17%	5.22%	3.76%
Cl•	6.40%	5.24%	4.06%
Cl_2^-•	Negligible	Negligible	Negligible
ClO•	61.0%	71.0%	78.7%
UV	25.5%	18.6%	13.5%

(d) For 2-Iodobenzoic Acid Degradation

Reactive Radicals	Relative Contribution		
	0.5 ppm HOCl/OCl^-	1 ppm HOCl/OCl^-	2 ppm HOCl/OCl^-
HO•	3.62%	2.99%	2.41%
Cl•	2.46%	2.32%	2.02%
Cl_2^-•	Negligible	Negligible	Negligible
ClO•	33.8%	44.1%	54.1%
UV	60.1%	50.6%	41.5%

(e) For 3-Cyanobenzoic Acid Degradation

Reactive Radicals	Relative Contribution		
	0.5 ppm HOCl/OCl^-	1 ppm HOCl/OCl^-	4 ppm HOCl/OCl^-

HO•	11.1%	7.09%	3.14%
Cl•	1.77%	1.33%	0.70%
Cl_2^-•	Negligible	Negligible	Negligible
ClO•	87.1%	91.6%	96.2%
UV	NA	NA	NA

(f) For 3-Nitrobenzoic Acid Degradation

Reactive Radicals	Relative Contribution		
	0.5 ppm HOCl/OCl^-	1 ppm HOCl/OCl^-	2 ppm HOCl/OCl^-
HO•	14.2%	9.68%	6.66%
Cl•	1.56%	1.24%	0.93%
Cl_2^-•	Negligible	Negligible	Negligible
ClO•	82.2%	87.6%	91.4%
UV	2.07%	1.46%	1.04%

Table C.3. Ranking of relative contribution of reactive radicals and photolysis for each SBAC

Rank	3-Methybenzoic acid			2-Fluorobenzoic acid			2-Chlorobenzoic acid		
	HOCl/OCl^- dosage (ppm)			HOCl/OCl^- dosage (ppm)			HOCl/OCl^- dosage (ppm)		
	0.5	1	4	1	2	4	0.5	1	2
1	ClO•	ClO•	ClO•	ClO•	ClO•	ClO•	ClO•	ClO•	ClO•
2	Cl•	Cl•	Cl•	Cl•	Cl•	Cl•	UV	UV	UV
3	HO•	HO•	HO•	HO•	HO•	HO•	HO•	Cl•	Cl•
4	Cl_2^-•	Cl_2^-•	Cl_2^-•	UV	UV	UV	Cl•	HO•	HO•
5	NA	NA	NA	Cl_2^-•	Cl_2^-•	Cl_2^-•	Cl_2^-•	Cl_2^-•	Cl_2^-•

Rank	2-Iodobenzoic acid			3-Cyanobenzoic acid			3-Nitrobenzoic acid		
	HOCl/OCl^- dosage (ppm)			HOCl/OCl^- dosage (ppm)			HOCl/OCl^- dosage (ppm)		
	0.5	1	2	0.5	1	4	0.5	1	2
1	UV	UV	ClO•	ClO•	ClO•	ClO•	ClO•	ClO•	ClO•
2	ClO•	ClO•	UV	HO•	HO•	HO•	HO•	HO•	HO•
3	HO•	HO•	HO•	Cl•	Cl•	Cl•	UV	UV	UV
4	Cl•	Cl•	Cl•	Cl_2^-•	Cl_2^-•	Cl_2^-•	Cl•	Cl•	Cl•
5	Cl_2^-•	Cl_2^-•	Cl_2^-•	NA	NA	NA	Cl_2^-•	Cl_2^-•	Cl_2^-•

C.4 Dominant reaction pathways of reactive radicals

In the UV/free chlorine process, the reactive radicals include OH•, Cl•, Cl_2^-• and ClO•. A reaction network was developed to describe all possible important elementary reactions for the UV/free chlorine system in **Figure 3.10**. To simplify the analysis, the reactions between

radicals were not included because of these reactions are insignificant. According to the **Figure 3.10**, (i) OH· can react with free chlorine and organic compounds. **Figure C. 3** indicates the comparison results about the reaction rate of HO· reacting with free chlorine and the rate of reacting with SBACs; (ii) Cl· can react with free chlorine, SBACs, H_2O and chloride ions. **Figure C.4** indicates the comparison results about the reaction rate of Cl· reacting with free chlorine, SBACs, H_2O and chloride ions; (iii) $Cl_2^-\cdot$ mainly: ***(1)*** reacts with SBACs ($k_{Cl_2^-\cdot/R}$ ranges from 1×10^4 $M^{-1}s^{-1}$ to 6×10^4 $M^{-1}s^{-1}$); ***(2)*** reacts with H_2O ($k_{34}[H_2O]$ = 1.3×10^3 s^{-1}); ***(3)*** dissociates to generate Cl· (k_{26} = 5.3×10^4 s^{-1}). When we compare the reaction rate of these three reactions ($k_{Cl_2^-\cdot/R}[R][Cl_2^-\cdot]$, $k_{34}[H_2O]$ $[Cl_2^-\cdot]$, $k_{26}[Cl_2^-\cdot]$), the SBACs initial concentration is 5×10^{-6} M and SBACs concentration decreases as time increases. Consequently, the fastest reaction rate regarding $Cl_2^-\cdot$ is the dissociation reaction and produces Cl· again. For ClO·, it mainly reacts with SBACs because other species that react with ClO· are radicals (radicals concentration are much smaller than SBACs). As a result, ClO· reacts with SBACs fastest. Since the free chlorine acts as an important role to generate ClO·, the free chlorine decay during the degradation of these SBACs is shown in **Figure C. 5**.

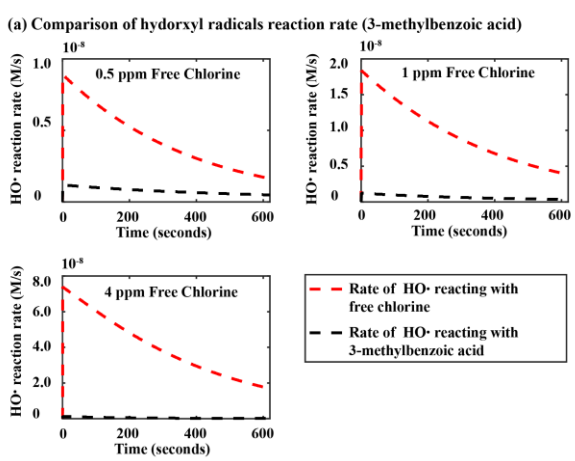

(b) Comparison of hydorxyl radicals reaction rate (4-Fluorobenzoic acid)

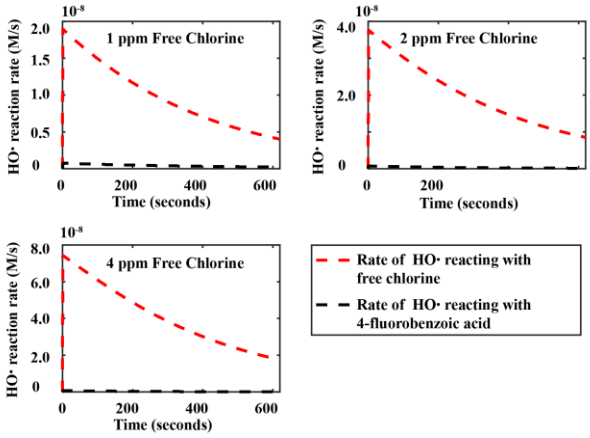

(c) Comparison of hydroxyl radicals reaction rate (2-Chlorobenzoic acid)

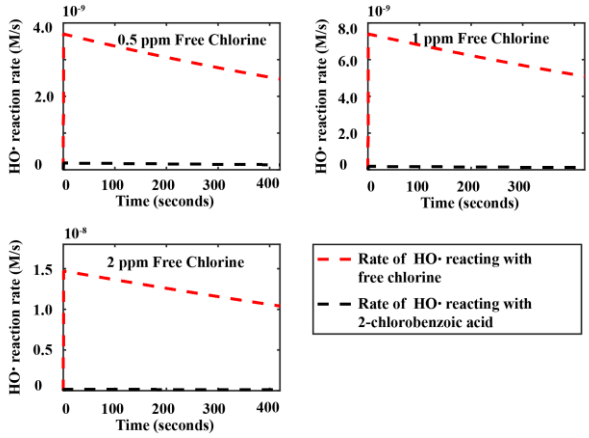

(d) Comparison of hydroxyl radicals reaction rate (2-Iodobenzoic acid)

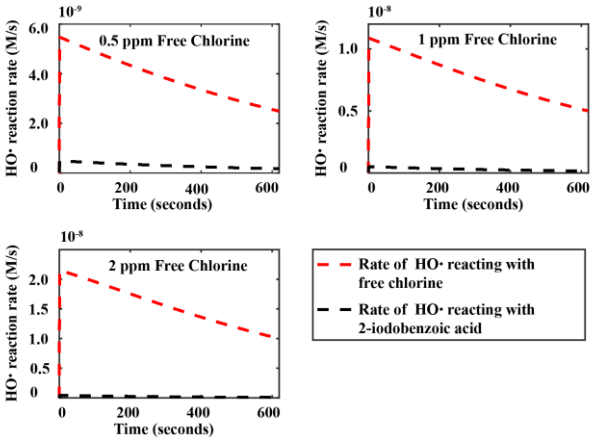

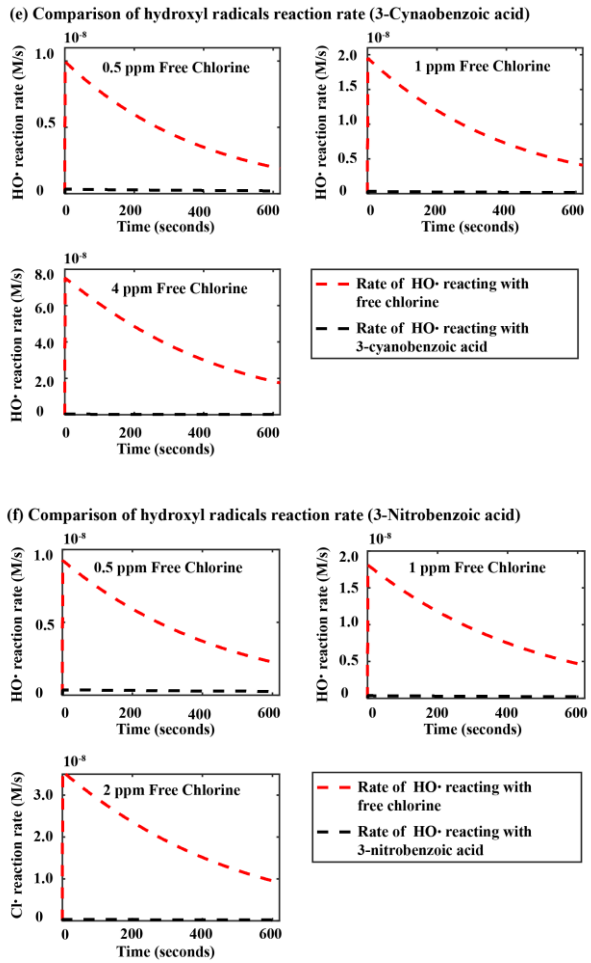

Figure C. 3. Comparison of the reaction rate of HO· reacting with free chlorine and SBACs. Simulation Conditions: UV intensity $=1.97\times10^{-6}$ Einstein/L·s; free chlorine dosage range, 0.5 ppm to 4 ppm; initial concentration of SBACs = 5×10^{-6} M; pH was buffered at 7.2.

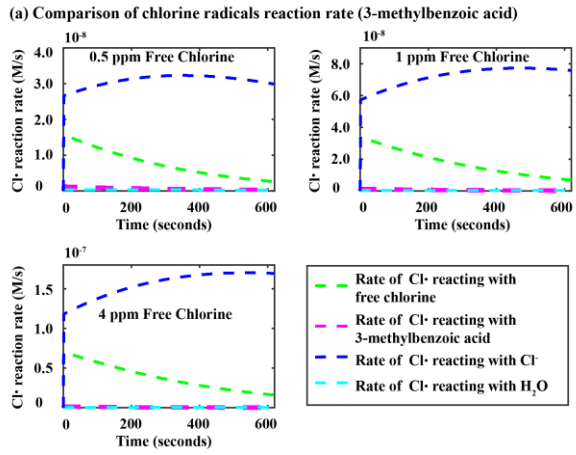

(b) Comparison of chlorine radicals reaction rate (4-Fluorobenzoic acid)

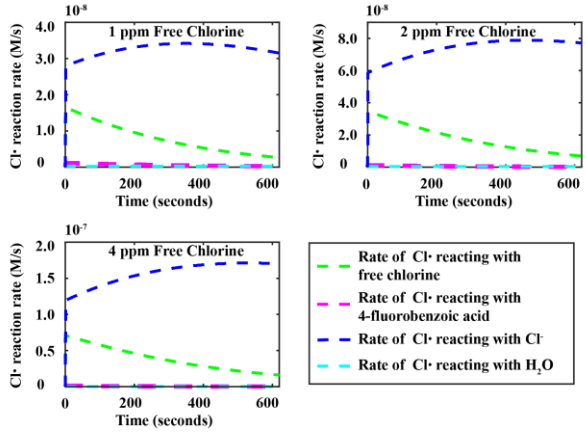

(c) Comparison of chlorine radicals reaction rate (2-Chlorobenzoic acid)

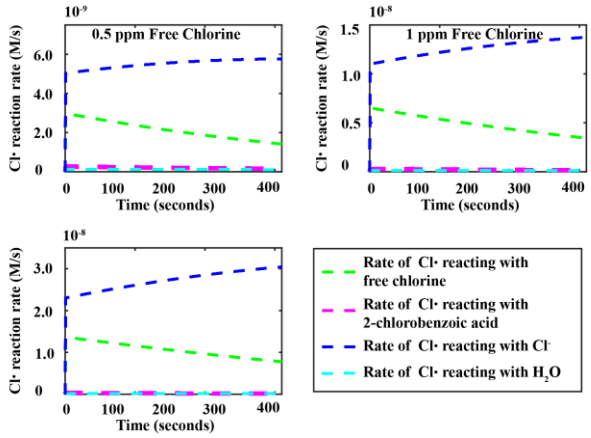

(d) Comparison of chlorine radicals reaction rate (2-Iodobenzoic acid)

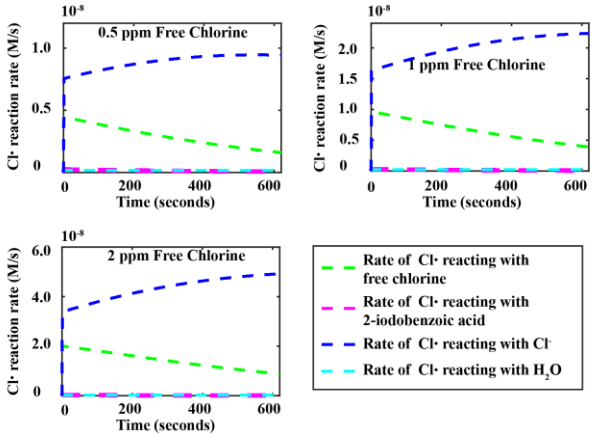

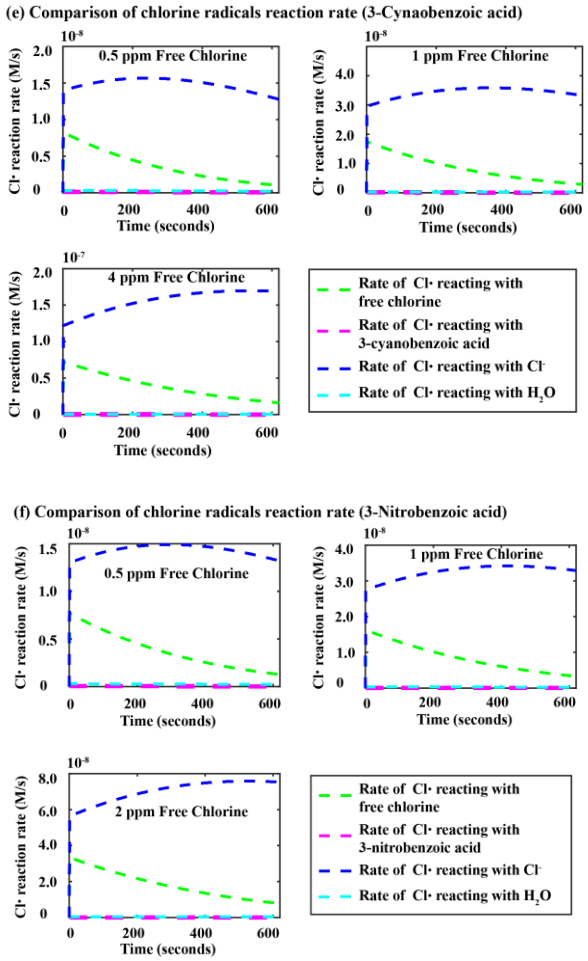

Figure C.4. Comparison of the reaction rate of Cl· reacting with free chlorine, SBACs, H2O and chloride ions. Simulation Conditions: UV intensity = 1.97×10^{-6} Einstein/L·s; free chlorine dosage range, 0.5 ppm to 4 ppm; initial concentration of SBACs = 5×10^{-6} M; pH was buffered at 7.2. The symbols represent experimental data and the lines represent model results.

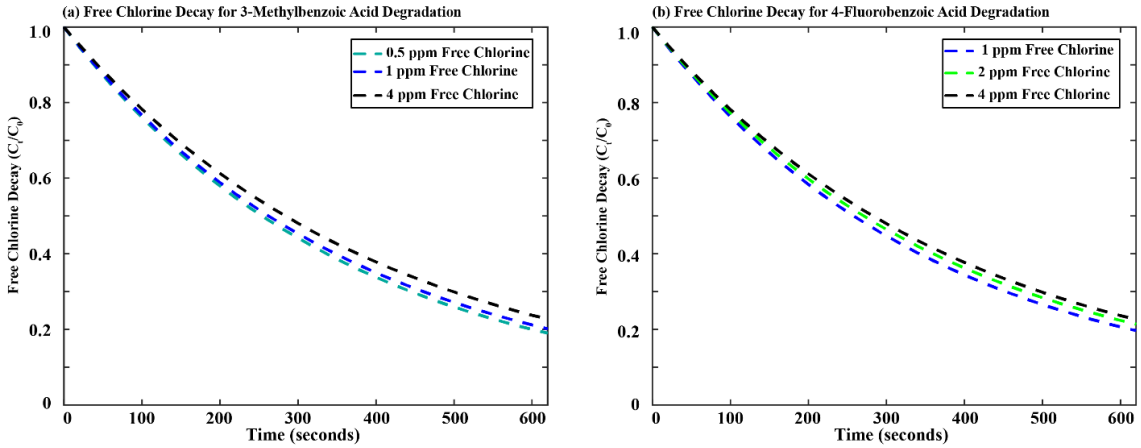

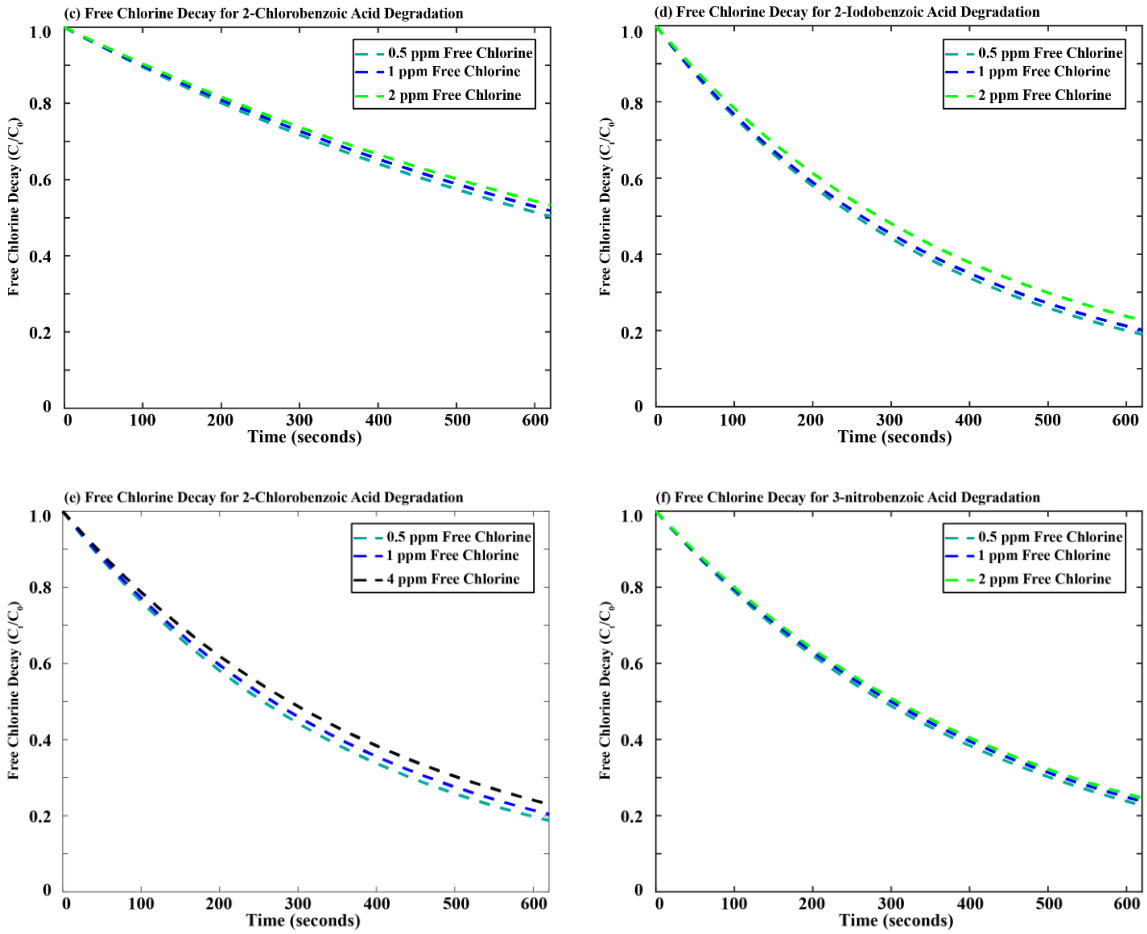

Figure C. 5. Free chlorine Decay during the degradation of SBACs in the UV/free chlorine process. Simulation Conditions: UV intensity = 1.97×10^{-6} Einstein/L·s; free chlorine dosage range, 0.5 ppm to 4 ppm; initial concentration of SBACs = 5×10^{-6} M; pH was buffered at 7.2.

C.5 EE/O Results

Table C.4. Minimal EE/O and optimal optional conditions for the SBACs degradation in the UV/free chlorine process.

(a) NOM is not present

No.	Target Organic Compounds	Minimum EE/O (kWh/m^3)	Optimal Conditions	
			UV Intensity (Einstein/L-s)	Free Chlorine Dosage (mM)
1	3-Methylbenzoic Acid	0.153	2.56×10^{-7}	0.089
2	4-Fluorobenzoic Acid	0.147	2.44×10^{-7}	0.085
3	2-Chlorobenzoic Acid	0.271	2.70×10^{-7}	0.151
4	2-Iodobenzoic Acid	0.196	2.13×10^{-7}	0.104

5	3-Cyanobenzoic Acid	0.211	2.86×10^{-7}	0.120
6	3-Nitrobenzoic Acid	0.280	2.50×10^{-7}	0.175

(b) NOM is present

No.	Target Organic Compounds	Minimum EE/O (kWh/m^3)	Optimal Conditions	
			UV Intensity (Einstein/L-s)	Free Chlorine Dosage (mM)
1	3-Methylbenzoic Acid	9.1	3.43×10^{-6}	0.060
2	4-Fluorobenzoic Acid	11.5	3.33×10^{-6}	0.036
3	2-Chlorobenzoic Acid	10.8	8.61×10^{-6}	0.039
4	2-Iodobenzoic Acid	2.9	1.89×10^{-6}	0.032
5	3-Cyanobenzoic Acid	46.8	3.56×10^{-6}	0.016
6	3-Nitrobenzoic Acid	17.8	6.41×10^{-6}	0.018

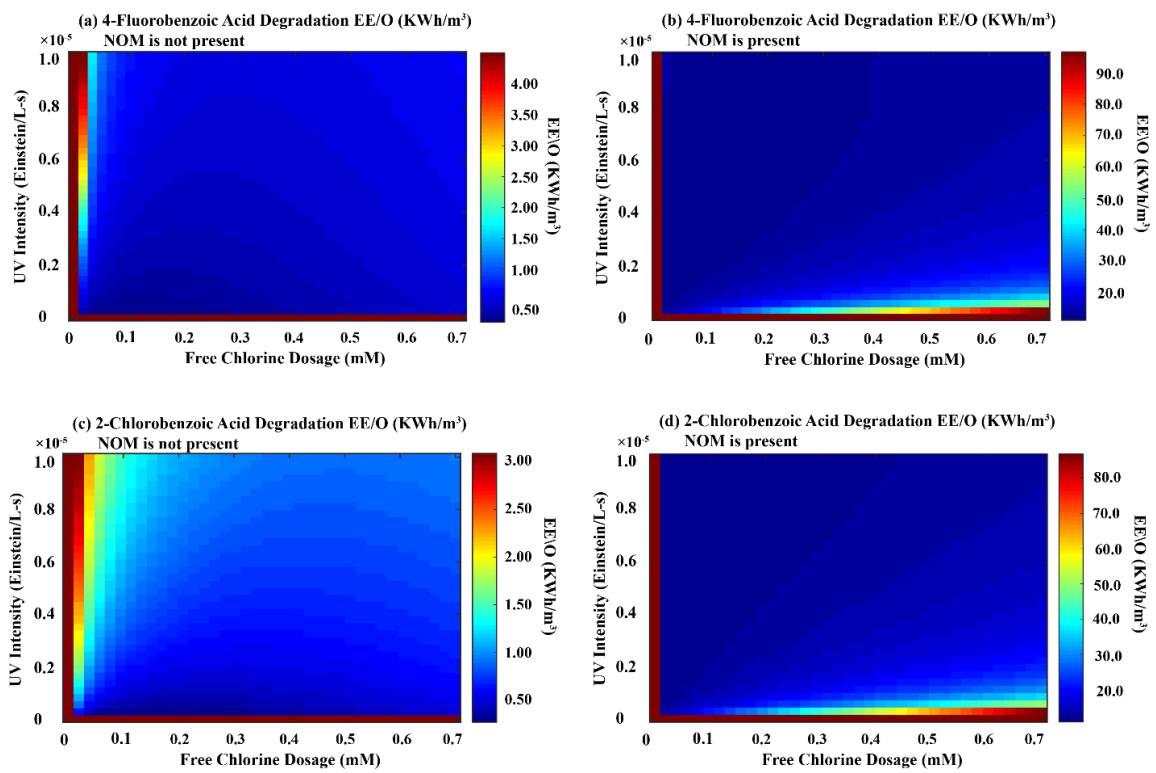

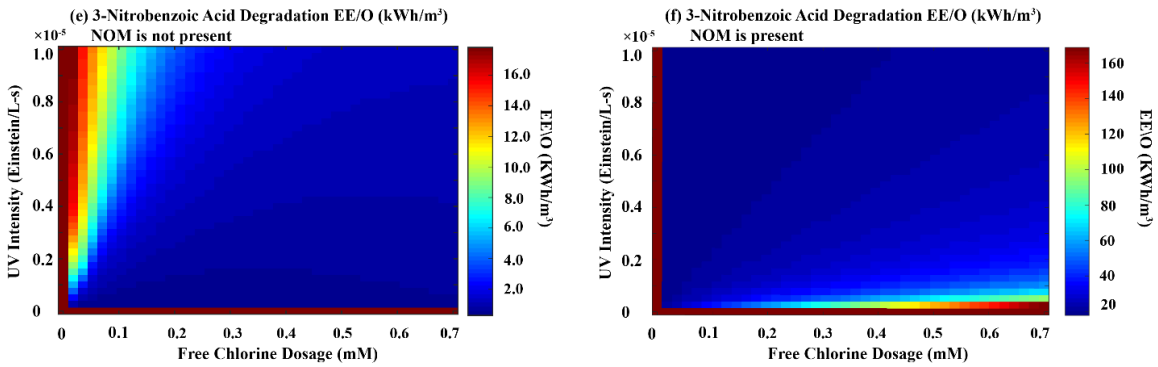

Figure C.6. EE/O (in kWh·m-3) estimation for 4-fluorobenzoic acid, 2-chlorobenzoic acid and 3-nitrobenzoic acid degradation by the UV/free chlorine process with varying UV intensity and free chlorine dosage. Simulation conditions: UV intensity range, 0 to 1×10^{-5} Einstein/L·s ; free chlorine dosage range, 0 ppm to 50 ppm; initial concentration of each SBAC = 5×10^{-6} M; pH was buffered at 7.2. If NOM is present: initial concentration of NOM = 2 mg/L; mass absorption coefficient of NOM = 0.107 L/mgC · cm.

C.6 Free Chlorine Residual Under Optimal Operational Conditions

Under the optimal operational conditions with the minimal EE/O, our first-principles based kinetic model predicted the free chlorine residual for one order magnitude of SBACs degradation. As the **Figure C.7** indicates, the residual free chlorine for one order magnitude of 3-methylbenzoic acid degradation is 70.55%, 4-fluorobenzoic acid degradation is 71.60%, 2-chlorobenzoic acid degradation is 78.17%, 2-iodobenzoic acid degradation is 75.76%, 2-cyanobenzoic acid degradation is 67.19%, 3-nitrobenzoic acid degradation is 58.27%.

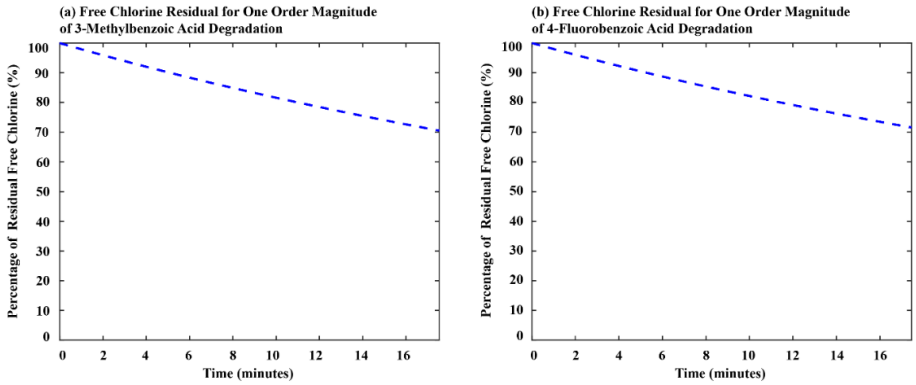

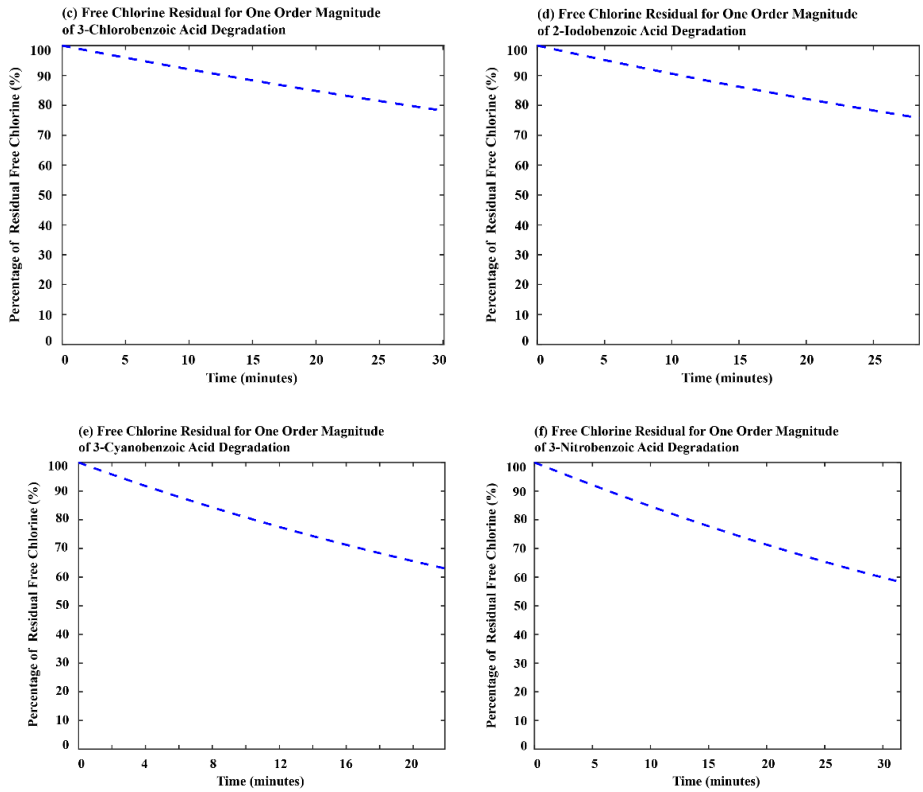

Figure C.7. Free chlorine residual for SBACs degradation under optimal operational conditions

APPENDIX D. OBJECTION FUNCTION

```
%%%%%%%%%%%%%%%%%%%%%%%%%%%%%%%%%%%%%%%%%%%%
% This subroutine contains the code about the objective function             %
% Three groups experimental data are simutaneously fitted in this example    %
%                                                                             %
% Author: Weiqiu Zhang and John Crittenden                                   %
%       School of Civil and Environmental Engineering                        %
%       Georgia Institute of Technology                                      %
%Date: 10/25/2019                                                             %
%                                                                             %
%Input Parameters:                                                            %
%(1)t0:an array stores time points of experiment data                         %
%(2)ExpData: a 2D matrix stores experimental observed time-dependent         %
%           concentration profiles of target organic compounds                %
%(3)Initial_Conditons: Intial experimental condition correspoinding to the   %
%                   experimental data                                         %
%(4)uk:an array stores the estimations for unknown rate constants            %
%(5)ts:time step                                                              %
%Outputs:                                                                     %
%objectfun:objective function value                                          %
%%%%%%%%%%%%%%%%%%%%%%%%%%%%%%%%%%%%%%%%%%%%

function objectfun = objective_rhocl(t0,ExpData,Initial_Conditons,uk,ts)
%OBJECTIVEFUN


    %available measurements
    ym1=ExpData(1,:);
    ym2=ExpData(2,:);
    ym3=ExpData(3,:);
    ym=[ym1 ym2 ym3];

    %Initial conditions
    y01=Initial_Conditons(1,:);
    y02=Initial_Conditons(2,:);
    y03=Initial_Conditons(3,:);

    opt=odeset('RelTol', 1*10^-9, 'AbsTol', 1*10^-20);
    [t,y1] = ode15s(@rhocl,0:ts:t0(end), y01, opt,uk);
    %rhocl is the stiff odes eqautions system includes eq B.1 to eq B.40 in Appendix
    B (this is an exmple without NOM,and Bicarbonate/Carbonate in water matrix)

    %retrive estimated values at known measurement points
    estimates1=interp1(t,y1(:,21),t0);

    [t,y2] = ode15s(@rhocl,0:1:t0(end), y02, opt,uk);
```

```
    estimates2=interp1(t,y2(:,21),t0);

    [t,y3] = ode15s(@rhocl,0:1:t0(end), y03, opt,uk);
    estimates3=interp1(t,y3(:,21),t0);

    %Collect all estimated values at known measurement points together
    estimates=[estimates1 estimates2 estimates3];
    % Total experimental data point
    len1=length(ym1);
    len2=length(ym2);
    len3=length(ym3);
    len=len1+len2+len3;

    %objective function calculation
    objectfun=sqrt(1/(len-1)*sum((((estimates-ym)./ym)).^2));


end
```

Published with MATLAB® R2018b

APPENDIX E. PATTERN SEARCH ALGORITHM

```
%%%%%%%%%%%%%%%%%%%%%%%%%%%%%%%%%%%%%%%%%%%%%%%%
% This subroutine contains the code example about the implementation of          %
% Pattern Search Algorithm to fit experimental data for unknown rate             %
% constants estimation                                                           %
%                                                                                %
%Author: Weiqiu Zhang and John Crittenden                                        %
%       School of Civil and Environmental Engineering                            %
%       Georgia Institute of Technology                                          %
%Date: 10/25/2019                                                                %
%                                                                                %
%Input Parameters:                                                               %
%(1)t0:an array stores time points of experiment data                            %
%(2)ExpData: a 2D matrix stores experimental observed time-dependent             %
%          concentration profiles of target organic compounds                    %
%(3)pH: pH of experimental condition                                             %
%(4)TOT_HOCl: initial total free chlorine dosage                                 %
%(5)Conc_R:initial concentration of target organic compound                      %
%(6)LB:an array stores the lower boundary for kCl_R,kCl2_R and kClO_R            %
%(7)UB:an array stores the upper boundary for kCl_R,kCl2_R and kClO_R            %
%(8)Guess:an array stores initial guess for kCl_R,kCl2_R and kClO_R              %
%(9)ts:time step                                                                 %
%Output:                                                                         %
%(1)estk:an array stores the estimated rate constants between:                   %
%       (a)chlorine radicals and target organic compound (kCl_R)                 %
%       (b)dichloride ion radicals and target organic compound (kCl2_R)          %
%       (c)chlorine monoxide radicals and target organic compound (kClO_R)       %
%(2)OF:minimal objective function                                                %
%%%%%%%%%%%%%%%%%%%%%%%%%%%%%%%%%%%%%%%%%%%%%%%%

function [Estk,OF]=PS_Algorithm(t0,ExpData,pH,TOT_HOCl,Conc_R,LB,UB,Guess,ts)


        % HOCl and OCl equilibrium
        pka=7.53; %Free Chlorine pKa
        ratio1=(10^(-pH)/(10^(-pH)+10^(-pka)));  %Fraction of HOCl
        ratio2=(10^(-pka)/(10^(-pH)+10^(-pka))); %Fraction of OCl-

        % Experimental Data
        % Here is an example of simutaneously fitting 3 groups exepermiental data
        ym1=ExpData(1,:);   % First Group Experimental Data
        ym2=ExpData(2,:);   % Second Group Experimental Data
        ym3=ExpData(3,:);   % Third Group Experimantal Data
```

```
    % Initial experimental conditions of first group experimental data
    y01(1)=ratio1*TOT_HOCl(1,1); %HOCl initial concentration
    y01(4)=ratio2*TOT_HOCl(1,1); %OCl- initial concentration
    y01(13)=TOT_HOCl(1,1);       %Chloride initial concentration
    y01(21)=Conc_R;              %Initial target organic compound concentration
    %  Initial experimental conditions of second group experimental data
    y02(1)=ratio1*TOT_HOCl(1,2);
    y02(4)=ratio2*TOT_HOCl(1,2);
    y02(13)=TOT_HOCl(1,2);
    y02(21)=Conc_R;
    % Initial experimental conditions of third group experimental data
    y03(1)=ratio1*TOT_HOCl(1,3);
    y03(4)=ratio2*TOT_HOCl(1,3);
    y03(13)=TOT_HOCl(1,3);
    y03(21)=Conc_R;
    %Collect all linitial experimental condtions together
    Initial_Conditions=[y01;y02;y03];

    %Paramenters for patternsearch
    x0=Guess;  % An array includes the initial guess for kCl_R,kCl2_R and kClO_R
    lb=LB;     % Lower boundaries for kCl_R,kCl2_R and kClO_R
    ub=UB;     % Upper boundaries for kCl_R,kCl2_R and kClO_R

    %Call objective function
    objectfun=@(uk)  objective_rhocl(t0,ExpData,Initial_Conditions,uk,ts);
    %Pattern search options setting
    opts = psoptimset('CompletePoll','on','Display','iter');
    %opts=optimoptions('patternsearch','Display','iter','MaxIter',18);
    %Call MATLAB R2018B built-in function: patternshearch
    [estk,fval]=patternsearch(objectfun,x0,[],[],[],[],lb,ub,opts);

    %Print Outputs
    Estk(1,1)=estk(1,1);  %Estimated kCl_R
    Estk(1,2)=estk(1,2);  %Estimated kCl2_R
    Estk(1,3)=estk(1,3);  %Estimated kClO_R
    OF=fval; %Minimum objective function


end
```

Published with MATLAB® R2018b

APPENDIX F. GENETIC ALGORITHM AND GEAR’S SOLVER

```
%%%%%%%%%%%%%%%%%%%%%%%%%%%%%%%%%%%%%%%%%%%%%
% This subroutine contains the code example about:                    %
%(1) Implementation of Genetic Algorithm to fit experimental           %
%     data for unknown rate constants estimation                       %
%(2) Implementation of Gear's method to solve sitff odes system using  %
%      estimated rate constants                                        %
%                                                                      %
%Author: Weiqiu Zhang and John Crittenden                              %
%             School of Civil and Environmental Engineering            %
%             Georgia Institute of Technology                          %
%Date: 10/25/2019                                                      %
%                                                                      %
%Input Parameters:                                                     %
%(1)t0:an array stores time points of experiment data                  %
%(2)ExpData: a 2D matrix stores experimental observed time-dependent   %
%                    concentration profiles of target organic compounds %
%(3)pH: pH of experimental condition                                   %
%(4)TOT_HOCl: initial total free chlorine dosage                       %
%(5)Conc_R:initial concentration of target organic compound            %
%(6)LB:an array stores the lower boundary for kCl_R,kCl2_R and kClO_R  %
%(7)UB:an array stores the upper boundary for kCl_R,kCl2_R and kClO_R  %
%(8)ts:time step                                                       %
%Output Parameters:                                                    %
%(1)estk:an array stores the estimated rate constants between:         %
%              (a)chlorine radicals and target organic compound (kCl_R) %
%               (b)dichloride ion radicals and target organic compound (kCl2_R) %
%                    (c)chlorine monoxide radicals and target organic compound
(kClO_R)                                                               %
%(2)OF:minimual objective function                                     %
%(3)Plotting the fitting restuls                                       %
%%%%%%%%%%%%%%%%%%%%%%%%%%%%%%%%%%%%%%%%%%%%%


function [Estk,OF]=GA_Algorithm(t0,ExpData,pH,TOT_HOCl,Conc_R,LB,UB,ts)

      % HOCl and OCl equilibrium
     pka=7.53;   %Free Chlorine pKa
     ratio1=(10^(-pH)/(10^(-pH)+10^(-pka)));  %Fraction of HOCl
     ratio2=(10^(-pka)/(10^(-pH)+10^(-pka))); %Fraction of OCl-


      % Experimental Data
     % Here is an example of simutaneously fitting 3 groups exepermiental data
     ym1=ExpData(1,:);   % First Group Experimental Data
     ym2=ExpData(2,:);   % Second Group Experimental Data
```

```
ym3=ExpData(3,:);   % Third Group Experimantal Data

% Initial experimental conditions of first group experimental data
y01(1)=ratio1*TOT_HOCl(1,1); %HOCl initial concentration
y01(4)=ratio2*TOT_HOCl(1,1); %OCl- initial concentration
y01(13)=TOT_HOCl(1,1);       %Chloride initial concentration
y01(21)=Conc_R;              %Initial target organic compound concentration
%  Initial experimental conditions of second group experimental data
y02(1)=ratio1*TOT_HOCl(1,2);
y02(4)=ratio2*TOT_HOCl(1,2);
y02(13)=TOT_HOCl(1,2);
y02(21)=Conc_R;
% Initial experimental conditions of third group experimental data
y03(1)=ratio1*TOT_HOCl(1,3);
y03(4)=ratio2*TOT_HOCl(1,3);
y03(13)=TOT_HOCl(1,3);
y03(21)=Conc_R;
%Collect all linitial experimental condtions together
Initial_Conditions=[y01;y02;y03];

%Paramenters for genetic algorithm
lb=LB;    % Lower boundaries for kCl_R,kCl2_R and kClO_R
ub=UB;    % Upper boundaries for kCl_R,kCl2_R and kClO_R

%Call objective function
objectfun=@(uk)  objective_rhocl(t0,ExpData,Initial_Conditions,uk,ts);
%Genetic algorithm options setting
%options=optimoptions('ga','MaxGenerations',5,'MaxTime',12,'MaxStallTime',12
);
%Call MATLAB R2018B built-in function ga for Genetic Algorithm
%[estk,fval]=ga(objectfun,3,[],[],[],[],lb,ub,[],options);
 [estk,fval]=ga(objectfun,1,[],[],[],[],lb,ub);

%Print Outputs
Estk(1,1)=estk(1,1);     %Estimated kCl_R
Estk(1,2)=estk(1,2);     %Estimated kCl2_R
Estk(1,3)=estk(1,3);     %Estimated kClO_R

OF=fval;                 %Minimum objective function


% Gear's method to solve stiff odes system using estimated rate constants
%rhocl is the stiff odes eqautions system includes eq B.1 to eq B.4 in Appendix B
(this is an exmple without NOM,and Bicarbonate/Carbonate in water matrix)


% Absolute and Relative error setting for ode solver
```

```
    opt=odeset('RelTol', 1*10^-9, 'AbsTol', 1*10^-20);
    % Call MATLAB R2018b built-in function ode15s for Gear's method
    [t,y1] = ode15s(@rhocl,0:ts:t0(end),y01,opt,estk);
    [t,y2] = ode15s(@rhocl,0:ts:t0(end),y02,opt,estk);
    [t,y3] = ode15s(@rhocl,0:ts:t0(end),y03,opt,estk);

    % Plot the fitting results between model calculation and experimental data
    plot(t0,ym1,'or','LineWidth',2);
    hold on
    plot(t,y1(:,21),'--r','LineWidth',2); %Time-dependent concentration profile
    hold on                               %for target organic compound
    plot(t0,ym2,'ok','LineWidth',2);
    hold on
    plot(t,y2(:,21),'--k','LineWidth',2);
    hold on
    plot(t0,ym3,'ob','LineWidth',2);
    hold on
    plot(t,y3(:,21),'--b','LineWidth',2);
    title('Degradation of organic compound in UV/Free Chlorine')
    xlabel('Time(seconds)','Fontsize',16)
    ylabel('Target Organic Compound Concentration(mole/L)'

end
```

Published with MATLAB® R2018b

APPENDIX G. RADICALS CONCENTRATIONS AND CONTRIBUTION CALCULATION

```
%%%%%%%%%%%%%%%%%%%%%%%%%%%%%%%%%%%%%%%%%%%%%%%%%%%%%%%%
% This subroutine contains the code example about the calculation for the        %
% time-dependent concentration profiles of reactive radicals, and the            %
% average concentration of reactive radicals                                     %
%                                                                                %
%Author: Weiqiu Zhang and John Crittenden                                        %
%       School of Civil and Environmental Engineering                            %
%       Georgia Institute of Technology                                          %
%Date: 10/25/2019                                                                %
%                                                                                %
%Input Parameters:                                                               %
%(1)Y:time-dependent concentration of each species                               %
%(2)tend:the simulation time                                                     %
%(3)ts:time steps                                                                %
%Output Parameters:                                                              %
%(1)Time-dependent concentration profiles of reactive radicals in the            %
%   UV/Free Chlorine process                                                     %
%(2)Average concentrations of reactive radicals in the UV/Free Chlorine          %
%   process                                                                      %
%%%%%%%%%%%%%%%%%%%%%%%%%%%%%%%%%%%%%%%%%%%%%%%%%%%%%%%%

function [Radicals_Ave_Conc]=Radicals(Y,tend,ts)

    %Calculation and plotting for the time-dependent concentration profiles of
    %reactive radicals in the UV/Free Chlorine process
    %Hydroxyl Radicals
    tt=0:ts:tend;
    subplot(2,2,1)
    plot(tt,Y(:,2),'--r','LineWidth',2)
    title('Hydroxyl Radicals vs. Time')
    xlabel('Time(seconds)','Fontsize',16)
    ylabel('Hydroxyl Radicals Concentration(mole/L)')
    hold on
    %Chlorine radicals
    subplot(2,2,2)
    plot(tt,Y(:,3),'--g','LineWidth',2)
    title('Chlorine Radicals vs. Time')
    xlabel('Time(seconds)','Fontsize',16)
    ylabel('Chlorine Radicals Concentration(mole/L)')
    hold on
    %Dichloride Ions Radicals
```

```
subplot(2,2,3)
plot(tt,Y(:,14),'--b','LineWidth',2)
title('Dichloride Ions Radicals vs. Time')
xlabel('Time(seconds)','Fontsize',16)
ylabel('Dichloride Ions Radicals Concentration(mole/L)')
hold on
%Chlorine Monoxide Radicals
subplot(2,2,4)
plot(tt,Y(:,6),'--k','LineWidth',2)
title('Chlorine Monoxide Radicals vs. Time')
xlabel('Time(seconds)','Fontsize',16)
ylabel('Chlorine Monoxide Radicals Concentration(mole/L)')


%Average concentration of reactive radicals in the UV/Free Chlorine
%For hydorxyl radicals
%Integral of hydorxyl radicals concentrations vs.time
OH_Integral=trapz(0:ts:tend,Y(:,2));  % Trapezoidal Integration
%Average concentration of hydorxyl radicals
OH_Ave=OH_Integral/tend;

%For chlorine radicals
%Integral of chlorine radicals concentrations vs.time
Cl_Integral=trapz(0:ts:tend,Y(:,3));
%Average concentration of chlorine radicals
Cl_Ave=Cl_Integral/tend;

%For dichloride ions radicals
%Integral of dichloride ions radicals concentrations vs.time
Cl2_Integral=trapz(0:ts:tend,Y(:,14));
%Average concentration of dichloride ions radicals
Cl2_Ave=Cl2_Integral/tend;

%For chlorine monoxide radicals
%Integral of chlorine monoxide radicals concentrations vs.time
ClO_Integral=trapz(0:ts:tend,Y(:,6));
%Average concentration of monoxide radicals
ClO_Ave=ClO_Integral/tend;

%Print outputs of average concentrations of reactive radicals
Radicals_Ave_Conc=[OH_Ave,Cl_Ave,Cl2_Ave,ClO_Ave];


end
```

Published with MATLAB® R2018b

```
%%%%%%%%%%%%%%%%%%%%%%%%%%%%%%%%%%%%%%%%%%%%%%%%
%This subroutine contains the code example about the calculation for the             %
%time-dependent contributions and average contributions of reactive                   %
%radicals,UV photolysis and free chlorination                                         %
%                                                                                     %
%Author: Weiqiu Zhang and John Crittenden                                             %
%       School of Civil and Environmental Engineering                                 %
%       Georgia Institute of Technology                                               %
%Date: 10/25/2019                                                                     %
%                                                                                     %
%Input Parameters:                                                                    %
%(1)Y:time-dependent concentration of each species                                    %
%(2)tend:the simulation time                                                          %
%(3)ts:time steps                                                                     %
%(4)qR:quantum yield of target organic compound                                       %
%(5)P:UV intensity                                                                    %
%(6)K:an array stores rate constants between:                                         %
%    (a)Hydroxyl radicals and target organic compound (kOH_R)                         %
%    (b)Chlroine radicals and target organic compound (kCl_R)                         %
%    (c)Dichloride ions radicals and target organic compound (kCl2_R)                 %
%    (d)Chlorine monoxide radicals and target organic compound (kClO_R)               %
%    (e)HOCl and target organic compound (kHOCl_R)                                    %
%    (f)OCl and target organic compound (KOCl_R)                                      %
% (7)E:an array stores extinction coefficients of all species that abosrb             %
%     UV light in the system                                                          %
% (8)C:an array stores concentration of all species that abosrb UV light              %
% (9)L:effective path length                                                          %
%Output Parameters:                                                                   %
%(1)Time-dependent contributions of reactive radicals, UV photolysis and              %
%   free chlorination in the UV/Free Chlorine process                                 %
%(2)Average contributions of reactive radicals, UV photolysis and free                %
%   chlorination in the UV/Free Chlorine process                                      %
%%%%%%%%%%%%%%%%%%%%%%%%%%%%%%%%%%%%%%%%%%%%%%%%

function [Ave_Contribute]=Contributions(Y,tend,ts,qR,P,K,E,C,L)


        kOH_R=K(1,1);
        kCl_R=K(1,2);
        kCl2_R=K(1,3);
        kClO_R=K(1,4);
        kHOCl_R=K(1,5);
        kOCl_R=K(1,6);

        %Organic compound destruction rate by UV vs.time
        [~,m]=size(0:ts:tend);
        Absorbance=zeros(m,1);
```

```
[~,n]=size(E);
for i=1:n
  Absorbance=Absorbance+E(1,i)*C(:,i);
end
fraction=(Y(:,21)*E(1,1))./Absorbance;
A=Absorbance*L;
ff=1-10.^(-A);
UV_rate=qR*P.*fraction.*ff;


%Organic compound destruction rate by hydorxyl radicals vs. time
OH_rate=kOH_R*Y(:,2).*Y(:,21);
%Organic compound destruction rate by chlorine radicals vs.time
Cl_rate=kCl_R*Y(:,3).*Y(:,21);
%Organic compound destruction rate by dichloride ions radicals vs.time
Cl2_rate=kCl2_R*Y(:,14).*Y(:,21);
%Organic compound destruction rate by chlorine monoxide radicals vs.time
ClO_rate=kClO_R*Y(:,6).*Y(:,21);
%Organic compound destruction rate by HOCl vs.time
HOCl_rate=kHOCl_R*Y(:,1).*Y(:,21);
%Organic compound destruction rate by OCl vs.time
OCl_rate=kOCl_R*Y(:,4).*Y(:,21);
%Organic compound overall destruction rate
Overall_rate=UV_rate+OH_rate+Cl_rate+Cl2_rate+ClO_rate+HOCl_rate+OCl_r
ate;

%UV contribution vs.time
UV_contribute=UV_rate./Overall_rate;
%Hydroxyl radicals contribution vs.time
OH_contribute=OH_rate./Overall_rate;
%Chlorine radicals contribution vs.time
Cl_contribute=Cl_rate./Overall_rate;
%Dichloride ions radicals contribution vs. time
Cl2_contribute=Cl2_rate./Overall_rate;
%Chlorine monoxide ions radicals contribution vs. time
ClO_contribute=ClO_rate./Overall_rate;
%HOCl/OCl contribution vs.time
Free_chlorine_contribute=(HOCl_rate+OCl_rate)./Overall_rate;

t=0:ts:tend;
UV_contribute(1,1)=0;
OH_contribute(1,1)=0;
Cl_contribute(1,1)=0;
Cl2_contribute(1,1)=0;
ClO_contribute(1,1)=0;
Free_chlorine_contribute(1,1)=0;
```

```
%Plot contributions of UV,reactive radicals and free chlorination vs.time
plot(t,UV_contribute,'--k','LineWidth',4);
hold on
plot(t,OH_contribute,'--r','LineWidth',2);
hold on
plot(t,Cl_contribute,'--g','LineWidth',2);
hold on
plot(t,Cl2_contribute,'--b','LineWidth',8);
hold on
plot(t,ClO_contribute,'--m','LineWidth',2);
hold on
plot(t,Free_chlorine_contribute,'--c','LineWidth',6);
axis([0 tend 0 1]);
%Average contribution of UV photolysis,reactive radicals and free chlorination
%For UV photolysis
UV_contribute(1,1)=0;
%Integral of UV photolysis contribution vs.time
UV_contribute_Integral=trapz(0:ts:tend,UV_contribute);
%Average contribution of UV photolysis
UV_Ave_Contribute=UV_contribute_Integral/tend;

%For hydorxyl radicals
OH_contribute(1,1)=0;
%Integral of hydorxyl radicals contribution vs.time
OH_contribute_Integral=trapz(0:ts:tend,OH_contribute);
%Average contribution of hydorxyl radicals
OH_Ave_Contribute=OH_contribute_Integral/tend;

%For chlorine radicals
Cl_contribute(1,1)=0;
%Integral of chlorine radicals contribution vs.time
Cl_contribute_Integral=trapz(0:ts:tend,Cl_contribute);
%Average contribution of chlorine radicals
Cl_Ave_Contribute=Cl_contribute_Integral/tend;

%For dichloride ions radicals
Cl2_contribute(1,1)=0;
%Integral of dichloride ions radicals contribution vs.time
Cl2_contribute_Integral=trapz(0:ts:tend,Cl2_contribute);
%Average contribution of dichloride ions radicals
Cl2_Ave_Contribute=Cl2_contribute_Integral/tend;

%For chlorine monoxide radicals
ClO_contribute(1,1)=0;
%Integral of chlorine monoxide radicals contribution vs.time
ClO_contribute_Integral=trapz(0:ts:tend,ClO_contribute);
```

```
    %Average contribution of chlorine monoxide radicals
    ClO_Ave_Contribute=ClO_contribute_Integral/tend;

    %For Free chlorine chlorination
    Free_chlorine_contribute(1,1)=0;
    %Integral of chlorine monoxide radicals contribution vs.time
    Free_chlorine_contribute_Integral=trapz(0:ts:tend,Free_chlorine_contribute);
    %Average contribution of chlorine monoxide radicals
    Free_chlorine_Ave_Contribute=Free_chlorine_contribute_Integral/tend;

    Ave_Contribute=[UV_Ave_Contribute*100,OH_Ave_Contribute*100,Cl_Ave_C
    ontribute*100,Cl2_Ave_Contribute*100,ClO_Ave_Contribute*100,Free_chlorine
    _Ave_Contribute*100];


end
```

Published with MATLAB® R2018b

APPENDIX H. EE/O CALCULATION

```
%%%%%%%%%%%%%%%%%%%%%%%%%%%%%%%%%%%%%%%%%%%%%%%%%%%%%%%%%%%%%%%%%%%%%%%%%%%
% This subroutine contains the code example about the calculation for the          %
% minimal EEO with optimal UV intensity and Free Chlorine Dosage, and the          %
% plotting of a heatmap for EE/O                                                   %
%                                                                                  %
%Author: Weiqiu Zhang and John Crittenden                                          %
%       School of Civil and Environmental Engineering                              %
%       Georgia Institute of Technology                                            %
%Date: 10/25/2019                                                                  %
%                                                                                  %
%Input Parameters:                                                                 %
%(1)UV:an array stores UV intensities                                              %
%(2)HOCl:an array stores free chlorine doseages                                    %
%(3)V:UV reactor volume                                                            %
%(4)pH                                                                             %
%(5)Conc_R:initial concentration of target organic compound                        %
%(6)A1:activity coefficient for +1/-1 charged specises                             %
%(7)A2:activity coefficient for +2/-2 charged species                              %
%(8)ts:time steps                                                                  %
%(9)tend:the simulation time                                                       %
%(10)Matrix:concentration of chloride,NOM and bicarbonate/carbonate in             %
%         water materix                                                            %
%Output Parameters:                                                                %
%(1)Time-dependent concentration profiles of reactive radicals in the              %
%   UV/Free Chlorine process                                                       %
%(2)Average concentrations of reactive radicals in the UV/Free Chlorine            %
%   process                                                                        %
%%%%%%%%%%%%%%%%%%%%%%%%%%%%%%%%%%%%%%%%%%%%%%%%%%%%%%%%%%%%%%%%%%%%%%%%%%%
function
    [EEO_Min,UV_OPT,HOCl_OPT]=EEO_UVHOCl(UV,HOCl,V,pH,Conc_R,A1,
    A2,ts,tend,Matrix)
    m=length(UV);
    n=length(HOCl);
    EEO=Inf(m,n);
    Terminate=zeros(m,n);

    % Initial Conditions
    pka_HOCl=7.35;
    %Carbonate Species
    pka_C_1=6.35;
    pka_C_2=10.33;
    a_HCO3=10^(-pka_C_1)*10^(-pH)/((10^(-pH))^2+10^(-pka_C_1)*10^(-
    pH)+10^(-pka_C_1)*10^(-pka_C_2));
    a_CO32=10^(-pka_C_1)*10^(-pka_C_2)/((10^(-pH))^2+10^(-pka_C_1)*10^(-
```

```
pH)+10^(-pka_C_1)*10^(-pka_C_2));

Cl=Matrix(1,1);
NOM=Matrix(1,2);
TOT_C=Matrix(1,3);

for i=2:m
   for j=2:n
   CHOCl=HOCl(j)*(10^(-pH)/(10^(-pH)+10^(-pka_HOCl)));  % HOCl initial
concentration
   COCl=HOCl(j)*(10^(-pka_HOCl)/(10^(-pH)+10^(-pka_HOCl))); %OCl initial
concentration
   y0(1,1)=CHOCl;
   y0(4,1)=COCl;
   y0(13,1)=HOCl(j)+Cl;
   y0(21,1)=Conc_R;
   y0(22,1)=a_HCO3*TOT_C;
   y0(24,1)=a_CO32*TOT_C;
   y0(25,1)=NOM;
   %A=UV(i);
   %B=HOCl(j);
   UVth=i
   Clth=j
  % ODE Slover
  opt=odeset('RelTol', 1*10^-9, 'AbsTol', 1*10^-15);
  [t,y1] = ode15s(@rhocl,0:ts:tend,y0,opt,UV(i),A1,A2);

  %Find the time requried to degrade 90% of organic target compound
  mm=length(y1);
  for k=1:mm
      if(y1(k,21)<=0.1*Conc_R)
        break
      end
  end
  c=y1(k,21);
  logC=log10(Conc_R/c);
  tt=1*(k-1)
  Terminate(i,j)=tt;


  %EEO calculation under each condition
  %1 Einstine is 0.1308 kWh
  %UV light efficiency is 35%
  %Energy used to produce free chlorine is 5.1 kWh/lb

eeo=(((UV(i)*0.1308)/0.35)*tt*V)/(V*logC)+(52.46*(HOCl(j)*0.0022*5.1)/logC
);
```

```
    EEO(i,j)=eeo;
    end
  end

  %Plot heatmap for EEO
  imagesc(HOCl,UV,EEO*1e3)
  set(gca,'YDir','normal')
  colorbar
  xlabel('HOCl Dosage (M)');
  ylabel('UV intensity (Einsteine/L.s)');
  title('UV/HOCl EEO, KWh/m3')

  %find minimal EEO, corrponding UV and HOCl dosage
  EEO_Min=min(min(EEO));
  [minUV_index, minHOCl_index]=find(EEO==min(min(EEO)));
  UV_OPT=UV(minUV_index);
  HOCl_OPT=HOCl(minHOCl_index);
  toc


end
```

Published with MATLAB® R2018b

APPENDIX I. ELEMENTARY REACTIONS FOR CBZ DEGRADATION IN UV/H_2O_2 PROCESS

Table I.1. Elementary Reactions for CBZ degradation in the UV/H_2O_2 process

No.	REACTIONS	RATE CONSTANTS, $M^{-1}\,s^{-1}$ (OR REACTION RATES FOR PHOTOLYSIS REACTIONS, AND EQUILIBRIUM CONSTANTS FOR EQUILIBRIUM REACTIONS)
UV/H_2O_2		
1	$H_2O_2 + h\nu \rightarrow 2HO\bullet$	$r_{HO\bullet} = -2r_{UV,H_2O_2} = 2\phi_{H_2O_2} P_{UV} f_{H_2O_2}\left[1-10^{(-A)}\right]$ $\phi_{H_2O_2,254nm} = 0.5$ $\varepsilon_{H_2O_2,254nm} = 19.6\,M^{-1}cm^{-1}$ $A = \left(\varepsilon_{H_2O_2} C_{H_2O_2} + \varepsilon_R C_R + \varepsilon_{Background} C_{Background}\right)L$ $f_{H_2O_2} = \varepsilon_{H_2O_2} C_{H_2O_2} L / A$
2	$HO\bullet + H_2O_2 \rightarrow HO_2\bullet + H_2O$	$k_2 = 2.7\times10^7$
3	$HO\bullet + HO_2^- \rightarrow HO_2\bullet + OH^-$	$k_3 = 7.5\times10^9$
4	$H_2O_2 + HO_2\bullet \rightarrow H_2O + O_2 + HO\bullet$	$k_4 = 3$
5	$H_2O_2 + O_2^-\bullet \rightarrow OH^- + O_2 + HO\bullet$	$k_5 = 0.13$
6	$HO\bullet + HO\bullet \rightarrow H_2O_2$	$k_6 = 5.5\times10^9$
7	$HO\bullet + HO_2\bullet \rightarrow H_2O + O_2$	$k_7 = 6.6\times10^9$
8	$HO_2\bullet + HO_2\bullet \rightarrow H_2O_2 + O_2$	$k_8 = 8.3\times10^5$
9	$HO_2\bullet + O_2^-\bullet \rightarrow HO_2^- + O_2$	$k_9 = 9.7\times10^7$
10	$HO\bullet + O_2^-\bullet \rightarrow OH^- + O_2$	$k_{10} = 7\times10^9$
In the presence of Cl^-		
11	$OH\bullet + Cl^- \rightarrow ClOH^-\bullet$	$k_{11} = 4.3\times10^9$
12	$ClOH^-\bullet + H^+ \rightarrow Cl\bullet + H_2O$	$k_{12} = 2.1\times10^{10}$
13	$Cl\bullet + H_2O \rightarrow ClOH^-\bullet + H^+$	$k_{13}[H_2O] = 1.3\times10^3\,s^{-1}$
14	$ClOH^-\bullet \rightarrow OH\bullet + Cl^-$	$k_{14} = 6.1\times10^9\,s^{-1}$
15	$ClOH^-\bullet + Cl^- \rightarrow Cl_2^-\bullet + OH^-$	$k_{15} = 1\times10^4$
16	$Cl\bullet + Cl^- \rightarrow Cl_2^-\bullet$	$k_{16} = 8\times10^9$
17	$Cl_2^-\bullet \rightarrow Cl\bullet + Cl^-$	$k_{17} = 5.3\times10^4\,s^{-1}$
18	$Cl\bullet + Cl\bullet \rightarrow Cl_2$	$k_{18} = 8.8\times10^7$

19	$Cl_2^-\bullet + Cl_2^-\bullet \rightarrow Cl_2 + 2Cl^-$	$k_{19} = 6.41\times10^9$
20	$Cl\bullet + Cl_2^-\bullet \rightarrow Cl_2 + Cl^-$	$k_{20} = 2.1\times10^9$
21	$Cl_2^-\bullet + H_2O_2 \rightarrow H^+ + 2Cl^- + HO_2\bullet$	$k_{21} = 1.4\times10^5$
22	$Cl_2^-\bullet + HO_2\bullet \rightarrow H^+ + 2Cl^- + O_2$	$k_{22} = 3\times10^9$
23	$Cl_2^-\bullet + H_2O \rightarrow Cl^- + HClOH$	$k_{23}[H_2O] = 1.3\times10^3\ s^{-1}$
24	$HClOH \rightarrow ClOH\bullet^- + H^+$	$k_{24} = 1.0\times10^2\ s^{-1}$
25	$HClOH \rightarrow Cl\bullet + H_2O$	$k_{25} = 5.0\times10^9\ s^{-1}$
26	$HClOH + Cl^- \rightarrow Cl_2^-\bullet + H_2O$	$k_{26} = 1.0\times10^8$
27	$Cl\bullet + H_2O_2 \rightarrow H^+ + Cl^- + HO_2\bullet$	$k_{27} = 2.0\times10^9$
28	$Cl_2^-\bullet + HO\bullet \rightarrow HClO + Cl^-$	$k_{28} = 1.0\times10^9$
29	$Cl_2 + H_2O \rightarrow HOCl + Cl^- + H^+$	$k_{29}[H_2O] = 15 s^{-1}$
30	$HO\bullet + HOCl \rightarrow ClO\bullet + H_2O$	$k_{30} = 2\times10^9$
31	$HO\bullet + OCl^- \rightarrow ClO\bullet + OH^-$	$k_{31} = 8.8\times10^{10}$
32	$Cl\bullet + HOCl \rightarrow H^+ + Cl^- + ClO\bullet$	$k_{32} = 3.0\times10^9$
33	$Cl\bullet + OCl^- \rightarrow Cl^- + ClO\bullet$	$k_{33} = 8.2\times10^9$
34	$Cl_2^-\bullet + O_2^-\bullet \rightarrow 2Cl^- + O_2$	$k_{34} = 2\times10^9$
In the presence of HCO_3^-		
35	$HO\bullet + HCO_3^- \rightarrow CO_3^-\bullet + H_2O$	$k_{35} = 8.5\times10^6$
36	$HO\bullet + CO_3^{2-} \rightarrow CO_3^-\bullet + OH^-$	$k_{36} = 3.9\times10^9$
37	$H_2O_2 + CO_3^-\bullet \rightarrow HCO_3^- + HO_2\bullet$	$k_{37} = 4.3\times10^5$
38	$HO_2^- + CO_3^-\bullet \rightarrow CO_3^{2-} + HO_2\bullet$	$k_{38} = 3\times10^7$
39	$Cl\bullet + HCO_3^- \rightarrow CO_3^-\bullet + Cl^- + H^+$	$k_{39} = 2.2\times10^8$
40	$Cl\bullet + CO_3^{2-} \rightarrow CO_3^-\bullet + Cl^-$	$k_{40} = 5\times10^8$
41	$HCO_3^- + Cl_2^-\bullet \rightarrow CO_3^-\bullet + H^+ + 2Cl^-$	$k_{41} = 8\times10^7$
42	$CO_3^{2-} + Cl_2^-\bullet \rightarrow CO_3^-\bullet + 2Cl^-$	$k_{42} = 1.6\times10^8$
In the presence of NOM		
43	NOM+HO• $\rightarrow$ byproduct	$k_{HO\bullet/NOM}$ (Fitted)
In the presence of CBZ		
44	CBZ + HO• $\rightarrow$ byproduct	$k_{HO\bullet/CBZ} = 1.28\times10^9$ (Fitted)
45	CBZ + Cl• $\rightarrow$ byproduct	$k_{Cl\bullet/CBZ}$
46	CBZ + $Cl_2^-\bullet$ $\rightarrow$ byproduct	$k_{Cl_2^-\bullet/CBZ}$
47	CBZ + $CO_3^-\bullet$ $\rightarrow$ byproduct	$k_{CO_3^-\bullet/CBZ}$

APPENDIX J. BYPRODUCTS OF TCE OXIDATION IN UV/FREE CHLORINE PROCESS

J.1 Byproducts of TCE Oxidation by Free Chlorine Alone

$CHCl_2COOH$ (Molecule Weight = (12+1+35+35+12+16+16+1) g/mol = 128 g/mol)

LC-Mass m/z under negative ionization charged mode ($[M-H]^-$) is 126.9 g/mol, and hence the detected uncharged molecule weight is 127.9 g/mol.

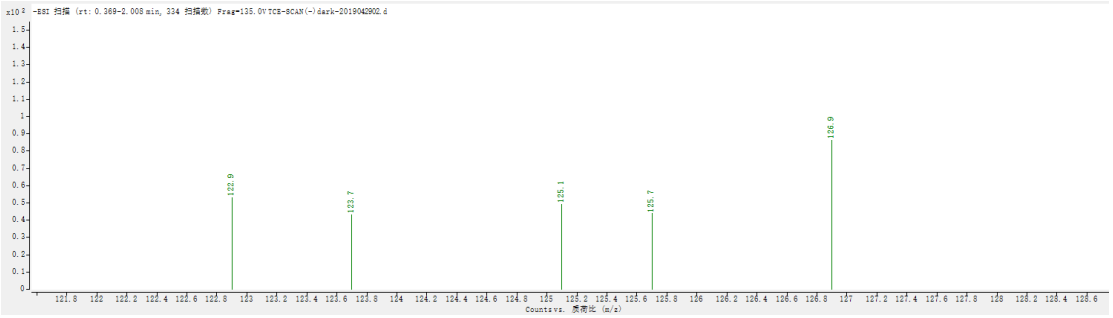

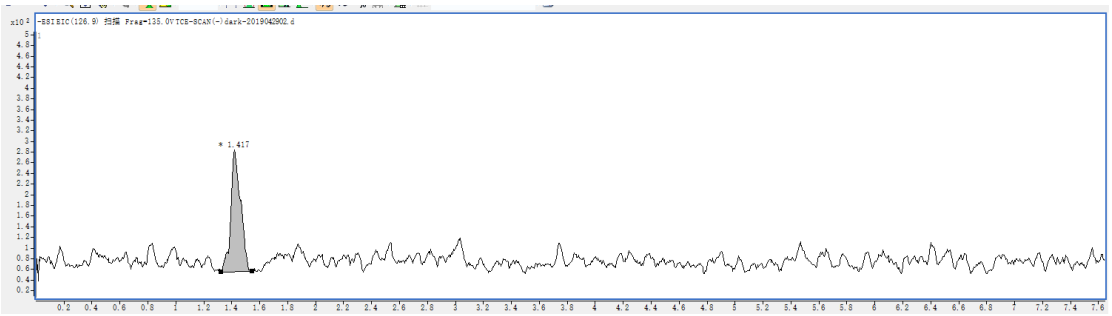

J.2 Byproducts of TCE Oxidation in UV/Free Chlorine Process

(1) CH_3COOH (Molecule Weight = 12 + 1+1+1 + 12 + 16 +16 +1 = 60 g/mol)

The mobile phase of LC-Mass consisted of 1% formic acid, and hence the detected uncharged molecule weight is 105 g/mol – 45 g/mol = 60 g/mol.

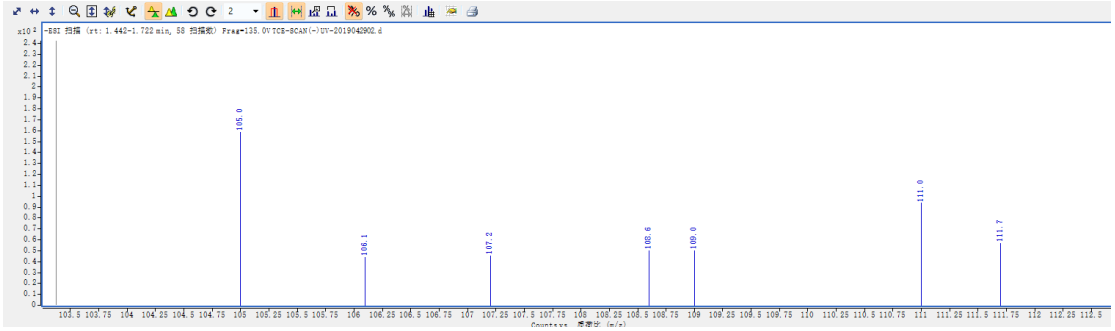

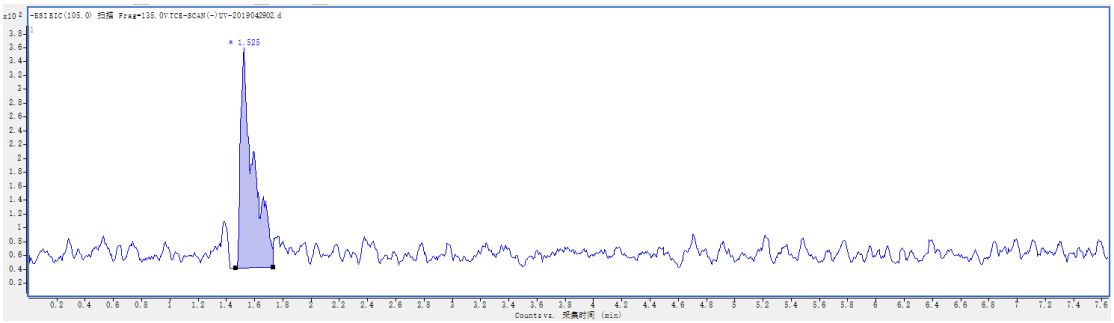

(2) ClC≡CH (Molecule Weight = 12 + 1+1+1 + 12 + 16 +16 +1 = 60 g/mol)

The mobile phase of LC-Mass consisted of 1% formic acid, and hence the detected uncharged molecule weight is 105 g/mol – 45 g/mol = 60 g/mol.

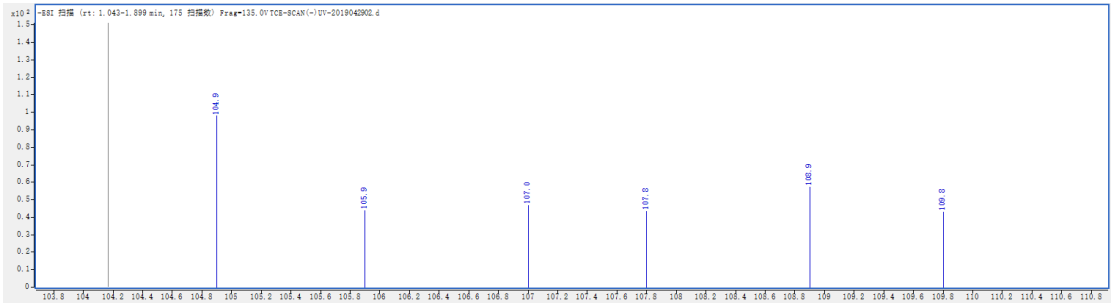

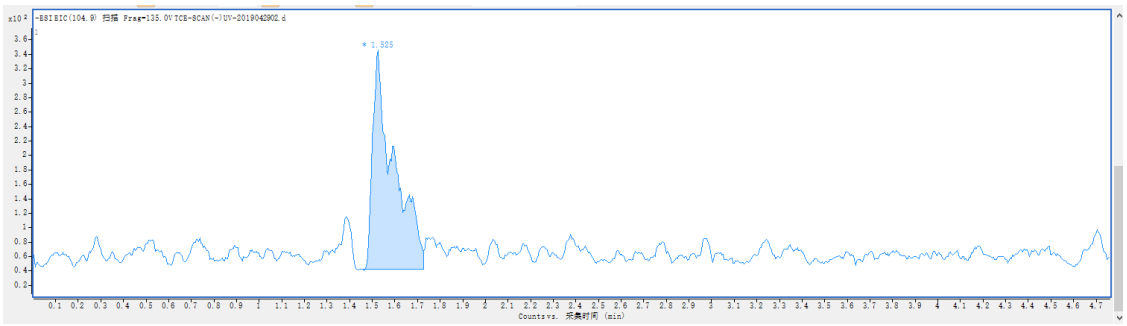

(3) $CHCl_2CHO$ (Molecule Weight = (12+1+35+35+12+1+16) g/mol = 112 g/mol

LC-Mass m/z under negative ionization charged mode ($[M-H]^-$) is 110.9 g/mol, and hence the detected uncharged molecule weight is 111.9 g/mol.

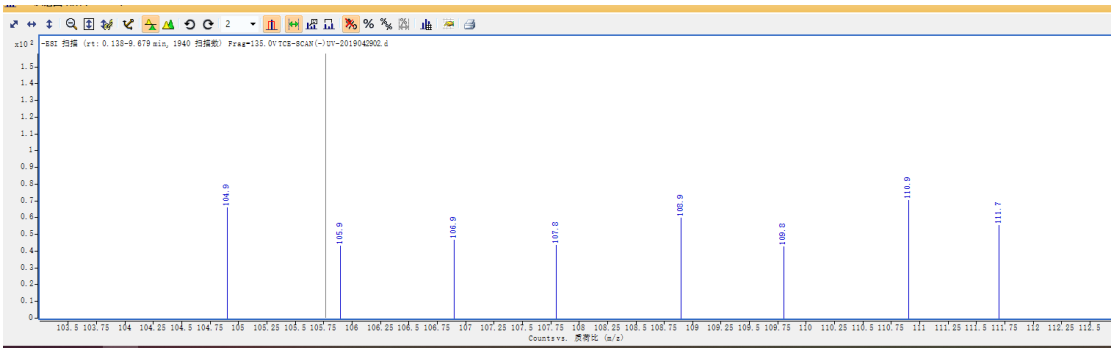

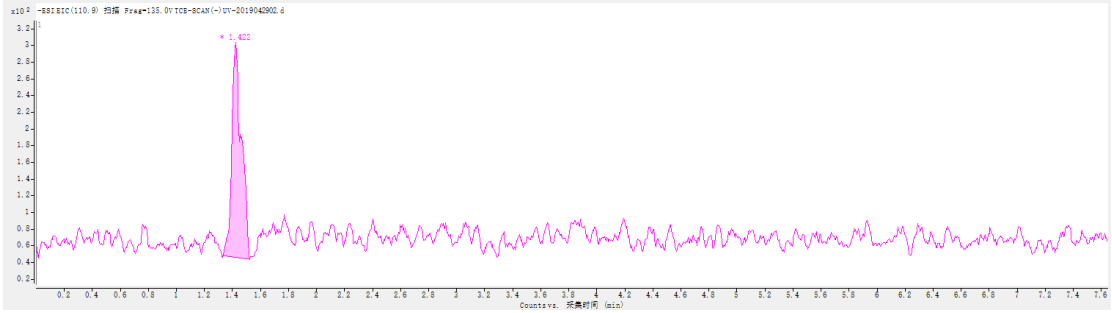

(4) $CHCl_2COOH$ (Molecule Weight = (12+1+35+35+12+16+16+1) g/mol = 128 g/mol)

LC-Mass m/z under negative ionization charged mode ($[M-H]^-$) is 126.9 g/mol, and hence the detected uncharged molecule weight is 127.9 g/mol.

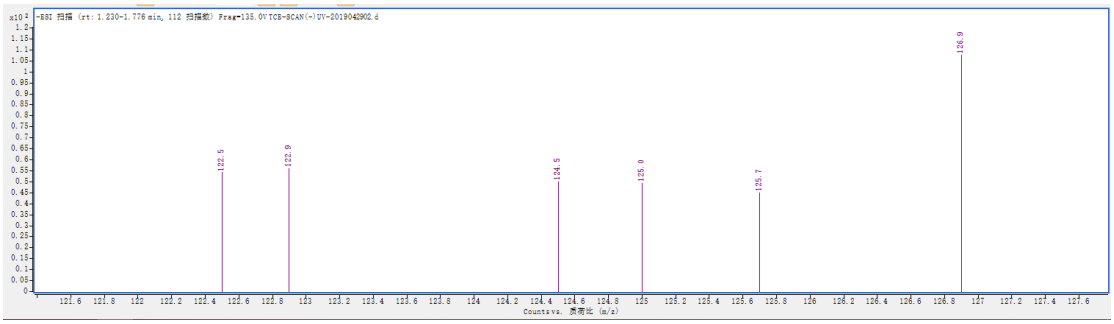

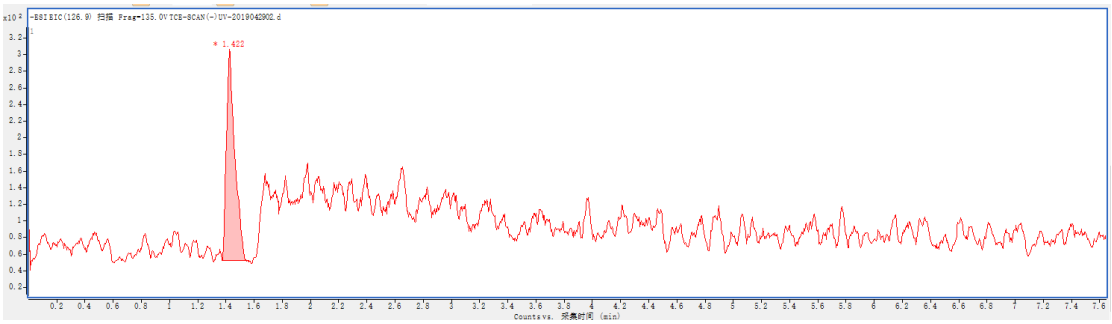

(5) $CHCl_2CHCl(OH)$ (Molecule Weight = (12+1+35+35+12+1+35+16+1) g/mol = 148 g/mol)

LC-Mass m/z under negative ionization charged mode ($[M-H]^-$) is 146.9 g/mol, and hence the detected uncharged molecule weight is 147.9 g/mol.

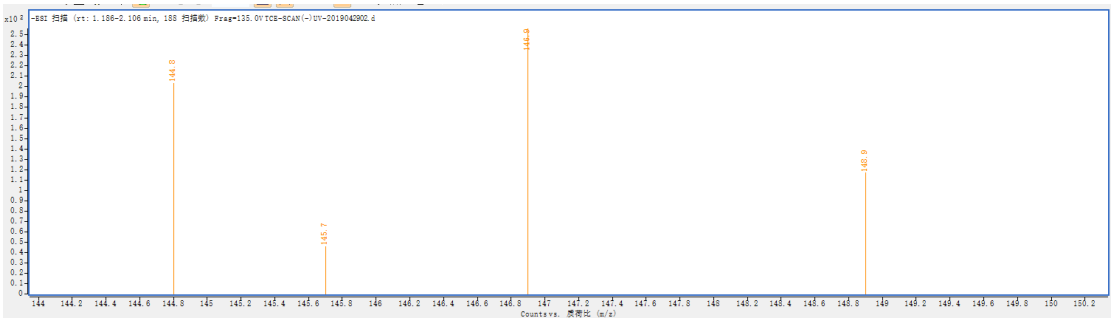

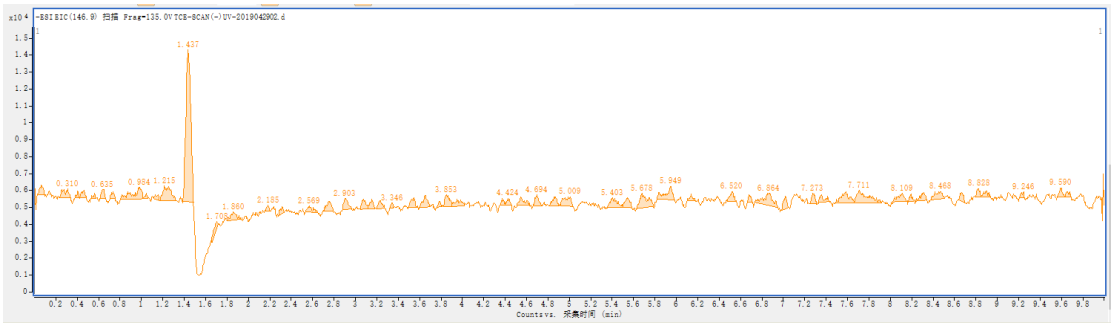

(6) CHCl(OCl)COOH (Molecule Weight = (12+1+35+16+35+12+16+16+1) g/mol = 144 g/mol)

LC-Mass m/z under negative ionization charged mode ($[M-H]^-$) is 142.9 g/mol, and hence the detected uncharged molecule weight is 143.9 g/mol.

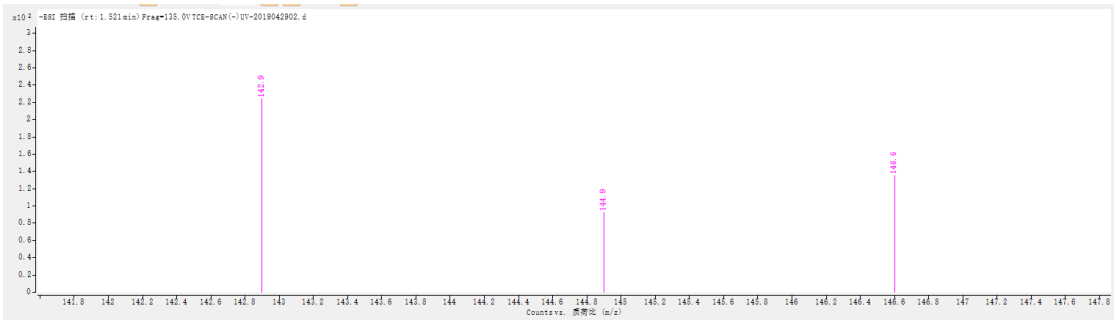

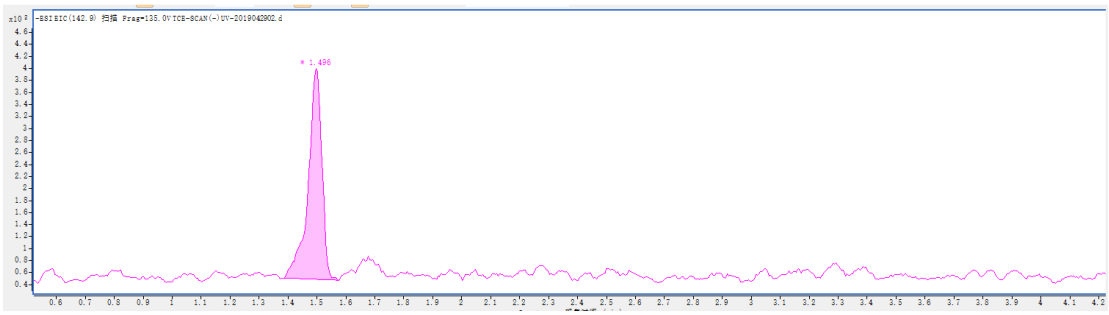

(7) $CHCl_3$

丰 度

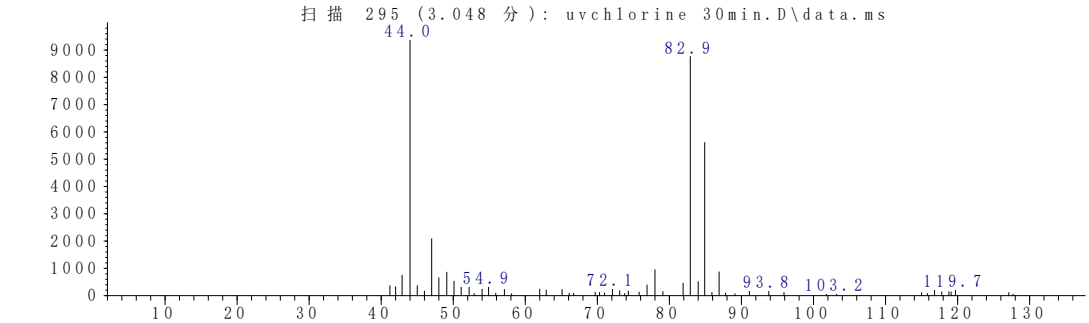

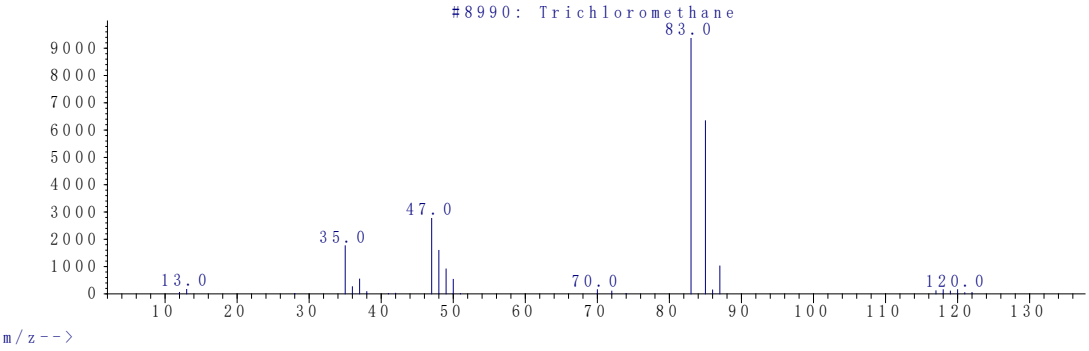

(8) $CHCl_2COCl$

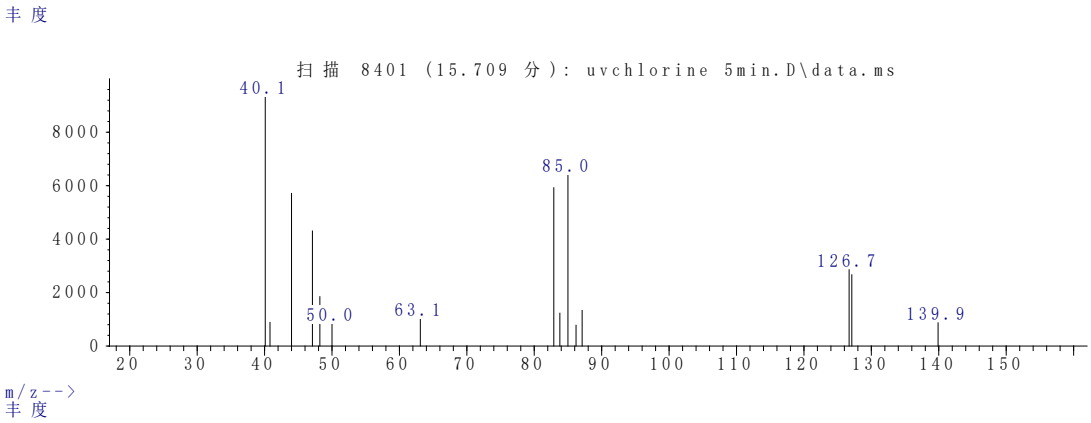
丰 度
扫 描 8401 (15.709 分): uvchlorine 5min.D\data.ms
40.1
85.0
126.7
50.0
63.1
139.9
m/z-->

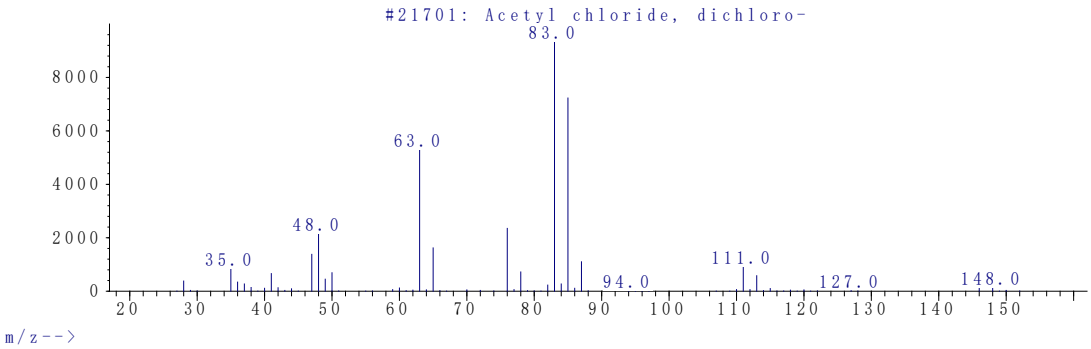
丰 度
#21701: Acetyl chloride, dichloro-
83.0
63.0
48.0
35.0
111.0
94.0
127.0
148.0
m/z-->

APPENDIX K. PATHWAY GENERAOTR CODE (EXAMPLE: HYDROGEN ABSTRACTION BY CHLORINE MONOXIDE RADICALS)

```
////////////////////////////////////////////////////////////////////////////////////////////////////////////////////////////////////////////////
//This subroutine contains the code about the implementation of hydrogen  abstraction   //
// from molecules induced by ClO·                                                        //
//                                                                                       //
// Author: Weiqiu Zhang and John Crittenden                                              //
//        School of Civil and Environmental Engineering                                  //
//        Georgia Institute of Technology                                                //
// Date: 10/25/2019                                                                      //
////////////////////////////////////////////////////////////////////////////////////////////////////////////////////////////////////////////////

void Generator::OCl_ABS(int MR, bool *R)
{
        *R = false;
        if (MR == 1)
        {
                CoReactant = &OCl;
                OCl_ABSHelper(CurReactant->RootPtr(), R);
        }
        else
        {
                if (!strcmp(CurReactant->RootPtr()->Node.Name, AtomC))
                {
                        CoReactant = CurReactant;
                        listNode<moleTree*>* CorPtr = ReactedM.ListHead();
                        while (CorPtr)
                        {
                                CurReactant = new moleTree(*CorPtr->item);
                                OCl_ABSHelper(CurReactant->RootPtr(), R);
                                CorPtr = CorPtr->next;
                        }
                }
        }
}

void Generator::OCl_ABSHelper(treeNode* aNode, bool* Match)
{
    //Determine if there any matched tree node at first
    if (!aNode || !aNode->Child[0])
                return;
        else
        {

                if (!strcmp(aNode->Node.Name, AtomC) || !strcmp(aNode->Node.Name, AtomO))
                {
                        bool HasH = false;
                        int k = 0;
```

```
while (aNode->Child[k] && k < 4)
{
        if (!strcmp(aNode->Child[k]->Node.Name, AtomH))
        {
                HasH = true;
                *Match = true;
                break;
        }
        k++;
}

if (!strcmp(aNode->Node.Name, AtomO) && Complexity < 1)
{
        HasH = false;
}

if (HasH)  //HasH=True indicates matched tree node is found
{
        Prod1 = new moleTree(*CurReactant); //make a copy to operate


       //Find the pointer in Prod1 that point to the atom with aNode->Node.ID.
        int MatchId = aNode->Node.ID;
        treeNode* MatchPtr = new treeNode();

        rtemp = new vector<species*>();
        ptemp = new vector<species*>();
        rsto = new vector<int>();
        psto = new vector<int>();

        //Double check the matched tree node is in Prod1 tree
        MatchPtr = Prod1->FindNode(Prod1->RootPtr(), MatchId);

        if (MatchPtr)
        {//below is the reaction
                MatchPtr->RemoveChild(k);
                MatchPtr->SetR(true);
                MatchPtr->Node.Valence--;

                int size = Prod1->SizeOfTree();
                size--;
                Prod1->SetSize(size);
               //Find the Root tree node for Prod1
                Prod1->KnownRootCanon(MatchPtr);

                //copy for product2 that will change.
                Prod2 = new moleTree(*CoReactant);
                //add valence was done in SetR
                Prod2->RootPtr()->SetR(false);
                //attach H to the root of prod2
                char H[3] = "H";
                nodeItem* Item1 = new nodeItem(H, 0, 0);

                Prod2->AttachChild(Prod2->RootPtr(), *Item1, 1,  SUCCESS1);
                //Prod2->PreOrderTraverse(Disp);
                PostGen(2);
                (*RStr) += " [HA]";
```

```
                                        //Set the rsto and psto vector, and build the reaction class
                                        rsto->push_back(-1);
                                        rsto->push_back(-1);
                                        psto->push_back(1);
                                        psto->push_back(1);
                                        reac = new reaction(rlist.size(), *RStr, true, 0.1, *rtemp, *ptemp,
                                                                *rsto, *psto)
                                        //End

                                        int p = 0;
                                        bool RedR = false;
                                        RedR = StrInList(RStr, Reaction, &p);
                                        if (!RedR)
                                        {
                                                Reaction.ListAppend(*RStr, SUCCESS1);
                                                rlist.push_back(reac);
                                        }


                                }
                        }
                }
                int I = 0;
                while (aNode->Child[I] && I < 4) //Traverse tree in preorder order
                {
                        OCl_ABSHelper(aNode->Child[I], Match);
                        I++;
                }
                return;
        }

}
```

APPENDIX L. GENERATED BYPRODUCTS/INTERMEDIATES AND REACTIONS OF ORGANIC COMPOUNDS DEGRADATION IN THE UV/FREE CHLORINE PROCESS

L.1 Pathways Generated for TCE Degradation in the UV/Free Chlorine Process (Complexity =1)

Table L.1. Species generated for TCE degradation in the UV/free chlorine process (Complexity = 1)

#	SMILES	Species
1	C(ClCl//C(ClH))	CCl_2=CClH
2	O*(H)	HO•
3	O(//O) C*(ClClC(//OH))	O_2
4	Cl*	Cl•
5	O*(Cl)	ClO•
6	Cl-*(Cl)	Cl_2^-•
7	C*(C(ClO(H)H)ClCl)	•CCl_2CHCl(OH)
8	C*(C(ClClH)ClCl)	•CCl_2CHCl_2
9	C*(C(O(Cl)ClH)ClCl)	•CCl_2CHCl(OCl)
10	Cl-	Cl^-
11	C*(ClClC(//OH))	•CCl_2CHO
12	O*(O(C(C(ClClH)ClCl)))	•O$OCCl_2CHCl_2$
13	O*(O(C(C(O(Cl)ClH)ClCl)))	•O$OCCl_2$CHCl(OCl)
14	O*(O(C(ClClC(//OH))))	•O$OCCl_2$CHO
15	O*(C(C(ClClH)ClCl))	•OCCl_2CHCl_2
16	O*(C(C(O(Cl)ClH)ClCl))	•OCCl_2CHCl(OCl)
17	O*(C(ClClC(//OH)))	•OCCl_2CHO
18	C(ClCl//O)	$COCl_2$
19	C(//O//O)	CO_2
20	C*(ClClH)	•$CHCl_2$
21	C(ClClHC(Cl//O))	$CHCl_2$CClO
22	C*(O(Cl)ClH)	•CHCl(OCl)
23	C(C(Cl//O)O(Cl)ClH)	CHCl(OCl)COCl
24	C(Cl//OC(//OH))	CClOCHO
25	C*(//OH)	•CHO
26	C(ClClClH)	$CHCl_3$
27	O*(O(C(ClClH)))	•O$OCHCl_2$
28	C(C(ClClH)O(H)//O)	$CHCl_2$COOH

29	O*(O(C(O(Cl)ClH)))	•OOCHCl(OCl)
30	C(O(Cl)ClHC(O(H)//O))	CHCl(OCl)COOH
31	C(C(//OH)O(H)//O)	OHCCOOH
32	C(//OHO(H))	HCOOH
33	H2O2	H_2O_2
34	*COO-	•COO^-
35	HO2*	HO_2•
36	C*(O(H)O(H)H)	•$CH(OH)_2$
37	C*(ClClCl)	•CCl_3
38	O(HH)	H_2O
39	C(ClClHC(ClClH))	$CHCl_2CHCl_2$
40	C(C(ClClH)O(Cl)ClH)	$CHCl(OCl)CHCl_2$
41	C(ClClHC(//OH))	$CHCl_2CHO$
42	C(ClClHH)	CH_2Cl_2
43	O(ClC(ClHH))	$CH_2Cl(OCl)$
44	Cl(H)	HCl
45	O(ClH)	HOCl
46	O*(C(ClClH))	•$OCHCl_2$
47	C(ClClHO(H))	$CHCl_2(OH)$
48	C*(C(O(H)//O)ClCl)	•CCl_2COOH
49	O*(C(C(ClClH)//O))	•$OCOCHCl_2$
50	O*(C(O(Cl)ClH))	•OCHCl(OCl)
51	C(Cl//OO(Cl))	OClC(OCl)
52	C(O(Cl)ClO(H)H)	CHCl(OH)(OCl)
53	C*(O(Cl)C(O(H)//O)Cl)	•CCl(OCl)COOH
54	O*(C(C(O(Cl)ClH)//O))	•OCOCHCl(OCl)
55	C(O(H)//OC(O(H)//O))	HOOCCOOH
56	O*(O(C(O(H)O(H)H)))	•$OOCH(OH)_2$
57	O*(O(C(ClClCl)))	•$OOCCl_3$
58	C(O(H)O(H)HH)	$CH_2(OH)_2$
59	C*(C(ClClH)O(Cl)Cl)	•$CCl(OCl)CHCl_2$
60	C*(ClClO(H))	•$CCl_2(OH)$
61	C(Cl//OH)	COHCl
62	CO	CO
63	O*(O(C(C(O(H)//O)ClCl)))	•$OOCCl_2COOH$
64	C*(O(Cl)ClO(H))	•CCl(OH)(OCl)
65	C(O(Cl)O(H)//O)	(OCl)COOH
66	O(ClC(//OH))	OHC(OCl)
67	O*(O(C(O(Cl)C(O(H)//O)Cl)))	•OOCCl(OCl)COOH
68	O*(C(ClClCl))	•$OCCl_3$
69	O*(C(O(H)HH))	•$OCH_2(OH)$
70	O*(O(C(C(ClClH)O(Cl)Cl)))	•$OOCCl(OCl)CHCl_2$
71	O*(O(C(ClClO(H))))	•$OOCCl_2(OH)$

72	O*(C(C(O(H)//O)ClCl))	•$OCCl_2COOH$
73	O*(O(C(O(Cl)ClO(H))))	•OOCCl(OH)(OCl)
74	O*(C(O(Cl)C(O(H)//O)Cl))	•OCCl(OCl)COOH
75	O*(C(C(ClClH)O(Cl)Cl))	•$OCCl(OCl)CHCl_2$
76	C(//OHH)	HCHO
77	C*(O(H)//O)	•COOH
78	C(C(Cl//O)O(H)//O)	OClCCOOH
79	C(C(ClClH)O(Cl)//O)	$CHCl_2CO(OCl)$
80	O*(O(C(O(H)//O)))	•OOCOOH
81	C*(C(O(Cl)//O)ClCl)	•$CCl_2CO(OCl)$
82	O*(O(C(C(O(Cl)//O)ClCl)))	•$OOCCl_2CO(OCl)$
83	O*(C(C(O(Cl)//O)ClCl))	•$OCCl_2CO(OCl)$
84	C*(O(Cl)//O)	•CO(OCl)
85	C(C(Cl//O)O(Cl)//O)	OClCCO(OCl)
86	O*(O(C(O(Cl)//O)))	•OOCO(OCl)
87	C(O(Cl)//OC(O(H)//O))	CO(OCl)COOH
88	O*(C(O(Cl)//O))	•OCO(OCl)
89	O*(C(C(O(Cl)//O)//O))	•OCOCO(OCl)
90	OH-	OH^-
91	O-*	O^-•
92	ClOH-*	$ClOH^-$•
93	H+	H^+
94	Cl(Cl)	Cl_2
95	HClOH	HClOH
96	Cl2O2	Cl_2O_2
97	ClO2-	ClO_2^-
98	ClO2*	ClO_2•
99	ClO3-	ClO_3^-
100	C*(//C(ClH)Cl)	•CClCHCl
101	O*(O(C(//C(ClH)Cl)))	•OOCClCHCl
102	O*(C(//C(ClH)Cl))	•OCClCHCl
103	C*(C(Cl//O)ClH)	•CHClCOCl
104	O*(O(C(C(Cl//O)ClH)))	•OOCHClCOCl
105	O*(C(C(Cl//O)ClH))	•OCHClCOCl
106	C(//C(ClH)//O)	COCHCl
107	C(C(ClHH)O(H)//O)	$CH_2ClCOOH$
108	C(C(ClClH)ClO(H)H)	$CHCl_2CHCl(OH)$
109	C(Cl#C(H))	CCl≡CH
110	C(ClC(HHH)//O)	CH_3COCl
111	C(//OC(HHH)O(H))	CH_3COOH
112	C(C(ClClH)ClClO(H))	$CHCl_2CCl_2(OH)$

Table L.2. Elementary reactions generated for TCE degradation in the UV/free chlorine process

#	Reactions	Type
1	$CCl_2{=}CClH + HO\bullet \rightarrow \bullet CCl_2CHCl(OH)$	DA
2	$CCl_2{=}CClH + Cl\bullet \rightarrow \bullet CCl_2CHCl_2$	DA
3	$CCl_2{=}CClH + ClO\bullet \rightarrow \bullet CCl_2CHCl(OCl)$	DA
4	$CCl_2{=}CClH + Cl_2^-\bullet \rightarrow \bullet CCl_2CHCl_2 + Cl^-$	DA
5	$\bullet CCl_2CHCl(OH) \rightarrow \bullet CCl_2CHO + HCl$	XE
6	$\bullet CCl_2CHCl_2 + O_2 \rightarrow \bullet OOCCl_2CHCl_2$	OA
7	$\bullet CCl_2CHCl(OCl) + O_2 \rightarrow \bullet OOCCl_2CHCl(OCl)$	OA
8	$\bullet CCl_2CHO + O_2 \rightarrow \bullet OOCCl_2CHO$	OA
9	$2\ \bullet OOCCl_2CHCl_2 \rightarrow 2\ \bullet OCCl_2CHCl_2 + O_2$	PB3
10	$2\ \bullet OOCCl_2CHCl(OCl) \rightarrow 2\ \bullet OCCl_2CHCl(OCl) + O_2$	PB3
11	$2\ \bullet OOCCl_2CHO \rightarrow 2\ \bullet OCCl_2CHO + O_2$	PB3
12	$COCl_2 + H_2O \rightarrow CO_2 + 2HCl$	S
13	$\bullet OCCl_2CHCl_2 \rightarrow COCl_2 + \bullet CHCl_2$	BS
14	$\bullet OCCl_2CHCl_2 \rightarrow CHCl_2CClO + Cl\bullet$	BS
15	$\bullet OCCl_2CHCl(OCl) \rightarrow COCl_2 + \bullet CHCl(OCl)$	BS
16	$\bullet OCCl_2CHCl(OCl) \rightarrow CHCl(OCl)COCl + Cl\bullet$	BS
17	$\bullet OCCl_2CHO \rightarrow CClOCHO + Cl\bullet$	BS
18	$\bullet OCCl_2CHO \rightarrow COCl_2 + \bullet CHO$	BS
19	$\bullet CHCl_2 + Cl\bullet \rightarrow CHCl_3$	XR
20	$\bullet CHCl_2 + Cl_2^-\bullet \rightarrow CHCl_3 + Cl^-$	XR
21	$\bullet CHCl_2 + O_2 \rightarrow \bullet OOCHCl_2$	OA
22	$CHCl_2CClO + H_2O \rightarrow CHCl_2COOH + HCl$	HX
23	$\bullet CHCl(OCl) + O_2 \rightarrow \bullet OOCHCl(OCl)$	OA
24	$CHCl(OCl)COCl + H_2O \rightarrow CHCl(OCl)COOH + HCl$	HX
25	$OHCCOOH + H_2O_2 \rightarrow HCOOH + CO_2 + H_2O$	S
26	$HCOOH + HO\bullet \rightarrow \bullet COO^- + H^+ + H_2O$	S
27	$\bullet COO^- + O_2 + H^+ \rightarrow CO_2 + HO_2\bullet$	S
28	$\bullet COO^- + H_2O_2 \rightarrow CO_2 + H_2O + HO\bullet$	S
29	$CClOCHO + H_2O \rightarrow OHCCOOH + HCl$	HX
30	$\bullet CHO + H_2O \rightarrow \bullet CH(OH)_2$	HC
31	$CHCl_3 + HO\bullet \rightarrow \bullet CCl_3 + H_2O$	HA
32	$CHCl_3 + \bullet CCl_2CHCl_2 \rightarrow \bullet CCl_3 + CHCl_2CHCl_2$	HA
33	$CHCl_3 + \bullet CCl_2CHCl(OCl) \rightarrow \bullet CCl_3 + CHCl(OCl)CHCl_2$	HA
34	$CHCl_3 + \bullet CCl_2CHO \rightarrow \bullet CCl_3 + CHCl_2CHO$	HA
35	$CHCl_3 + \bullet CHCl_2 \rightarrow \bullet CCl_3 + CH_2Cl_2$	HA
36	$CHCl_3 + \bullet CHCl(OCl) \rightarrow \bullet CCl_3 + CH_2Cl(OCl)$	HA
37	$CHCl_3 + Cl\bullet \rightarrow \bullet CCl_3 + HCl$	HA
38	$CHCl_3 + \bullet ClO \rightarrow \bullet CCl_3 + HOCl$	HA
39	$CHCl_3 + Cl_2^-\bullet \rightarrow \bullet CCl_3 + Cl^- + HCl$	HA
40	$2\ \bullet OOCHCl_2 \rightarrow 2\ \bullet OCHCl_2 + O_2$	PB3

41	2 •$OOCHCl_2$ → 2 $COCl_2$ + H_2O_2	PB2
42	2 •$OOCHCl_2$ → $COCl_2$ + $CHCl_2(OH)$ + O_2	PB1
43	$CHCl_2COOH$ + HO• → •CCl_2COOH+ H_2O	HA
44	$CHCl_2COOH$ + HO• → •$OCOCHCl_2$ + H_2O	HA
45	$CHCl_2COOH$ + •CCl_2CHCl_2 → •CCl_2COOH+ $CHCl_2CHCl_2$	HA
46	$CHCl_2COOH$ + •CCl_2CHCl_2 → •$OCOCHCl_2$ + $CHCl_2CHCl_2$	HA
47	$CHCl_2COOH$ + •$CCl_2CHCl(OCl)$ → •CCl_2COOH + $CHCl(OCl)CHCl_2$	HA
48	$CHCl_2COOH$ + •$CCl_2CHCl(OCl)$ → •$OCOCHCl_2$ + $CHCl(OCl)CHCl_2$	HA
49	$CHCl_2COOH$ + •CCl_2CHO → •CCl_2COOH + $CHCl_2CHO$	HA
50	$CHCl_2COOH$ + •CCl_2CHO → •$OCOCHCl_2$ + $CHCl_2CHO$	HA
51	$CHCl_2COOH$ + •$CHCl_2$ → •CCl_2COOH + CH_2Cl_2	HA
52	$CHCl_2COOH$ + •$CHCl_2$ → •$OCOCHCl_2$ + CH_2Cl_2	HA
53	$CHCl_2COOH$ + •$CHCl(OCl)$ → •CCl_2COOH + $CH_2Cl(OCl)$	HA
54	$CHCl_2COOH$ + •$CHCl(OCl)$ → •$OCOCHCl_2$ + $CH_2Cl(OCl)$	HA
55	$CHCl_2COOH$ + Cl• → •CCl_2COOH + HCl	HA
56	$CHCl_2COOH$ + Cl• → •$OCOCHCl_2$ + HCl	HA
57	$CHCl_2COOH$ + ClO• → •CCl_2COOH + HOCl	HA
58	$CHCl_2COOH$ + ClO• → •$OCOCHCl_2$ + HOCl	HA
59	$CHCl_2COOH$ + Cl_2^-• → •CCl_2COOH + Cl^- + HCl	HA
60	$CHCl_2COOH$ + Cl_2^-• → •$OCOCHCl_2$ + Cl^- + HCl	HA
61	2 •$OOCHCl(OCl)$ → 2 •$OCHCl(OCl)$ + O_2	PB3
62	2 •$OOCHCl(OCl)$ → 2 $OClC(OCl)$ + H_2O_2	PB2
63	2 •$OOCHCl(OCl)$ → $OClC(OCl)$ + $CHCl(OH)(OCl)$ + O_2	PB1
64	$CHCl(OCl)COOH$ + HO• → •$CCl(OCl)COOH$ + H_2O	HA
65	$CHCl(OCl)COOH$ + HO• → •$OCOCHCl(OCl)$ + H_2O	HA
66	$CHCl(OCl)COOH$ + •CCl_2CHCl_2 → •$CCl(OCl)COOH$ + $CHCl_2CHCl_2$	HA
67	$CHCl(OCl)COOH$ + •CCl_2CHCl_2 → •$OCOCHCl(OCl)$ + $CHCl_2CHCl_2$	HA
68	$CHCl(OCl)COOH$ + •$CCl_2CHCl(OCl)$ → •$CCl(OCl)COOH$ + $CHCl(OCl)CHCl_2$	HA
69	$CHCl(OCl)COOH$ + •$CCl_2CHCl(OCl)$ → •$OCOCHCl(OCl)$ + $CHCl(OCl)CHCl_2$	HA
70	$CHCl(OCl)COOH$ + •CCl_2CHO → •$CCl(OCl)COOH$ + $CHCl_2CHO$	HA
71	$CHCl(OCl)COOH$ + •CCl_2CHO → •$OCOCHCl(OCl)$ + $CHCl_2CHO$	HA
72	$CHCl(OCl)COOH$ + •$CHCl_2$ → •$CCl(OCl)COOH$ + CH_2Cl_2	HA
73	$CHCl(OCl)COOH$ + •$CHCl_2$ → •$OCOCHCl(OCl)$ + CH_2Cl_2	HA
74	$CHCl(OCl)COOH$ + •$CHCl(OCl)$ → •$CCl(OCl)COOH$ + $CH_2Cl(OCl)$	HA
75	$CHCl(OCl)COOH$ + •$CHCl(OCl)$ → •$OCOCHCl(OCl)$ + $CH_2Cl(OCl)$	HA
76	$CHCl(OCl)COOH$ + Cl• → •$CCl(OCl)COOH$ + HCl	HA
77	$CHCl(OCl)COOH$ + Cl• → •$OCOCHCl(OCl)$ + HCl	HA
78	$CHCl(OCl)COOH$ + ClO• → •$CCl(OCl)COOH$ + HOCl	HA
79	$CHCl(OCl)COOH$ + ClO• → •$OCOCHCl(OCl)$ + HOCl	HA
80	$CHCl(OCl)COOH$ + Cl_2^-• → •$CCl(OCl)COOH$ + Cl^- + HCl	HA
81	$CHCl(OCl)COOH$ + Cl_2^-• → •$OCOCHCl(OCl)$ + Cl^- + HCl	HA
82	HOOCCOOH + HO• → CO_2 + •COO^- + H_2O + H^+	S

83	$OHCCOOH + H_2O \rightarrow HOOCCOOH$	HC
84	$\bullet CH(OH)_2 + O_2 \rightarrow \bullet OOCH(OH)_2$	OA
85	$\bullet CCl_3 + O_2 \rightarrow \bullet OOCCl_3$	OA
86	$CHCl_2CHCl_2 + HO\bullet \rightarrow \bullet CCl_2CHCl_2 + H_2O$	HA
87	$CHCl_2CHCl_2 + \bullet CCl_2CHCl(OCl) \rightarrow \bullet CCl_2CHCl_2 + CHCl(OCl)CHCl_2$	HA
88	$CHCl_2CHCl_2 + \bullet CCl_2CHO \rightarrow \bullet CCl_2CHCl_2 + CHCl_2CHO$	HA
89	$CHCl_2CHCl_2 + \bullet CHCl_2 \rightarrow \bullet CCl_2CHCl_2 + CH_2Cl_2$	HA
90	$CHCl_2CHCl_2 + \bullet CHCl(OCl) \rightarrow \bullet CCl_2CHCl_2 + CH_2Cl(OCl)$	HA
91	$CHCl_2CHCl_2 + \bullet CH(OH)_2 \rightarrow \bullet CCl_2CHCl_2 + CH_2(OH)_2$	HA
92	$CHCl_2CHCl_2 + \bullet CCl_3 \rightarrow \bullet CCl_2CHCl_2 + CHCl_3$	HA
93	$CHCl_2CHCl_2 + Cl\bullet \rightarrow \bullet CCl_2CHCl_2 + HCl$	HA
94	$CHCl_2CHCl_2 + ClO\bullet \rightarrow \bullet CCl_2CHCl_2 + HOCl$	HA
95	$CHCl_2CHCl_2 + Cl_2^-\bullet \rightarrow \bullet CCl_2CHCl_2 + Cl^- + HCl$	HA
96	$CHCl(OCl)CHCl_2 + HO\bullet \rightarrow \bullet CCl(OCl)CHCl_2 + H_2O$	HA
97	$CHCl(OCl)CHCl_2 + HO\bullet \rightarrow \bullet CCl_2CHCl(OCl) + H_2O$	HA
98	$CHCl(OCl)CHCl_2 + \bullet CCl_2CHCl_2 \rightarrow \bullet CCl(OCl)CHCl_2 + CHCl_2CHCl_2$	HA
99	$CHCl(OCl)CHCl_2 + \bullet CCl_2CHCl_2 \rightarrow \bullet CCl_2CHCl(OCl) + CHCl_2CHCl_2$	HA
100	$CHCl(OCl)CHCl_2 + \bullet CCl_2CHO \rightarrow \bullet CCl(OCl)CHCl_2 + CHCl_2CHO$	HA
101	$CHCl(OCl)CHCl_2 + \bullet CCl_2CHO \rightarrow \bullet CCl_2CHCl(OCl) + CHCl_2CHO$	HA
102	$CHCl(OCl)CHCl_2 + \bullet CHCl_2 \rightarrow \bullet CCl(OCl)CHCl_2 + CH_2Cl_2$	HA
103	$CHCl(OCl)CHCl_2 + \bullet CHCl_2 \rightarrow \bullet CCl_2CHCl(OCl) + CH_2Cl_2$	HA
104	$CHCl(OCl)CHCl_2 + \bullet CHCl(OCl) \rightarrow \bullet CCl(OCl)CHCl_2 + CH_2Cl(OCl)$	HA
105	$CHCl(OCl)CHCl_2 + \bullet CHCl(OCl) \rightarrow \bullet CCl_2CHCl(OCl) + CH_2Cl(OCl)$	HA
106	$CHCl(OCl)CHCl_2 + \bullet CH(OH)_2 \rightarrow \bullet CCl(OCl)CHCl_2 + CH_2(OH)_2$	HA
107	$CHCl(OCl)CHCl_2 + \bullet CH(OH)_2 \rightarrow \bullet CCl_2CHCl(OCl) + CH_2(OH)_2$	HA
108	$CHCl(OCl)CHCl_2 + \bullet CCl_3 \rightarrow \bullet CCl(OCl)CHCl_2 + CHCl_3$	HA
109	$CHCl(OCl)CHCl_2 + \bullet CCl_3 \rightarrow \bullet CCl_2CHCl(OCl) + CHCl_3$	HA
110	$CHCl(OCl)CHCl_2 + Cl\bullet \rightarrow \bullet CCl(OCl)CHCl_2 + HCl$	HA
111	$CHCl(OCl)CHCl_2 + Cl\bullet \rightarrow \bullet CCl_2CHCl(OCl) + HCl$	HA
112	$CHCl(OCl)CHCl_2 + ClO\bullet \rightarrow \bullet CCl(OCl)CHCl_2 + HOCl$	HA
113	$CHCl(OCl)CHCl_2 + ClO\bullet \rightarrow \bullet CCl_2CHCl(OCl) + HOCl$	HA
114	$CHCl(OCl)CHCl_2 + Cl_2^-\bullet \rightarrow \bullet CCl(OCl)CHCl_2 + Cl^- + HCl$	HA
115	$CHCl(OCl)CHCl_2 + Cl_2^-\bullet \rightarrow \bullet CCl_2CHCl(OCl) + Cl^- + HCl$	HA
116	$CHCl_2CHO + H_2O \rightarrow CHCl_2COOH$	HC
117	$CH_2Cl_2 + HO\bullet \rightarrow \bullet CHCl_2 + H_2O$	HA
118	$CH_2Cl_2 + \bullet CCl_2CHCl_2 \rightarrow \bullet CHCl_2 + CHCl_2CHCl_2$	HA
119	$CH_2Cl_2 + \bullet CCl_2CHCl(OCl) \rightarrow \bullet CHCl_2 + CHCl(OCl)CHCl_2$	HA
120	$CH_2Cl_2 + \bullet CCl_2CHO \rightarrow \bullet CHCl_2 + CHCl_2CHO$	HA
121	$CH_2Cl_2 + \bullet CHCl(OCl) \rightarrow \bullet CHCl_2 + CH_2Cl(OCl)$	HA
122	$CH_2Cl_2 + \bullet CH(OH)_2 \rightarrow \bullet CHCl_2 + CH_2Cl_2$	HA
123	$CH_2Cl_2 + \bullet CCl_3 \rightarrow \bullet CHCl_2 + CHCl_3$	HA
124	$CH_2Cl_2 + Cl\bullet \rightarrow \bullet CHCl_2 + HCl$	HA
125	$CH_2Cl_2 + ClO\bullet \rightarrow \bullet CHCl_2 + HOCl$	HA
126	$CH_2Cl_2 + Cl_2^-\bullet \rightarrow \bullet CHCl_2 + Cl^- + HCl$	HA

127	$CH_2Cl(OCl) + HO\bullet \rightarrow \bullet CHCl(OCl) + H_2O$	HA
128	$CH_2Cl(OCl) + \bullet CCl_2CHCl_2 \rightarrow \bullet CHCl(OCl) + CHCl_2CHCl_2$	HA
129	$CH_2Cl(OCl) + \bullet CCl_2CHCl(OCl) \rightarrow \bullet CHCl(OCl) + CHCl(OCl)CHCl_2$	HA
130	$CH_2Cl(OCl) + \bullet CCl_2CHO \rightarrow \bullet CHCl(OCl) + CHCl_2CHO$	HA
131	$CH_2Cl(OCl) + \bullet CHCl_2 \rightarrow \bullet CHCl(OCl) + CH_2Cl_2$	HA
132	$CH_2Cl(OCl) + \bullet CH(OH)_2 \rightarrow \bullet CHCl(OCl) + CH_2(OH)_2$	HA
133	$CH_2Cl(OCl) + \bullet CCl_3 \rightarrow \bullet CHCl(OCl) + CHCl_3$	HA
134	$CH_2Cl(OCl) + Cl\bullet \rightarrow \bullet CHCl(OCl) + HCl$	HA
135	$CH_2Cl(OCl) + ClO\bullet \rightarrow \bullet CHCl(OCl) + HOCl$	HA
136	$CH_2Cl(OCl) + Cl_2^-\bullet \rightarrow \bullet CHCl(OCl) + Cl^- + HCl$	HA
137	$\bullet OCHCl_2 \rightarrow \bullet CCl_2(OH)$	OT
138	$COHCl \rightarrow HCl + CO$	S
139	$\bullet OCHCl_2 \rightarrow COHCl + Cl\bullet$	BS
140	$CHCl_2(OH) \rightarrow COHCl + HCl$	XE
141	$\bullet CCl_2COOH + O_2 \rightarrow \bullet OOCCl_2COOH$	OA
142	$\bullet OCOCHCl_2 \rightarrow CO_2 + \bullet CHCl_2$	BS
143	$\bullet OCHCl(OCl) \rightarrow \bullet CCl(OH)(OCl)$	OT
144	$\bullet OCHCl(OCl) \rightarrow COHCl + ClO\bullet$	BS
145	$\bullet OCHCl(OCl) \rightarrow OHC(OCl) + Cl\bullet$	BS
146	$(OCl)COOH \rightarrow CO_2 + HOCl$	S
147	$OClC(OCl) + H_2O \rightarrow (OCl)COOH + HCl$	HX
148	$CHCl(OH)(OCl) \rightarrow OHC(OCl) + HCl$	XE
149	$\bullet CCl(OCl)COOH + O_2 \rightarrow \bullet OOCCl(OCl)COOH$	OA
150	$\bullet OCOCHCl(OCl) \rightarrow CO_2 + \bullet CHCl(OCl)s$	BS
151	$\bullet OOCH(OH)_2 \rightarrow HCOOH + HO_2\bullet$	PH
152	$2 \bullet OOCCl_3 \rightarrow 2 \bullet OCCl_3 + O_2$	PB3
153	$CH_2(OH)_2 + HO\bullet \rightarrow \bullet CH(OH)_2 + H_2O$	HA
154	$CH_2(OH)_2 + HO\bullet \rightarrow \bullet OCH_2(OH) + H_2O$	HA
155	$CH_2(OH)_2 + \bullet CCl_2CHCl_2 \rightarrow \bullet CH(OH)_2 + CHCl_2CHCl_2$	HA
156	$CH_2(OH)_2 + \bullet CCl_2CHCl_2 \rightarrow \bullet OCH_2(OH) + CHCl_2CHCl_2$	HA
157	$CH_2(OH)_2 + \bullet CCl_2CHCl(OCl) \rightarrow \bullet CH(OH)_2 + CHCl(OCl)CHCl_2$	HA
158	$CH_2(OH)_2 + \bullet CCl_2CHCl(OCl) \rightarrow \bullet OCH_2(OH) + CHCl(OCl)CHCl_2$	HA
159	$CH_2(OH)_2 + \bullet CCl_2CHO \rightarrow \bullet CH(OH)_2 + CHCl_2CHO$	HA
160	$CH_2(OH)_2 + \bullet CCl_2CHO \rightarrow \bullet OCH_2(OH) + CHCl_2CHO$	HA
161	$CH_2(OH)_2 + \bullet CHCl_2 \rightarrow \bullet CH(OH)_2 + CH_2Cl_2$	HA
162	$CH_2(OH)_2 + \bullet CHCl_2 \rightarrow \bullet OCH_2(OH) + CH_2Cl_2$	HA
163	$CH_2(OH)_2 + \bullet CHCl(OCl) \rightarrow \bullet CH(OH)_2 + CH_2Cl(OCl)$	HA
164	$CH_2(OH)_2 + \bullet CHCl(OCl) \rightarrow \bullet OCH_2(OH) + CH_2Cl(OCl)$	HA
165	$CH_2(OH)_2 + \bullet CCl_3 \rightarrow \bullet CH(OH)_2 + CHCl_3$	HA
166	$CH_2(OH)_2 + \bullet CCl_3 \rightarrow \bullet OCH_2(OH) + CHCl_3$	HA
167	$CH_2(OH)_2 + \bullet CCl_2COOH \rightarrow \bullet CH(OH)_2 + CHCl_2COOH$	HA
168	$CH_2(OH)_2 + \bullet CCl_2COOH \rightarrow \bullet OCH_2(OH) + CHCl_2COOH$	HA
169	$CH_2(OH)_2 + \bullet CCl(OCl)COOH \rightarrow \bullet CH(OH)_2 + CHCl(OCl)COOH$	HA
170	$CH_2(OH)_2 + \bullet CCl(OCl)COOH \rightarrow \bullet OCH_2(OH) + CHCl(OCl)COOH$	HA

171	$CH_2(OH)_2 + Cl\bullet \rightarrow \bullet CH(OH)_2 + HCl$	HA
172	$CH_2(OH)_2 + Cl\bullet \rightarrow \bullet OCH_2(OH) + HCl$	HA
173	$CH_2(OH)_2 + ClO\bullet \rightarrow \bullet CH(OH)_2 + HOCl$	HA
174	$CH_2(OH)_2 + ClO\bullet \rightarrow \bullet OCH_2(OH) + HOCl$	HA
175	$CH_2(OH)_2 + Cl_2^-\bullet \rightarrow \bullet CH(OH)_2 + Cl^- + HCl$	HA
176	$CH_2(OH)_2 + Cl_2^-\bullet \rightarrow \bullet OCH_2(OH) + Cl^- + HCl$	HA
177	$\bullet CCl(OCl)CHCl_2 + O_2 \rightarrow \bullet OOCCl(OCl)CHCl_2$	OA
178	$\bullet CCl_2(OH) + O_2 \rightarrow \bullet OOCCl_2(OH)$	OA
179	$2\ \bullet OOCCl_2COOH \rightarrow 2\ \bullet OCCl_2COOH + O_2$	PB3
180	$\bullet CCl(OH)(OCl) + O_2 \rightarrow \bullet OOCCl(OH)(OCl)$	OA
181	$OHC(OCl) + H_2O \rightarrow (OCl)COOH$	HC
182	$2\ \bullet OOCCl(OCl)COOH \rightarrow 2\ \bullet OCCl(OCl)COOH + O_2$	PB3
183	$\bullet OCCl_3 \rightarrow COCl_2 + Cl\bullet$	BS
184	$\bullet OCH_2(OH) \rightarrow HCHO + HO\bullet$	BS
185	$2\ \bullet OOCCl(OCl)CHCl_2 \rightarrow 2\ \bullet OCCl(OCl)CHCl_2 + O_2$	PB3
186	$\bullet OOCCl_2(OH) \rightarrow COCl_2 + HO_2\bullet$	PH
187	$\bullet OCCl_2COOH \rightarrow COCl_2 + \bullet COOH$	BS
188	$\bullet OCCl_2COOH \rightarrow OClCCOOH + Cl\bullet$	BS
189	$\bullet OOCCl(OH)(OCl) \rightarrow OClC(OCl) + HO_2\bullet$	PH
190	$\bullet OCCl(OCl)COOH \rightarrow OClCCOOH + ClO\bullet$	BS
191	$\bullet OCCl(OCl)COOH \rightarrow OClC(OCl) + \bullet COOH$	BS
192	$HCHO + H_2O \rightarrow HCOOH$	HC
193	$\bullet OCCl(OCl)CHCl_2 \rightarrow OClC(OCl) + \bullet CHCl_2$	BS
194	$\bullet OCCl(OCl)CHCl_2 \rightarrow CHCl_2CClO + ClO\bullet$	BS
195	$\bullet OCCl(OCl)CHCl_2 \rightarrow CHCl_2CO(OCl) + Cl\bullet$	BS
196	$\bullet COOH + O_2 \rightarrow \bullet OOCOOH$	OA
197	$OClCCOOH + H_2O \rightarrow HOOCCOOH + HCl$	HX
198	$CHCl_2CO(OCl) + HO\bullet \rightarrow \bullet CCl_2CO(OCl) + H_2O$	HA
199	$CHCl_2CO(OCl) + \bullet CCl_2CHCl_2 \rightarrow \bullet CCl_2CO(OCl) + CHCl_2CHCl_2$	HA
200	$CHCl_2CO(OCl) + \bullet CCl_2CHCl(OCl) \rightarrow \bullet CCl_2CO(OCl) + CHCl(OCl)CHCl_2$	HA
201	$CHCl_2CO(OCl) + \bullet CCl_2CHO \rightarrow \bullet CCl_2CO(OCl) + CHCl_2CHO$	HA
202	$CHCl_2CO(OCl) + \bullet CHCl_2 \rightarrow \bullet CCl_2CO(OCl) + CH_2Cl_2$	HA
203	$CHCl_2CO(OCl) + \bullet CHCl(OCl) \rightarrow \bullet CCl_2CO(OCl) + CH_2Cl(OCl)$	HA
204	$CHCl_2CO(OCl) + \bullet CH(OH)_2 \rightarrow \bullet CCl_2CO(OCl) + CH_2(OH)_2$	HA
205	$CHCl_2CO(OCl) + \bullet CCl_3 \rightarrow \bullet CCl_2CO(OCl) + CHCl_3$	HA
206	$CHCl_2CO(OCl) + \bullet CCl_2COOH \rightarrow \bullet CCl_2CO(OCl) + CHCl_2COOH$	HA
207	$CHCl_2CO(OCl) + \bullet CCl(OCl)COOH \rightarrow \bullet CCl_2CO(OCl) + CHCl(OCl)COOH$	HA
208	$CHCl_2CO(OCl) + \bullet CCl(OCl)CHCl_2 \rightarrow \bullet CCl_2CO(OCl) + CHCl(OCl)CHCl_2$	HA
209	$CHCl_2CO(OCl) + \bullet CCl_2(OH) \rightarrow \bullet CCl_2CO(OCl) + CHCl_2(OH)$	HA
210	$CHCl_2CO(OCl) + \bullet CCl(OH)(OCl) \rightarrow \bullet CCl_2CO(OCl) + CHCl(OH)(OCl)$	HA
211	$CHCl_2CO(OCl) + \bullet COOH \rightarrow \bullet CCl_2CO(OCl) + HCOOH$	HA

212	$CHCl_2CO(OCl) + Cl\bullet \rightarrow \bullet CCl_2CO(OCl) + HCl$	HA
213	$CHCl_2CO(OCl) + ClO\bullet \rightarrow \bullet CCl_2CO(OCl) + HOCl$	HA
214	$CHCl_2CO(OCl) + Cl_2^-\bullet \rightarrow \bullet CCl_2CO(OCl) + Cl^- + HCl$	HA
215	$\bullet OOCOOH \rightarrow CO_2 + HO_2\bullet$	PH
216	$\bullet CCl_2CO(OCl) + O_2 \rightarrow \bullet OOCCl_2CO(OCl)$	OA
217	$2\ \bullet OOCCl_2CO(OCl) \rightarrow 2\ \bullet OCCl_2CO(OCl) + O_2$	PB3
218	$\bullet OCCl_2CO(OCl) \rightarrow COCl_2 + \bullet CO(OCl)$	BS
219	$\bullet OCCl_2CO(OCl) \rightarrow OClCCO(OCl) + Cl\bullet$	BS
220	$\bullet CO(OCl) + O_2 \rightarrow \bullet OOCO(OCl)$	OA
221	$OClCCO(OCl) + H_2O \rightarrow CO(OCl)COOH + HCl$	HX
222	$2\ \bullet OOCO(OCl) \rightarrow 2\ \bullet OCO(OCl) + O_2$	PB3
223	$CO(OCl)COOH + HO\bullet \rightarrow \bullet OCOCO(OCl) + H_2O$	HA
224	$CO(OCl)COOH + \bullet CCl_2CHCl_2 \rightarrow \bullet OCOCO(OCl) + CHCl_2CHCl_2$	HA
225	$CO(OCl)COOH + \bullet CCl_2CHCl(OCl) \rightarrow \bullet OCOCO(OCl) + CHCl(OCl)CHCl_2$	HA
226	$CO(OCl)COOH + \bullet CCl_2CHO \rightarrow \bullet OCOCO(OCl) + CHCl_2CHO$	HA
227	$CO(OCl)COOH + \bullet CHCl_2 \rightarrow \bullet OCOCO(OCl) + CH_2Cl_2$	HA
228	$CO(OCl)COOH + \bullet CHCl(OCl) \rightarrow \bullet OCOCO(OCl) + CH_2Cl(OCl)$	HA
229	$CO(OCl)COOH + \bullet CH(OH)_2 \rightarrow \bullet OCOCO(OCl) + CH_2(OH)_2$	HA
230	$CO(OCl)COOH + \bullet CCl_3 \rightarrow \bullet OCOCO(OCl) + CHCl_3$	HA
231	$CO(OCl)COOH + \bullet CCl_2COOH \rightarrow \bullet OCOCO(OCl) + CHCl_2COOH$	HA
232	$CO(OCl)COOH + \bullet CCl(OCl)COOH \rightarrow \bullet OCOCO(OCl) + CHCl(OCl)COOH$	HA
233	$CO(OCl)COOH + \bullet CCl(OCl)CHCl_2 \rightarrow \bullet OCOCO(OCl) + CHCl(OCl)CHCl_2$	HA
234	$CO(OCl)COOH + \bullet CCl_2(OH) \rightarrow \bullet OCOCO(OCl) + CHCl_2(OH)$	HA
235	$CO(OCl)COOH + \bullet CCl(OH)(OCl) \rightarrow \bullet OCOCO(OCl) + CHCl(OH)(OCl)$	HA
236	$CO(OCl)COOH + \bullet COOH \rightarrow \bullet OCOCO(OCl) + HCOOH$	HA
237	$CO(OCl)COOH + \bullet CCl_2CO(OCl) \rightarrow \bullet OCOCO(OCl) + CHCl_2CO(OCl)$	HA
238	$CO(OCl)COOH + \bullet CO(OCl) \rightarrow \bullet OCOCO(OCl) + OHC(OCl)$	HA
239	$CO(OCl)COOH + Cl\bullet \rightarrow \bullet OCOCO(OCl) + HCl$	HA
240	$CO(OCl)COOH + ClO\bullet \rightarrow \bullet OCOCO(OCl) + HOCl$	HA
241	$CO(OCl)COOH + Cl_2^-\bullet \rightarrow \bullet OCOCO(OCl) + Cl^- + HCl$	HA
242	$\bullet OCO(OCl) \rightarrow CO_2 + ClO\bullet$	BS
243	$\bullet OCOCO(OCl) \rightarrow CO_2 + \bullet CO(OCl)$	BS
244	$HO\bullet + OH^- \rightarrow O^-\bullet + H_2O$	S
245	$O^-\bullet + H_2O \rightarrow HO\bullet + OH^-$	S
246	$HO\bullet + HOCl \rightarrow ClO\bullet + H_2O$	S
247	$HO\bullet + HO\bullet \rightarrow H_2O_2$	S
248	$H_2O_2 + HO\bullet \rightarrow HO_2\bullet + H_2O$	S
249	$HO\bullet + HO_2\bullet \rightarrow O_2 + H_2O$	S
250	$H_2O_2 + HO_2\bullet \rightarrow HO\bullet + O_2 + H_2O$	S
251	$HO_2\bullet + HO_2\bullet \rightarrow H_2O_2 + O_2$	S
252	$Cl\bullet + H_2O \rightarrow ClOH^-\bullet + H^+$	S

253	$ClOH^{-}\bullet + H^{+} \rightarrow Cl\bullet + H_2O$	S
254	$ClOH^{-}\bullet \rightarrow HO\bullet + Cl^{-}$	S
255	$HO\bullet + Cl^{-} \rightarrow ClOH^{-}\bullet$	S
256	$ClOH^{-}\bullet + Cl^{-} \rightarrow Cl_2^{-}\bullet + OH^{-}$	S
257	$Cl\bullet + Cl^{-} \rightarrow Cl_2^{-}\bullet$	S
258	$Cl_2^{-}\bullet \rightarrow Cl\bullet + Cl^{-}$	S
259	$Cl\bullet + Cl\bullet \rightarrow Cl_2$	S
260	$Cl_2 + OH^{-} \rightarrow HOCl + Cl^{-}$	S
261	$Cl_2^{-}\bullet + Cl_2^{-}\bullet \rightarrow Cl_2 + 2Cl^{-}$	S
262	$Cl\bullet + Cl_2^{-}\bullet \rightarrow Cl_2 + Cl^{-}$	S
263	$Cl_2^{-}\bullet + H_2O_2 \rightarrow HO_2\bullet + 2Cl + H^{+}$	S
264	$Cl_2^{-}\bullet + HO_2\bullet \rightarrow O_2 + 2Cl + H^{+}$	S
265	$Cl_2^{-}\bullet + H_2O \rightarrow HClOH + Cl^{-}$	S
266	$Cl_2^{-}\bullet + OH^{-} \rightarrow ClOH^{-}\bullet + Cl^{-}$	S
267	$HClOH \rightarrow ClOH^{-}\bullet + H^{+}$	S
268	$HClOH \rightarrow Cl\bullet + H_2O$	S
269	$HClOH + Cl^{-} \rightarrow Cl_2^{-}\bullet + H_2O$	S
270	$Cl\bullet + H_2O_2 \rightarrow HO_2\bullet + Cl^{-} + H^{+}$	S
271	$Cl_2^{-}\bullet + HO\bullet \rightarrow HOCl + Cl^{-}$	S
272	$Cl_2 + H_2O \rightarrow HOCl + Cl^{-} + H^{+}$	S
273	$Cl_2 + HO_2\bullet \rightarrow Cl_2^{-}\bullet + O_2 + H^{+}$	S
274	$HOCl + HO_2\bullet \rightarrow Cl\bullet + O_2 + H_2O$	S
275	$Cl\bullet + HOCl \rightarrow ClO\bullet + Cl^{-} + H^{+}$	S
276	$Cl\bullet + OH^{-} \rightarrow ClOH^{-}\bullet$	S
277	$ClO\bullet + ClO\bullet \rightarrow Cl_2O_2$	S
278	$Cl_2O_2 + H_2O \rightarrow HOCl + ClO_2^{-} + H^{+}$	S
279	$ClO\bullet + HO\bullet \rightarrow ClO_2^{-} + H^{+}$	S
280	$ClO_2^{-} + HO\bullet \rightarrow ClO_2\bullet + OH^{-}$	S
281	$ClO_2\bullet + HO\bullet \rightarrow ClO_3^{-} + H^{+}$	S
282	$ClO_2^{-} + Cl_2^{-}\bullet \rightarrow ClO_2\bullet + 2Cl^{-}$	S
283	$ClO_2^{-} + ClO\bullet + H^{+} \rightarrow ClO_2\bullet + HOCl$	S
284	$CCl_2{=}CClH + UV \rightarrow \bullet CClCHCl + Cl\bullet$	UV
285	$\bullet CClCHCl + O_2 \rightarrow \bullet OOCClCHCl$	OA
286	$2\ \bullet OOCClCHCl \rightarrow 2\ \bullet OCClCHCl + O_2$	PB3
287	$\bullet OCClCHCl \rightarrow \bullet CHClCOCl$	S
288	$\bullet CHClCOCl + H_2O \rightarrow\rightarrow HCOOH + H^{+} + Cl^{-}$	S
289	$\bullet CHClCOCl + O_2 \rightarrow \bullet OOCHClCOCl$	OA
290	$2\ \bullet OOCHClCOCl \rightarrow 2\ \bullet OCHClCOCl + O_2$	PB3
291	$\bullet OCHClCOCl \rightarrow CClOCHO + Cl\bullet$	ClE
292	$CClOCHO + H_2O + \rightarrow\rightarrow OHCCOOH + HCl$	HS
293	$\bullet OCClCHCl \rightarrow COCHCl + Cl\bullet$	ClE
294	$COCHCl + H_2O \rightarrow\rightarrow CH_2ClCOOH$	HS
295	$CH_2ClCOOH + HOCl \rightarrow CHCl_2COOH + H2O$	ClR
296	$CCl_2{=}CClH + UV + H_2O \rightarrow CHCl_2CHCl(OH)$	UV

297	$CHCl_2CHCl(OH) \rightarrow CHCl_2CHO + HCl$	XE
298	$CHCl_2CHO + H_2O \rightarrow\rightarrow CHCl_2COOH$	HC
299	$CHCl_2CHO + UV + \rightarrow \bullet CHO + \bullet CHCl_2$	UV
300	$CCl_2{=}CClH + UV + H_2O \rightarrow\rightarrow CCl{\equiv}CH$	UV
301	$CCl{\equiv}CH + H_2O \rightarrow CH_3COCl$	HC
302	$CH_3COCl + H_2O \rightarrow CH_3COOH + HCl$	HX
303	$CH_3COOH + HOCl \rightarrow CH_2ClCOOH + H_2O$	ClR
304	$CCl_2{=}CClH + HOCl \rightarrow CHCl_2CCl_2(OH)$	ClR
305	$CHCl_2CCl_2(OH) \rightarrow CHCl_2CClO + HCl$	XE

L.2 Pathways Generated for Various Organic Compounds Degradation in the UV/Free Chlorine Process

Our pathway generator also predicted mechanisms of (1) TCE degradation under complexity 2, (2) methane degradation under complexity 1 and complexity 2, (3) methanol degradation under complexity 1 and complexity 2, (4) acetone degradation under complexity 1 and complexity 2, (5) IPA degradation under complexity 1 and complexity 2, and, (6) MTBE degradation under complexity 1 and complexity 2. These prediction results have been uploaded on GitHub: https://github.com/jadezwq/Results-of-Pathway-Generator-for-UV-Free-Chlorine-Process

REFERENCES

1 Qing Li, Q.; Loganath, A.; Seng Chong, Y.; Tan, J.; Philip Obbard, J. Persistent organic pollutants and adverse health effects in humans. *Journal of Toxicology and Environmental Health, Part A* 2006, *69*, 1987-2005.

2 El-Shahawi, M.; Hamza, A.; Bashammakh, A.; Al-Saggaf, W. An overview on the accumulation, distribution, transformations, toxicity and analytical methods for the monitoring of persistent organic pollutants. *Talanta* 2010, *80*, 1587-1597.

3 Bonito, L. T.; Hamdoun, A.; Sandin, S. A. Evaluation of the global impacts of mitigation on persistent, bioaccumulative and toxic pollutants in marine fish. *PeerJ* 2016, *4*, e1573.

4 Chiu, W. A.; Jinot, J.; Scott, C. S.; Makris, S. L.; Cooper, G. S.; Dzubow, R. C.; Bale, A. S.; Evans, M. V.; Guyton, K. Z.; Keshava, N. Human health effects of trichloroethylene: key findings and scientific issues. *Environ. Health Perspect.* 2012, *121*, 303-311.

5 Shore, R. F.; Taggart, M. A.; Smits, J.; Mateo, R.; Richards, N. L.; Fryday, S. Detection and drivers of exposure and effects of pharmaceuticals in higher vertebrates. *Phil. Trans. R. Soc. B* 2014, *369*, 20130570.

6 Sammarco, P. W.; Kolian, S. R.; Warby, R. A.; Bouldin, J. L.; Subra, W. A.; Porter, S. A. Distribution and concentrations of petroleum hydrocarbons associated with the BP/Deepwater Horizon Oil Spill, Gulf of Mexico. *Marine pollution bulletin* 2013, *73*, 129-143.

7 Rossi, L.; Queloz, P.; Brovelli, A.; Margot, J.; Barry, D. A. Enhancement of micropollutant degradation at the outlet of small wastewater treatment plants. *PloS one* 2013, *8*, e58864.

8 Petrović, M.; Gonzalez, S.; Barceló, D. Analysis and removal of emerging contaminants in wastewater and drinking water. *TrAC, Trends Anal. Chem.* 2003, *22*, 685-696.

9 Rizzo, L.; Selcuk, H.; Nikolaou, A.; Meriç Pagano, S.; Belgiorno, V. A comparative evaluation of ozonation and heterogeneous photocatalytic oxidation processes for reuse of secondary treated urban wastewater. *Desalin Water Treat.* 2014, *52*, 1414-1421.

10 Crittenden, J. C.; Howe, K.; Hand, D. W.; Trussell, R. R.; Tchobanoglous, G., *MWH's Water Treatment: Principles and Design*. 3rd, ed.; John Wiley & Sons: Hoboken, NJ, 2012.

11 Deng, Y.; Zhao, R. Advanced Oxidation Processes (AOPs) in Wastewater Treatment. *Curr.Pollution.Rep.* 2015, *1*, 167-176.

12 Buxton, G. V.; Greenstock, C. L.; Helman, W. P.; Ross, A. B. Critical review of rate constants for reactions of hydrated electrons, hydrogen atoms and hydroxyl radicals (·OH/·O^-) in aqueous solution. *J. Phys. Chem. Ref. Data.* 1988, *17*, 513-886.

13 Armstrong, D. A.; Huie, R. E.; Koppenol, W. H.; Lymar, S. V.; Merényi, G.; Neta, P.; Ruscic, B.; Stanbury, D. M.; Steenken, S.; Wardman, P. Standard electrode potentials involving radicals in aqueous solution: inorganic radicals (IUPAC Technical Report). *Pure Appl. Chem.* 2015, *87*, 1139-1150.

14 Michalski, R.; Mathews, B. Occurrence of Chlorite, Chlorate and Bromate in Disinfected Swimming Pool Water. *Pol.J.Engl.Stud.* 2007, *16*.

15 Crittenden, J. C.; Hu, S.; Hand, D. W.; Green, S. A. A kinetic model for H_2O_2/UV process in a completely mixed batch reactor. *Water Res.* 1999, *33*, 2315-2328.

16 Jasim, S.; Ndiongue, S.; Alshikh, O.; Jamal, A. Impact of Ozone and Hydrogen Peroxide vs. UV and Hydrogen Peroxide on Chlorine Residual. *Ozone: Sci Eng.* 2012, *34*, 16-25.

17 Espana, V. A. A.; Mallavarapu, M.; Naidu, R. Treatment technologies for aqueous perfluorooctanesulfonate (PFOS) and perfluorooctanoate (PFOA): A critical review with an emphasis on field testing. *Environmental.Technol. Innovation.* 2015, *4*, 168-181.

18 Neta, P.; Madhavan, V.; Zemel, H.; Fessenden, R. W. Rate constants and mechanism of reaction of sulfate radical anion with aromatic compounds. *J. Am. Chem. Soc.* 1977, *99*, 163-164.

19 Lian, L.; Yao, B.; Hou, S.; Fang, J.; Yan, S.; Song, W. Kinetic Study of Hydroxyl and Sulfate Radical-Mediated Oxidation of Pharmaceuticals in Wastewater Effluents. *Environ. Sci. Technol.* 2017, *51*, 2954-2962.

20 Qian, Y.; Guo, X.; Zhang, Y.; Peng, Y.; Sun, P.; Huang, C.-H.; Niu, J.; Zhou, X.; Crittenden, J. Perfluorooctanoic Acid Degradation Using UV/Persulfate Process: Modeling of the Degradation and Chlorate Formation. *Environ. Sci. Technol.* 2015, *50*, 772-781.

21 Dodgen, H.; Taube, H. The exchange of chlorine dioxide with chlorite ion and with chlorine in other oxidation states. *J. Am. Chem. Soc.* 1949, *71*, 2501-2504.

22 Naeini, M. R.; Khoshgoftarmanesh, A. H.; Lessani, H.; Fallahi, E. Effects of sodium chloride-induced salinity on mineral nutrients and soluble sugars in three commercial cultivars of pomegranate. *J.Plant.Nutr.* 2005, *27*, 1319-1326.

23 Kelly, W. R.; Panno, S. V.; Hackley, K. *The sources, distribution, and trends of chloride in the waters of Illinois*; Illinois State Water Survey Bulletin 74: Champaign, Illinois, 2012; https://www.isws.illinois.edu/pubdoc/B/ISWSB-74.pdf.

24 Govindaraj, M.; Muthukumar, M.; Bhaskar Raju, G. Electrochemical oxidation of tannic acid contaminated wastewater by RuO2/IrO2/TaO2-coated titanium and graphite anodes. *Environ. Technol.* 2010, *31*, 1613-1622.

25 Luo, C.; Jiang, J.; Ma, J.; Pang, S.; Liu, Y.; Song, Y.; Guan, C.; Li, J.; Jin, Y.; Wu, D. Oxidation of the odorous compound 2, 4, 6-trichloroanisole by UV activated persulfate: Kinetics, products, and pathways. *Water Res.* 2016, *96*, 12-21.

26 Fang, G.-D.; Dionysiou, D. D.; Wang, Y.; Al-Abed, S. R.; Zhou, D.-M. Sulfate radical-based degradation of polychlorinated biphenyls: effects of chloride ion and reaction kinetics. *J. Hazard. Mater.* 2012, *227*, 394-401.

27 Zhang, Y.; Zhang, J.; Xiao, Y.; Chang, V. W.; Lim, T.-T. Kinetic and mechanistic investigation of azathioprine degradation in water by UV, UV/H_2O_2 and UV/persulfate. *Chem. Eng. J.* 2016, *302*, 526-534.

28 Lou, X.; Xiao, D.; Fang, C.; Wang, Z.; Liu, J.; Guo, Y.; Lu, S. Comparison of UV/hydrogen peroxide and UV/peroxydisulfate processes for the degradation of humic acid in the presence of halide ions. *Environ.Sci.Pollut.Res.* 2016, *23*, 4778-4785.

29 Wang, P.; Yang, S.; Shan, L.; Niu, R.; Shao, X. Involvements of chloride ion in decolorization of Acid Orange 7 by activated peroxydisulfate or peroxymonosulfate oxidation. *J.Environ.Sci.* 2011, *23*, 1799-1807.

30 Zhang, R.; Sun, P.; Boyer, T. H.; Zhao, L.; Huang, C.-H. Degradation of pharmaceuticals and metabolite in synthetic human urine by UV, UV/H_2O_2, and UV/PDS. *Environ. Sci. Technol.* 2015, *49*, 3056-3066.

31 Yang, Y.; Pignatello, J. J.; Ma, J.; Mitch, W. A. Effect of matrix components on UV/H_2O_2 and UV/$S_2O_8^{2-}$ advanced oxidation processes for trace organic degradation in reverse osmosis brines from municipal wastewater reuse facilities. *Water Res.* 2016, *89*, 192-200.

32 Tan, C.; Fu, D.; Gao, N.; Qin, Q.; Xu, Y.; Xiang, H. Kinetic degradation of chloramphenicol in water by UV/persulfate system. *J. Photochem. Photobiol., A.* 2017, *332*, 406-412.

33 Tan, C.; Gao, N.; Zhou, S.; Xiao, Y.; Zhuang, Z. Kinetic study of acetaminophen degradation by UV-based advanced oxidation processes. *Chem. Eng. J.* 2014, *253*, 229-236.

34 Luo, C.; Jiang, J.; Guan, C.; Ma, J.; Pang, S.; Song, Y.; Yang, Y.; Zhang, J.; Wu, D.; Guan, Y. Factors affecting formation of deethyl and deisopropyl products from atrazine degradation in UV/H_2O_2 and UV/PDS. *RSC. Adv.* 2017, *7*, 29255-29262.

35 Fang, C.; Lou, X.; Huang, Y.; Feng, M.; Wang, Z.; Liu, J. Monochlorophenols degradation by UV/persulfate is immune to the presence of chloride: Illusion or reality? *Chem. Eng. J.* 2017, 124-133.

36 Park, K.-M.; Lee, H.-K.; Do, S.-H.; Kong, S.-H., Degradation of TCE using persulfate (PS) and peroxymonosulfate (PMS): effect of inorganic ions in groundwater. In *Proceedings of the world congress on engineering and computer science*, San Francisco, CA, USA, 2010.

37 Fang, J.; Fu, Y.; Shang, C. The roles of reactive species in micropollutant degradation in the UV/free chlorine system. *Environ. Sci. Technol.* 2014, *48*, 1859-1868.

38 Rosenfeldt, E.; Boal, A. K.; Springer, J.; Stanford, B.; Rivera, S.; Kashinkunti, R. D.; Metz, D. H. Comparison of UV-mediated Advanced Oxidation. *J Am Water Works Assoc.* 2013, *105*, 29-33.

39 Zhang, W.; Zhou, S.; Sun, J.; Meng, X.; Luo, J.; Zhou, D.; Crittenden, J. C. Impact of Chloride Ions on UV/H_2O_2 and UV/Persulfate Advanced Oxidation Processes. *Environ. Sci. Technol.* 2018, *52*, 7380-7389.

40 Feng, Y.; Smith, D. W.; Bolton, J. R. Photolysis of aqueous free chlorine species (HOCl and OCl) with 254 nm ultraviolet light. *J. Environ. Eng. Sci.* 2007, *6*, 277-284.

41 Sichel, C.; Garcia, C.; Andre, K. Feasibility studies: UV/chlorine advanced oxidation treatment for the removal of emerging contaminants. *Water Res.* 2011, *45*, 6371-6380.

42 Council, C. C.; Council, A. C., Drinking Water Chlorination: A Review of Disinfection Practices and Issues. *WATER CONDITIONING AND PURIFICATION INTERNATIONAL.* 2006, p 68.

43 Guo, K.; Wu, Z.; Shang, C.; Yao, B.; Hou, S.; Yang, X.; Song, W.; Fang, J. Radical Chemistry and Structural Relationships of PPCP Degradation by UV/Chlorine Treatment in Simulated Drinking Water. *Environ. Sci. Technol.* 2017, *51*, 10431-10439.

44 Tang, Y.; Shi, X.; Liu, Y.; Feng, L.; Zhang, L. Degradation of clofibric acid in UV/chlorine disinfection process: kinetics, reactive species contribution and pathways. *R Soc Open Sci.* 2018, *5*, 171372.

45 Xiang, Y.; Fang, J.; Shang, C. Kinetics and pathways of ibuprofen degradation by the UV/chlorine advanced oxidation process. *Water Res.* 2016, *90*, 301-308.

46 Wang, W.-L.; Wu, Q.-Y.; Huang, N.; Wang, T.; Hu, H.-Y. Synergistic effect between UV and chlorine (UV/chlorine) on the degradation of carbamazepine: influence factors and radical species. *Water Res.* 2016, *98*, 190-198.

47 Sun, P.; Lee, W.-N.; Zhang, R.; Huang, C.-H. Degradation of DEET and caffeine under UV/chlorine and simulated sunlight/chlorine conditions. *Environ. Sci. Technol.* 2016, *50*, 13265-13273.

48 Boal, A. *Groundwater Remediation Using a Chlorine/Ultraviolet Advanced Oxidation Process.* NGWA Groundwater Summit, Ngwa, 2014.

49 Wang, D.; Bolton, J. R.; Andrews, S. A.; Hofmann, R. UV/chlorine control of drinking water taste and odour at pilot and full-scale. *Chemosphere.* 2015, *136*, 239-244.

50 Kong, X.; Jiang, J.; Ma, J.; Yang, Y.; Liu, W.; Liu, Y. Degradation of atrazine by UV/chlorine: efficiency, influencing factors, and products. *Water Res.* 2016, *90*, 15-23.

51 Guo, K.; Wu, Z.; Yan, S.; Yao, B.; Song, W.; Hua, Z.; Zhang, X.; Kong, X.; Li, X.; Fang, J. Comparison of the UV/chlorine and UV/H_2O_2 processes in the degradation of PPCPs in simulated drinking water and wastewater: Kinetics, radical mechanism and energy requirements. *Water Res.* 2018, *147*, 184-194.

52 Huang, N.; Wang, T.; Wang, W.-L.; Wu, Q.-Y.; Li, A.; Hu, H.-Y. UV/chlorine as an advanced oxidation process for the degradation of benzalkonium chloride: synergistic effect, transformation products and toxicity evaluation. *Water Res.* 2017, *114*, 246-253.

53 Pan, M.; Wu, Z.; Tang, C.; Guo, K.; Cao, Y.; Fang, J. Emerging investigators series: comparative study of naproxen degradation by the UV/chlorine and the UV/H_2O_2 advanced oxidation processes. *Environ Sci: Wat Res.* 2018.

54 Dao, Y.; Tran, H.; Tran-Lam, T.; Pham, T.; Le, G. Degradation of Paracetamol by an UV/Chlorine Advanced Oxidation Process: Influencing Factors, Factorial Design, and Intermediates Identification. *International journal of environmental research and public health* 2018, *15*, 2637.

55 Gao, Z.-C.; Lin, Y.-L.; Xu, B.; Pan, Y.; Xia, S.-J.; Gao, N.-Y.; Zhang, T.-Y.; Chen, M. Degradation of acrylamide by the UV/chlorine advanced oxidation process. *Chemosphere.* 2017, *187*, 268-276.

56 Zhu, Y.; Wu, M.; Gao, N.; Chu, W.; Li, K.; Chen, S. Degradation of phenacetin by the UV/chlorine advanced oxidation process: Kinetics, pathways, and toxicity evaluation. *Chem. Eng. J.* 2018, *335*, 520-529.

57 Ye, B.; Li, Y.; Chen, Z.; Wu, Q.-Y.; Wang, W.-L.; Wang, T.; Hu, H.-Y. Degradation of polyvinyl alcohol (PVA) by UV/chlorine oxidation: Radical roles, influencing factors, and degradation pathway. *Water Res.* 2017, *124*, 381-387.

58 Dong, H.; Qiang, Z.; Hu, J.; Qu, J. Degradation of chloramphenicol by UV/chlorine treatment: Kinetics, mechanism and enhanced formation of halonitromethanes. *Water Res.* 2017, *121*, 178-185.

59 Wang, A.-Q.; Lin, Y.-L.; Xu, B.; Hu, C.-Y.; Xia, S.-J.; Zhang, T.-Y.; Chu, W.-H.; Gao, N.-Y. Kinetics and modeling of iodoform degradation during UV/chlorine advanced oxidation process. *Chem. Eng. J.* 2017, *323*, 312-319.

60 Wu, Z.; Fang, J.; Xiang, Y.; Shang, C.; Li, X.; Meng, F.; Yang, X. Roles of reactive chlorine species in trimethoprim degradation in the UV/chlorine process: Kinetics and transformation pathways. *Water Res.* 2016, *104*, 272-282.

61 Shi, X.-T.; Liu, Y.-Z.; Tang, Y.-Q.; Feng, L.; Zhang, L.-Q. Kinetics and pathways of Bezafibrate degradation in UV/chlorine process. *Environ.Sci.Pollut.Res.* 2018, *25*, 672-682.

62 Zhang, R.; Meng, T.; Huang, C.-H.; Ben, W.; Yao, H.; Liu, R.; Sun, P. PPCP degradation by chlorine-UV processes in ammoniacal water: new reaction insights, kinetic modeling and DBP formation. *Environ. Sci. Technol.* 2018.

63 Guo, X.; Minakata, D.; Crittenden, J. Computer-Based First-Principles Kinetic Monte Carlo Simulation of Polyethylene Glycol Degradation in Aqueous Phase UV/H_2O_2 Advanced Oxidation Process. *Environ. Sci. Technol.* 2014, *48*, 10813-10820.

64 Guo, X.; Minakata, D.; Niu, J.; Crittenden, J. Computer-Based First-Principles Kinetic Modeling of Degradation Pathways and Byproduct Fates in Aqueous-Phase Advanced Oxidation Processes. *Environ. Sci. Technol.* 2014, *48*, 5718-5725.

65 Guo, X.; Minakata, D.; Crittenden, J. On-the-Fly Kinetic Monte Carlo Simulation of Aqueous Phase Advanced Oxidation Processes. *Environ. Sci. Technol.* 2015, *49*, 9230-9236.

66 Zeng, H.; Zhang, W.; Deng, L.; Luo, J.; Zhou, S.; Liu, X.; Pei, Y.; Shi, Z.; Crittenden, J. Degradation of dyes by peroxymonosulfate activated by ternary CoFeNi-layered double hydroxide: catalytic performance, mechanism and kinetic modeling. *J. Colloid Interface Sci.* 2018, *515*, 92-100.

67 Zhou, S.; Yu, Y.; Zhang, W.; Meng, X.; Luo, J.; Deng, L.; Shi, Z.; Crittenden, J. Oxidation of Microcystin-LR via Activation of Peroxymonosulfate Using Ascorbic Acid: Kinetic Modeling and Toxicity Assessment. *Environ. Sci. Technol.* 2018, *52*, 4305-4312.

68 Li, K.; Crittenden, J. Computerized pathway elucidation for hydroxyl radical-induced chain reaction mechanisms in aqueous phase advanced oxidation processes. *Environ. Sci. Technol.* 2009, *43*, 2831-2837.

69 Minakata, D.; Li, K.; Westerhoff, P.; Crittenden, J. Development of a group contribution method to predict aqueous phase hydroxyl radical (HO•) reaction rate constants. *Environ. Sci. Technol.* 2009, *43*, 6220-6227.

70 Lee, Y.; Von Gunten, U. Quantitative structure–activity relationships (QSARs) for the transformation of organic micropollutants during oxidative water treatment. *Water Res.* 2012, *46*, 6177-6195.

71 Minakata, D.; Crittenden, J. Linear Free Energy Relationships between Aqueous phase Hydroxyl Radical Reaction Rate Constants and Free Energy of Activation. *Environ. Sci. Technol.* 2011, *45*, 3479-3486.

72 Minakata, D.; Kamath, D.; Maetzold, S. Mechanistic Insight into the Reactivity of Chlorine-derived Radicals in the Aqueous-phase UV/chlorine Advanced Oxidation Process: Quantum Mechanical Calculations. *Environ. Sci. Technol.* 2017.

73 Minakata, D.; Mezyk, S. P.; Jones, J. W.; Daws, B. R.; Crittenden, J. C. Development of Linear Free Energy Relationships for Aqueous Phase Radical-Involved Chemical Reactions. *Environ. Sci. Technol.* 2014, *48*, 13925-13932.

74 Zhou, S.; Zhang, W.; Sun, J.; Zhu, S.; Li, K.; Meng, X.; Luo, J.; Shi, Z.; Zhou, D.; Crittenden, J. C. Oxidation Mechanisms of the UV/Free Chlorine Process: Kinetic Modeling and Quantitative Structure Activity Relationships. *Environ. Sci. Technol.* 2019, *53*, 4335-4345.

75 Zhang, R.; Yang, Y.; Huang, C.-H.; Li, N.; Liu, H.; Zhao, L.; Sun, P. UV/H_2O_2 and UV/PDS Treatment of Trimethoprim and Sulfamethoxazole in Synthetic Human Urine: Transformation Products and Toxicity. *Environ. Sci. Technol.* 2016, *50*, 2573-2583.

76 Liu, X.; Fang, L.; Zhou, Y.; Zhang, T.; Shao, Y. Comparison of UV/PDS and UV/H_2O_2 processes for the degradation of atenolol in water. *J.Environ.Sci.* 2013, *25*, 1519-1528.

77 Brillas, E. A review on the degradation of organic pollutants in waters by UV photoelectro-Fenton and solar photoelectro-Fenton. *J. Braz. Chem. Soc.* 2014, *25*, 393-417.

78 Chu, W.; Gao, N.; Yin, D.; Krasner, S. W.; Mitch, W. A. Impact of UV/H_2O_2 pre-oxidation on the formation of haloacetamides and other nitrogenous disinfection byproducts during chlorination. *Environ. Sci. Technol.* 2014, *48*, 12190-12198.

79 Chu, W.; Li, D.; Gao, N.; Templeton, M. R.; Tan, C.; Gao, Y. The control of emerging haloacetamide DBP precursors with UV/persulfate treatment. *Water Res.* 2015, *72*, 340-348.

80 Prieto-Rodríguez, L.; Oller, I.; Klamerth, N.; Agüera, A.; Rodríguez, E.; Malato, S. Application of solar AOPs and ozonation for elimination of micropollutants in municipal wastewater treatment plant effluents. *Water Res.* 2013, *47*, 1521-1528.

81 Collivignarelli, M. C.; Pedrazzani, R.; Sorlini, S.; Abbà, A.; Bertanza, G. H_2O_2 Based Oxidation Processes for the Treatment of Real High Strength Aqueous Wastes. *Sustainability.* 2017, *9*, 244.

82 Seid-Mohammadi, A.; Asgari, G.; Poormohammadi, A.; Ahmadian, M.; Rezaeivahidian, H. Removal of phenol at high concentrations using UV/Persulfate from saline wastewater. *Desalin Water Treat.* 2016, *57*, 19988-19995.

83 Xiao, Y.; Zhang, L.; Yue, J.; Webster, R. D.; Lim, T.-T. Kinetic modeling and energy efficiency of UV/H_2O_2 treatment of iodinated trihalomethanes. *Water Res.* 2015, *75*, 259-269.

84 Yao, H.; Sun, P.; Minakata, D.; Crittenden, J. C.; Huang, C.-H. Kinetics and modeling of degradation of ionophore antibiotics by UV and UV/H_2O_2. *Environ. Sci. Technol.* 2013, *47*, 4581-4589.

85 NDRL/NIST Solution Kinetics Database; http://kinetics.nist.gov/solution/.

86 Dilmeghani, M.; Zahir, K. O. Kinetics and mechanism of chlorobenzene degradation in aqueous samples using advanced oxidation processes. *J. Environ. Qual.* 2001, *30*, 2062-2070.

87 Li, Y.; Song, W.; Fu, W.; Tsang, D. C.; Yang, X. The roles of halides in the acetaminophen degradation by UV/H_2O_2 treatment: kinetics, mechanisms, and products analysis. *Chem. Eng. J.* 2015, *271*, 214-222.

88 Hou, S.; Ling, L.; Shang, C.; Guan, Y.; Fang, J. Degradation kinetics and pathways of haloacetonitriles by the UV/persulfate process. *Chem. Eng. J.* 2017, *320*, 478-484.

89 He, X.; Armah, A.; Dionysiou, D. D. Destruction of cyanobacterial toxin cylindrospermopsin by hydroxyl radicals and sulfate radicals using UV-254nm activation of hydrogen peroxide, persulfate and peroxymonosulfate. *J. Photochem. Photobiol., A.* 2013, *251*, 160-166.

90 Yang, Y.; Jiang, J.; Lu, X.; Ma, J.; Liu, Y. Production of sulfate radical and hydroxyl radical by reaction of ozone with peroxymonosulfate: a novel advanced oxidation process. *Environ. Sci. Technol.* 2015, *49*, 7330-7339.

91 Hori, H.; Hayakawa, E.; Einaga, H.; Kutsuna, S.; Koike, K.; Ibusuki, T.; Kiatagawa, H.; Arakawa, R. Decomposition of environmentally persistent perfluorooctanoic acid in water by photochemical approaches. *Environ. Sci. Technol.* 2004, *38*, 6118-6124.

92 Li, K.; Stefan, M. I.; Crittenden, J. C. Trichloroethene Degradation by UV/H2O2 Advanced Oxidation Process: Product Study and Kinetic Modeling. *Environ. Sci. Technol.* 2007, *41*, 1696-1703.

93 Lutze, H. Sulfate radical based oxidation in water treatment. P.h.D. Dissertation, Duisburg-Essen University, Disburg, Germany, 2013.

94 Perez-Tejeda, P.; Maestre, A.; Delgado-Cobos, P.; Burgess, J. Single-ion Setschenow coefficients for several hydrophobic non-electrolytes in aqueous electrolyte solutions. *Can. J. Chem.* 1990, *68*, 243-246.

95 Davies, C. W.; Shedlovsky, T. Ion association. *J. Electrochem. Soc.* 1964, *111*, 85C-86C.

96 Du, Y.; Zhou, M.; Lei, L. The role of oxygen in the degradation of p-chlorophenol by Fenton system. *J. Hazard. Mater.* 2007, *139*, 108-115.

97 Lutze, H. V.; Bircher, S.; Rapp, I.; Kerlin, N.; Bakkour, R.; Geisler, M.; von Sonntag, C.; Schmidt, T. C. Degradation of chlorotriazine pesticides by sulfate radicals and the influence of organic matter. *Environ. Sci. Technol.* 2015, *49*, 1673-1680.

98 Lutze, H. V.; Kerlin, N.; Schmidt, T. C. Sulfate radical-based water treatment in presence of chloride: formation of chlorate, inter-conversion of sulfate radicals into hydroxyl radicals and influence of bicarbonate. *Water Res.* 2015, *72*, 349-360.

99 Millero, F. J. The physical chemistry of seawater. *Annu.Rev.Earth Planet.Sci.* 1974, *2*, 101-150.

100 Grebel, J. E.; Pignatello, J. J.; Mitch, W. A. Effect of halide ions and carbonates on organic contaminant degradation by hydroxyl radical-based advanced oxidation processes in saline waters. *Environ. Sci. Technol.* 2010, *44*, 6822-6828.

101 Wander, R.; Neta, P.; Dorfman, L. M. Pulse radiolysis studies. XII. Kinetics and spectra of the cyclohexadienyl radicals in aqueous benzoic acid solution. *J. Phys. Chem.* 1968, *72*, 2946-2949.

102 Alegre, M. L.; Gerones, M.; Rosso, J. A.; Bertolotti, S. G.; Braun, A. M.; Martire, D. O.; Gonzalez, M. C. Kinetic study of the reactions of chlorine atoms and Cl_2^-•radical anions in aqueous solutions. 1. Reaction with benzene. *J. Phys. Chem.A.* 2000, *104*, 3117-3125.

103 Luo, C.; Ma, J.; Jiang, J.; Liu, Y.; Song, Y.; Yang, Y.; Guan, Y.; Wu, D. Simulation and comparative study on the oxidation kinetics of atrazine by UV/H 2 O 2, and. *Water Res.* 2015, *80*, 99-108.

104 Li, W. Sulfate Radical-Based Advanced Oxidation Treatment for Groundwater Water Treatment and Potable Water Reuse. Ph.D. Dissertation, University of California Riverside, Riverside, CA, 2017.

105 Lu, X.; Shao, Y.; Gao, N.; Chen, J.; Zhang, Y.; Xiang, H.; Guo, Y. Degradation of diclofenac by UV-activated persulfate process: Kinetic studies, degradation pathways and toxicity assessments. *Ecotoxicol Environ Saf.* 2017, *141*, 139-147.

106 Wang, Z.; Shao, Y.; Gao, N.; Lu, X.; An, N. Degradation of diethyl phthalate (DEP) by UV/persulfate: An experiment and simulation study of contributions by hydroxyl and sulfate radicals. *Chemosphere.* 2018, *193*, 602-610.

107 Li, K.; Stefan, M. I.; Crittenden, J. C. UV photolysis of trichloroethylene: Product study and kinetic modeling. *Environ. Sci. Technol.* 2004, *38*, 6685-6693.

108 Daneshvar, N.; Behnajady, M.; Asghar, Y. Z. Photooxidative degradation of 4-nitrophenol (4-NP) in UV/H 2 O 2 process: Influence of operational parameters and reaction mechanism. *J. Hazard. Mater.* 2007, *139*, 275-279.

109 Liu, T.; Yin, K.; Liu, C.; Luo, J.; Crittenden, J.; Zhang, W.; Luo, S.; He, Q.; Deng, Y.; Liu, H. The role of reactive oxygen species and carbonate radical in oxcarbazepine degradation via UV, UV/H2O2: kinetics, mechanisms and toxicity evaluation. *Water Res.* 2018, *147*, 204-213.

110 Heponiemi, A.; Lassi, U., Advanced oxidation processes in food industry wastewater treatment–a review. In *Food Industrial Processes-Methods and Equipment*, InTech: 2012.

111 Watts, M. J.; Linden, K. G. Chlorine photolysis and subsequent OH radical production during UV treatment of chlorinated water. *Water Res.* 2007, *41*, 2871-2878.

112 Guan, Y.-H.; Ma, J.; Liu, D.-K.; Ou, Z.-f.; Zhang, W.; Gong, X.-L.; Fu, Q.; Crittenden, J. C. Insight into chloride effect on the UV/peroxymonosulfate process. *Chem. Eng. J.* 2018, *352*, 477-489.

113 Canonica, S.; Tratnyek, P. G. Quantitative structure-activity relationships for oxidation reactions of organic chemicals in water. *Environ. Toxicol. Chem.* 2003, *22*, 1743-1754.

114 Hansch, C.; Leo, A.; Taft, R. A survey of Hammett substituent constants and resonance and field parameters. *Chem. Rev.* 1991, *91*, 165-195.

115 Hessler, D.; Gorenflo, V.; Frimmel, F. Degradation of Aqueous Atrazine and Metazachlor Solutions by UV and UV/H2O2—Influence of pH and Herbicide Concentration. *Acta Hydroch. Hydrob.* 1993, *21*, 209-214.

116 Khan, J. A.; He, X.; Shah, N. S.; Khan, H. M.; Hapeshi, E.; Fatta-Kassinos, D.; Dionysiou, D. D. Kinetic and mechanism investigation on the photochemical degradation of atrazine with activated H2O2, S2O82− and HSO5−. *Chem. Eng. J.* 2014, *252*, 393-403.

117 Torczon, V. *Pattern search methods for nonlinear optimization.* SIAG/OPT Views and News, Citesser, 1995.

118 McCall, J. Genetic algorithms for modelling and optimisation. *J. Comput. Appl. Math.* 2005, *184*, 205-222.

119 Toolbox, G. O. User's Guide (r2011b). *The MathWorks Inc.* 2011.

120 Finlayson, B. A. *Introduction to chemical engineering computing*.; John Wiley & Sons Press: 2012.

121 Hansch, C.; Leo, A.; Livingstone, D. Exploring QSAR fundamentals and applications in chemistry and biology. *Pestic. Biochem. Physiol.* 1996, *56*, 78.

122 Sudhakaran, S.; Amy, G. L. QSAR models for oxidation of organic micropollutants in water based on ozone and hydroxyl radical rate constants and their chemical classification. *Water Res.* 2013, *47*, 1111-1122.

123 Guan, C.-t.; Jiang, J.; Luo, C.-w.; Ma, J.; Pang, S.-y.; Zhou, Y.; Yang, Y. Oxidation kinetics of bromophenols by nonradical activation of peroxydisulfate in the presence of carbon nanotube and formation of brominated polymeric products. *Environ. Sci. Technol.* 2017.

124 Hammett, L. P. The effect of structure upon the reactions of organic compounds. Benzene derivatives. *J. Am. Chem. Soc.* 1937, *59*, 96-103.

125 Draper, N. R.; Smith, H. *Applied regression analysis.* John Wiley & Sons Press: 2014.

126 Mártire, D. O.; Rosso, J. A.; Bertolotti, S.; Le Roux, G. C.; Braun, A. M.; Gonzalez, M. C. Kinetic study of the reactions of chlorine atoms and Cl2•-radical anions in aqueous solutions. II. Toluene, benzoic acid, and chlorobenzene. *J. Phys. Chem.A.* 2001, *105*, 5385-5392.

127 Li, K.; Hokanson, D. R.; Crittenden, J. C.; Trussell, R. R.; Minakata, D. Evaluating UV/H2O2 processes for methyl tert-butyl ether and tertiary butyl alcohol removal: Effect of pretreatment options and light sources. *Water Res.* 2008, *42*, 5045-5053.

128 Cheng, S.; Zhang, X.; Yang, X.; Shang, C.; Song, W.; Fang, J.; Pan, Y. The multiple role of bromide ion in PPCPs degradation under UV/chlorine treatment. *Environ. Sci. Technol.* 2018, *52*, 1806-1816.

129 Dotson, A. D.; Metz, D.; Linden, K. G. UV/H_2O_2 treatment of drinking water increases post-chlorination DBP formation. *Water Res.* 2010, *44*, 3703-3713.

130 Pisarenko, A. N.; Stanford, B. D.; Snyder, S. A.; Rivera, S. B.; Boal, A. K. Investigation of the use of chlorine based advanced oxidation in surface water: oxidation of natural organic matter and formation of disinfection byproducts. *J Adv Oxid Technol.* 2013, *16*, 137-150.

131 Jeong, J.; Song, W.; Cooper, W. J.; Jung, J.; Greaves, J. Degradation of tetracycline antibiotics: mechanisms and kinetic studies for advanced oxidation/reduction processes. *Chemosphere.* 2010, *78*, 533-540.

132 Dodd, M. C.; Huang, C.-H. Aqueous chlorination of the antibacterial agent trimethoprim: reaction kinetics and pathways. *Water Res.* 2007, *41*, 647-655.

133 Kodešová, R.; Klement, A.; Golovko, O.; Fér, M.; Kočárek, M.; Nikodem, A.; Grabic, R. Soil influences on uptake and transfer of pharmaceuticals from sewage sludge amended soils to spinach. *J. Environ. Manage.* 2019, *250*, 109407.

134 Bolton, J. R.; Stefan, M. I.; Shaw, P.-S.; Lykke, K. R. Determination of the quantum yields of the potassium ferrioxalate and potassium iodide–iodate actinometers and a method for the calibration of radiometer detectors. *J. Photochem. Photobiol., A.* 2011, *222*, 166-169.

135 Baeza, C.; Knappe, D. R. Transformation kinetics of biochemically active compounds in low-pressure UV Photolysis and UV/H2O2 advanced oxidation processes. *Water Res.* 2011, *45*, 4531-4543.

136 Miklos, D.; Wang, W.-L.; Linden, K.; Drewes, J.; Hübner, U. Comparison of UV-AOPs (UV/H2O2, UV/PDS and UV/Chlorine) for TOrC removal from municipal wastewater effluent and optical surrogate model evaluation. *Chem. Eng. J.* 2019, *362*, 537-547.

137 Mandal, S. Reaction Rate Constants of Hydroxyl Radicals with Micropollutants and Their Significance in Advanced Oxidation Processes. *J Adv Oxid Technol.* 2018, *21*, 178-195.

138 Ji, Y.; Xie, W.; Fan, Y.; Shi, Y.; Kong, D.; Lu, J. Degradation of trimethoprim by thermo-activated persulfate oxidation: reaction kinetics and transformation mechanisms. *Chem. Eng. J.* 2016, *286*, 16-24.

139 Quiroz, M. A.; Martínez-Huitle, C. A.; Bandala, E. R., Advanced oxidation processes (AOPs) for removal of pesticides from aqueous media. INTECH Open Access Publisher: 2011.

140 Yang, X.; Sun, J.; Fu, W.; Shang, C.; Li, Y.; Chen, Y.; Gan, W.; Fang, J. PPCP degradation by UV/chlorine treatment and its impact on DBP formation potential in real waters. *Water Res.* 2016, *98*, 309-318.

141 Duan, X.; Sanan, T.; de la Cruz, A. A.; He, X.; Kong, M.; Dionysiou, D. D. Susceptibility of the Algal Toxin Microcystin-LR to UV/Chlorine Process: Comparison with Chlorination. *Environ. Sci. Technol.* 2018.

142 Cerreta, G.; Roccamante, M. A.; Plaza-Bolaños, P.; Oller, I.; Aguera, A.; Malato, S.; Rizzo, L. Advanced treatment of urban wastewater by UV-C/free chlorine process: Micro-pollutants removal and effect of UV-C radiation on trihalomethanes formation. *Water Res.* 2019, 115220.

143 Bu, L.; Zhou, S.; Zhu, S.; Wu, Y.; Duan, X.; Shi, Z.; Dionysiou, D. D. Insight into carbamazepine degradation by UV/monochloramine: Reaction mechanism, oxidation products, and DBPs formation. *Water Res.* 2018, *146*, 288-297.

144 Sun, J.; Kong, D.; Aghdam, E.; Fang, J.; Wu, Q.; Liu, J.; Du, Y.; Yang, X.; Shang, C. The influence of the UV/chlorine advanced oxidation of natural organic matter for micropollutant degradation on the formation of DBPs and toxicity during post-chlorination. *Chem. Eng. J.* 2019, *373*, 870-879.

145 Gao, Z.-C.; Lin, Y.-L.; Xu, B.; Xia, Y.; Hu, C.-Y.; Zhang, T.-Y.; Cao, T.-C.; Chu, W.-H.; Gao, N.-Y. Effect of UV wavelength on humic acid degradation and disinfection by-product formation during the UV/chlorine process. *Water Res.* 2019, *154*, 199-209.

146 Wang, W.-L.; Zhang, X.; Wu, Q.-Y.; Du, Y.; Hu, H.-Y. Degradation of natural organic matter by UV/chlorine oxidation: molecular decomposition, formation of oxidation byproducts and cytotoxicity. *Water Res.* 2017, *124*, 251-258.

147 Zhang, X.; Li, W.; Blatchley III, E. R.; Wang, X.; Ren, P. UV/chlorine process for ammonia removal and disinfection by-product reduction: comparison with chlorination. *Water Res.* 2015, *68*, 804-811.

148 Li, M.; Xu, B.; Liungai, Z.; Hu, H.-Y.; Chen, C.; Qiao, J.; Lu, Y. The removal of estrogenic activity with UV/chlorine technology and identification of novel estrogenic disinfection by-products. *J. Hazard. Mater.* 2016, *307*, 119-126.

149 Xiang, H.; Shao, Y.; Gao, N.; Lu, X.; Chu, W.; An, N.; Tan, C.; Zheng, X.; Gao, Y. The influence of bromide on the degradation of sulfonamides in UV/free chlorine treatment: Degradation mechanism, DBPs formation and toxicity assessment. *Chem. Eng. J.* 2019, *362*, 692-701.

150 Wu, Y.; Zhu, S.; Zhang, W.; Bu, L.; Zhou, S. Comparison of diatrizoate degradation by UV/chlorine and UV/chloramine processes: Kinetic mechanisms and iodinated disinfection byproducts formation. *Chem. Eng. J.* 2019, 121972.

151 Stefan, M. I.; Hoy, A. R.; Bolton, J. R. Kinetics and Mechanism of the Degradation and Mineralization of Acetone in Dilute Aqueous Solution Sensitized by the UV Photolysis of Hydrogen Peroxide. *Environ. Sci. Technol.* 1996, *30*, 2382-2390.

152 Stefan, M. I.; Bolton, J. R. Mechanism of the degradation of 1, 4-dioxane in dilute aqueous solution using the UV/hydrogen peroxide process. *Environ. Sci. Technol.* 1998, *32*, 1588-1595.

153 Stefan, M. I.; Bolton, J. R. Reinvestigation of the Acetone Degradation Mechanism in Dilute Aqueous Solution by the UV/H2O2 Process. *Environ. Sci. Technol.* 1999, *33*, 870-873.

154 Stefan, M. I.; Mack, J.; Bolton, J. R. Degradation pathways during the treatment of methyl tert-butyl ether by the UV/H2O2 process. *Environ. Sci. Technol.* 2000, *34*, 650-658.

155 Cooper, W. J.; Cramer, C. J.; Martin, N. H.; Mezyk, S. P.; O'Shea, K. E.; Sonntag, C. v. Free radical mechanisms for the treatment of methyl tert-butyl ether (MTBE) via advanced oxidation/reductive processes in aqueous solutions. *Chem. Rev.* 2009, *109*, 1302-1345.

156 Schuchmann, M. N.; Von Sonntag, C. Hydroxyl radical-induced oxidation of 2-methyl-2-propanol in oxygenated aqueous solution. A product and pulse radiolysis study. *J. Phys. Chem.* 1979, *83*, 780-784.

157 Weininger, D. SMILES, a chemical language and information system. 1. Introduction to methodology and encoding rules. *Journal of chemical information and computer sciences* 1988, *28*, 31-36.

158 Westerhoff, P.; Mezyk, S. P.; Cooper, W. J.; Minakata, D. Electron pulse radiolysis determination of hydroxyl radical rate constants with Suwannee River fulvic acid and other dissolved organic matter isolates. *Environ. Sci. Technol.* 2007, *41*, 4640-4646.

159 Sugioka, M. The Relationship Between UV-VIS Absorption and Structure of Organic Compounds. *UV Talk Letter February. Shimadzu* 2009, *2*, 5-6.

160 Li, W.; Jain, T.; Ishida, K.; Liu, H. A mechanistic understanding of the degradation of trace organic contaminants by UV/hydrogen peroxide, UV/persulfate and UV/free chlorine for water reuse. *Environ Sci: Wat Res.* 2017, *3*, 128-138.